Circumvention of bottlenecks in the manufacture of influenza subunit vaccines using aqueous two-phase systems.

By Adetoun Olufolake Aiyedebinu

A Thesis submitted to the Faculty of Engineering
The University of Birmingham
For the degree of doctor of Philosophy

School of
The Faculty of
The University of Birmingham
Birmingham, UK
September 2001.

ABSTRACT

The experiments documented in this thesis investigate the use of aqueous two-phase systems (ATPS) as a viable method for the processing of influenza virus particles in a feedstock derived from embryonated hen's eggs. The virus particles are currently purified in an industrial process using stages of sucrose density gradient ultracentrifugation that produce a subunit vaccine Fluvirin™ which consists of the immunoprotective antigens haemagglutinin (HA) and neuraminidase (NA). The current purification scheme suffers process bottlenecks in particular, limitations of scale hence volumetric throughput and time taken to produce a batch that could be circumvented by ATPS.

Manipulations of polyethylene glycol (PEG) molecular weight, tie-line length (TLL) and volume ratio were exploited for the design of aqueous two-phase systems. A simple two-stage process was designed in which, (i) 60 % (by mass) of contaminating proteins were eliminated in an ATPS comprising PEG 300 22.2 % w/w/ phosphate 17.9 % w/w at pH 7.5 and (ii) HA antigen was released from intact influenza particles in the presence of 1 % w/w Triton X100 in an optimised secondary ATPS comprising PEG 300 13.9 % w/w/ phosphate 24.3 % w/w, pH 7.5. The first purification stage using ATPS performed as well as the ultracentrifugation method. The material was produced with purification factor of 4.2 and intact virus recovery of 72 % within one hour, (as compared to a purification factor 4.0 and recovery of 109 % within 18 hours, using ultracentrifugation). Thus ATPS has demonstrated potential in fractionating particulate feedstocks in relatively short times, thus facilitating the circumvention of bottlnecks in the current commercial process.

DEDICATION.

This thesis is dedicated to my mother

Janet Bolanle Meshileya.

ACKNOWLEDGMENTS.

I firstly would like to express my gratitude to my Supervisor Professor Andrew Lyddiatt, for his support and drive from project outset to finish, culminating in this manuscript.

Thank you to Dr Mohamed Desai whose support and encouragement were much appreciated. To, Paul Sinclair for his continuous assistance with information, protocols and equipment. To, Drs Amanda Shipman and Simon Walker for their assistance in reading my drafts and providing encouragement and support.
A special thanks to my family, Eva Turner, Winifred Joan Smeath and all my friends within and without the department: the Biochemical Recovery Group, members of St John's Church.

I gratefully acknowledge the support at Medeva Pharma (now Powderject Pharmaceuticals Plc), the assistance of Mr Brian Getty for the transmission electron microscopy undertaken on my behalf. This project was funded by the BBSRC and Medeva Pharma.

ABBREVIATIONS.

ATPS(s)	aqueous two-phase system(s).
ADTPS(s)	aqueous-detergent two-phase system(s).
BCA	bicinchinonic acid.
BSA	bovine serum albumin.
CAM	chorio allantoic membrane.
CBER	Center for Biologics Evaluation and Research.
cm	centimetres.
Con A	concanavalin A lectin.
CsCl	caesium chloride.
CV	coefficient of variance.
° C	degrees centrigrade.
g	grammes.
$H_x N_y$	haemagglutinin and neuraminidase sub type respectively (x =1 to 5; y =1 to 9).
HA	haemagglutinin.
HAU	haemagglutination unit.
HCl	hydrochloric acid.
IBF	inactivated bulk fluid.
IgG	immunoglobulin Gamma.
K	partition coefficient.
kDa	kilodalton.
kg	kilogramme.
M	molar.
MMWR	Morbidity and Mortality Weekly Report.
µg	micrograms.
µl	microlitres.
Ml	millilitres.
Mwt.	Molecular weight.
NA	neuraminidase.
NANA	n-acetylneuraminic acid.
NAN lactose	N-acetylneuraminyllactose.
NELLAM	neuraminidase enzyme-linked assay in microplates.
NIBSC	National Institute of Biological Standards and Controls.
nm	nanometres.
OPD	O-phenylamine diamine.
PBS	phosphate buffered saline.
Pfu	plaque-forming units.
pNPP	para-nitrophenyl phosphate.
Po-PNA	peroxidase-labelled peanut lectin.
PMR	partition mass ratio.
PTA	phosphotungstic acid
PZC	purified zonal concentrate.
RNA	ribonucleic acid.
SDS	sodium dodecyl sulphate.
SDS PAGE	sodium dodecyl sulphate polyacrylamide gel electrophoresis.
SRD	serial radial immunodiffusion.
TEM	transmission electron microscopy.

ABBREVIATIONS.

TBS	tris-buffered saline.
TCA	trichloroacetic acid.
v/v	volume per volume.
WHO	World Health Organisation.
w/v	weight per volume.

CONTENTS.

Circumvention of Bottlenecks in the manufacture of an influenza subunit vaccines using aqueous two-phase systems.

List of Figures.

List of Tables.

CHAPTER ONE.

1. INTRODUCTION TO VACCINES AND THEIR COMMERCIAL MANUFACTURE.

1.1 Vaccine development: A historical perspective.

Vaccination is an efficient, cost-effective means to protect human and animal populations against a variety of diseases such as cholera, polio, diphtheria, measles and influenza (Cryz Jr., 1991; Liljeqvist and Ståhl, 1999). More recently with the advent of recombinant DNA technology, the range of diseases that can be safely treated has been extended. The concept of vaccination is not a new one, dating back to 1000 BC in China and India. At the end of 18th century the first "rational" approaches to vaccination were made by Jenner, (using naturally attenuated cowpox to immunise against smallpox), followed by vaccines produced by Pasteur (Cryz Jr., 1991). The development, large-scale production of vaccines (which has perhaps surprisingly, changed very little) and the establishment of immunisation programmes began at the turn of the 20th century. These vaccines permitted the management of many diseases including the eradication of smallpox (Breman and Arita, 1980; WHO, 1980).

1.2. Definition and function of a vaccine.

A vaccine is defined as heterogeneous class of anti-infective medicinal product containing antigenic substances capable of inducing specific and active immunity against the infecting agent or the toxin or other important antigenic substances produced by this agent (definition in the *Ph. Eur.* 1998: 0153). The primary aim of a vaccine is that it stimulates an appropriate immune response when administered; that it should provide

immunoprophylaxis upon subsequent exposure to the disease for a period of time and that it should protect populations from that disease. These vaccines act as immunogens by stimulating (to varying degrees) the cellular and humoral arms of the immune system. Different factors influence the arm that is preferentially stimulated (as discussed by Shearer and Clerici, 1997), which could impact upon the vaccine design. Vaccine development has progressed significantly over the decades from "first generation" highly purified vaccines consisting of whole organisms, killed- inactivated or live- attenuated (Plotkin, 1993) through to specific organism-derived components such as detoxified toxins- purified subunit vaccines (Liljeqvist and Stahl, 1999). In addition "second generation" recombinant subunit vaccines utilised plasmid DNA that encoded the protective subunit proteins and were expressed in hosts such as yeast cells. The first such vaccine licensed in the US in 1986, consisted of the surface antigen (S antigen) of Hepatitis B and was produced in *Saccharomyces cerevisiae* (for example Energix B™, GlaxoSmithKline) whilst Hepagene™ (Medeva Pharma, now Powderject Pharmaceuticals plc) contained the S antigen in addition to other protective antigens which were derived from a mammalian cell line. These vaccines are useful in minimising both risk of pyrogenicity caused by other viral proteins (Salk, 1948) and the reversion back to wild type, virulent genotypes. More recently "third generation" vaccines consisting of naked DNA (containing the information required to encode the protective antigens) are delivered directly to the nucleus (Ulmer *et al*, 1993; Ulmer *et al,* 1996c and Donnelly *et al*, 1997). It was shown that both arms of the immune response were stimulated in animal models for bacterial, parasitic and viral diseases.

1.3. Purification of traditional vaccines.

"First generation" vaccines are usually the type of vaccine that comes to mind- the type that is given paraenterally (or in some cases such as polio, orally). In the context of this discussion they are referred to as traditional vaccines. Such vaccines originate from a range of organisms: bacteria (pertussis from *Bordetella pertussis*, Madsen, 1933; typhoid from *Salmonella typhi*, Germanier and Fürer, 1975), parasites (as described in an overview by Cryz Jr., 1991) and viruses (polio, Sabin, 1985 and influenza A, Burnet, 1941). Safety and obtaining the appropriate responses (specific, at required therapeutic levels, for defined periods) are the biggest issues surrounding the production of vaccines. Thus the fractionation and elimination of impurities (undesirable components internal to the system such as cell debris and proteins) and contaminants (undesirable substances added to the system such as detergents) away from the target organism is necessary to prevent inappropriate (potentially fatal) responses or to ensure that the true response is not masked. As discussed in the previous section, some "first generation" vaccines have an excellent safety record hence the reluctance by manufacturers to change their production methods.

1.3.1. An introduction to down-stream processing (DSP).

The degree of purification required for therapeutic proteins including protein-based vaccines is very high >99.9998 % since their end-use are as therapeutics (Wheelwright, 1989). Their recovery depends upon bioprocesses that incorporate a range of technological activities including the design of a sequence of purification steps, (leading to the generation of purified target molecules from an initially crude feedstock) to facilitation of the process operation at larger scales. The purification process is called a down-stream process, DSP,

(Wheelwright, 1989). Information regarding mass transfer and reaction kinetics which in turn depend upon the different phase separations required, (solid-liquid, liquid-liquid or gas-liquid), and thermodynamics of the system all contribute to the development and design of a process and the process equipment. Each individual step is known as a unit operation. By rational selection of these operations, one may obtain the optimal process conditions with respect to safety and efficacy and also requirements such as high purity and yield, cost-effective economics or speed to market.

1.3.1.1. Large scale purification of organisms and components comprising traditional vaccines.

Traditional vaccine manufacture has remained relatively consistent with respect to the purification schemes employed. Bacterial and some parasitic traditional vaccines (for example vaccines for diphtheria and malaria) are produced by a combination of fermentation (upstream processing), primary and secondary (downstream) processing. Primary processing involves microfiltration to remove cells (if a toxin is the vaccine, for example, diphtheria) and a detoxification step (chemically or using heat treatment). Secondary processing involves a combination of diafiltration or ultracentrifugation and precipitation (with ammonium sulphate or ethanol). Polishing is often achieved using adsorption chromatography including size exclusion media (Cryz Jr., 1991). This thesis focuses on the manufacture of a traditional viral vaccine (influenza). Viral vaccines are often sourced from viral seed stocks, which are inoculated and propagated into hosts *in vivo* (embryonated fertile hens egg or suckling mice) or *in vitro* using cell cultures, (O'Neil and Balkovic, 1993). These vaccines are often attenuated, that is their virulence is naturally tempered to

the disease whilst still retaining the ability to stimulate an appropriate immune response. Alternatively the vaccines are killed (inactivated) chemically or with the use of heat treatment. They are usually harvested as intact particles thus the type of impurities observed in these preparations are likely to be similar between viral feedstocks (cell membrane fragments, proteins, endotoxins and adventitious agents) and hence their primary purification strategies are likely to be comparable. However further downstream, depending on the vaccine requirements (such as a subunit vaccine) and the physico-chemical properties of the virus particles, the purification strategies are expected to diverge as different characteristics are exploited. Most of the unit operations used in the commercial production of bacterial and parasite vaccines are commonly applied to the purification of components comprising traditional viral vaccines and include: filtration, centrifugation and chromatography (see Figure 1.1). Precipitation is often used in the recovery of viruses on laboratory scale but not so frequently on larger scales because of poor selectivity and the high precipitant concentrations can affect their infectivity in cases where this is required (O'Neil and Balkovic, 1993).

1.3.1.2 Unit operations used in viral vaccine manufacture.

Utilisation of conventional unit operations such as filtration, centrifugation and adsorption chromatography exploit physico-chemical differences between biomolecules. For example filtration separates on the basis of particle size, density centrifugation, on the basis of particle size and density, adsorption chromatography on the basis of size, charge, hydrophobicity or affinity. Microfiltration (a primary processing step) and ultrafiltration (used in secondary processing) are solid-liquid separation techniques that isolate particles

across a membrane according to size (Zydney and Kuriyel, 2000). Microfiltration can be used to fractionate particles with a diameter of 5.0 x 10^2 to 2.0 x 10^4 nm (Schmidt-Kastner and Gölker, 1987). Ultrafiltration handles a smaller particle size range- 5.0 x 10^0 to 2.0 x 10^3 nm (Schmidt-Kastner and Gölker, 1987). The feed flow is pumped parallel (under pressure) to a synthetic polymer membrane with pore sizes that have been pre-selected to permit or to prevent the passage of target molecules. A fraction of the feed is driven through the membrane due to a pressure drop (the transmembrane pressure, TMP). At large scale these processes are operated in cross-flow (tangential flow) mode, whereby flow at a tangent to the feed flow continually "sweeps" the membrane surface to minimise protein and debris binding to the membrane, leading to the phenomena of concentration polarisation (Porter, 1972) and fouling. Membrane performance often depends upon the characteristics and concentration of the feedstock (which allows selection of the most suitable membrane).

Density gradient ultracentrifugation is a processing technique that fractionates molecules on the basis of both density and size differences between solids and liquids. The use of a density gradient makes this a highly resolving fractionation technique (van Holde, 1986). The density gradient is magnified by the application of large centrifugal forces (in the order of 2.5 x 10^4 *xg*) that cause the particles to rotate at high speeds and is suitable for handling particles of diameter 2.0 x 10^1 to 2.0 x 10^3 nm (Schmidt-Kastner and Gölker, 1987). Two types of density gradient ultracentrifugation are often employed. The first is rate zonal ultracentrifugation, which often uses a sucrose density gradient. In this technique, sedimentation transport of molecules occurs through the gradient causing a mixture of molecules to be fractionated according to their density and size (see Equation 1.1). The second is equilibrium density gradient ultracentrifugation, which (commonly) uses caesium

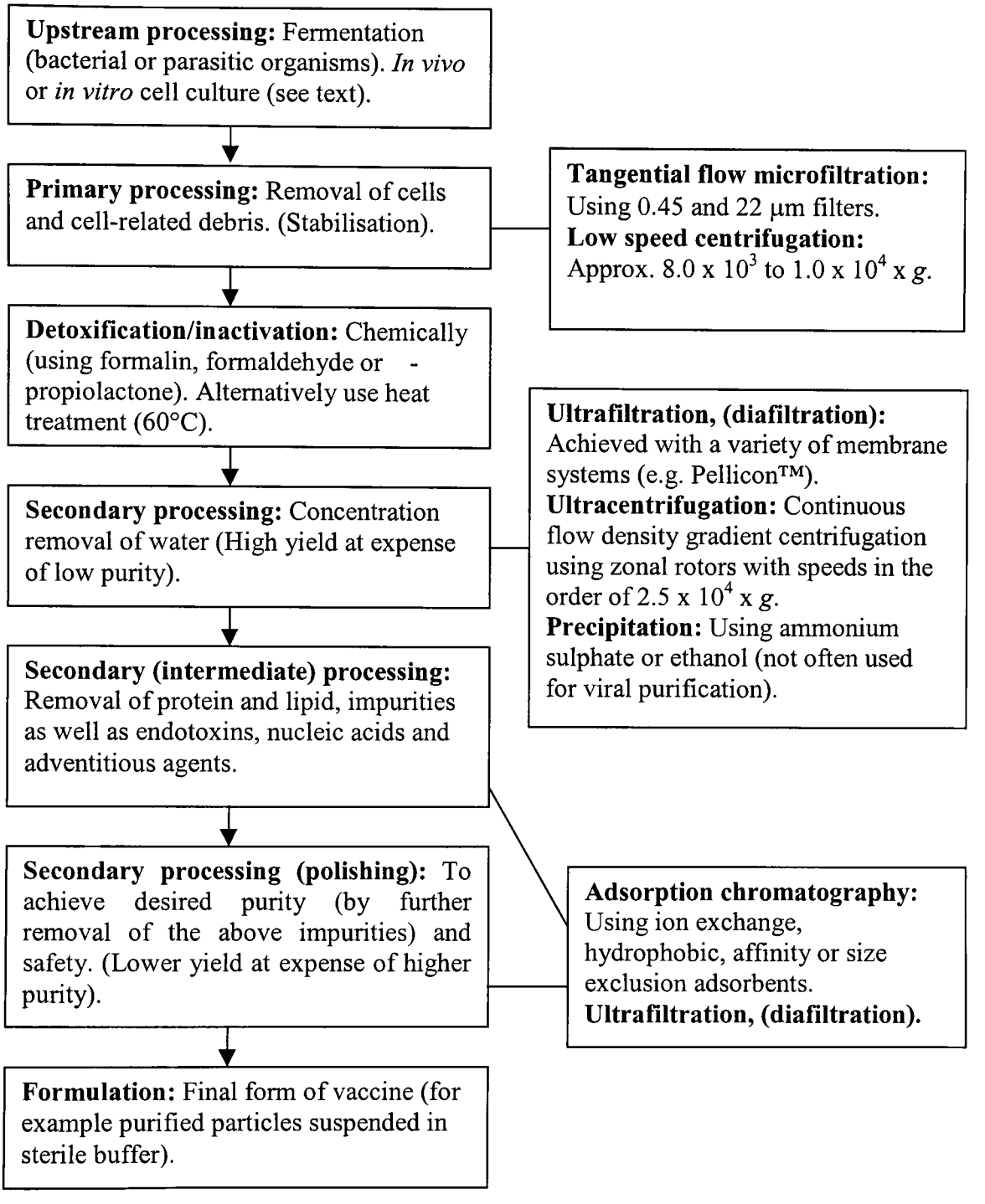

FIGURE 1.1. Flow chart depicting typical stages in a down-stream process scheme commercial scale traditional vaccine manufacture.
A general process outlining the steps in the large scale purification of organisms (to be used as vaccines) using conventional unit operations. These operations are shown on the right hand side. A more specific scheme for processing influenza virus nanoparticles is presented in Chapter Two Sections 2.1.5 and 2.16.

chloride as the gradient former. This type of centrifugation is run until equilibrium is attained and no transport of the molecules occurs. At this point the buoyant density and ultimately the molecular weight of the molecules can be determined (van Holde, 1986). Sucrose gradients are often preferred because they are better at maintaining viral integrity (Faff *et al*, 1993). Zonal rotors are often used in fractionation because both types of centrifugation can be used. Also continuous flow centrifuges are often employed on commercial scales in order to process large feedstock volumes, whereby fresh feedstock is continually pumped across the centripetal surface of the density gradient (Cline and Ryel, 1971).

Sedimentation follows Stokes Law:

$t = 18\eta / d^2 \omega^2 \Delta\rho * L+z_1/L+z_2$ *Equation 1.1.*

t = time taken for single sphere of particle diameter (d) to settle a distance z_1 to z_2 in a radial direction;. η = liquid viscosity; ω = angular velocity; $\Delta\rho$ = difference in density between particle and liquid; L = radius of inner liquid surface.

From this equation it is observed that if the particle diameter, the angular velocity or the density difference (between particle and liquid) are small, then the longer it takes for the particles to sediment (hence the reason for inducing precipitation using flocculants to increase the density difference).

Adsorption chromatography (once optimised) can permit highly selective and specific interactions between molecules and adsorbent based on size, charge, and affinity differences between the target molecules and impurities (Hammond and Scawen, 1989). The most frequently used mode of operation involves binding of the target molecules to the adsorbent (allowing the impurities to pass through), followed by elution of the target molecules by manipulating conditions (such as salt concentration or pH).

Examples in literature detailing the use of these techniques for traditional viral vaccine production at commercial scale are scarce. In addition since many of these commercial processes have been in place for some decades, improved materials (filtration membranes, ultracentrifugation density media and chromatographic adsorbents) were probably not available at the time of establishment of the purification protocols. Thus if the bioprocess scientists had a commercial process that worked, then there was no real impetus to evaluate alternatives (also contributing to the lack of information in the public domain). However there are recent examples in literature whereby viruses have been purified using anion exchange chromatography on a relatively smaller (milligram to decigram) scale (Walin *et al*, 1994). Inactivated HIV-1 particles purified by anion exchange chromatography followed by diafiltration produced enough virus particles for Phase III clinical trial, (Richieri *et al*, 1998). O'Keefe *et al*, (1999) showed that DISC-HSV-1 Type 2 viruses cultured from Vero cells could be isolated in relatively high titre from impurities whilst maintaining their infectivity. The chromatographic matrix used (heparin sulphate) was also proposed for use with other similarly charged enveloped viruses: human cytomegalovirus (CMV) and human immunodeficiency virus (HIV-1). Cation exchange chromatography for the purification of herpesviruses was also reported by (Karger *et al* 1998). However the following discussion

1.3.1.3. Highlighting problems associated with the use of conventional unit operations for commercial scale virus purification.

The unit operations previously discussed depend upon the size, density or surface properties of the target particles. Most viruses have a particle diameter of between 2.0×10^1 to 2.0×10^2 nm thus they can be classed as nanoparticulates. These unit operations are designed for the recovery of proteins (particle diameter of 1.0×10^0 to 1.0×10^1 nm). Microfiltration (operating range 5.0×10^2 to 2.0×10^4 nm) is often used as a gross clarification step (retaining debris and cells, whilst permitting proteins to pass through) ultrafiltration (operating range 5.0×10^0 to 2.0×10^3 nm) is used further downstream (refer to Figure 1.1). These techniques are fine when there is a relatively large difference in size between the proteins and debris or cells. In fact ultrafiltration (and nanofiltration) are often used as process scale methods of removing viruses from feedstocks (Hoffer *et al*, 1995; Graf *et al*, 1999 and Azari *et al*, 2000). However when the target molecule is in the nanoparticulate range, the size difference between the nanoparticles and debris is less thus decreasing the resolution of the technique. In addition during the filtration process, the flux of liquid per unit membrane decreases due to fouling. This contributes significantly to the operational cost. Scale up increases the volumetric capacity but also the cost.

In the case of ultracentrifugation, proteins can be efficiently fractionated from debris and viruses (when these are a contaminant) since there is a large difference in density between the surrounding liquid and the proteins and the debris; in addition there is a large difference in size between the proteins (particle diameters of between 1.0×10^0 to 1.0×10^1 nm) and debris and cells (particle diameters in excess of 1.0×10^2 nm). However when nanoparticulates such as viruses (particle diameters of between 2.0×10^1 to 2.0×10^2 nm)

are fractionated, one observes that the size differences between the molecules and densities differences between the debris and liquid are much smaller, leading to a decrease in resolution. Thus long process times are required in order to fractionate the nanoparticles from the debris, (refer to Equation 1.1 and O'Neil and Balkovic, 1993) rendering this unit operation energy-intensive. Another disadvantage lies in the limited volumetric capacity of the rotors. Even if a continuous flow rotor was used, there is only a finite volume of feedstock that can be processed at any one time. In practice this is circumvented by using multiple rotors (which adds to the cost of the process). The preparation and set up of gradients on large scale is labour-intensive (Braas *et al*, 1996) and gradient forming chemicals such as caesium chloride (CsCl) are relatively expensive and high concentrations can place the virion (of enveloped viruses) under osmotic stress leading to viral disruption that can affect viral infectivity; although this is circumvented to some degree by the introduction of synthetic gradient media (Karger *et al*, 1998). This is not a problem for traditional viral vaccines (that are not required to maintain their infectivity for their end purpose) but it could be a problem with viruses required for other purposes such as gene therapy vectors that require infectivity to gain access to target cells.

Conventional packed bed adsorption chromatography can be specific but requires that the feedstock be clarified prior to loading onto a column (this was the case in all the examples described at the end of Section 1.3.1.2), which adds to the process time and costs. Conventional gel adsorbents contain pores in the 3.0×10^1 to 4.0×10^2 nm range (O'Keefe *et al*, 1999). This is fine for penetration of proteins (1.0×10^0 to 1.0×10^1 nm range) but the pores tend to exclude viruses (in the 1.0×10^2 nm range) leading to diminished capacity (Walin *et al*, 1994) Although a promising report concerning the capacity of heparin-HP

media and HSV-2 virus, documented a capacity in excess of 5.0 x 10^9 pfu ml^{-1} gel (O'Keefe *et al*, 1999). This would just about be adequate for the production of traditional viral vaccines but with future ambitions of meeting the commercial demand for viral gene therapy vectors, this capacity needs to be improved by at least three orders of magnitude, which could be realised with improved matrix design (Braas *et al*, 1996). The scale-up of unit operations using adsorption chromatography can be problematic; the large amount of adsorbent and requirements for rigorous sanitation also add to the process cost. Thus each conventional unit operation suffers from specific problems that prevent their maximal utilisation when applied to the processing of nanoparticles. This provides the stimulus to look at alternative techniques to handle such particles.

1.3.1.4. A commercial example of viral vaccine production using conventional unit operations.

The discussion has so far centred on the commercial manufacture of traditional vaccines with emphasis on those of a viral nature. The theme of this thesis concerns the commercial production of an influenza virus vaccine. Influenza disease is still a potential killer (Reid *et al*, 1999). Medeva Pharma (now Powderject Pharmaceuticals plc) the UK's premier vaccine manufacturing company produces an attenuated, inactivated influenza subunit vaccine. Medeva Pharma identified problems with one of their processes- using influenza particles (approximately 1.0 x 10^2 nm particle diameter). The vaccine is currently produced by stages of sucrose density ultracentrifugation (further details are given in Section 2.1.5 of this thesis), which as previously discussed is an energy-intensive, scale-limited unit operation. Multiple rotors are employed to increase throughput (which again adds to the energy

consumption). This creates a bottleneck (or rate-limiting step), which (i) compromises the throughput (due to the long processing times required), (ii) possibly affects the potency of the vaccine (prolonged residency) and (iii) definitely impacts upon the profitability of the process. This is a prime example of a successful bench-scale process (Brady, PhD Thesis, 1974), which has been directly scaled up without investigation of alternative (and possibly better) purification commercial-scale strategies. Density gradient ultracentrifugation is frequently used in harvesting viruses and thus is employed in the experimental work herein as a benchmark by which to judge the performance of alternative techniques.

The pressure to find and test out alternative techniques is even more urgent in the light that companies continue to use sub-optimised processes consisting of conventional DSP unit operations in order to qualify their products through regulatory bodies. This is governed by a number of reasons: a reluctance to change the existing dogmas; speed to market (particularly if a new product); constraints of costs; accountability to shareholders and the existing wealth of validation data at both small and large scale that perpetuates the use of the conventional techniques in regulatory submissions. In practice the techniques, which meet the required purification criteria first, tend to set the regulatory ground rules and the precedent for subsequent techniques. Therefore the only way that alternative techniques could be considered would be if a company decides that their process (using conventional techniques) was not cost effective. In the interim, field researchers must continue to build up a body of evidence for alternatives in order to convince the companies. Hopefully a "domino effect" would ensue in that other companies begin to adopt alternative techniques and so change existing regulatory frameworks.

1.4. A brief survey of alternative bioseparation technologies useful for processing nanoparticulates.

A selection of alternative techniques is briefly discussed in order to give an insight into exciting developments in the field of bioseparation. All are being currently investigated to handle proteins but it may be possible that some will successfully be used to handle nanoparticles such as the influenza virus.

1.4.1. Fluidised bed adsorption chromatography.

Fluidised bed adsorption chromatography has been used as a purification technique since the 1950's. This technique consisted of the adsorbent being placed in a stirred tank to allow binding of target biomolecules such as the recovery of antibiotics from broths (Bartels *et al*, 1958). These fluidised beds were inefficient (providing a single equilibrium stage) with extensive channelling and turbulence and poor recoveries. It was in the late 1980's and early 1990's that stable fluidised (so-called, expanded) beds were created with similar characteristics (plug flow, low back-mixing) to a packed bed. Not long after that that these beds were being used to recover proteins from particulate feedstocks (Wells and Lyddiatt, 1987) such as whole cell fermentation broths and cell disruptates. This technique was proposed as a means of circumventing some of the solid-liquid separation problems (outlined in Section 1.3.1.3) such as removal of particulate material from proteins (without the requirement for clarification), decreasing the number of unit operations and process integration. This unit operation employs porous adsorbents (like those used in packed bed adsorbent chromatography) but in order to acquire different settling velocities between the feedstock molecules and the adsorbent particles during fluidisation, it was necessary to

integration. This unit operation employs porous adsorbents (like those used in packed bed adsorbent chromatography) but in order to acquire different settling velocities between the feedstock molecules and the adsorbent particles during fluidisation, it was necessary to increase the density of the latter. This was achieved by creating an inert core of increased density, 1.15- 1.3 g ml^{-1}, (Hjorth, 1997; Zhang *et al,* 1999) and then derivatising these with the required ligands. The frequently used STREAMLINE™ range of adsorbents (manufactured by Amersham Pharmacia Biotech., Uppsala, Sweden) employ a crystalline quartz inert core. The feedstock is loaded onto the column in an upward flow which separates the particles allowing passage of the feedstock molecules, permitting the proteins to bind to the chromatography matrix and the particulate material to be washed away. Protein elution occurs in packed bed mode (Hjorth, 1997; Pharmacia Handbook, Edition AA). Much research has been undertaken on the performance of proteins. The current focus is on designing new matrices including novel ligands and engineered proteins to enhance recovery on chromatographic matrices (Asplund *et al*, 2000; Hober, *et al*, 2000), processing strategies such as process integration (Bierau *et al*, 1999) were designed to improve recovery and minimise residence times of labile proteins. In addition the hydrodynamic performances of these matrices was also investigated (Thömmes *et al*, 1995). This technique is thought not to generate shear and has been used for separations involving mammalian cell culture (Batt *et al*, 1995). In addition it has been demonstrated on large scale to showing significant improvement over packed bed with respect to decreased time and process volumes and increased throughput (Johansson *et al*, 1996). However this technique has been primarily demonstrated for protein recovery. Its potential for handling nanoparticles has only so far been undertaken using plasmids (Varley *et al*, 1999; Ferreira *et al*, 2000).

chromatography could be applied to other nanoparticulate feedstocks such as those containing viruses.

1.4.2. Selective precipitation.

Chemicals such as alcohol, PEG 6000 ammonium sulphate have been used as precipitants. (Ingham, 1990 and 1984), which involves the removal of water from the surface of the proteins leading to a decrease in solubility. This technique is not utilised frequently due to poor understanding of the mechanisms involved that make it possible to precipitate selectively. The commercial use of precipitation for the preparation of bacterial and parasitic vaccines was briefly discussed in Section 1.3.1.1. However this method tended to be used when the vaccine component was secreted into the fermentation medium (for example, diphtheria toxin) and the cells removed prior to adding the precipitant. Utilisation of this technique for the purification of nanoparticulates such as viruses would probably affect their infectivity (important for gene therapy vectors) and require time-consuming desalting techniques (Braas *et al*, 1996).

1.4.3. Aqueous two-phase systems (ATPS).

Albertsson (1958) first looked at aqueous two-phase systems (ATPS) as a potential purification technique for partition of proteins in polymer-polymer solutions. This technique is highly versatile being able to selectively fractionate secondary metabolites, proteins, nanoparticles and macromolecules (Albertsson, 1986). Each phase contains in excess of 70% water. Thus ATPS has been used in partitioning biomolecules due to the mild environment provided. The conventional bioseparation techniques discussed in Section

1.3.1.2 were effective within certain particle size ranges. ATPS has demonstrated fractionation procedures over a much wider range of particle sizes, which points to its utility as a versatile purification technique that will be discussed in detail further in the text.

1.4.4. Selection of a potential alternative bioseparation technology to process influenza particles.

Separation using ATPS was initially considered because it could offer a solution to the problems faced in the Medeva Fluvirin™ Process. Ideally, time-consuming (rate-limiting) unit operations could be circumvented with the elimination of process bottlenecks (Hustedt 1985; Huddleston *et al*, 1991b). In addition this process could provide a suitable environment for the influenza particles and is relatively easy to scale up.

1.5. A Description of ATPS.

Aqueous two-phase extraction using aqueous two-phase systems (ATPS) is a liquid-liquid separation technique that was initially used to partition proteins (enzymes), nanoparticles (viruses) and macromolecules- cells and organelles, (Albertsson, 1986). An ATPS consists of a polymer pair (for example polyethylene glycol-PEG and dextran) or a polymer salt pair (for example- PEG and phosphate). When these are mixed in common solvent- water above critical concentrations, their incompatibility leads to the formation of two phases that coexist and are in equilibrium with each other. Each phase is enriched with one of the polymers (or salts). For example in a polymer-salt ATPS, the top phase is enriched in polymer and the bottom in salt.

1.5.1. Mechanism of phase separation in ATPS.

Explanations regarding the mechanism of phase separation in polymer-polymer ATPS have been attempted using thermodynamics. As the polymers mix, the enthalpy of mixing is great; there is a concomitant decrease in entropy to compensate as the polymers separate to their respective phases. This forms the basis of several models reviewed by (Abbott *et al*, 1990). There are many combinations of polymer-polymer or polymer salt systems that can form ATPS (for example polyvinyl alcohol-Dextran; methylcellulose-PEG). The most studied use polyethylene glycol (PEG) and Dextran and PEG-phosphate (or sulphate). Polyethylene glycol is a homopolymer consisting of repeating ethylene units linked by an ether bond. It possesses some unique features that are responsible for its solubility such as the ability to efficiently order a hydration layer because some molecules with similar structures exist that are less soluble (Huddleston *et al*, 1991b). Dextran is derived from *Leuconostoc mesenteroides*. Dextran possibly orders a layer of water leading to H-bonding between water and hydroxyl groups on the polymer. It is thought that water surrounding these polymers are orientated differently and therefore when mixed (above critical concentrations) repel each other leading to phase separation. Phase separation in PEG-salt (for example phosphate) ATPS is thought to be brought about by a balance between enthalpic and entropic interactions (Huddleston *et al*, 1991b). Phase separation in a PEG-salt ATPS depends on the type of salt used. The ions form a lyotropic series based on ability to salt out (Ananthapadmanabhan and Goddard, 1987). In this series, the anion is more important than the cation in phase separation and multivalent ions more important than monovalent ions. This is because the larger, more-charged ions cannot interact with PEG and are thus repelled leading to phase separation. If the interactions were closer (such as

between PEG of longer chain length) this would occur more readily. Thus an ATPS comprising PEG of high molecular weight and potassium (K^+) and phosphate (HPO_4^{2-}) ions would be very effective at phase separation.

1.5.2. Factors affecting phase separation in ATPS.

When a two-phase system is mixed, droplets from one of the phase formants coalesce and as the ordered water molecules surrounding the phase formant are disrupted, there are interactions with the other phase formant. Mass transfer of the molecules occurs across the interface. As the water molecules regain order, the interactions between phase formants becomes unfavourable and phase separation occurs. The rate of droplets coalescing depends on the interfacial tension (Bamberger *et al*, 1984), which provides the driving force for adsorption of particles at the interface. Adsorption of particles at the interface can lead to their denaturation (presumably due to changes in conformation as a result of osmotic effects and high shear forces). The relatively low interfacial tension in ATPS provides the reason why aqueous-aqueous systems are preferred for processing biological molecules instead of aqueous-organic systems. The former exhibit interfacial tensions in the order of 0.1-2 mN^{-1} for PEG-salt ATPS and 0.0001-0.1 mN^{-1} for PEG-dextran ATPS, whilst the latter possess interfacial tensions of at least an order of magnitude greater (Hustedt *et al*, 1985). Lowering of the interfacial tension is thermodynamically favourable since energy is used to decrease the interfacial area and thus decrease the number of particles adsorbing at the interface (Sadana, 1993). This is important in context of the work presented in this thesis since it has been observed and reported that systems loaded with nanoparticles partition to the interface (Braas, PhD Thesis, 2000). Thus it is probable that the influenza virus particles will exhibit

similar partition behaviour. In addition, such a strategy of lowering the interfacial tension has been employed in the experimental work documented in this thesis. In this case, the target particles require harvesting from the interphase. This is not conventional since this phase is often overlooked. However this presents the advantage of harvesting a de-watered, relatively concentrated product (which can reduce process costs of removing excess water further downstream) and also the challenges of how to harvest such a phase at process scale and how to characterise ATPS consisting of both solid and liquid phases. The interfacial tension is also affected by temperature (increased temperature decreases the interfacial tension), differences in polymer concentration and salt concentration (increases in these variables increases the interfacial tension). Physico-chemical properties of the phases such as density and viscosity of the phases affect phase separation. The densities of the phase formants determine which predominantly occupies the top and bottom phases. The viscosity of the phases determines the scale up feasibility of a separation. Denser more viscous phases are slower to phase separate than less dense and less viscous phases, which could have an impact upon the stability of labile proteins or particles. Temperature affects both of these parameters therefore affects the phase separation. The type of phase formant and their relative concentration in the ATPS determines the type and strength of interaction during mixing.

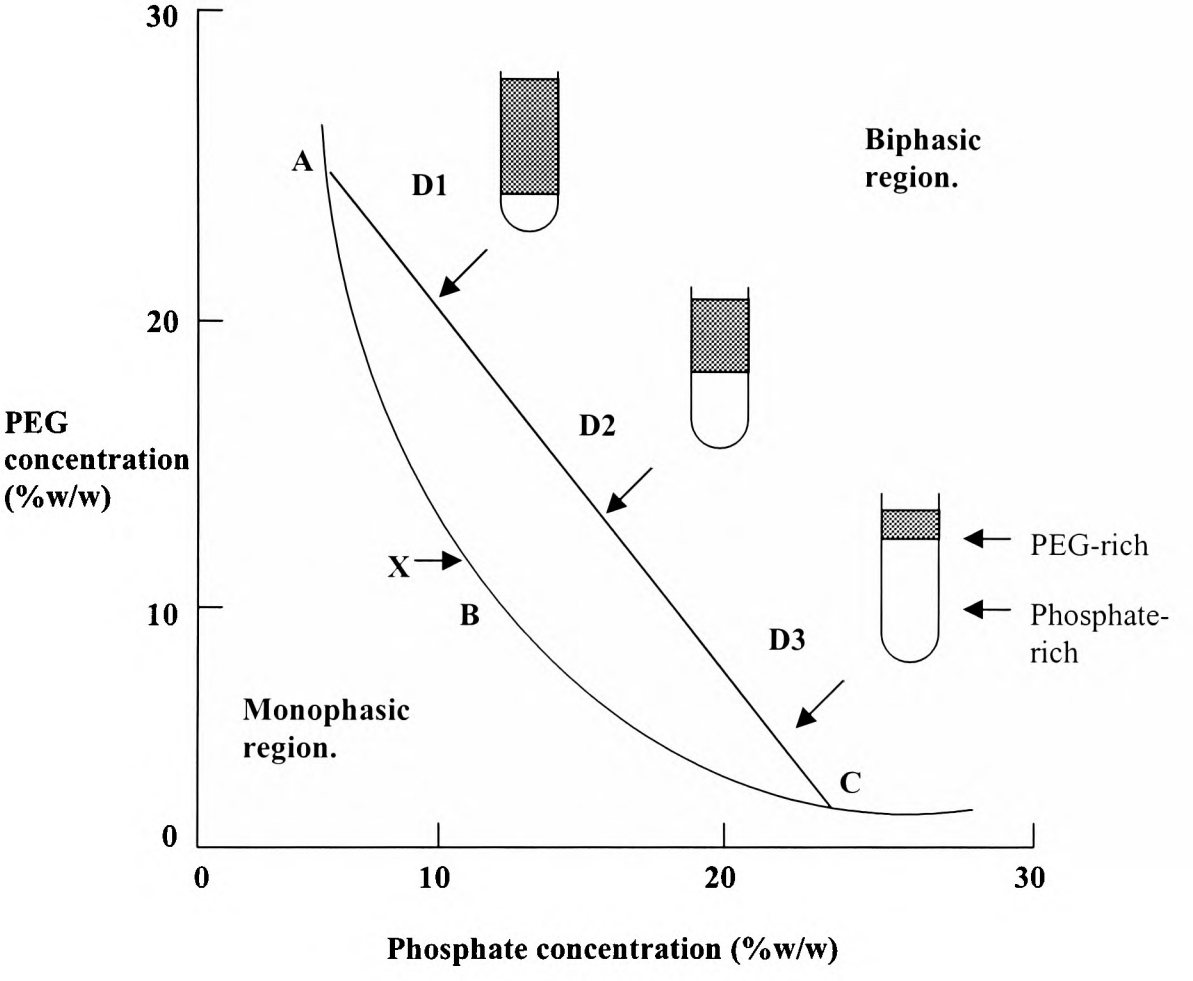

FIGURE 1.2. A schematic illustration of a binodal curve showing a PEG-phosphate aqueous two-phase system.

All systems above the curve are biphasic and those below are monophasic. The line AC denotes a tie line. All systems on this tie line will have the same tie line length (TLL). Thus the tie line provides a positional co-ordinate on the binodal. These systems have different overall compositions but the same final phase compositions thus the top phases are all of equal composition and the bottom phases are all of equal composition. Thus the only difference is in the ratio of the volumes. This parameter provides a locational coordinate on the binodal curve. The point X marks the critical point, which is the point where the phase transition from monophasic to biphasic just occurs. Theoretically it is the point where the volume ratio is equal to unity and the TLL is equal to zero. The shaded areas on the test tubes represent PEG-rich phases and the clear areas represent phosphate-rich phases.

1.5.3. Characterisation of ATPS.

Aqueous two-phase systems (ATPS) are characterised by a phase diagram or binodal (Figure 1.2). The phase diagram is ternary in nature but simplified in the binodal by showing only two axes (the remaining solute is water by inference). On the binodal depicted in Figure 1.2, systems with compositions above the binodal are biphasic and those below monophasic. Systems on the binodal curve with different overall composition but same final phase composition can be connected by a tie line. The length of a tie line is referred to as the tie-line length (TLL) and is one of the characteristics used to describe an ATPS. The TLL can be easily estimated from a Pythagorean procedure using Equation 1.2 (Huddleston *et al*, 1991b);

$$TLL = (\Delta C_{top}^{2} + \Delta C_{bottom}^{2})^{1/2} \qquad \textit{Equation 1.2.}$$

Where ΔC_{top} and ΔC_{bottom} are differences in concentration (determined from the binodal) of the top and bottom phases respectively. Any selected co-ordinates along the tie-line gives a volume ratio (Vr), Equation 1.3.

$$Vr = V_{top} / V_{bottom} \qquad \textit{Equation 1.3.}$$

This can be estimated from the binodal as the ratio of tie-line segments bisected by the overall system composition (for example in the case of system D2, Equation 1.4).

$$V_{top} / V_{bottom} = CD2/AD2 \qquad \textit{Equation 1.4.}$$

The volume ratio is an approximation assuming that the density (ρ) of each phase is unity. Therefore a more accurate estimation is to use the mass ratio, Equation 1.5.

$$Mr = V_{top} * \rho_{top} / V_{bottom} * \rho_{top} \qquad \textit{Equation 1.5.}$$

Thus the TLL gives *positional* co-ordinates and volume ratio gives *locational* co-ordinates. The binodal also possesses a unique point (X) in Figure 1.2 This is known as the critical point; theoretically it is the point where the TLL is zero and the volume ratio is equal to unity. At this region, ideal partition is obeyed. This gives rise to systems that are highly sensitive to changes such as those of composition, temperature, and pH. These systems will be referred to herein as "sensitive" systems, while those systems distant from the critical point will be referred to as "robust" since they are robust with respect to such changes. However there is evidence to suggest that even robust systems can behave in a sensitive manner, using plasmids (personal communication, F. Luechau, 2001).

1.5.4. Factors controlling molecular partition.

Partitioned material distributes unequally between the two phases and can be estimated from the partition coefficient (K) a useful parameter as shown in Equation 1.6 (Hariri *et al*, 1989).

$$K = C_t/C_b \qquad \textit{Equation 1.6.}$$

Where C_t is the concentration of target solute in the top phase and C_b is the concentration of target solute in the bottom phase. K is a function of many parameters: $K = K_{electrostatic} + K_{hydrophobic} + K_{conformation} + K_{size} + K_{affinity} + K_{temp} + K_{other}$ (Albertsson, 1986). In addition $K_{electrostatic}$ is influenced by system pH and the addition of neutral salts; $K_{hydrophobic}$ influenced by type and molecular weight of the phase-forming chemicals such as PEG; the concentration difference between the phases; $K_{conformation}$ and K_{size} are influenced by the shape and surface area of the particles. These factors can be manipulated to direct impurities away from the target particle(s) or to control partition characteristics. For example BSA in PEG 1000-salt ATPS partitions to the top phase (at high TLL) whilst in a PEG 3350-salt ATPS this protein partitions to the bottom phase, (Huddleston *et al*, 1991a). The determination of K is so important because of its thermodynamic origins and the fact that it can be used to assess the performance of a bioseparation procedure. The ATPS have been described so far with respect to containing only the phase forming chemicals (and a low concentration- < 0.1 % of protein, which has little effect on the binodal, Baskir *et al*, 1988); these systems will be defined as "blank" systems; when the protein concentration is higher than this, and/or contains biomass, they will be defined as "loaded" systems.

1.5.5. Loaded ATPS.

In practical working systems (that is, loaded ATPS), the binodal curve is shifted towards lower concentrations of phase formants (Figure 1.3), suggesting that the biomass contributes to the overall composition of the system. Different feedstocks impact upon the binodal in

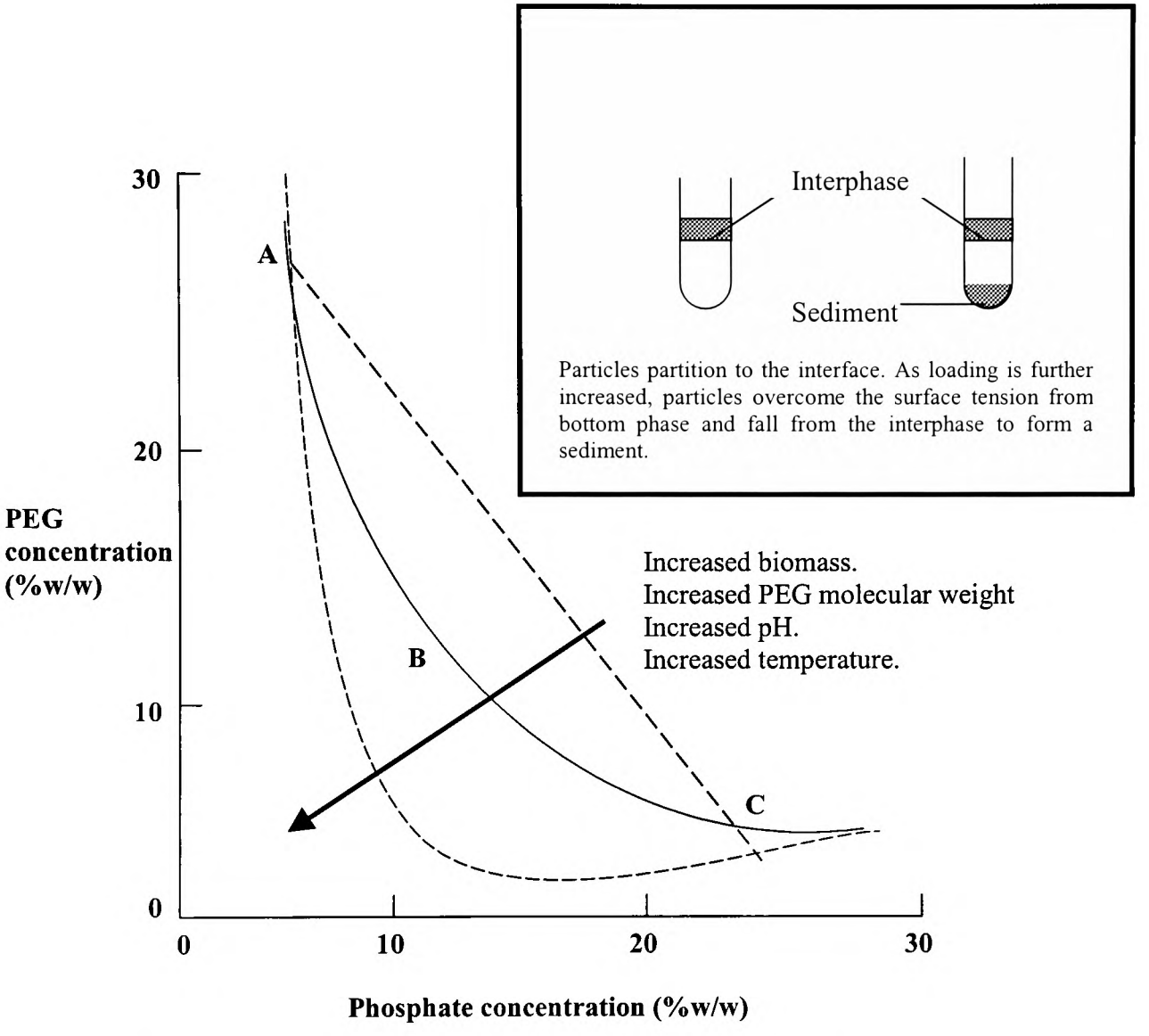

FIGURE 1.3. Schematic binodal curve showing the effect of biomass.
The presence of biomass (forming a loaded ATPS) has shifted the binodal towards the origin (towards lower concentrations of phase-forming chemicals). The dashed line curve indicates the new position of the binodal curve. The solid line curve indicates the original position of the binodal (that is with a blank ATPS). Note that the shift depicted is stylised since different feedstocks impact on the binodal in different ways (and also depends on the loading). Also note that the tie line length (TLL) has increased. These effects are observed when pH or temperature is increased. The bold arrow indicates the general direction of the shift of the binodal. There is often multiple phase formation in the presence of biomass. The shaded areas of the two tubes in the insert represent the types of multiple phases observed; refer to main text for details.

different ways and this is manifested in the presence of multiple phases (see insert of Figure 1.3). Some researchers disregard the solid phases accepting that some loss of product is inevitable (Boland, 1991); others treat them as belonging to one of the bulk phases (Rito-Palomares and Cueto, 2000; Lebreton, PhD Thesis, 1998) or some assume that it belongs equally to either phase, (as discussed by Walker, PhD Thesis, 1998). In this thesis, multiple phases (including interphases and sediments) are treated as discrete phases wherever possible and the description proposed by (Walker, PhD Thesis, 1998) was used to interpret the results (refer to Section 2.18). Kim, (PhD Thesis, 1986) first modelled the formation of interphases in PEG-salt ATPS. These effects (which are used to explain partitioning phenomena in these systems) involve a combination of salting out (Melander and Horváth, 1977) from the bottom phase and excluded volume from the PEG-rich phase. The latter effect is simply envisaged as increased entanglement of PEG chains as their length (or average molecular weight increases) that leads to an exclusion of molecules from their surfaces. Ideally one wishes the target molecules to partition to one of the bulk phases. The bottom phase is preferred because in a PEG-salt ATPS, salt can be more easily removed than PEG allowing for interfacing with other unit operations such as hydrophobic interaction chromatography (Huddleston *et al*, 1996) or ultrafiltration (Guan *et al*, 1992). There are many examples whereby a protein favouring the top phase has been deliberately back-extracted to achieve this (Boland, 1991; Rito-Palomares, PhD Thesis, 1995; 1996a). In addition this permits PEG recycling to save on process costs (Rito-Palomares, 1996a). However in a recent publication Walker and Lyddiatt, (1999) suggest the potential for recovering target particles as a sediment.

1.5.6. The diversity of purification problems handled by ATPS.

It is exciting to note that ATPS is playing a role in the harvesting of commercially relevant enzymes that affect many areas of our lives: medical, chemical, textiles and paper production, (refer to Figure 1.4). A strategy that has been employed in using ATPS on large scale has been to look at current industrial processes with problems, identify them, and attempt to propose where ATPS may be used to overcome these problems. Since the exploitation of ATPS as a separation technique began (Albertsson, 1958), it has been mainly used in the isolation of intracellular enzymes from debris (Kroner *et al*, 1978; Veide *et al* 1983.) Although the potential of ATPS for fractionating particles such as blood cells, chloroplasts and viruses has been demonstrated (Albertsson, 1986). This technique has demonstrated versatility in isolating proteins from different sources: bacteria, yeasts, plants (Hustedt *et al*, 1978; Kulkarni *et al*, 1999; Guan *et al*, 1992; Flanagan *et al* 1991; Huddleston *et al*, 1991a; Cole, 1993; Miranda and Cascone, 1997) and also with biomolecules of different size ranges from secondary metabolites (antibiotics; Paquet *et al*, 1994 and organic acids; Planas *et al*, 1997), through to proteins and finally to nanoparticles larger organelles. The many diverse areas of current research in this field are outlined in Figure 1.4. Successful commercial processes (incidentally originating from the US) offer significant advantages such as high partition coefficient (K) values, the ability to interface with other unit operations or procedures (for example, Genencor, patented a process for the production of chymosin from a fermentation broth with K in excess of 80. The high K occurs at low pH (2.0- 2.5). The ATPS is interfaced further downstream with ion exchange chromatography to remove the PEG. Also Genentech, San Francisco, CA,

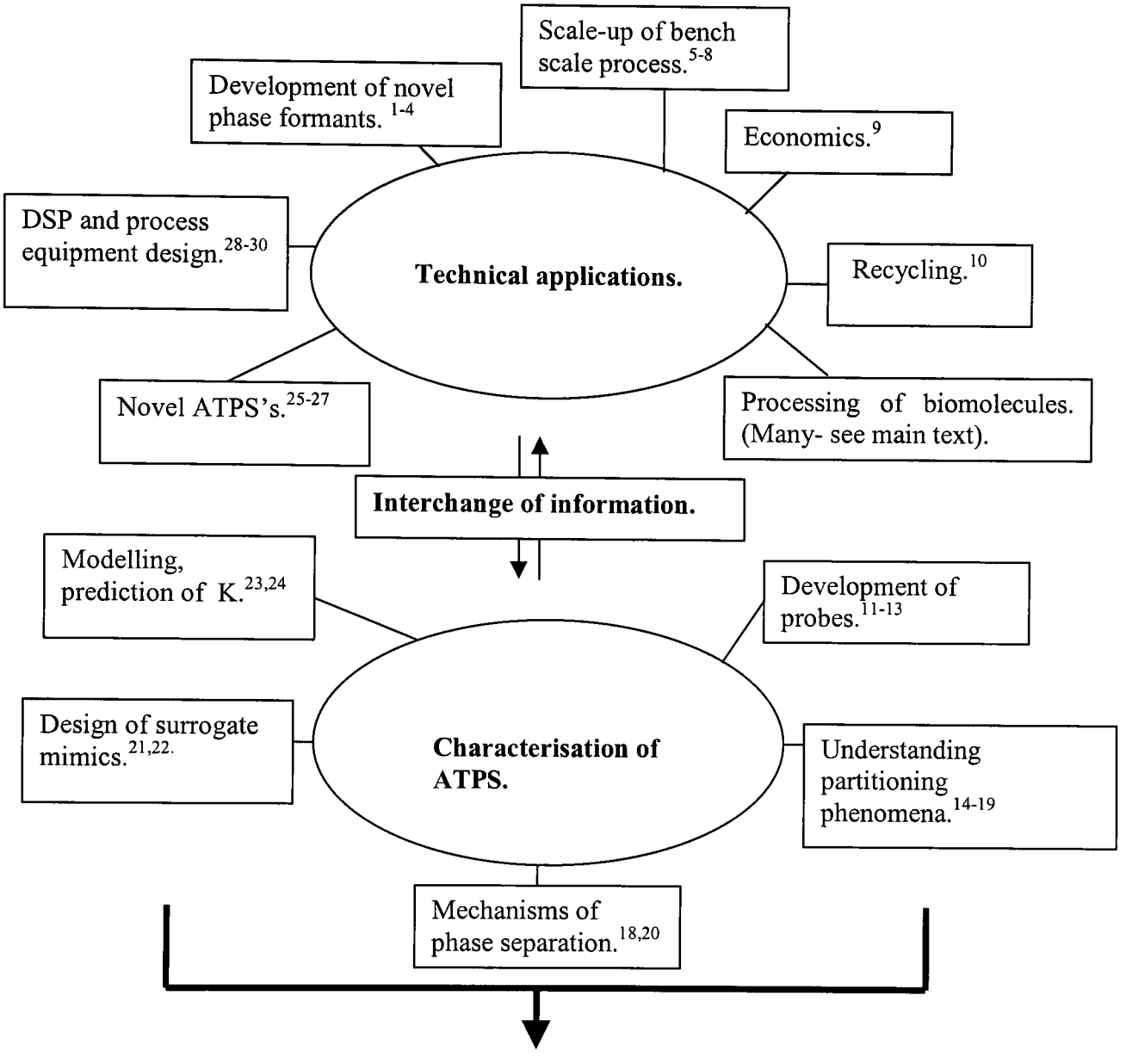

FIGURE 1.4. A summary of the current research areas in the field of ATPS. On the basis of the data obtained from the two major areas, a case could be presented for the consideration of ATPS as a serious candidate for the large scale processing of nanoparticles (including viruses).

Persson et al, 2000;1999[1-2]; Skuse et al, 1992[3]; Hughes and Lowe, 1988[4]; Veide et al, 1984[5]; Kroner and Kula, 1982[6]; Hustedt et al, 1978[7]; Kroner et al, 1978[8]; Kroner et al, 1984[9]; Rito-Palomares,1996a[10]; Lebreton and Lyddiatt 2000[11];1998[12-13];Huddleston et al, 1991[a, b 14-15]; Forciniti and Hall, 1992[16];Eitman and Gainer, 1990[17];Abbott et al, 1990[18];Albertsson, 1986[19];Cabezas et al, 1990[20];Braas et al, 2000[21];Walker and Lyddiatt, 1998[22]; Sebastião et al, 1997[23]; Zhou et al, 1997[24]; Sivars and Tjerneld, 2000[25]; Terstappen et al, 1993[26]; Johansson 1985[27];Su and Feng, 1999[28];Huddleston, 1996[29]; Joshi et al, 1990[30]

USA obtained human insulin-like growth factor I inclusion bodies using PEG 8000-salt ATPS. They were able to use process conditions to directly resolubilise the protein and to simultaneously remove cells from the fermentation broth (Hart *et al*, 1994). Examples of ATPS used in the processing of nanoparticulates include: surrogate mimics (Braas and Lyddiatt, 2000), vaccines on small scale, (Hammar *et al*, 1990; 1989a and 1989b); small inclusion bodies of alpha glucosidase (Walker and Lyddiatt, 1998; 1999), and surrogate mimics (Braas and Lyddiatt, 2000); virus-like particles (Andrews, 1995); and prion protein aggregates (transmissible spongiform encephalopathy) required in large amount for research and diagnostic assays, (Walker *et al*, 1996).

1.6. Aims of investigation.

The aim (and emphasis) of this thesis was to investigate the laboratory scale fractionation of influenza virus nanoparticles that form the basis of a commercial subunit vaccine (Fluvirin™) using ATPS. The decision to use PEG-salt ATPS was made on the basis of favourable process economics (salt being relatively inexpensive compared to Dextran; the ability to work at a wider range of volume ratios for similar cost); faster de-mixing kinetics due to lower phase viscosities (Sikdar, 1991) and also due to literature reporting the potential of these systems in the handling of nanoparticulates (Walker and Lyddiatt, 1998; 1999). The next objective was to design a downstream process whose end product was similar to that produced by the Medeva Fluvirin™ Process. Once it was demonstrated that ATPS was useful in the processing of the influenza virus, the next goal was to evaluate its performance (with respect to purity and yield) against a benchmark method: sucrose density ultracentrifugation (and more importantly in this case, the method currently employed by

Medeva Pharma). A critical analysis of these techniques would enable one to weigh up their relative advantages and disadvantages and also help decide where in the DSP scheme, ATPS could be employed. This would provide conclusions regarding the technique that was most suitable for handling influenza virus particles. Successful meeting of all or most of these objectives would further demonstrate the processing of nanoparticles by ATPS and also permit the description of systems containing real feedstocks and multiple phase formation which could point to generic partition mechanisms thus aiding process design.

1.7. Structure of thesis.

The requirement for a bioseparation process that can selectively fractionate the target molecules away from impurities is the central theme of this project. In this context the target molecules were influenza virus nanoparticles and the impurities consisted of (for the most part) proteins and cell membrane debris. This feedstock originated from a commercial process (Medeva Fluvirin™ Process), which suffered from various bottlenecks. It was proposed to use ATPS as a candidate bioseparation technique that could overcome these bottlenecks (for reasons discussed previously). Initially, potential ATPS were evaluated using purified influenza viral particles (refer to Appendix I). This allowed characterisation (using Medeva-sourced assays) of the virus particles with respect to their surface antigens (haemagglutinin and neuraminidase) and also permitted tracking of virus partition within the ATPS. The PEG molecular weight, tie-line length (TLL) and volume ratio were manipulated. The purified virus particles spiked with a major protein contaminant (ovalbumin) was also investigated to allow selection of ATPS capable of fractionating the virus particles away from the ovalbumin. Chapter Two describes the method scouting

experiments undertaken to define potentially useful systems for the partitioning of the conditioned crude feedstock from the Medeva Fluvirin™ Process, inactivated bulk fluid (IBF). This material contained the influenza virus particles in allantoic fluid (derived from fertile hen's eggs). The IBF feedstock was characterised with respect to the viral proteins and the protein impurities using an in-house method developed using SDS PAGE and one-dimensional densitometry. In addition to manipulation of the PEG molecular weight and TLL, the volume ratios of selected ATPS were varied and from this the most promising ATPS was taken forward for further process development. Chapter Three describes the employment of the candidate ATPS (defined in the previous chapter) in a DSP scheme. The use of detergent in ATPS was evaluated and then employed to solubilise the surface antigens. This was followed by further purification using tangential flow ultrafiltration. The material generated by ATPS at the end the DSP scheme was compared with material generated at the end of the Medeva Fluvirin™ Process (using sucrose density ultracentrifugation). The comparison was made on the basis of purity, yield and time to produce an equivalent batch. Preliminary conclusions and discussions regarding experimental work undertaken were presented at the end of each chapter and final conclusions were given in Chapter Four. Further work and was discussed along with how it contributes to work undertaken by other field researchers. Finally, future directions and trends were indicated for the processing of other nanoparticles using ATPS.

CHAPTER TWO.

2. SCREENING FOR SUITABLE AQUEOUS TWO PHASE SYSTEMS FOR PARTITIONING A CRUDE FEEDSTOCK CONTAINING INFLUENZA VIRUS PARTICLES.

2.1. INTRODUCTION.

2.1.1. Aims of Chapter Two.

The technique of ATPS is suited to fractionation of nanoparticles (Walker and Lyddiatt, 1998; 1999). Influenza virus is considered a nanoparticle and will be described in the following section. This chapter focuses on the utilisation of ATPS in the screening for suitable ATPSs capable of fractionating influenza virus particles in a crude feedstock originating from the commercial Medeva Fluvirin™ Process. Structural information regarding the components of this feedstock is given along with details of the current Medeva Fluvirin™ Process.

2.1.2. The structure of Influenza virus.

Influenza virus is an enveloped, RNA orthomxyovirus approximately 80 to 120 nm in diameter (Kilbourne, 1975) that is of extreme biological importance from an epidemiological viewpoint in humans and other species. The advent of electron microscopy, negative staining techniques and other biochemical techniques have contributed in providing detailed description of this virus (Choppin *et al*, 1961 and Hoyle *et al*, 1961). Influenza is a heterogeneous virus and is composed of 70 to 75 % protein, 20 to 24 % lipid, 5 to 8 % carbohydrate and 0.8 to 1.1 % RNA. It has a molecular mass of between 270 x 10^3 to 290 x 10^3 kDa as determined by electron microscopy and sedimentation analysis, (Kilbourne, 1975). Key characteristics of the virus are illustrated

in Figure 2.1. Influenza virus consists of strains of type A, B and C. Only A and B strains cause significant human disease (Murray *et al*, 1994). Influenza virions possess two important antigenic proteins: haemagglutinin (HA) and neuraminidase (NA). Haemagglutinin is a 224 kDa "triangular-shaped" (when viewed end-on), homotrimer, which is approximately 14 nm long and 4 nm across (Laver and Valentine, 1969; Kilbourne, 1975). HA is composed of monomers of approximately 80 kDa (Kilbourne, 1975), which are held together by disulphide bonds to form the homotrimer. Cleavage (enzymatic or reductive) of the monomers generates two polypeptides of approximately 50 kDa, (HA_1) and 25 kDa (HA_2). These are referred to as heavy and light chain polypeptides respectively. They are both glycosylated, but the majority of the oligosaccharides are attached to the HA_1 sub unit. This sub unit carries the molecular domains exposed to the environment and thus carries the majority of antigenic sites (suggesting that these oligoscaacharides are at least partly implicated in antigenic recognition). The HA_2 subunit possesses some antigenic sites, but is primarily responsible for the hydrophobic properties which include anchorage of the HA to the lipid bilayer (see Figure 2.2). When viewed end-on, the NA molecule is observed as a "mushroom-shaped" tetramer (see Figure 2.2), which has a molecular mass of 240 kDa (Laver and Valentine, 1969; Varghese *et al*, 1983). In most strains, each subunit is approximately 60 kDa in size. The antigenic and enzymatic activities of NA are located in separate domains of the NA (Ada *et al,* 1963; Kobasa *et al*, 1997). The major structural protein of the viral envelope is the matrix (M) protein, subdivided into M1 and M2 proteins. Other proteins present in an influenza virion are nucleoprotein- NP (associated with RNA in the nucleus), the polymerase, P proteins that are also located in the nucleus and are associated with the nucleocapsid (possibly involved in RNA

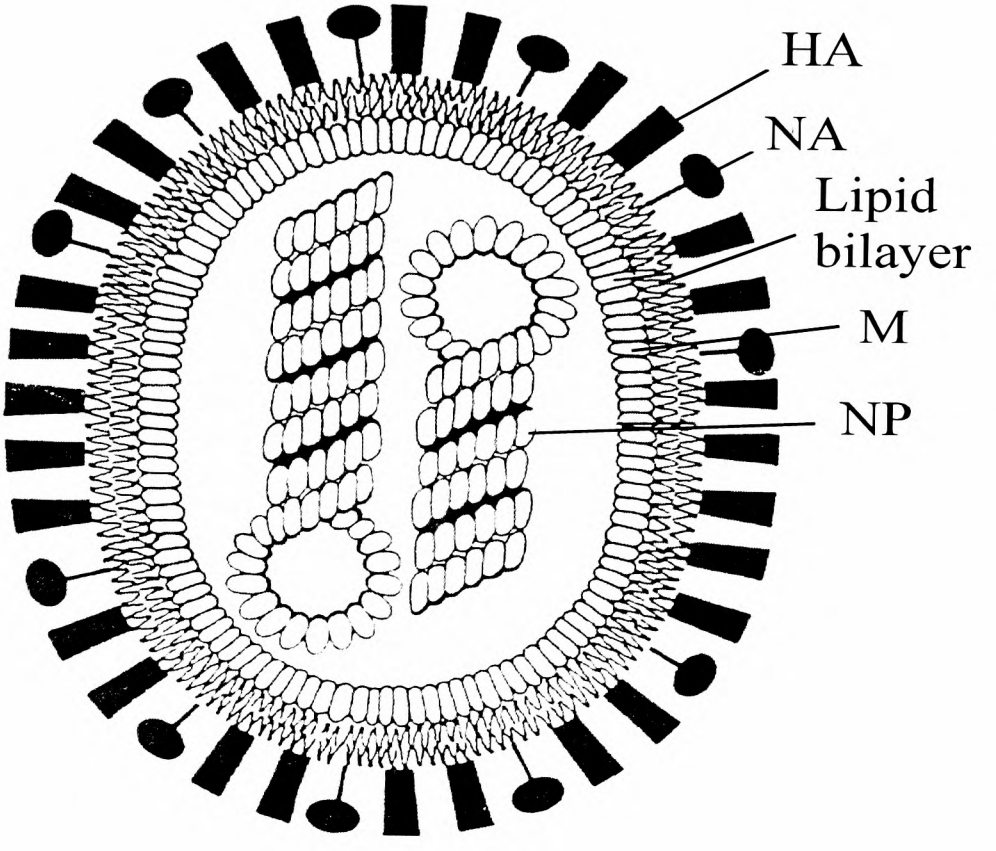

FIGURE 2.1. Model of the influenza virus.
Haemagglutinin (HA) spikes consist of trimers of HA polypeptides. The HA_1 sub unit represents the more exposed part of the spike and the HA_2 sub unit represents the region embedded into the lipid bilayer. The neuraminidase (NA) spikes consist of tetramers of NA polypeptides. Non-glycosylated matrix, (M) protein lines the inner surface of the lipid bilayer. Within the envelope, are the nucleocapsids that contain single-stranded RNA. The protein sub unit of the nucleocapsid is the nucleoprotein, (NP) polypeptide. (Reproduced from Compans and Choppin, 1968).

transcriptase activity of the virion) and the non-structural (NS) proteins. The occurrence of these proteins are summarised in Table 2.1. An unusual feature of the virus is its segmented genome. There are eight strands of RNA (seven in C strains) and it is this arrangement that is implicated in the virus's ability to create antigenic variability so successfully (Kilbourne, 1975).

2.1.2.1. Functions of antigenic influenza virus components.

The HA and NA are implicated in influenza disease therefore any influenza virus vaccine, would include these components. The HA attaches to sialic acid on cell membrane receptors thus promoting fusion and subsequent infection (Murray *et al*, 1994). It is the causative agent in antigenic drift and shift (which involves a continual generation of new influenza viral A strains, Laver and Webster, 1968). The NA (also known as sialidase or receptor-destroying enzyme) is an acyl neuraminyl hydrolase, EC 3.2.1.18. It is attached to the viral membrane via the N terminus (see Figure 2.2); it binds to α-ketosidic linkages in NANA (N-acetyl neuraminic acid) and cleaves this sialic acid post infection, thereby preventing self-aggregation of the progeny resulting in virus release. In so doing, the host cell receptor is destroyed (Webster and Laver, 1967).

Protein identity.	**Molecular Weight (kDa).**	**Abundance (%).**
Haemagglutinin (HA)	75 to 80	Approx. 30
Neuraminidase (NA)	55 to 70	Up to 5
Matrix Protein (M)	21 to 27	Up to 35
Nucleoprotein (NP)	55 to 65	Up to 25
Polymerase proteins (P)	81 to 94	Up to 3
Non-structural protein (NS).	Not given.	Up to 3

TABLE 2.1. The main proteins of the Influenza virion.
The Table gives ranges of molecular weights and abundance relative to the total protein of a typical virion. These ranges indicate the variation between strains. (Taken from Kilbourne, 1987).

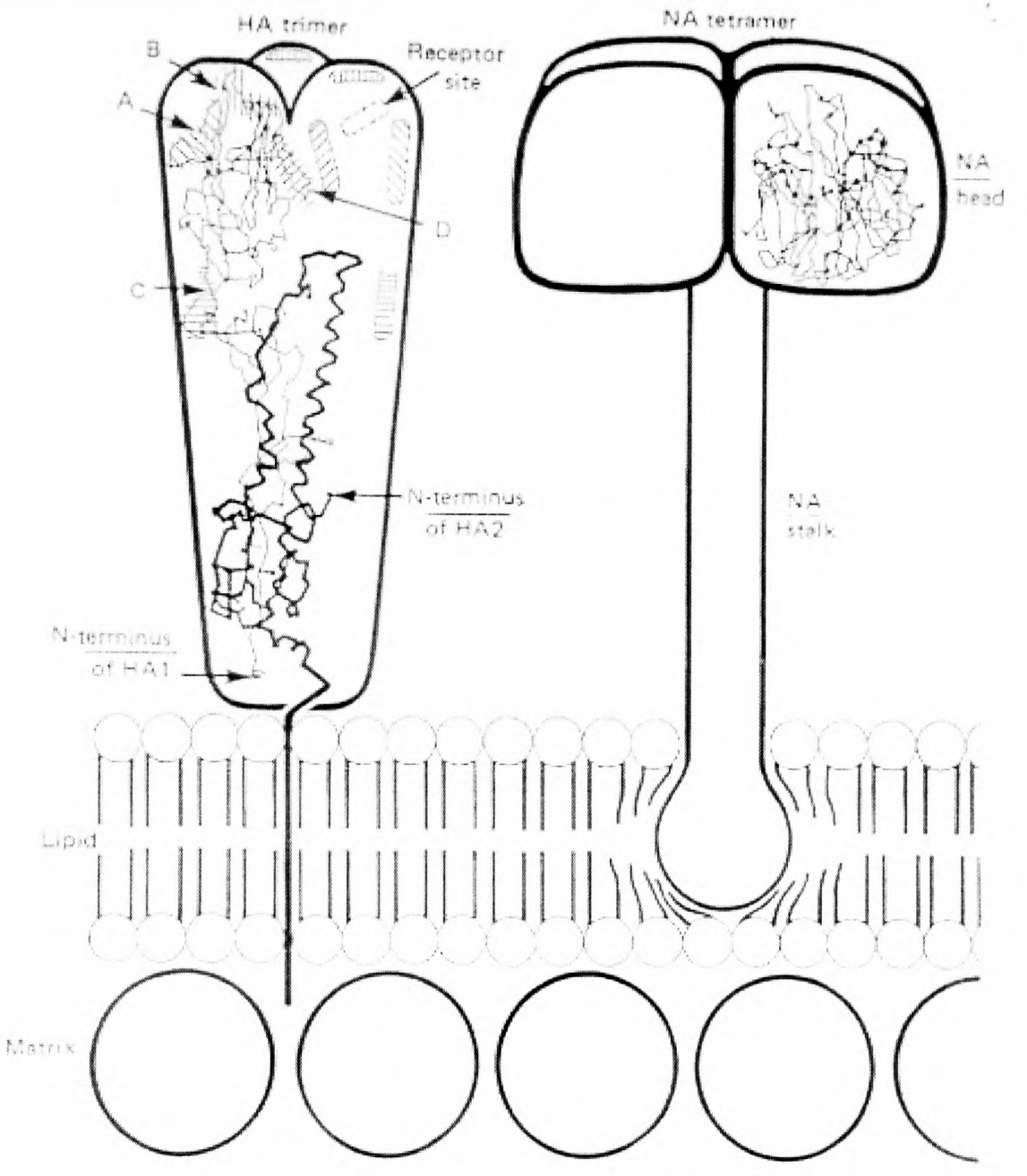

FIGURE 2.2. Diagrammatic representation of influenza virus HA and NA structure.

The HA trimer and NA tetramer are inserted into the viral lipid membrane. A carbon chain representation of the polypeptide (from x-ray crystallography studies by Wilson et al, 1981; Colman et al, 1983) is shown for a single HA and NA subunit. The HA_2 polypeptide is designated in thicker line whilst HA_1 is shown in thinner line. The host cell receptor-binding site is indicated along with four antigenic sites (A-D). The N terminus of HA_2 has fusion activity whilst the C terminus penetrates through the lipid layer to contact the M monolayer. The epitopes on NA are more widely distributed around the enzyme active site.

(Reproduced from Kilbourne, 1987).

Neuraminidase, like HA is also characterised by antigenic changes associated with evolutionary drift and shifts (Kilbourne, 1975). Research has shown that the ratio of HA: NA is 5:1 and whilst HA is uniformly distributed over the viral surface, NA has been found in localised patches, (Lamb, 1983). This distribution was confirmed by immunoelectron microscopy using indirect immunogold staining. It was thought that this distribution prevented premature cleavage by NA (thus preventing infection) and prohibited blockage by NA of the fusion peptide (Murti and Webster, 1986).

2.1.3. Influenza strain designation.

The World Health Organisation (WHO), established in 1971, the current naming system for the antigenic subtypes of HA and NA produced by the virus. The subtypes are named by type: A, B or C followed by the place of original isolation (for example, Sydney), the date of original isolation (month/year) and finally the antigen subtype: HA followed by NA. The B strain is named in the same way but without mention of H or N antigens. The strains are chosen approximately 9 months prior to commencement of the influenza season (to allow time for subtle antigenic variations to be detected).

2.1.4. Current manufacture of Fluvirin™ vaccine (upstream processing).

Although influenza disease can be treated with drugs (such as rimantidine and oseltamivir), they are not always effective against certain viral strains. As a result, vaccination is still regarded as the best method of protection. Influenza vaccination campaigns occur annually to ensure at risk persons are treated to minimise illness (MMWR, 1997). Hence the requirement for high-yielding, generic purification strategies that meet demands for the production of efficacious, non-allergenic influenza vaccines.

Exploitation of the fact that HA and NA are the key immunoprotective antigens in influenza illness (Hobson *et al*, 1972), *and* that these antigens could be released from the viral lipid membrane leaving an intact sub viral particle (Skehel 1971), lead to production methodologies for subunit vaccines. These types of vaccines are less pyrogenic (better for immunocompromised vaccinees) as compared to whole virus-based vaccines (Webster and Laver, 1966). Pyrogenicity was thought to be caused by other viral proteins and co-purifying bacterial components (Salk, 1948). In addition, subunit vaccines are advantageous because the pathological organism is eliminated and there is no possibility of reversion to wild type in attenuated vaccines (Liljeqvist and Ståhl, 1999). However the drawback in using such vaccines lay in their low antigenicity, (which could be improved by the use of an adjuvant, Brady and Furminger, 1976 b).

Fluvirin™ is an attenuated, inactivated sub unit influenza vaccine that derives from X31 recombinant virus (which has the HA and NA of A3/Aichi/2/68 and the growth characteristics of A0/PR8/34). Non-infective, high growth virions are produced in large titre by a process of adaptation, which attenuates the virus, making it less virulent and produces a predominance of spherical progeny. Adaptation occurs after a total of 10 passage cycles- a process that begins at NIBSC, (National Institute of Biological Standards) and is then completed at Medeva Pharma whereby a seed of the attenuated virus is inoculated into the allantoic cavity of an embryonated hens egg (Figure 2.3). Following an 11-day incubation period, the virus infects the chorio-allantoic membrane (CAM) and the allantoic fluid is harvested to collect the released virus particles, which contains the H3N2 antigens that have originated from the A/Hong Kong 1968 virus. The WHO reviews the world epidemiological situation annually. If it is necessary, it will

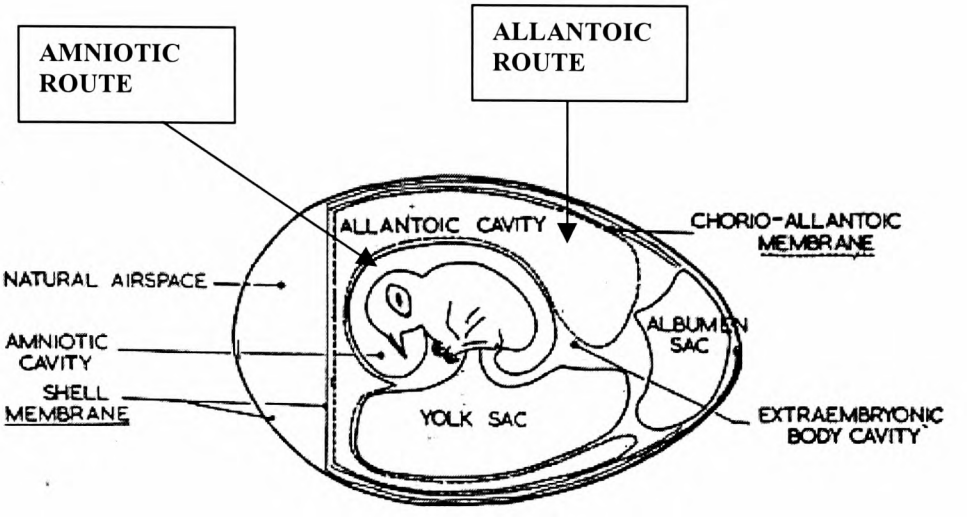

FIGURE 2.3. Diagram illustrating the compartments within an embryonated hen's egg.

Chick embryos were first used for influenza virus propagation by (Smith, 1935). The virus can be inoculated via two routes: the allantoic and the amniotic the latter is more sensitive. The virions used to make Fluvirin™ were produced by the allantoic route (see Section 2.1.4). Reproduced from (Barrett and Inglis, 1985).

recommend new strains to be used in vaccine manufacture on the basis of epidemiological evidence.

2.1.5. Manufacture of Fluvirin™ vaccine (downstream processing).

Earlier attempts to purify the viral proteins, before and after splitting (disruption) failed because of the co-purification of bacteria and egg proteins from the egg cultivation procedures. These were pyrogenic and allergenic- (Salk, 1948; Peck, 1968 and Walsh *et al*, 1988). The arrival of the KII continuous flow zonal ultracentrifuge (Electro-Nucleonics Incorporated) superseded conventional centrifuges (such as the Sharples tubular bowl centrifuge). Using rate zonal centrifugation followed by isopycnic banding (with sucrose), permitted both clarification (kilogramme quantities of impurities were removed from gram quantities of virus) and concentration of the virus (Reimer, 1967; Guerin and Anderson, 1969). In addition, Triton N101 was used to release the surface antigens leaving the core intact (Corbel *et al.* 1970; Corbel and Rondle, 1970).

The major steps in the processing of Fluvirin™ as used commercially by Medeva Pharma are illustrated in Figure 2.4. The Fluvirin™ process uses low-speed centrifugation (Westfalia) to remove gross contaminants such as chick erythrocytes followed by zonal centrifugation (using the KII rotor) to remove further contaminants. Starting with inactivated bulk fluid, IBF, (pre-concentrated allantoic fluid containing inactivated influenza virus particles) the initial sucrose density ultracentrifugation procedure, (Stage 5, Figure 2.4), eliminates contaminating proteins and debris producing purified whole virus as a purified zonal concentrate (PZC). Addition of Triton N101, (Stage 6) selectively releases surface antigen from the viral lipid envelope leaving an intact core particle. The resulting size and mass differences permitted separation of these

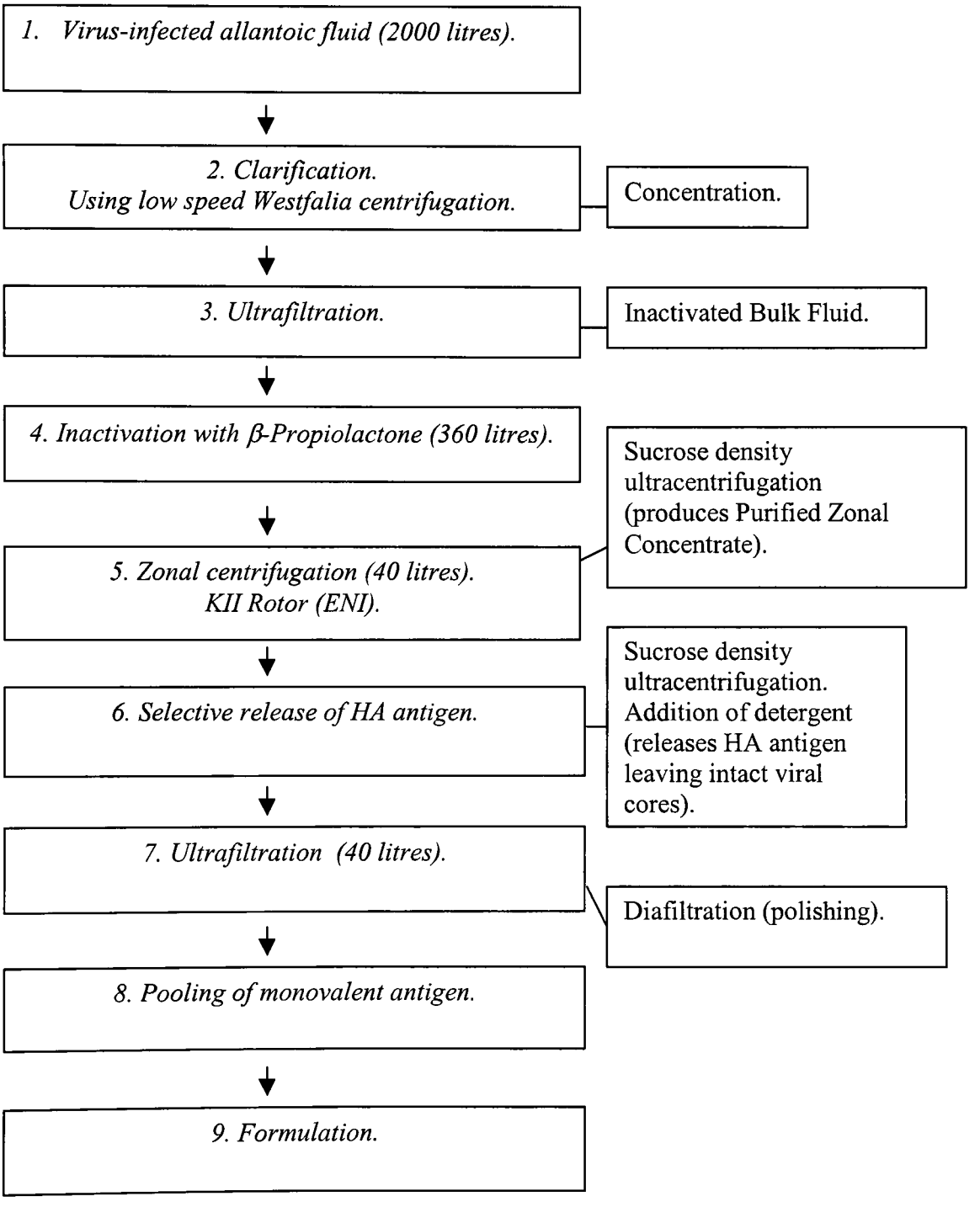

FIGURE 2.4. An outline of the down-stream processing stages in the current Medeva Fluvirin™ Process.

components. The detergent is removed by adding phosphate (salting out) and a diafiltration step (Stage 7) eliminates traces of salt, detergent and exchanges the buffer to yield a monovalent blend antigen pool (MBP). The final vaccine (Fluvirin™) is a formulation of two A strains and one B strain and conforms to the definition of an inactivated influenza vaccine (as stated in the *British Pharmacoepia, BP*, 1997 and the *European Pharmacoepia, EP*, 1997). The total time taken to produce one batch from IBF to MPB is between 36 to 48 hours.

2.1.6. Re-evaluation of the current Medeva Fluvirin™ Process process and the potential for utilising ATPS.

In the face of commercial pressures and regulatory demands, the Fluvirin™ manufacturing process has not significantly altered since the investigations undertaken by Brady PhD Thesis, (1974). As is often the case, these demands meant that there was insufficient time/funds to further optimise a process, although it is important to stress that an optimised process may not necessarily be the most economically feasible one. However in the case of Fluvirin™ manufacture, stages of sub-optimal performance (so-called bottlenecks) have been identified (in particular: the capacity of the rotors used at Stages 5 and 6, Figure 2.4). The use of zonal centrifugation results in long processing times to eliminate impurities from the virus particles (to standards stated in *BP* and *EP* guidelines). This makes the process energy-intensive. However, it would be desirable to circumvent these bottlenecks and reduce the processing times in order to increase process productivity and throughput. Alternative purification techniques therefore deserve examination from both processing and economic viewpoints.

Partitioning using aqueous two-phase systems (ATPS) has been recognised as a candidate technology whose potential has been discussed previously (see Section 1.4.4). For application in the Medeva Fluvirin™ Process, it would be necessary to demonstrate significant advantages over the existing technique, of sucrose density gradient ultracentrifugation. Previous researchers demonstrated a role for ATPS in the processing of nanoparticulates (Walker *et al*, 1996; Walker and Lyddiatt, 1998; 1999 and Braas *et al*, 2000). The current study aims to extend this role by demonstrating the application of ATPS in the processing of influenza virus nanoparticles that are currently used in a commercial vaccine manufacture process. This provides the unique opportunity to compare the performance of ATPS with a commercially used purification process for virus particles and to highlight the challenges faced when applying this technique on large scale.

2.1.7. Strategy for the utilisation of ATPS as a technique for the processing of Fluvirin™.

In order to evaluate the success of ATPS as a potential technique in the processing of Fluvirin™, it was necessary to decide from the outset what criteria the process should meet. It was envisaged that ATPS would serve as a primary down-stream processing step for the selective removal of bulk impurities from intact viral particles in allantoic fluid. During the early stages, it was desirable to maintain the integrity of the virus (in spite of the final product being of subunit form) in order to simplify and to monitor the purification.

2.1.7.1. Establishing the analytical methods.

The first essential activity to undertake in such a development study was the establishment of analytical methods. This would permit the characterisation of components in the feedstock and underpin aspects of process design. In addition, the analytical techniques used could decide the success of the process, since they enable the detection and quantitation of the feedstock components and monitoring of the purity and recovery throughout the process. An important thermodynamic and bioprocess parameter in ATPS is the partition coefficient (K), which enables quantitative monitoring of partition between phases (see Section 1.5.4). One of the main methods developed in this study was the use of sodium dodecyl sulphate polyacrylamide gel electrophoresis (SDS PAGE) and quantitative one-dimensional densitometry to estimate K of individual proteins in loaded ATPSs.

2.1.7.2. Characterisation of egg white proteins.

During harvest of the allantoic fluid, the albumen sac is ruptured (due to its close proximity to the allantoic cavity, Figure 2.3), and released contents contaminate the allantoic fluid. These contents comprise egg white proteins, which make up roughly 50 % of the egg components (Romanoff and Romanoff, 1949). The key components are listed in Table 2.2. Ovalbumin is the major egg white protein and provides the chick with a nutrient source. The proteins ovotransferrin (a haem protein), ovoglobin and lysosoyme prevent bacterial growth. Ovomucoid has protease inhibiting activity (mainly trypsin). Ovalbumin is also one of the most allergenic proteins in egg white, followed by ovotransferrin, lysosyme and ovomucoid. Thus it is desirable to remove these proteins in the purification process from the virus.

Egg white proteins.	Percentage (%) of egg white proteins.	Molecular weight (kDa).
Ovalbumin	54	43
Ovotransferrin (conalbumin)	12 to 13	75
Ovomucoid	11	28
Ovoglobin	8	25
Lysosyme	3.4 to 3.5	14
Ovomucin	1.5 to 3.5	0.22-270 $x10^6$

TABLE 2.2. Egg white proteins.
Egg white is a well-characterised feedstock (see main text). Thus Table 2.2 was used to confirm the identities of key egg white proteins that were partitioned using ATPS and fractionated using SDS PAGE gels (see Appendix I). The data was taken from ***Awadé and Efstathiou, (1999).***

2.1.7.3. Characterisation of egg yolk.

In addition to rupture of the albumen sac, during allantoic fluid harvest, the yolk sac is often ruptured too, leading to release of its contents. Therefore not only is the allantoic fluid contaminated with egg white proteins but also egg yolk components also. Egg yolk is composed of approximately 48 % water and 33 % (wet weight) lipid- in the form of triglycerides (Evans *et al*, 1973), 17 % protein and the remaining 2 % as, carbohydrates and minerals. Egg yolk is divided up into approximately three compartments: the granular compartment (consisting of phosvitins and lipovitellins), the very low-density lipoprotein (VLDL) compartment and the water-soluble compartment (Figure 2.5). Some

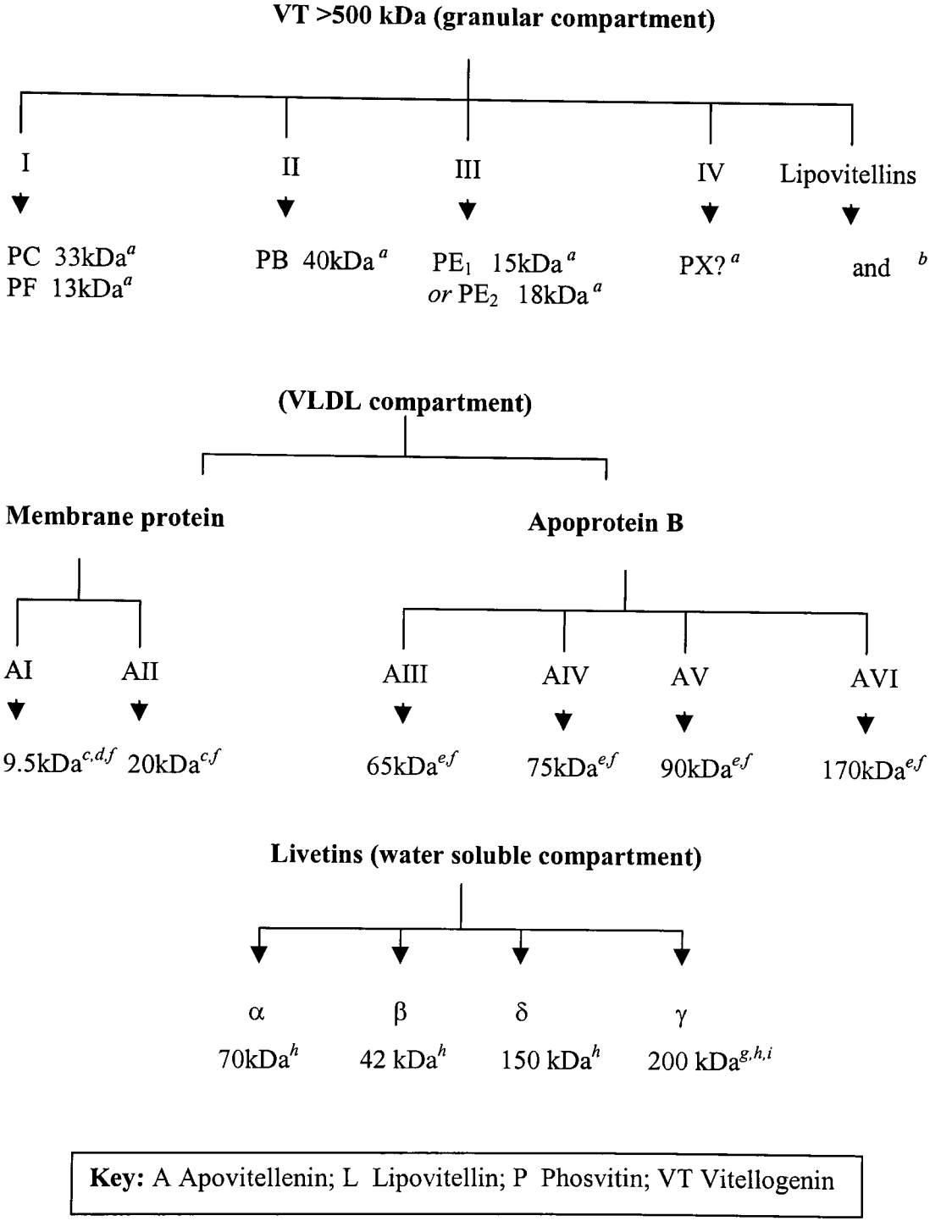

Figure 2.5. Showing origins and interrelationships of the proteins in egg yolk. *a: Wallace and Morgan, 1986[a, b]. b: Wang and Williams, 1980. c: Burley, 1975. d: Burley and Davies, 1976. e: Burley and Sleigh, 1980. f: Evans and Burley, 1987. g: Joubert and Cook, 1958. h: Burley and Vadehra, 1979 and i: Burley, 1978.*

of these proteins have been difficult to study due to their strong binding preference for lipids (Burley, 1975). The main constituents are apovitellenins, phosvitins and livetins. The apovitellenins (I and VI) and phosvitins have also been implicated in allergic responses (Walsh *et al*, 1988).

2.1.8. Rational investigation of suitable ATPSs to process IBF material.

This chapter documents and discusses the strategies employed in the selection of ATPSs suitable for the processing of influenza virus particles. Key variables, which are known to influence the partition of proteins and particles in ATPSs, were investigated including the molecular weight of PEG, the TLL and volume ratio, (Albertsson, 1986; Hustedt, 1986). Polyethylene glycol (PEG)-phosphate ATPSs were examined because the cost of salt were known to be less than for that of Dextran (Sigma Chemical Company). The wealth of information regarding PEG-salt systems provided the incentive for their further investigation with respect to the influenza particles, (Huddleston, PhD thesis, 1996; Rito-Palomares, PhD thesis, 1996; Walker, PhD thesis, 1998; Lebreton, PhD thesis, 1998 and Braas *et al*, 2000).

To broadly appreciate the partition behaviour of the influenza virions in an ATPS, it was decided to undertake initial experiments using PZC alone. Information from this study was then used in the deployment of selected ATPS suitable for handling the crude process feedstock, IBF as the start-point. Aqueous two-phase systems consisting of PEG of nominal molecular weight 300 to 8000 were used (since most useful separations had been obtained using PEG in this range). Systems with varying tie-lines lengths (TLLs) were selected to investigate how system composition affected the partition of virus and contaminants (refer to Appendix II). An arbitary designation of short (1-20 % w/w),

intermediate (21-34 % w/w) and long (>35 % w/w) TLLs was employed. The volume ratio was initially fixed at unity so that the observed partition behaviour would be a function of TLL and PEG molecular weight alone. Walker, (1998), argued that measurement of volume ratios for loaded systems were ambiguous where the presence of multiple solid phases such as an interphase, (Boland, 1989) compromised conventional estimates. Thus the term "Vrd" was coined (which will be used herein), defined as the volume ratio of a "dirty" or loaded ATPS (Walker PhD Thesis, 1998). This parameter takes account of the relative contribution each phase makes, whilst still calculating the phase ratio (where T is the top phase, I is the Interphase and B is the Bottom phase):

$$T\ (\%) = \frac{T}{(T + I + B)} \times 100 \qquad \textit{Equation 2.1.}$$

$$B\ (\%) = \frac{B}{(T + I + B)} \times 100 \qquad \textit{Equation 2.2.}$$

$$Vrd = \frac{T}{B} \qquad \textit{Equation 2.3.}$$

The Vrd can also be conveniently represented as T: I: B which indicates the proportion that each phase occupies. The benefit of the viral particles partitioning into an interphase or sediment include the concentration of product into a small volume making it easier to handle further downstream. Potentially useful ATPSs were studied in the optimisation and ultimately the design of a bench-scale process that could be compared with end-

stage material generated from the current, conventional ultracentrifugation process. Information from this study would also contribute to an evaluation of the generic application of ATPSs in the processing of nanoparticulates from a "real" process.

2.1.9. System nomenclature.

Each ATPS used in the study is assigned a number, which is used herein. Strictly speaking ATPSs in the presence of biomass are not the same (with respect to their compositions) as their parent blank system. For convenience the same system number was used. For example, S1, (PEG 300 20.0 % w/w/ phosphate 22.0 % w/w, pH 7.5), used in this study (see Appendix II) is also referred to as S1 in the presence of biomass.

2.2. MATERIALS and METHODS.

All reagents from Sigma unless stated otherwise.

2.2.1. Construction of blank ATPSs.

The systems were selected from a binodal constructed by the cloud point method (Bamberger *et al*, 1985). The ATPSs were constructed using a top-pan balance (Oertling RB153). Polyethylene glycol (PEG) of average molecular weights: 300, 600, 1000, 3350 and 8000 were used. Polyethylene glycol of average molecular weight 6000 was obtained from BDH. Dibasic and monobasic potassium orthophosphate was combined in the ratio of 18:7 to provide a system of pH 7.5. The appropriate masses of phase-forming chemicals, 2g inactivated fluid bulk (IBF) material and water were added to clean 15ml centrifuge tubes (Sarstedt) to a total of 10g w/w. The IBF loading represented 20 % of this total. The samples were mixed for one hour at 20-22 °C using a rotary mixer (SB1, Stuart Scientific) and centrifuged for 5 minutes at 2000 *xg* (Jouan, C422 bench top

centrifuge). After noting the volume ratios, (Vrd's- the volumes of the top phase:interphase:bottom phase) the top phase was harvested into a clean bijou tube. The interphase was carefully harvested using a clean pipette tip and resuspended into 1ml of 0.01M PBS pH 7.4. Finally, piercing the bottom of the tube allowed the bottom phase to be collected into a clean bijou. For a complete summary of the ATPSs studied, refer to Appendix II.

2.2.2. Construction of loaded ATPSs.

The loaded ATPSs were constructed as in Section 2.2.1 but with the addition of biomass. The biomass used was IBF reserve material (A/Sydney batch 753134) provided by Medeva Pharma, Liverpool, UK.

2.2.3. SDS PAGE.

Homogeneous gels consisting of 12 % monomer concentration were made with 30 % Acrylamide/Bis: acrylamide in the ratio of 37.5:1 and containing a crosslinker (N N N^1N^1 tetramethyl ethylenediamine, TEMED), of concentration, 2.6 % (BioRad), were used along with stacking gels consisting of 4 % monomer concentration. The resolving gel contained 1.5M Tris-HCl, pH 8.8, SDS at a concentration of 1 % w/v and ammonium persulphate at a final concentration of 0.5 % v/v. The stacking gel contained 0.5M Tris-HCl, pH 6.8, as described by Laemmli, 1970). The gels were made and electrophoresed using 16x 20 cm glass plates giving a gel thickness of 1.5 mm The clamp system and gel tank were part of the PROTEAN® II xi cell from BioRad.

2.2.3.1. Sample preparation.

Partitioned samples from top, interphase or bottom phase were added to an equal volume of 10 % w/v TCA into 1.5 ml microfuge tubes and vortexed briefly. The samples were then placed in a –20 °C freezer for one hour, subsequently thawed out and centrifuged at 11,600 *xg* for 10 minutes (MSE bench centrifuge). The supernatant was discarded and washed with 1ml of 1:1 mixture of ethanol and ether in capped microcentrifuge tubes (that had been pierced to release the build-up of pressure). The centrifugation step was repeated twice more using this wash step. After the last wash, the supernatant was removed and the resulting pellet allowed to air dry. The sample was resolubilised in a 70 µl of reduced sample buffer (0.625M Tris-HCl pH 6.8, 4 % w/v SDS, 10 % v/v β-mercaptoethanol, 2 % w/v sucrose and trace bromophenol blue). Samples involved in the volume ratio (Vrd) study (Section 2.3.4), were prepared as described by Bensadoun and Weinstein, (1976). This was because the TCA was insufficient on its own to precipitate the proteins. The Bensadoun and Weinstein method appeared to work better due to the added deoxycholate, which acted as a carrier and possibly increased the availability of TCA to act as a precipitant.

2.2.3.2. Marker preparation.

The markers (low molecular weight kit from Pharmacia), were simply reconstituted in 100 µl reduced sample buffer and gently mixed. For IBF analysis (see Section 2.3.1) this stock mixture was directly applied to the gels. For all other analysis, the stock was diluted ten-fold in reduced sample buffer before gel application. This was due to the large format gels of greater thickness used in the analysis of IBF (which required a

higher protein concentration to visualise the bands after Coomassie staining). For economic reasons, the smaller mini gels utilised a more dilute mixture of the markers. The low molecular markers consisted of the following protein subunits: phosphorylase a (97 kDa), bovine serum albumin (67 kDa), ovalbumin (43 kDa), carbonic anhydrase (31 kDa), trypsin inhibitor, (21 kDa) and lysosyme (14 kDa).

2.2.3.3. Electrophoresis Conditions.

The samples and marker were placed in a boiling water bath for 5 minutes at 100 °C, allowed to cool and then a known volume applied to a lane on the gel. The samples were electrophoresed at 80 volts for approximately 18 hours. The electrophoresis stock buffer was made as a concentrate containing 1 % w/v SDS, 3M Tris-HCl and 1.92 M glycine. This was diluted 10-fold in Milli-Q water to provide the electrophoresis running buffer.

2.2.3.4. Staining/Destaining procedure.

The gels were removed from the electrophoresis tank and stained for a minimum of three hours in Coomassie Brilliant Blue stain (2 g Coomassie Blue R250 per litre in 5 parts methanol, 5 parts Milli-Q water and 2 parts glacial acetic acid (Fisher Scientific). The gels were rocked to promote the staining reaction. Coomassie Brilliant Blue could detect a lower limit of sensitivity 1 μg total protein ml^{-1}. The gels were destained with a solution of the stain solvent. The gels were dried using a gel drying kit (Promega) and then scanned using Ultroscan XL densitometer (LKB Pharmacia).

2.2.4. One- dimensional densitometry.

The densitometer consists of a helium-neon (He-Ne) laser source, which provides an intense coherent beam of monochromatic light at 633 nm. The laser beam light is split into two: 90 % goes to the sample bands and the remaining 10 % goes to the reference detector. The detector measures the portion of light absorbed by a sample band, which manifests as a photocurrent and is converted to a voltage. The voltage is proportional to the amount of light detected and is compared to the light from the reference detector. The resulting signal is proportional to the absorbance of sample. The detector signal is integrated by computer software to compute the absorbance area (in absorbance units or AU) x thickness of gel for each major band (in mm). These are represented as peaks on the computer printout.

2.2.4.1.Estimation of mass of proteins on gel using SDS PAGE and one-dimensional densitometry.

The mass of protein present in each band on the gel was estimated as follows. Firstly, the major protein bands in the IBF feedstock were identified. The concentration of the IBF feedstock was estimated by using the method of Lowry *et al*, (1951). The mass of IBF on the gel and the relative proportion of each major protein band were deduced. The IBF material was then serially diluted (to obtain a calibration curve), loaded onto a reduced SDS PAGE gel and electrophoresed (as described in Section 2.2.3). A typical calibration gel is shown in Figure 2.6. The insert shows a typical Rf plot used to deduce the molecular weight of the individual proteins (Weber and Osborn, 1969). Table 2.3 summarises the main proteins observed in the IBF material and their molecular weights. The relative proportion of each major protein is depicted in Figure 2.7. From this, it was possible to construct calibration curves of the individual proteins contained within the

IBF material (an example using ovalbumin is shown in Figure 2.8). Thus the amount of major proteins present in each experimental ATPS could be deduced. By knowing the amount of a certain protein (for example ovalbumin) in each phase, weight ratios could be deduced in a manner analogous to that of K. This will be further discussed in the following section. The SDS PAGE/densitometry method was evaluated for precision a total of six times. The error in recovery of proteins was estimated to be ± 20 %. This was primarily due to variability in TCA precipitation. It was decided to use this method since the major proteins (the viral proteins, ovalbumin and apovitellenins accounting for at least 80 % of the proteins) were quantitatively precipitated.

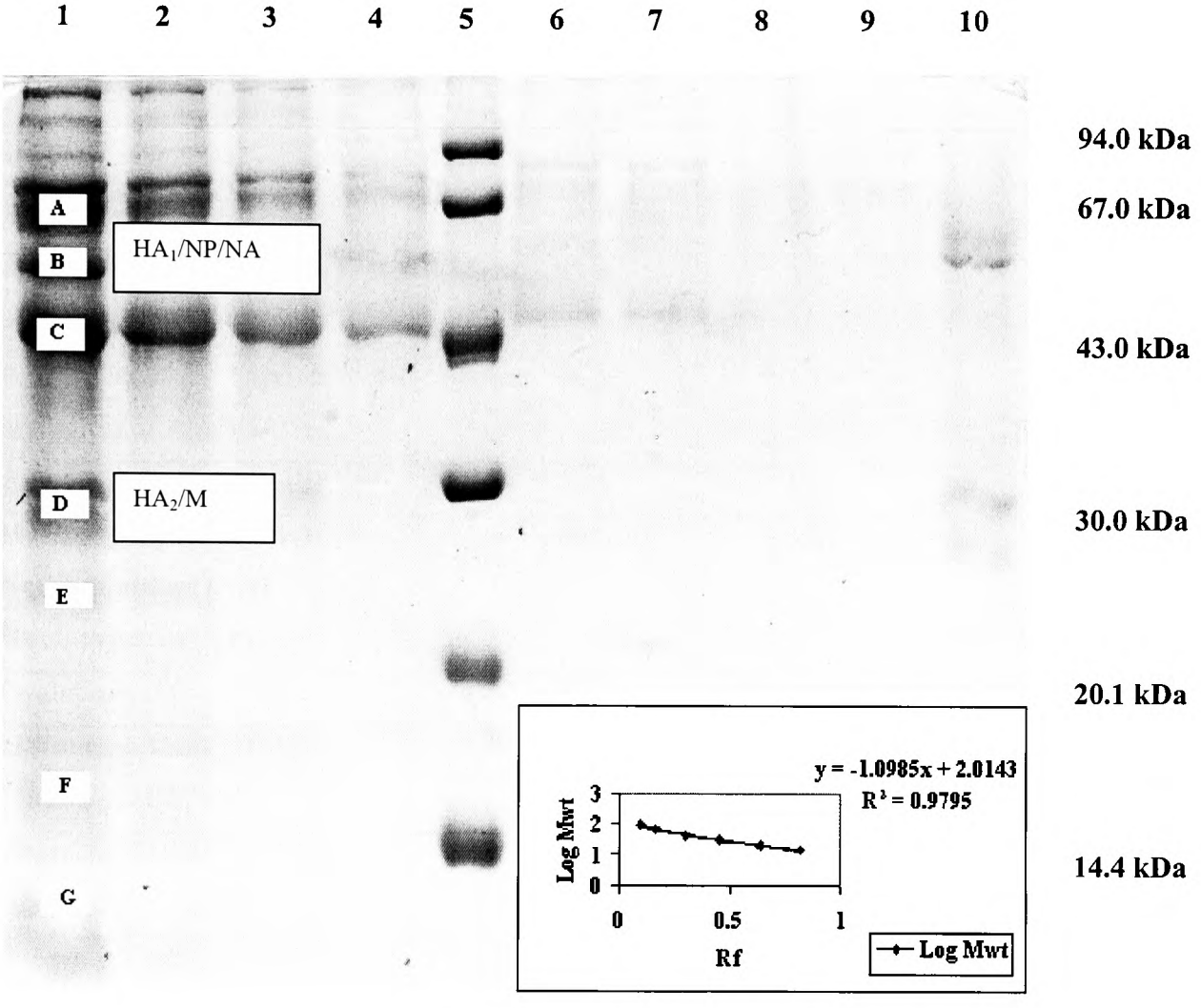

FIGURE 2.6. Typical calibration gel used to quantify the amounts of individual proteins within IBF feedstock.

One-dimensional densitometry was used to estimate the absorbance of each individual protein band. By knowing the amount of IBF protein loaded in each lane and the proportion each band represents out of the total, (see Figure 2.7), calibration curves of the individual proteins were constructed (see Figure 2.8). Thus the amount of each protein could be estimated in samples partitioned in ATPSs and Partition Mass Ratios could be deduced. The viral proteins are indicated on the gel as B and D.

***Lanes 1 to 4 inclusive**: IBF material diluted in the range 112.5 to 14.1 μg of protein.*
***Lane 5**: Low molecular weight marker (10 μl load).*
***Lanes 6 to 9 inclusive:** IBF material diluted in the range 7.0 to 0.9 μg of protein.*
***Lane 10:** PZC material 45 μg protein.*

***Key: A:** Apo III-V; **B:** HA_1/NP/NA; **C:** OA; **D:** HA_2/M; **E and F:** PB and PE_1; **G:** ApoI (refer to Table 2.3).*

Identification.	Mean Mwt. (kDa).	Coefficient of Variation (CV) %.
Apovitellenin VI (Apo VI)	> 97 kDa	3.7
Apovitellenin V (Apo V) plus reduced multimers of Apo VI	83.5	2.6
Apovitellenin IV (Apo IV) plus reduced multimers of Apo VI	76.5	1.8
Apovitellenin III (Apo III)	70.5	1.7
Haemagglutinin $_1$ (HA_1) **Neuraminidase (NA)** **Nucleoprotein (NP)**	60.9	3.3
Ovalbumin (OA)	49.9	2.3
Haemagglutinin $_2$ (HA_2) **Matrix protein (M)**	29.9	2.7
Phosvitin B (PB)*	24.5	2.7
Apovitellenin II (Apo II)	17.6	2.4
Phosvitin E_1 (PE_1)	14.6	2.6
Apovitellenin I (Apo I)	11.2	3.8

TABLE 2.3. A summary of the proteins observed in IBF material as deduced by SDS PAGE and Rf plots.

*The molecular weights were estimated as the mean of six individual runs. The error in the determination are shown as coefficient of variances. *The molecular weight determination of phosvitin B was flawed since it is known to behave anomalously on straight percentage gels (Wallace and Morgan, 1986b). The actual value should be nearer to 40 kDa. The identities of the proteins were confirmed from a literature review (see Figure 2.5). The viral proteins are highlighted in bold font. Abbreviated forms of the protein names are shown in bracket (refer to SDS PAGE gel presented in Figure 2.6). The relative proportions of the key proteins in IBF are presented in Figure 2.7.*

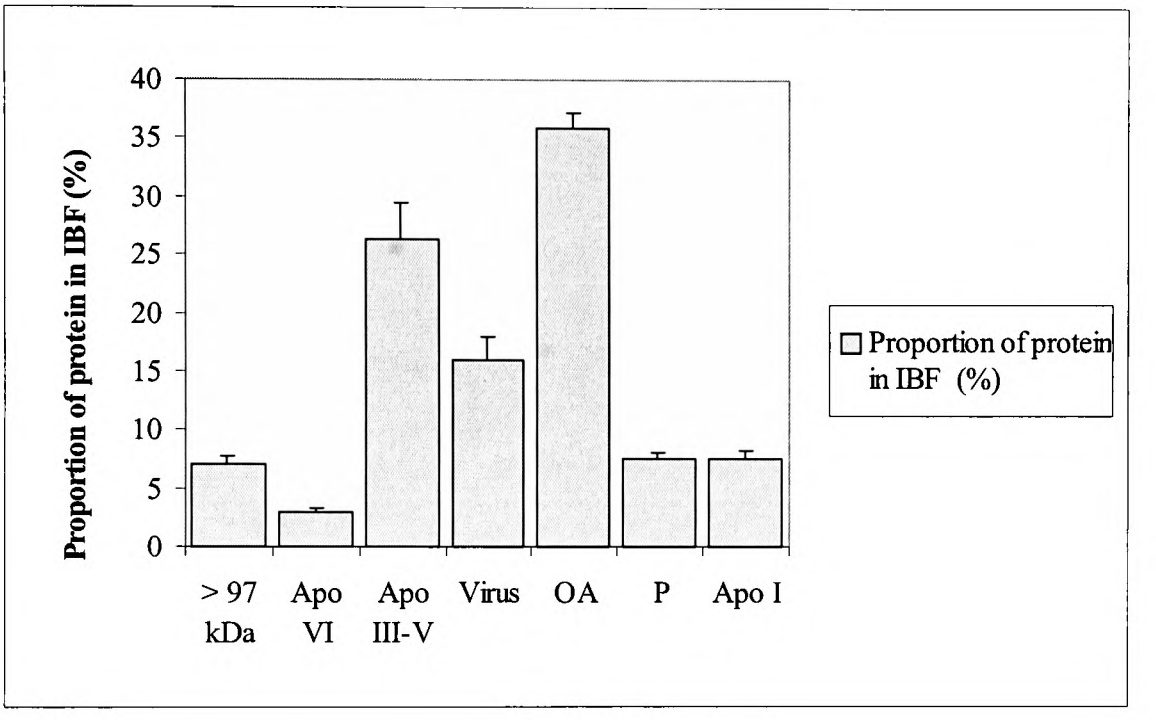

FIGURE 2.7. Histogram illustrating the proportion of key proteins within IBF. *The bars represent standard errors from six determinations. The proteins are presented in Table 2.3.*

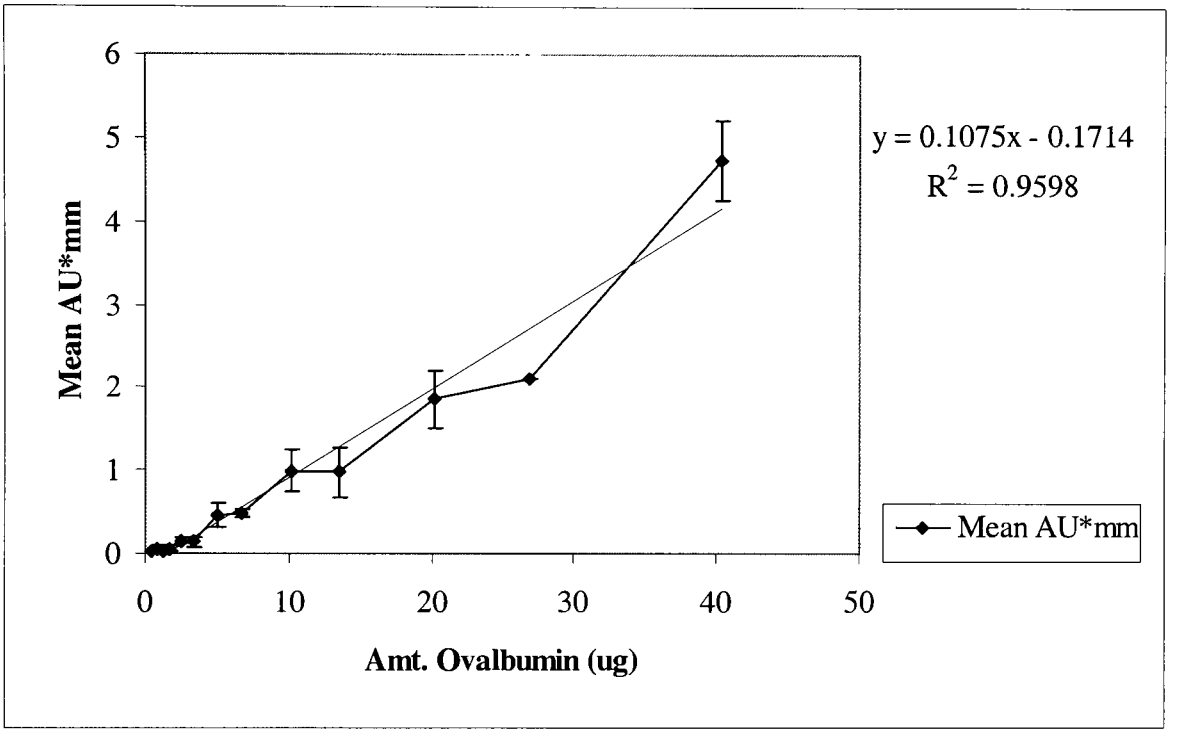

FIGURE 2.8. A typical calibration curve obtained from SDS PAGE and densitometric analysis of ovalbumin contained within IBF material.

*Ovalbumin (a key protein in IBF) was selected an example. Serially diluted IBF material was electrophoresed and individual proteins were quantified on a gel. This permitted calibration curves of main proteins within IBF to be produced. The data shown was calculated as a mean of six such typical calibration curves generated from gels typified by Figure 2.6. The mean absorbance units x thickness of area scanned (AU*mm) was obtained from densitometric analysis. The bars represent standard errors.*

2.2.4.2. Definition of Fractional Mass Ratio (FMR).

The partition behaviour of virus-derived proteins and protein contaminants were characterised using fractional mass ratios (FMRs), the authors own nomenclature. This provided a means of monitoring protein partition between the phases as well as permitting a quantitative description of the system in the presence of solid phases (since the conventional partition coefficient (K) has no relevance in such situations). Therefore the FMR for target molecules is defined in Equations 2.5d, 2.6c and 2.7c:

Top phase = mass target $protein_{top\ phase}$/ total mass protein x 100 *Equation 2.5a*

Interphase = mass target $protein_{interphase}$/ total mass protein x 100 *Equation 2.5b*

Bottom phase = mass target $protein_{bottom\ phase}$/ total mass protein x 100

Equation 2.5c

Thus the FMR = Top phase: Interphase: Bottom phase ***Equation 2.5d***

The FMR is redefined for purpose of the volume ratio study (Section 2.3.4) as follows:

For PEG 300-based ATPSs.

Top phase = mass target $protein_{top\ phase}$ / total mass protein x 100 *Equation 2.6a*

Interphase/bottom phase = mass target $protein_{Interphase/bottom\ phase}$ / total mass protein x 100

Equation 2.6b

Thus the FMR = Top phase: Interphase/ bottom phase ***Equation 2.6c***

For PEG 8000-based ATPSs.

Top phase/interphase = mass target protein$_{\text{top phase/interphase}}$ / total mass protein x 100

Equation 2.7a

Bottom phase = mass target protein$_{\text{bottom phase}}$ / total mass protein x 100

Equation 2.7b

Thus the FMR = Top phase/Interphase: Bottom phase ***Equation 2.7c***

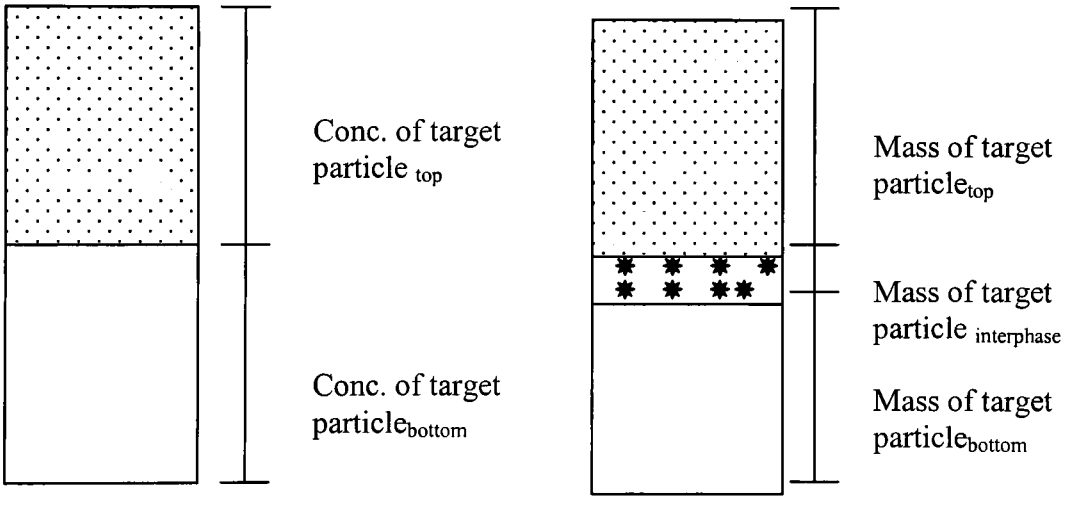

Blank ATPS (contains only phase-forming chemicals).

$K = C_{top}/C_{bottom}$, (see Equation 1.6).

Loaded ATPS (containing biomass).

FMR= Fractional mass $_{\text{top phase}}$/ Fractional mass $_{\text{interphase}}$ / Fractional mass $_{\text{bottom phase}}$ (see Equations 2.5a to2.5d).

FIGURE 2.9. Schematic interpreting the partition coefficient in blank and loaded ATPSs.

2.2.5. Total protein concentration determined by Lowry assay (Lowry et al, 1951).

Five reagents were prepared:

Reagent A: 20 g Na_2CO_3, 4 g NaOH made up to 1000 ml in Milli-Q water.

Reagent B-1: 1 g $CuSO_4$ .5 H_20 in 100 ml Milli-Q water.

Reagent B-2: 2 g sodium potassium tartrate in 100 ml Milli-Q water.

Reagent C: A mixture of Reagents B-1 and B-2 in a 1:1 volumetric ratio. Used on day of preparation.

Reagent D: 2N Folin Ciocalteau Reagent diluted in an equal volume of 10 % w/v TCA in Milli-Q water.

The samples were mixed with an equal volume of Reagent A post TCA precipitation (as in Section 2.2.3.1). A volume of 0.5 ml of this mixture was added to 2.5 ml Reagent C, vortexed and incubated for ten minutes at 23 °C. A volume of 0.5 ml Reagent D was added followed by immediate mixing. The solution was read at a transmission of 550 nm after an incubation period of 30 minutes at 23 °C.

2.2.6. The murexide test.

One drop of concentrated nitric acid was added to the test sample on a clean microscope slide (this lead to the production of alloxantin from uric acid present). The sample was heated then cooled. A drop of ammonia (26 % v/v) was added which lead to the formation of murexide from the alloxantin. Formation of a red-purple colour indicated a positive test for uric acid.

2.3. RESULTS AND DISCUSSIONS.

2.3.1. Partition of Inactivated Bulk Fluid (IBF).

In order to detect and quantitate the viral proteins in the ATPSs, it was decided to use validated assays that were already in place at Medeva Pharma and to modify them as necessary. Therefore the assays used initially to investigate the PZC were the HA test, the Neuraminidase enzyme-linked assay in microplates (NELLAM) and the Micro BCA assay for total protein (see Appendix I). With the exception of the NELLAM, these assays were relatively quick to perform. The assays used for the detection and quantitation of PZC partitioned in ATPS could not be used in the analysis of Inactivated Bulk Fluid (IBF). The NELLAM could not detect the NA perhaps due to masking of the response due to the presence of lipoproteins in the allantoic fluid (NA is less abundant than HA and could be more susceptible to this effect). Dilution of sample did not appear to overcome this effect. Alternatively, the result could be due to aggregation, (Cassidy, 1965). The Micro BCA assay was affected by the presence of uric acid at levels known to interfere with this assay, (Pierce Technical Bulletin) and confirmed upon undertaking the murexide test. The Lowry method was used (Lowry *et al,* 1951) and produced anomalous results in the presence of PEG 8000 thought to be due to the presence of lipoproteins such as the apovitellenins (Kashyap *et al,* 1980). The Coomassie binding protein assay (Bradford, 1976) was also attempted. An alternative was to use SDS PAGE with TCA precipitation followed by Coomassie Brilliant Blue staining and one-dimensional densitometry to quantitate the total protein within the bands (see Sections 2.2.3 and 2.2.4). Trichloroacetic acid (TCA) precipitation was the preferred method of preparing the samples for SDS PAGE to concentrate proteins of relatively low initial concentration and to remove salts derived from the phase formant. It was decided to use

this method since the major proteins (the viral proteins, ovalbumin and apovitellenins) were quantitatively precipitated.

Electrophoresis of IBF material on a reduced gel (Figure 2.6) showed it to be more complex than the simple gel pattern shown by the egg white proteins (Figure A4). In fact the gel pattern of IBF looked more like the proteins present in egg yolk. Possible explanations for this were that there were differences between a fertile and non-fertile hens egg; or the yolk sac had ruptured during harvesting of allantoic fluid causing it to be contaminated with the egg yolk proteins. The ovalbumin was present presumably because it served as a nutrient source for the chick. Thus the egg white spiking data (Appendix I) was only useful from a method development point of view. However, the data from partition of PZC could be used to support the data from the partition of the IBF. The main differences between reduced and non-reduced IBF samples included the loss of Apovitellenin I multimers upon reduction (and gain in the Apovitellenin monomer). In addition, bands in the 60 to 90 kDa region appeared on the reduced gels with a concurrent diminished staining intensity of the high molecular weight bands- > 97 kDa (data not shown). These were thought to be oxidation products from Apovitellenin VI. Therefore to simplify quantitation, the bands were identified as Apovitellenins III-V. This is correct to some extent (Apovitellenins IV and V are present in small amounts), but also present were the oxidation product of Apovitellenin VI.

2.3.2. Effect of PEG molecular weight and TLL upon Fractional Mass Ratios (FMRs) of the viral components.

Partition of the viral components in IBF material in ATPSs were monitored using SDS PAGE gels and Fractional Mass Ratios (FMRs) were used to characterise partition

in these systems. The viral components include haemagglutinin subunits 1 and 2, nucleoprotein, neuraminidase and matrix protein (HA_1 and HA_2, NP, NA and M respectively). In ATPSs comprising PEG 300, Systems S2 and S3 (refer to Appendix II) the FMRs for HA_1/NP/NA, indicate that the HA_1/NP/NA proteins are predominantly located at the interphase and that no proteins were detected in the bottom phase (Table 2.4). The increase in TLL has little effect on these partition characteristics. In ATPSs comprising PEG 1000, (Systems S7, S8 and S9), the viral proteins partition predominantly between the interface and the bottom phase. In ATPSs comprising PEG 3350, (Systems S10, S11 and S12), the HA_1/NP/NA proteins partition exclusively to the interphase at short to intermediate TLLs, but in S10 (at long TLL), approximately a third of these proteins partition to the top phase (refer to Table 2.4). This anomalous behaviour can be explained by an increase in precipitation (observed in PZC/ egg white analysis, Appendix AI) with increasing TLL, leading to saturation of the interphase. No HA_1/NP/NA proteins were detected in the bottom phase. This was attributed to large salting out effects (which was also observed in the PEG 300 ATPSs). These effects will be discussed later. Saturation of the interphase meant that the proteins partitioned to the top phase. The PEG 6000 ATPS (S13, S14 and S15) demonstrated that the viral proteins partitioned predominantly to the interphase in systems of short to intermediate TLL. At longer TLL, the proteins partition to the bulk phases. As the interphase becomes saturated and because the proteins cannot partition to the top phase (due to increased excluded volume effects, to be discussed later), these proteins partition increasingly to the bottom phase. This observation is replicated in PEG 8000 ATPSs, S22, S23 and S24 except that in S24, the both the interphases and bottom phases become saturated (with protein and debris) and these proteins partition to the top phase (overcoming any

TLL (%w/w)	Short	Intermediate	Long
PEG Mwt. 300	N/A	(S3) 13: 87: 0	(S2) 27: 73: 0
PEG Mwt 1000	(S9) 6: 77: 17	(S8) 26: 40: 34	(S7) 3: 80: 17
PEG Mwt 3350	(S12) 0: 100: 0	(S11) 0: 100: 0	(S10) 37: 63: 0
PEG Mwt 6000	(S15) 0: 71: 29	(S14) 0: 61: 39	(S13) 35: 65: 0
PEG Mwt 8000	(S24) 0: 88: 12	(S23) 0: 67: 33	(S22) 3: 97: 0

TABLE 2.4. The effect of PEG molecular weight and TLL upon FMR of the viral components HA_1/NP.

The systems used were shown in brackets (refer to Appendix II), followed by the fractional mass ratios of protein in the top: interphase: bottom phase (see Section 2.2.4.2 for a fuller explanation). Definitions of short, intermediate and long TLL are given in Section 2.1.8.

TLL (%w/w)	Short.	Intermediate.	Long.
PEG Mwt. 300	N/A	(S3) 23: 77: 0	(S2) 27: 73: 0
PEG Mwt 1000	(S9) 27: 62: 11	(S8) 19: 36: 45	(S7) 8: 87: 5
PEG Mwt 3350	(S12) 0: 100: 0	(S11) 0: 100: 0	(S10) 55: 45: 0
PEG Mwt 6000	(S15) 0: 56: 46	(S14) 10: 79: 10	(S13) 6: 38: 56
PEG Mwt 8000	(S24) 0: 76: 23	(S23) 39: 51: 10	(S22) 21: 75: 47

TABLE 2.5. The effect of PEG molecular weight and TLL upon FMR of the viral components HA_2/M.

The systems used were shown in brackets (refer to Appendix II), followed by the fractional mass ratios of protein in the top: interphase: bottom phase (see Section 2.2.4.2 for a fuller explanation). Definitions of short, intermediate and long TLL are given in Section 2.1.8.

excluded volume effects). The trends in partition of HA_2/M proteins are generally similar to those described for HA_1/NP/NA proteins except with systems comprising high molecular weight and long TLL PEG (Table 2.5). This suggests that in these relatively extreme conditions, the salting out effects are large so the proteins are "forced" to partition to the top phase.

In order to assess the usefulness of a system for processing IBF material, it is also essential to deduce the partition characteristics of the contaminant proteins. The FMR analysis described in the previous section was applied to examine the partition behaviour of the key protein contaminants, ovalbumin, apovitellenin I, apovitellenins III to VI and the phosvitins. Ideally useful systems would be those, which direct the contaminating proteins away from the interphase. Thus far it can be concluded that ATPSs of long TLL would be suitable for partitioning the virus.

2.3.2.1. Effect of PEG molecular weight and TLL upon Fractional Mass Ratios (FMRs) of ovalbumin.

In ATPSs comprising low molecular weight, PEG 300 the FMRs for ovalbumin indicate that as the TLL length increases, a greater proportion of this protein partitions to the top phase (approximately 7 times more in S2 compared to S3, refer to Table 2.6). In ATPSs comprising PEG 1000, the FMRs for ovalbumin indicate that as the TLL length increases, more ovalbumin partitions to the interphase. The same proportion of ovalbumin partitions to the bottom phase, therefore changes must be due to a in protein from the top phase. In ATPSs comprising PEG 3350, increasing TLL results in an increasing top phase preference and decreasing bottom phase preference. In ATPSs comprising PEG 6000, increasing TLL results in increased partition of ovalbumin to the

top and interphase and less to the bottom phase. In ATPSs comprising PEG 8000, the ovalbumin shows a bottom phase preference with all TLLs investigated.

TLL (%w/w)	Short.	Intermediate.	Long.
PEG Mwt. 300	N/A	(S3) 51: 49: 0	(S2) 87: 13: 0
PEG Mwt 1000	(S9) 51: 31: 18	(S8) 47: 13: 40	(S7) 35: 59 : 6
PEG Mwt 3350	(S12) 16: 24: 60	(S11) 26: 66: 8	(S10) 62: 38: 0
PEG Mwt 6000	(S15) 0: 16: 84	(S14) 4: 12: 84	(S13) 20: 32: 48
PEG Mwt 8000	(S24) 0: 7: 93	(S23) 0: 8: 92	(S22) 17: 1: 82

TABLE 2.6. The effect of PEG molecular weight and TLL upon FMR of ovalbumin (OA).
The systems used were shown in brackets (refer to Appendix II), followed by the fractional mass ratios of protein in the top: interphase: bottom phase (see Section 2.2.4.2 for a fuller explanation). Definitions of short, intermediate and long TLL are given in Section 2.1.8.

2.3.2.2. Effect of PEG molecular weight and TLL upon Fractional Mass Ratios of (FMRs) of apovitellenins III to V.

In ATPSs comprising low molecular weight, PEG 300 the FMRs for apovitellenins III to V, increasing TLL increases the proportion of these proteins partitioning to the top phase (refer to Table 2.7). In ATPSs comprising PEG 1000, increasing the TLL leads to an increase in apovitellenin II to V partition to the interphase (and a concurrent decrease in these proteins to the top phase). In ATPSs comprising PEG 3350, the apovitellenins III to V partition preferentially to the interphase at lower TLLs. (similar to PEG 300). At increased TLL, these proteins partition to the top phase as the interphase becomes

saturated (with protein and debris). In ATPSs comprising PEG 6000 and 8000, the intermediate TLLs. However as these phases became saturated (with protein and debris), the apovitellenins partition to the top phase.

TLL (%w/w)	Short	Intermediate	Long
PEG Mwt. 300	N/A	(S3) 29: 71: 0	(S2) 60: 40: 0
PEG Mwt 1000	(S9) 73: 0: 27	(S8) 50: 12: 38	(S7) 6: 72: 22
PEG Mwt 3350	(S12) 0: 86: 14	(S11) 0: 100: 0	(S10) 41: 59: 0
PEG Mwt 6000	(S15) 7: 43: 50	(S14) 0: 53: 47	(S13) 18: 54: 28
PEG Mwt 8000	(S24) 0: 55: 45	(S23) 0: 59: 41	(S22) 11: 50: 39

TABLE 2.7. The effect of PEG molecular weight and TLL upon FMR of apovitellinins III to V.
The systems used were shown in brackets (refer to Appendix II), followed by the fractional mass ratios of protein in the top: interphase: bottom phase (see Section 2.2.4.2 for a fuller explanation). Definitions of short, intermediate and long TLL are given in Section 2.1.8.

2.3.2.3. Effect of PEG molecular weight and TLL upon Fractional Mass Ratios of (FMRs) of apovitellenin I.

In ATPSs comprising molecular weights PEG 300 to 8000, > 60 % apovitellenin I partitioned to the interphase regardless of TLL (refer to Table 2.8). It is unclear why apovitellenin I should display different partitioning behaviour from the other apovitellenins in these systems.

TLL (%w/w)	Short	Intermediate	Long
PEG Mwt. 300	N/A	(S3) 31: 69: 0	(S2) 10: 90: 0
PEG Mwt 1000	(S9) 0: 76: 24	(S8) 0: 62: 38	(S7) 0: 100: 0
PEG Mwt 3350	(S12) 0: 100: 0	(S11) 0: 100: 0	(S10) 0: 100: 0
PEG Mwt 6000	(S15) 0: 100: 0	(S14) 8: 70: 22	(S13) 4: 96 0
PEG Mwt 8000	(S24) 0: 92: 8	(S23) 17: 65:18	(S22) 25: 75: 0

TABLE 2.8. The effect of PEG molecular weight and TLL upon FMR of apovitellinin I.

The systems used were shown in brackets (refer to Appendix II), followed by the fractional mass ratios of protein in the top: interphase: bottom phase (see Section 2.2.4.2 for a fuller explanation). Definitions of short, intermediate and long TLL are given in Section 2.1.8.

2.3.2.4. Effect of PEG molecular weight and TLL upon Fractional Mass Ratios of (FMRs) of remaining contaminant proteins.

Although ovalbumin and apovitellenins III to V comprised the majority contaminants (> 70 % by mass) in IBF feedstock, other contaminating proteins included the phosvitins. Phosvitin B (the main phosvitin) partitioned exclusively to the top phase regardless of PEG molecular weight or TLL used (data not shown, but refer to Figure 2.6, Band E to observe the solitary protein band between 20 and 30 kDa). Minor phosvitins such as E_1 partitioned in a manner similar to apovitellenin I.

2.3.3. Selection of ATPSs to fractionate protein contaminants from influenza virus particles.

The results using SDS PAGE gels and FMR data demonstrate that the virus favours the interphase at all TLLs and PEG molecular weight used in this study. This occurs because adsorption to the interface lowers the free energy of the system by lowering the

interfacial area (Walter *et al*, 1991). Systems that were especially useful in partitioning virus particles to the interphase were those comprising PEG 300 (and long TLL), 3350 (and short to intermediate TLL) and PEG 8000 (any TLL used in the study). The ATPSs comprising PEG 3350 were discontinued for use because of co-purification of contaminant proteins (particularly the apovitellenins). Also such systems were subject to impaired recovery of proteins (especially in systems of long TLL, for example S10). This result was in agreement with the findings regarding partitioned PZC and egg white (Appendix AI). Employing systems comprising PEG 300 and long TLL facilitated the partition of ovalbumin away from the interphase (see Table 2.6). Such PEG molecules are relatively hydrophilic and ovalbumin is a hydrophilic protein (Liu *et al*, 1995), thus this protein partitions to the phase that it is most compatible with. However, ovalbumin displayed a bottom phase preference in PEG 8000-based ATPSs (see Table 2.6). Thus it must be more compatible with the salt-rich phase in such systems. At least 50 % (by mass) of the apovitellenins III to V partitioned preferentially to the interphase regardless of the PEG molecular weight or TLL used (refer to Table 2.7). These proteins are lipoproteins, which possibly interact with membranous debris (or co-habit with the debris) at the interphase. Only S2 (comprising PEG 300 and long TLL) displayed a degree to elimination of these proteins to the top phase. This could be due to exclusion of these proteins to the top phase (as membraneous debris increases at the interphase upon increasing the TLL). The partition behaviour of the apovitellenins III-V proteins was similar because they were related, (Burley and Sleigh, 1980). Also included was the partition behaviour of apovitellenin VI, whose oxidation products have molecular weights in the same range as apovitellenin III-V. The behaviour of apovitellenin I could be explained by its ability to bind to lipids (possibly on the viral membrane) and to form

aggregates (Burley, 1975). This implies that it would be difficult to remove from the virus. The reason for the behaviour of phosvitin B was because it is highly phosphorylated (Joubert and Cook, 1958; Wallace and Morgan, 1986a). Interactions with phosphate anions cause repulsion from the bottom phase into the top phase. Although PEG molecules possess a lone pair of electrons on the ether oxygen, and there is a low concentration of phosphate present in the top phase, any possible repulsion effects between phosvitin B and PEG are expected to be minimal as compared to those between phosvitin B and the phosphate-rich phase. From point of view of elimination of contaminant proteins from the virus, the partition behaviour of phosvitin B is advantageous. The minor Phosvitins E_1 showed similar partition trends to the apovitellenin I (suggesting that these proteins are less phosphorylated than phosvitin B). These phosvitins are derived from different vitellogenin subunits than phosvitin B (refer to Figure 2.5) so maybe this is not surprising. The fact that these phosvitins could be observed at all suggested powerful resolution of ATPS as a technique since Wallace and Morgan, (1986a) had to undertake a lengthy centrifugation step to obtain these proteins. Livetins were not identified since they would have been associated with apovitellenin III-V at high salt concentration (Burley, 1978).

To conclude, on the basis of the FMR data presented here, ATPSs comprising low PEG molecular weight (and long TLL) or high PEG molecular weight (and low to intermediate TLL) would be useful for removing key protein contaminants ovalbumin and apovitellenins III to V. The fact that apovitellenin I and the minor phosvitins were not removed from the virus particles at the interphase was not critical at this stage since they could be separated further downstream using a unit operation (such as ultrafiltration) which could separate these low molecular weight contaminants from the

larger proteins. In addition, these proteins constitute approximately 20 % (by mass) of the protein contaminants (refer to Figure 2.7), so these proteins should not ultimately pose a problem for their removal from the process stream. Thus ATPSs that met the criteria discussed were ATPS S2 (PEG 300 20.0 % w/w/ phosphate 20.0 % w/w, pH 7.5, TLL, 43.4 % w/w) and ATPS S23 (PEG 8000 15.0 % w/w/ phosphate 11.1 % w/w, pH 7.5, TLL, 22.4 % w/w) and are investigated later. The required manipulations of PEG molecular weight and TLL to direct contaminating proteins away from virus particles at the interphase are summarised in Table 2.9.

The SDS PAGE/densitometry method was useful to monitor the distribution of the viral and contaminating proteins both qualitatively and quantitatively, allowing deduction of Fractional Mass Ratios (FMRs). The main source of error was introduced by the precipitation of proteins using TCA. An estimation of this error was determined by measuring the IBF concentration. This concentration, deduced by the method based on Lowry *et al*, (1951) was 1.4 $mgml^{-1}$ (± 18 %). This is similar to the value deduced using SDS PAGE/densitometry of 1.5 $mgml^{-1}$. The samples analysed using the Lowry Method were TCA precipitated which gives an indication of the error in the densitometry technique. It was previously noted that Coomassie Brilliant Blue stain produced differential staining effects of proteins (lysosyme and phosvitin B). The fact that the latter protein is highly phosphorylated and the dye is anionic in character meant that there would be repulsion between them and less binding. Use of a cationic dye such as Stains-all would have circumvented this (Wallace and Morgan, 1986a).

The behaviour of viral and contaminating proteins in IBF feedstock can be explained in terms of excluded volume and salting out effects. A summary of these effects upon PEG molecular weight and TLL are depicted in Figure 2.10.

	Top		Bottom	
Protein	**TLL**	**PEG Mwt.**	**TLL**	**PEG Mwt.**
OA	↑	↓	↓	↑
Apo III-V	↑	↓	↓	↑
Apo I	↓	↔	↔	↔
PB	↔	↔	N/A	N/A

TABLE 2.9. A summary of manipulations of PEG molecular weight and TLL required to direct contaminating proteins away from influenza virus particles in IBF feedstock.

The virus particles partition preferentially to the interphase, therefore the contaminant proteins must be directed away from this phase. Proteins such as ovalbumin (OA) are responsive to their environment and their partition can be manipulated by changing the PEG molecular weight and TLL. Other contaminating proteins such as apovitellenin 1 (Apo I) and phosvitin B (PB) are unresponsive to their environment so that manipulation of PEG molecular weight and TLL are not useful. This suggests that these proteins possess physico-chemical characteristics, which dominate their partition (see main text for details).

Key: N/A not applicable;

Decrease the parameter; ↓

Increase the parameter; ↑

Parameter insensitive. ↔

The virus favoured partition to the interphase at all TLLs and PEG molecular weights used. Systems of short TLL were precluded from use due to their low salting out

capacity. Systems of intermediate or long TLLs (and any PEG molecular weight in the range investigated) were suitable for use. Selection of optimal ATPSs depended upon how the contaminants partitioned in these systems. It can be concluded that ATPSs S2 (PEG 300 20.0 % w/w/ phosphate 20.0 % w/w, pH 7.5, TLL, 43.4 % w/w) and ATPS S23 (PEG 8000 15.0 % w/w/ phosphate 11.1 % w/w, pH 7.5, TLL, 22.4 % w/w) both met the required criteria. The next stage of the ATPS screening process involved further investigation of the candidate systems (S2 and S23), examining the effect of volume ratio manipulation upon fractionation of IBF material.

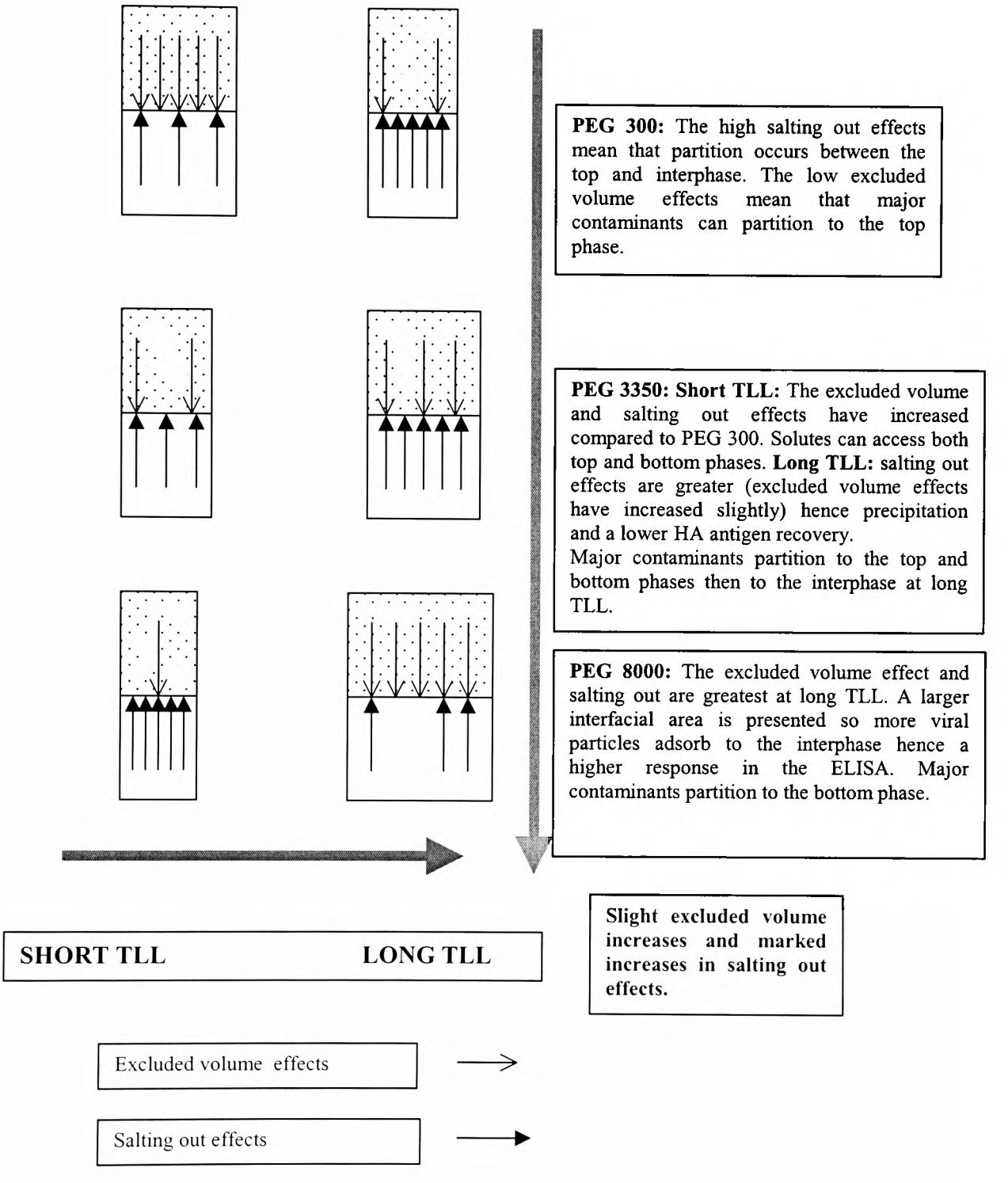

FIGURE 2.10. The effect of PEG molecular weight and TLL upon partition of IBF.

Schematic summarising the partitioning effects in PEG-phosphate ATPSs with Vrds of value unity. The partition behaviour is interpreted in terms of excluded volume and salting out effects. The widths of tubes represent the interfacial area.

2.3.4. Rationale for volume ratio manipulation.

Aqueous two-phase systems using extremes of PEG molecular weight appeared useful for selectively partitioning the IBF material. The virus partitioned preferentially to the interphase. The harvesting and preparation of the interphase on small scale could be quite time-consuming and difficult to undertake on larger scale. Therefore it was decided to ease this harvesting concern and take advantage of the observation that partition of proteins in these systems was between the interphase and a bulk phase. In the case of PEG 300, the bulk phase was the top phase (therefore the bottom phase was virtually free of proteins as judged by the analytical techniques used). For PEG 8000, the opposite was true. Low starting volumes would also be advantageous from a processing point of view. One way of achieving this using ATPS would be to manipulate the volume ratio and concentrate the product into a smaller top or bottom phase volume. The ATPSs that showed potential in the processing of IBF were systems S2 (PEG 300 20.0 % w/w/ phosphate 20.0 % w/w, TLL 43.3 % w/w, pH 7.5) and S23 (PEG 8000 15.0 % w/w/ phosphate 11.1 % w/w, TLL 22.4 % w/w, pH 7.5). Proteins partitioned preferentially between the top phase and interphase in the former ATPS and between the interphase and the bottom phase in the latter. These ATPSs were used as starting points from which to manipulate the volume ratio (see the schematic phase diagrams showing the manipulation of the volume ratio along the tie-line, Figures 2.11 and 2.12). In the PEG 300-based ATPSs, the top and interphase/bottom phases were harvested and in the PEG 8000-based ATPSs the top/interphase and bottom phases were harvested. The data was analysed using SDS PAGE/densitometry (as Section 2.3.2).

System identification number (PEG 300-based ATPS).	Volume ratio (Vrd)	System identification number (PEG 8000-based ATPS).	Volume ratio (Vrd)
S 2	1.33	S23	1.06
S25	1.50	S30	0.69
S26	1.92	S31	0.50
S27	6.00	S32	0.29
S28	7.80	S33	0.20
S29	Monophasic		

TABLE 2.10. Table listing the volume ratios (Vrds) of ATPSs used in volume ratio manipulation study.
The ATPSs S2, (TLL, 43.4 % w/w) and S23, (TLL, 22.4 % w/w) were useful in directing contaminant proteins away from the virus particles contained in IBF feedstock (see Section 2.3.2). The volume ratios of these systems were manipulated to obtain further process advantages in the purification of IBF. Refer to the schematics depicted in Figures 2.11 and 2.12 and to Appendix II for details of these systems.

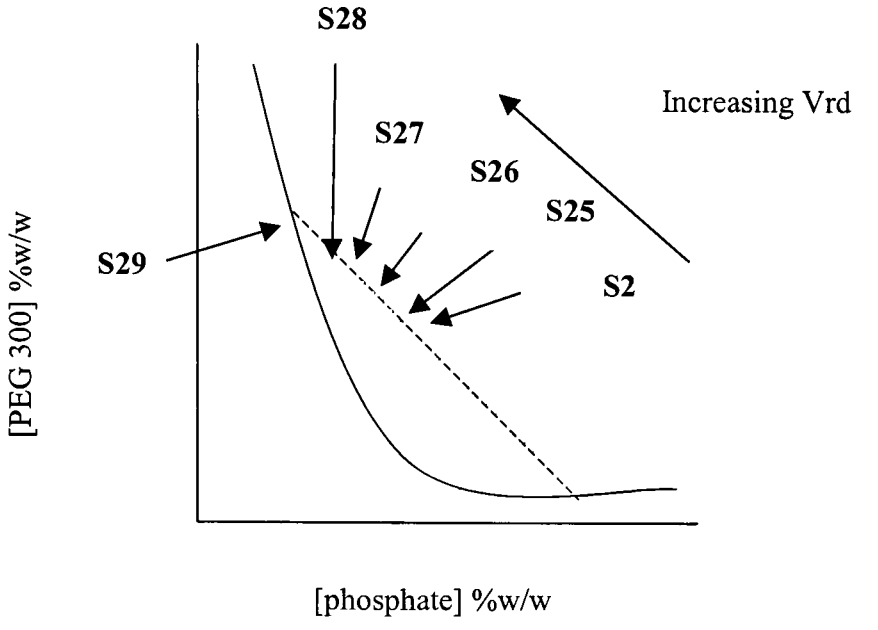

FIGURE 2.11. An illustration of the phase diagram and position of the PEG 300 ATPSs used in the manipulation of volume ratio (Vrd).
Refer to Appendix II for a complete list of systems used. See also Table 2.11 for details of the Vrds of these systems.

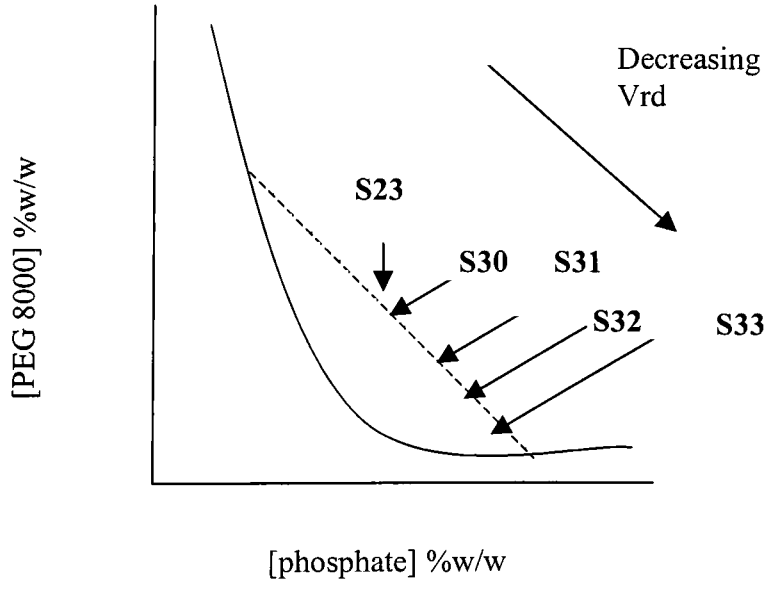

FIGURE 2.12. An illustration of the phase diagram and position of the PEG 8000 ATPSs used in the manipulation of volume ratio (Vrd).
Refer to Appendix II for a complete list of systems used. See also Table 2.11 for details of the Vrds of these systems.

2.3.4.1. Manipulation of volume ratio in ATPSs comprising PEG 300 and effect on FMR deduced by SDS PAGE and one-dimensional densitometry.

The data presented in Table 2.11 derives from the gels depicted in Figures 2.13 and 2.14. Manipulation of the Vrd such that the move is towards higher concentrations of PEG 300 (see Figure 2.11), increased the volume ratio. This resulted in ATPSs with a progressively smaller interphase/bottom phase. The FMR was redefined since the partition was essentially being monitored between two phases: top phase: interphase/ bottom phase (see Equation 2.6c for definition).

	ATPS				
PROTEINS	**S2**	**S25**	**S26**	**S27**	**S28**
> 97 kDa	1.9	IB	IB	IB	IB
Apo VI	NS	NS	IB	IB	IB
Apo III-V	7.2	12.6	0.4	4.3	2.0
HA_1/NP/NA	**IB**	**0.9**	**NR**	**0.2**	**IB**
OA	6.2	13.5	NR	1.7	1.8
HA_2/M	**IB**	**2.4**	**IB**	**0.4**	**IB**
PB	VF	T	NR	T	T
PE_1/F	VF	VF	VF	VF	VF
Apo I	1.3	1.5	1.5	IB	IB
INCREASING Vrd →					

TABLE 2.11. Summary table indicating the effect of volume ratio upon partitioning individual proteins within IBF material in PEG 300 ATPS (TLL, 43.4 % w/w).
The > 97 kDa protein refers to higher molecular weight species believed to be derived from higher molecular weight apovitellenins. The samples (from top phase and interphase/bottom phase) originated from SDS PAGE gels (Figures 2.13 and 2.14 respectively) and analysed using Quantiscan™ software, Biosoft. The viral proteins are highlighted in bold typeface. See Table 2.10 for details of system volume ratio.
Data for S29 was not shown since its corresponding blank ATPS was monophasic and therefore had not originated from the same TLL as S2 and S25 to 28 inclusive.
***Key:** NR: No result; NS: Not seen; VF: Very faint;* T: exclusive partition to the top phase; IB: exclusive partition to the interphase/bottom phase.

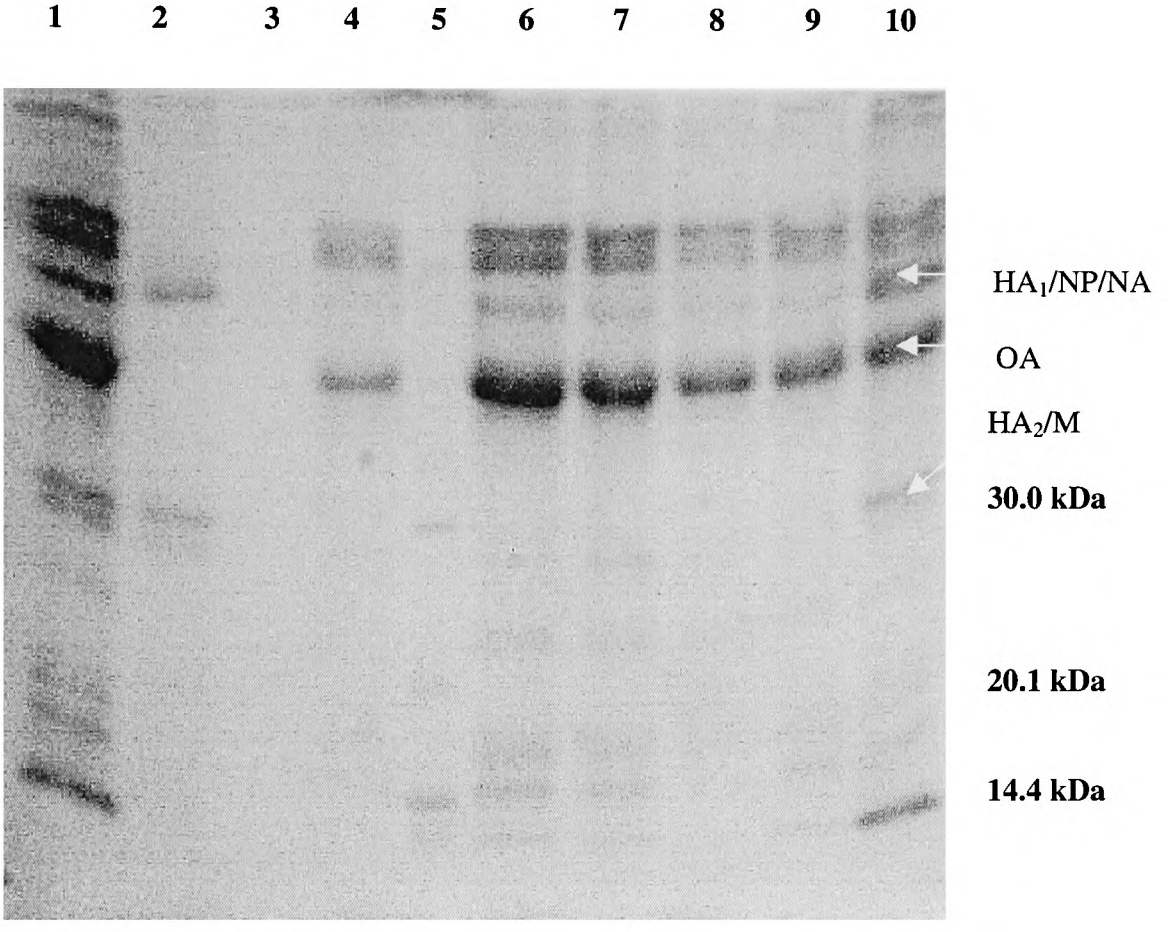

FIGURE 2.13. Partition of IBF material in PEG 300 ATPS of increasing Vrd (top phase samples).

Systems S2, S25 to S29 (all with of TLL 43.4 % w/w) were loaded with 20 % w/w IBF material used in Fluvirin™ processing (refer to Section 2.1.6) and partitioned as described in (Section 2.2.2). The top phase samples were prepared for analysis on 12 % SDS PAGE gels (see Section 2.2.3). Samples of IBF (pre-partition) and PZC were also shown for comparison. A volume of 150 µl sample was loaded into each lane. Refer to Table 2.11 for details of volume ratios of these ATPSs.

Lane 1: *IBF 112.5 µg protein.*
Lane 2: *PZC 45.0 µg protein.*
Lane 3: *Unused.*
Lane 4: *Top phase from S2 (PEG 300 20.0 % w/w/ phosphate 20.0 % w/w).*
Lane 5: Low molecular weight markers (5 µl load).
Lane 6: *Top phase from S25 (PEG 300 22.2 % w/w/ phosphate 17.9 % w/w).*
Lane 7: *Top phase from S26 (PEG 300 25.5 % w/w/ phosphate 15.0 % w/w).*
Lane 8: *Top phase from S27 (PEG 300 32.2 % w/w/ phosphate 10.0 % w/w).*
Lane 9: *Top phase from S28 (PEG 300 32.5 % w/w/ phosphate 8.4 % w/w).*
Lane 10: *Top phase from S29 (PEG 300 32.2 % w/w/ phosphate 7.3 % w/w).*

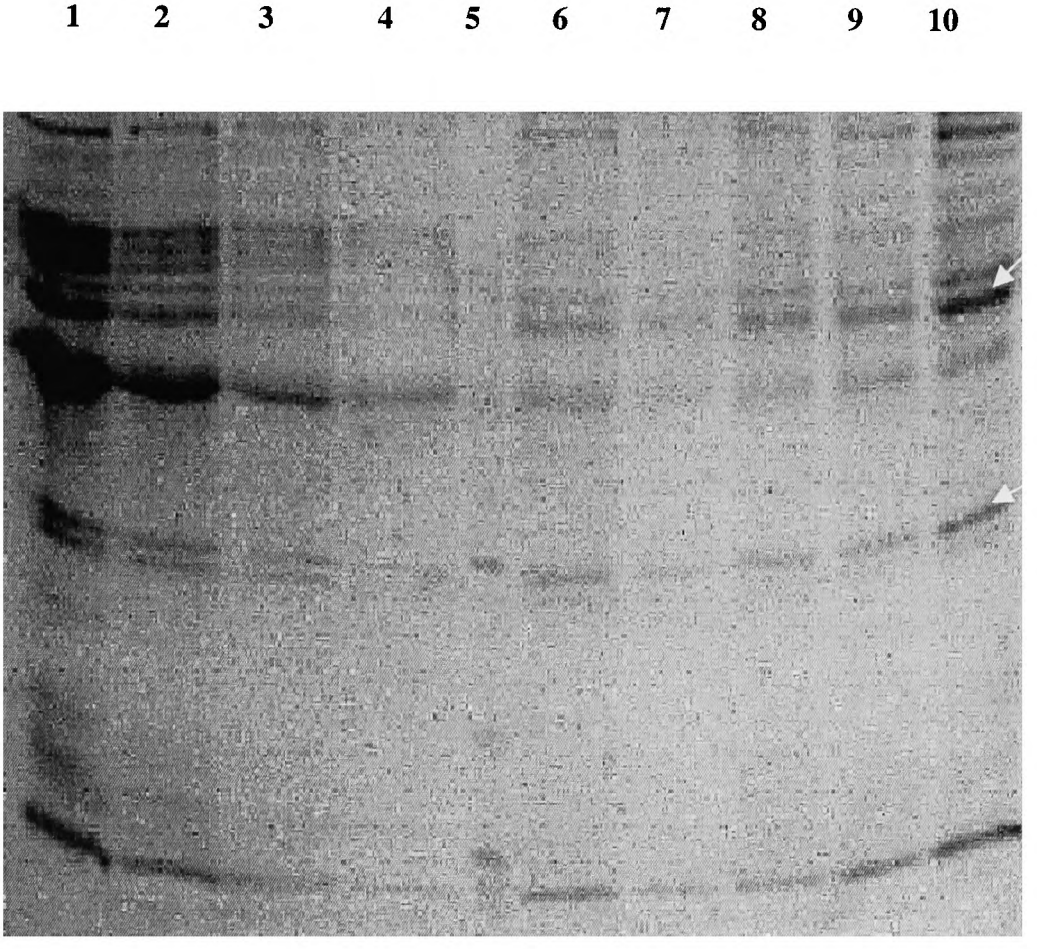

FIGURE 2.14. Partition of IBF material in PEG 300 ATPS of increasing Vrd (interphase/ bottom phase samples).
Systems S2, S25 to S29 (all with of TLL 43.4 % w/w) were loaded with 20 % w/w IBF material used in Fluvirin™ processing (refer to Section 2.1.6) and partitioned as described in (Section 2.2.2). The interphase/bottom phase samples were prepared for analysis on 12 % SDS PAGE gels (see Section 2.2.3). Samples of IBF (pre-partition) and PZC were also shown for comparison. A volume of 150 µl sample was loaded into each lane. Refer to Table 2.11 for details of volume ratios of these ATPSs.

Lane 1: *IBF 112.5 µg protein.*
Lane 2: *IBF 56.3 µg protein*
Lane 3: *IBF 28.1 µg protein.*
Lane 4: *IBF 14.1 µg protein*
Lane 5: Low molecular weight markers (5 µl load).
Lane 6: *Interphase/ bottom phase from S2 (PEG 300 20.0 % w/w/ phosphate 20.0 % w/w).*
Lane 7: *Interphase/ bottom phase S25 (PEG 300 22.2 % w/w/ phosphate 17.9 % w/w).*
Lane 8: *Interphase/ bottom from S26 (PEG 300 25.5 % w/w/ phosphate 15.0 % w/w).*
Lane 9: *Interphase/ bottom from S27 (PEG 300 32.2 % w/w/ phosphate 10.0 % w/w).*
Lane 10: *Interphase/ bottom from S28 (PEG 300 32.5 % w/w/ phosphate 8.4 % w/w).*

Thus the aim here was to concentrate this phase in order to ease its harvest. For information regarding the volume ratios used in this study, refer to Table 2.10. The FMR value was defined as the ratio of masses of target protein between the top phase and the interphase/bottom phase (Equation 2.6c). Since the virus preferentially partitions to the interphase, for successful fractionation of the contaminating proteins away from the virus, the contaminants should generate a relatively large FMR. The HA_1/ NP/NA proteins were located almost exclusively in the interphase/bottom phase in most of the ATPSs used (refer to Table 2.11). The HA_2/M followed a similar trend except with S25 where there was partition of these proteins to the top phase. The FMRs of the major contaminants (apovitellenins III to V and ovalbumin) were greatest with S25 (which demonstrated a two-fold increase in FMR, giving values of 12.6 and 13.5 for apovitellenins III to V and ovalbumin, respectively). Thus S25 demonstrated the most efficient removal of these key contaminants from the interphase/bottom phase with little loss of the virus. The > 97 kDa and apovitellenin I proteins co-purified with the virus in the interphase/bottom phase at all volume ratios used (however, as discussed in Section 2.3.3, this was not significant at this stage). Partition of phosvitin B partitioned independently of the volume ratio used (as it did with the TLL and PEG molecular weight used) and showed a top phase preference. The minor phosvitins also favoured this phase. The poor staining intensity of these bands was partly due to their relative low abundance, dilution effects in the ATPS and in the case of phosvitin B its highly phosphorylated state (as previously discussed).

2.3.4.2. Manipulation of volume ratio in ATPSs comprising PEG 8000 and effect on FMR deduced by SDS PAGE and one-dimensional densitometry.

Manipulation of the Vrd such that the move is towards lower concentrations of PEG 8000 (see Figure 2.12), decreased the volume ratio. This results in ATPSs with a progressively smaller top phase/interphase. The aim here was to concentrate this phase in order to ease its harvest. For information regarding the volume ratios, please refer to Table 2.10. The FMR was redefined since the partition was essentially being monitored between two phases: top phase/interphase: bottom phase (see Equation 2.7c for definition).

	ATPS				
PROTEINS	**S23**	**S30**	**S31**	**S32**	**S33**
> 97kDa	0.8	TI	TI	TI	TI
Apo VI	TI	TI	TI	TI	TI
Apo III-V	0.1	0.6	0.6	0.6	0.6
HA_1/NP/NA	**0.6**	**2.2**	**2.5**	**2.0**	**2.7**
OA	0.0	0.4	0.2	0.2	0.3
HA_2/M	**NR**	**1.3**	**1.3**	**1.7**	**1.9**
PB	VF (TI)	VF (TI)	TI	VF (TI)	VF (TI)
PE_1/F	0.2	B	NR	NR	TI
Apo I	1.0	TI	TI	TI	TI

DECREASING Vrd ⟶

TABLE 2.12. Summary table indicating the effect of volume ratio upon partitioning individual proteins within IBF material in PEG 8000 ATPS (TLL, 22.4 % w/w).
The > 97 kDa protein refers to higher molecular weight species believed to be derived from higher molecular weight apovitellenins. The samples (from top phase and interphase/bottom phase) originated from SDS PAGE gels (Figures 2.15 and 2.16 respectively) and analysed using Quantiscan™ software, Biosoft. The viral proteins are highlighted in bold typeface. See Table 2.10 for details of system volume ratio.

Key: *NR: No result; NS: Not seen; VF: Very faint;* TI: exclusive partition to the top phase/interphase; B: exclusive partition to the bottom phase.

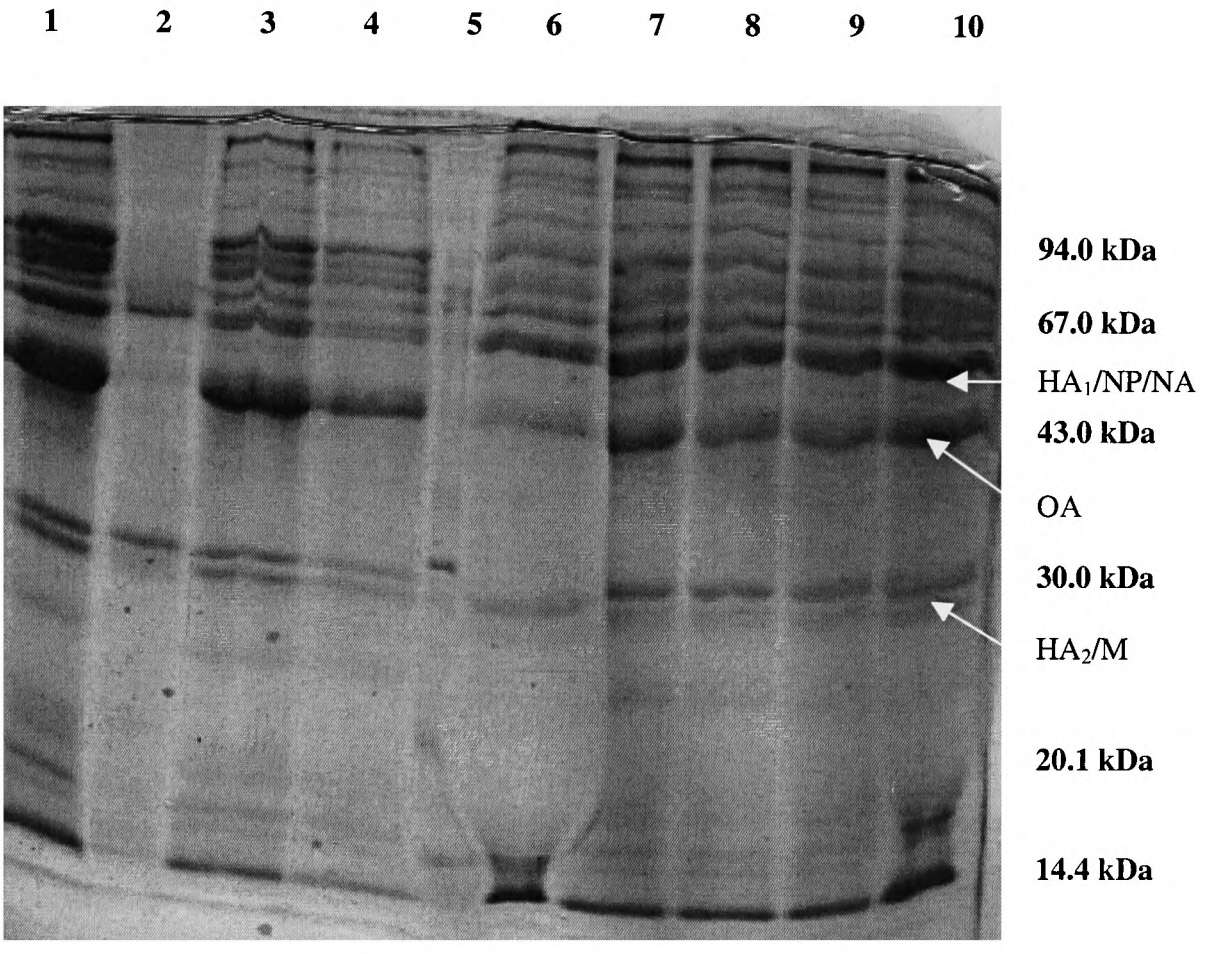

FIGURE 2.15. Partition of IBF material in PEG 8000 ATPS of decreasing Vrd (top/ interphase samples).

Systems S23, S30 to S33 (all with of TLL 22.4 % w/w) were loaded with 20 % w/w IBF material used in Fluvirin™ processing (refer to Section 2.1.6) and partitioned as described in (Section 2.2.2). The top/interphase bottom phase samples were prepared for analysis on 12 % SDS PAGE gels (see Section 2.2.3). Samples of IBF (pre-partition) and PZC were also shown for comparison. A volume of 150 µl sample was loaded into each lane. Refer to Table 2.11 for details of volume ratios of these ATPSs.

Lane 1: *IBF 112.5 µg protein.*
Lane 2: *IBF 56.3 µg protein*
Lane 3: *IBF 28.1 µg protein.*
Lane 4: *IBF 14.1 µg protein*
Lane 5: Low molecular weight markers (10 µl load).
Lane 6: *Top phase/ Interphase from S23 (PEG 8000 15.0 % w/w/ phosphate 11.1 % w/w).*
Lane 7: *Top phase/ Interphase from S30 (PEG 8000 12.5 % w/w/ phosphate 12.2 % w/w).*
Lane 8: *Top phase/ Interphase from S31 (PEG 8000 10.0 % w/w/ phosphate 13.5% w/w).*
Lane 9: *Top phase/ Interphase from S32 (PEG 8000 7.2% w/w/ phosphate 15.3% w/w).*
Lane 10: *Top phase/ Interphase from S33 (PEG 8000 5.3 % w/w/ phosphate 16.3 % w/w).*

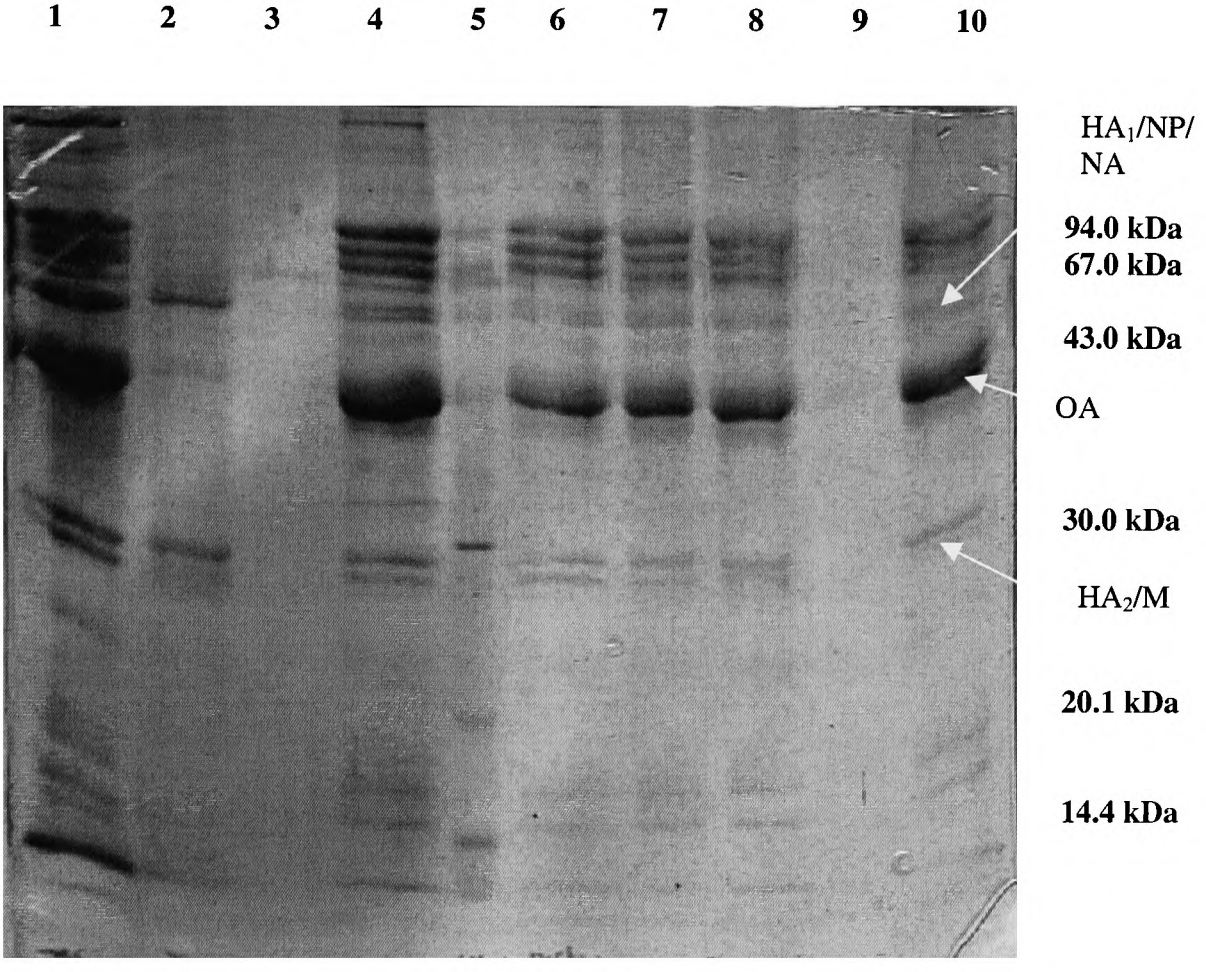

FIGURE 2.16. Partition of IBF material in PEG 8000 ATPS of decreasing Vrd (bottom phase samples).

Systems S23, S30 to S33 (all with of TLL 22.4 % w/w) were loaded with 20 % w/w IBF material used in Fluvirin™ processing (refer to Section 2.1.6) and partitioned as described in (Section 2.2.2). The bottom phase samples were prepared for analysis on 12 % SDS PAGE gels (see Section 2.2.3). Samples of IBF (pre-partition) and PZC were also shown for comparison. A volume of 150 µl sample was loaded into each lane. Refer to Table 2.11 for details of volume ratios of these ATPSs.

Lane 1: *IBF 112.5 µg protein.*
Lane 2: *PZC 45 µg protein.*
Lane 3: *Unused.*
Lane 4: *Bottom phase from S23 (PEG 8000 15.0 % w/w/ phosphate 11.1 % w/w).*
Lane 5: Low molecular weight markers (10 µl load).
Lane 6: *Bottom phase from S30 (PEG 8000 12.5 % w/w/ phosphate 12.2 % w/w).*
Lane 7: *Bottom phase from S31 (PEG 8000 10.0 % w/w/ phosphate 13.5% w/w).*
Lane 8: *Bottom phase from S32 (PEG 8000 7.2% w/w/ phosphate 15.3% w/w).*
Lane 9: *Unused.*
Lane 10:*Bottom phase from S33 (PEG 8000 5.3 % w/w/ phosphate 16.3 % w/w).*

Use was made of the parameter FMR (as defined in Section 2.2.4.2). Again, in this case only one FMR value was defined as the ratio of masses between the top phase/interphase and the bottom phase (see Equation 2.7c). For successful fractionation of the contaminant proteins away from the virus, the contaminant proteins should generate a relatively small FMR. The data presented in Table 2.12 demonstrated that the virus was located in the top/interphase fraction. The FMR increased slightly along the TLL (decreasing Vrd) indicating a small degree of concentration. The FMR values of ovalbumin and apovitellenin III to V are low (which is desirable) but there was no concentrating effect (since the PMR value did not alter significantly). The phosvitins and apovitellenin I co-purified with the virus in the top phase/interphase. To conclude manipulation of the volume ratio to concentrate the virus and remove contaminating proteins was most beneficial for PEG 300 ATPSs and in particular, ATPS, S25 (PEG 300 22.2 % w/w/ 17.9 % w/w phosphate, TLL 43.4 % w/w). Refer to Table 2.11.

2.4. Analytical Considerations.

2.4.1. PEG/salt vs PEG/Dextran ATPSs.

PEG-phosphate ATPSs were used in preference of PEG-Dextran systems because they were cheaper. The fact that the cost doesn't change significantly over a wide variety of volume ratio (Kroner *et al*, 1984) makes these systems attractive since this parameter can be manipulated with little regard for cost unlike PEG-Dextran systems. Data using PEG-Dextran was not shown primarily because it showed no benefit over PEG 6000 or 8000. Such systems could be used satisfactorily only at low TLLs since the viscosity increased dramatically at intermediate and long TLLs (hampering the overall virus recovery). This coupled with knowledge regarding the physico-chemical nature of the

feedstock components can enable one to manipulate partition variables accordingly (for example, the use of PEG 300-based ATPS S2, demonstrated its usefulness in directing key protein contaminants away from the virus). The influenza virus partitioned to the interphase, (more energetically favourable) in this study at all PEG molecular weights employed (in the range of 300 to 8000) and with Vrd of unity. The emphasis then was in directing protein contaminants away from the virus. Partition behaviour of these proteins was explained in terms of excluded volume and salting out effects. The partition was also monitored using an HA antigen ELISA. This method could be potentially adapted to confirm the identities and quantitate impurities using Western blot techniques, (Towbin *et al*, 1979), probing with antibodies specific for other proteins (such as neuraminidase, ovalbumin and M protein), or for nucleic acids.

The IBF material proved extremely sensitive to storage with the highest level of HA detected in the order of material stored at –70 °C, –20 °C and 4 °C. Samples of IBF analysed by SDS PAGE could detect no such difference in band pattern. An explanation for the instability of IBF could be the presence of proteases and other enzymes from the host cell membrane that were isolated along with the virus and are often not removed using sucrose density ultracentrifugation (Rosenbergová *et al*, 1981).

The neuraminidase (NA) antigens could not be monitored using the NELLAM. It was believed that the NA tetrameric structure was damaged in the presence of PEG, thus preventing its use. The release of NA was compared to a calibration curve generated by using *V.cholerae* from bacteria the NA source (Ada *et al*, 1961). This may not have been useful and ideally an NA source from the same influenza strain should be used (since variation occurs even between strains, Cabezas *et al*, 1980). Ultimately this would not have been detrimental since the data generated would contain a consistent systematic

error. Another reason that detection of the virus could not rely on monitoring NA alone is that its activity could suddenly "nose-dive". One suggested explanation for this could be due to aggregation and reversible polymerisation (Cassidy *et al,* 1965).

2.4.2. System Characterisation.

To enable understanding of partition on the molecular level, the system must be fully characterised. This is not an easy task when the system contains biological biomass and debris. During this study the impact of PBS and thiomerosal (present in PZC) and uric acid in IBF upon the phase diagram was ignored. This would require further investigation. Walker, PhD Thesis, (1998) suggested that true partition equilibria are never reached because they are inhibited by material accumulation at the interphase. It was therefore suggested that one talks in terms of an effective equilibrium. Finally, an observation was that ATPS S24 (PEG 8000) spiked with egg white (total protein- 12.5 mg) produced no visible interphase (see Appendix I). The same ATPS loaded with IBF (3 to 5 mg total protein) produced an interphase. This suggested that it is not necessarily the amount of protein loaded into a system that determines the formation of an interphase, but the composition of these components. For example, IBF contains a high proportion of lipoproteins (especially apovitellenin I known to aggregate at the pH used in this study).

Thus in conclusion, the study in this chapter has demonstrated the usefulness of SDS PAGE/ one-dimensional densitometry in monitoring the partition behaviour of influenza virus proteins and also of the contaminant proteins. Manipulation of volume ratio was useful in PEG 300 based ATPSs. The system that showed optimal and selective removal of contaminating proteins (mainly ovalbumin and apovitellenins) and concentration of

virus was achieved using ATPS S25 PEG 300 22.2 % w/w/ phosphate 17.9 % w/w, pH 7.5). This system will be investigated in detail in Chapter Three.

CHAPTER THREE.

3. OPTIMISATION OF AQUEOUS TWO-PHASE SYSTEMS AND COMPARISON WITH ULTRACENTRIFUGATION IN PROCESSING INACTIVATED BULK FLUID GENERATED BY THE MEDEVA FLUVIRIN™ PROCESS.

3.1. INTRODUCTION.

3.1.1. Proposed purification strategy using ATPS.

The ATPS S25 (PEG 300 22.2 % w/w / 17.9 % w/w phosphate, pH 7.5) was useful in partitioning virus and contaminating proteins to different phases. This system was incorporated in the strategy outlined in Figure 3.1. The virus particles and debris partitioned predominantly to the interface of the ATPS, forming an interphase, similar to that described (see Section 2.1.8). Removal of the top phase of this primary ATPS eliminated a significant proportion of the contaminant proteins (approximately 50 % by mass, as quantitated using densitometry). Options for harvesting nanoparticles, (such as influenza virus) from an interphase include (i) repartitioning into a second ATPS to maximise target particle yield and (ii) decreasing the interfacial tension of the primary ATPS to make particle adsorption to the interface less favourable, thereby facilitating true partition. The former option appeared to work with inclusion bodies, when some degree of phase selectivity existed already between polymer and salt-rich phases (Walker, PhD thesis, 1998). However, if (like the virus), partition was directed predominantly to one phase, then repartitioning the interphase would not be expected to do this. Therefore the latter option was taken. The interfacial tension (predominantly responsible for interphase formation) was reduced by use of a surface-active agent: (a detergent) and also by attempting to reduce the tie line length of the resulting secondary hybrid system. In such experiments, the interphase and bottom phase were harvested as

though a single discrete phase. This was justified by previous data, which demonstrated that no detectable protein (viral or otherwise), partitioned to the bottom phase. It was envisaged that harvesting the interphase and bottom phase together would circumvent the practical problems associated with harvesting discrete interphases at enhanced scales. The laboratory scale scheme (illustrated in Figure 3.1) employed an intermediate (blank) ATPS, which was constructed and the top phase removed. This phase was combined with the interphase/bottom phase from the primary ATPS and added detergent (for example Triton X100) to yield a hybrid system described as an aqueous-detergent two-phase system –ADTPS (Figure 3.1). The rationale behind using the ADTPS was to partition soluble antigens and detergent to the top phase whilst leaving contaminant proteins and core material in the interphase/bottom phase.

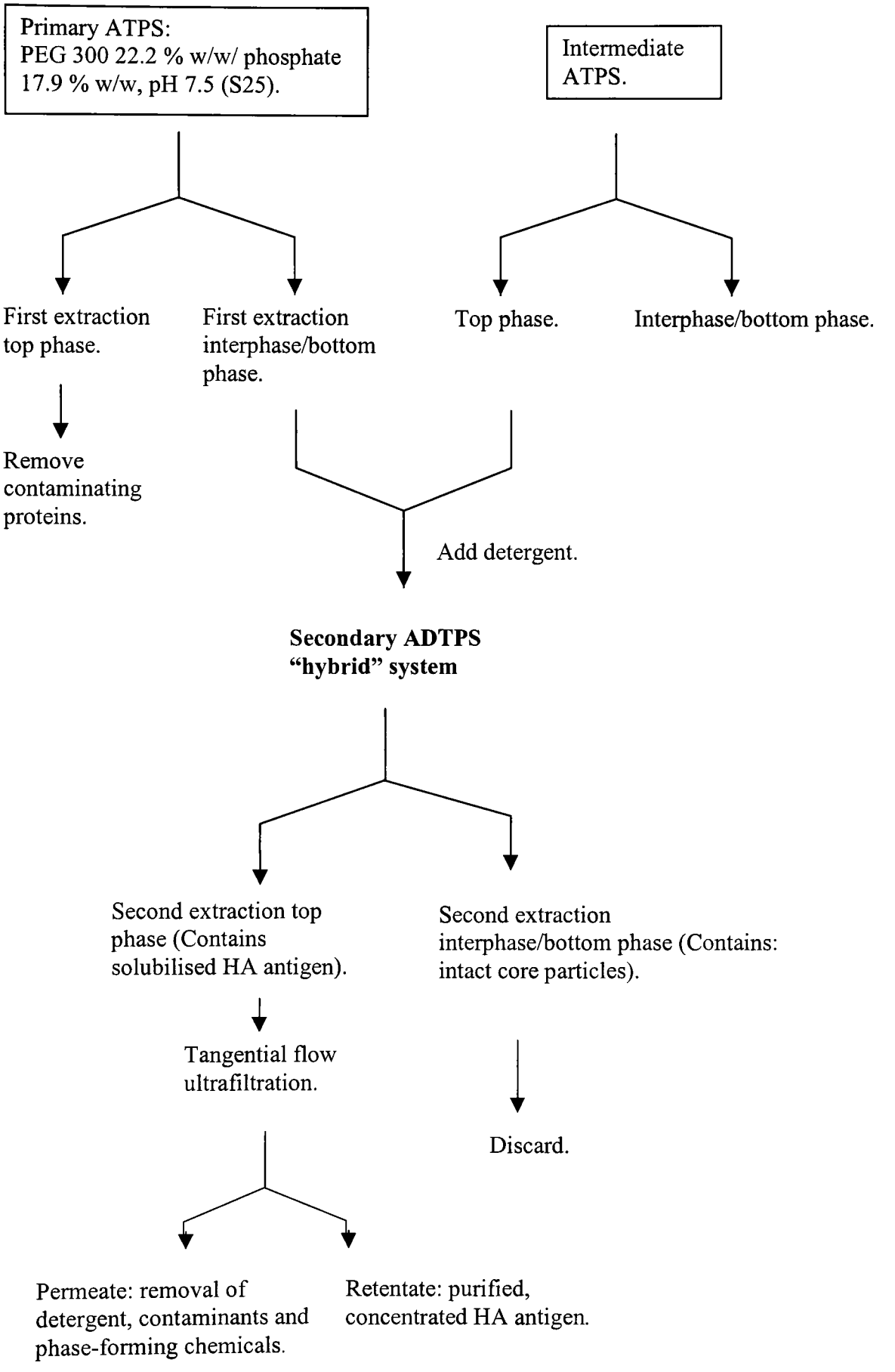

FIGURE 3.1. Proposed lab-scale route to purified HA antigen production from IBF material.

3.1.2. Solubilisation Study.

The production of Fluvirin™ subunit vaccine is possible because of selective release of surface antigens haemagglutinin (HA) and neuraminidase (NA) with detergent using sucrose density gradient ultracentrifugation (see Figure 2.4). Method development underpinning the Medeva Fluvirin™ Process relied upon screening a range of detergents for optimal detergent and operating concentration (Hjelmland and Chrambach, 1984; Hjelmland, 1990). The ability of ultracentrifugation to discriminate between the solubilised surface antigens and the denser intact core material permitted the separation of these components (Brady, PhD Thesis, 1974; Brady and Furminger, 1976a). The schematic depicted in Figure 3.2, illustrates typical situations encountered when monitoring detergent solubilisation of surface antigen from purified influenza virus in the ultracentrifuge. Analysis of resulting fractions collected from the ultracentrifuge during the run is undertaken using refractive indices to monitor sucrose concentration and absorbance at 280 nm, to monitor protein concentration. Such a scheme was employed in the detergent screening in the Medeva Fluvirin™ Process (Brady, PhD Thesis, 1974).

Profile "A" (Figure 3.2) is a typical profile obtained when the virus particles are completed disrupted. The viral components are located in sucrose of low concentration, approximately 20 % w/v (corresponding to a density of 1.081 g ml^{-1} at 20 °C, Bates, 1942). Profile "B" (Figure 3.2) is typical of selective solublisation of the surface antigens (as described by Bachmayer, 1975). The HA and NA antigens are located in sucrose of low concentration, approximately 20 % w/v, whilst the intact core material remains in sucrose of high concentration, approximately 40 % to 50 % w/v (corresponding to densities of 1.176 to 1.230 g ml^{-1} at 20 °C, Bates, 1942). Profile "C" (Figure 3.2) is

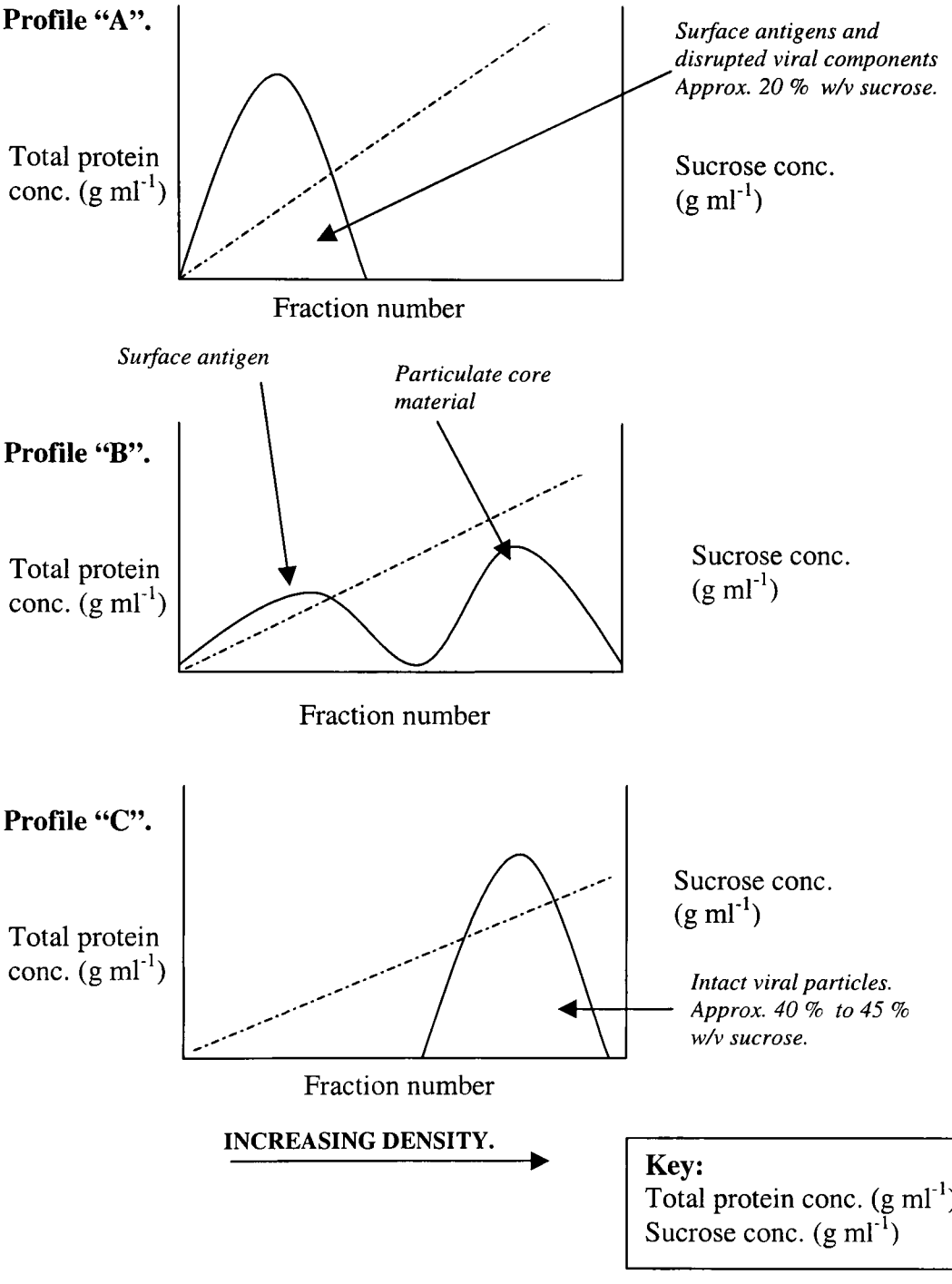

FIGURE 3.2. Schematic illustrating the possible outcomes when detergent is incubated with influenza virus and subjected to ultracentrifugation using a sucrose density gradient. Taken from Brady, PhD Thesis, (1974).

Profile "A". Depicts the virus in a fully disrupted state.

Profile "B". Depicts virus with solubilised HA and NA antigens leaving behind the dense core material.

Profile "C". Depicts the profile obtained when the detergent has been unable to solubilise surface antigen from the whole virus.

A detergent that produced a similar profile to Profile "B" (that is, maximum antigen release) would be judged suitable for further utilisation in an aqueous two-phase system.

"B". Maintaining intact core particles are important in simplifying the purification scheme, since the nucleoproteins, polymerase proteins and non-structural proteins (Figure 2.1 and Table 2.1) are contained inside.

In order to identify potential detergents that could selectively release surface antigens from influenza particles partitioned in an ATPS (as proposed in Figure 3.1), it was decided to use the same evaluation method as that used to develop the Medeva Fluvirin™ Process. Nonionic detergents were preferred to ionic ones since they would be less denaturing (Makino *et al*, 1973).

3.1.3. Considerations at the outset of the solubilisation study.

The use of detergents in an ATPS raises several concerns, which are summarised as follows. Modification of the established phase separation may occur such that new, more complex systems would require re-characterisation. Methods must be established to assess the efficiency of antigen release and to distinguish between solubilised and non-solubilised antigens. Consideration must also be given to removal of detergent from the partitioned product.

3.1.4. Description of detergents.

A detergent consists of soluble amphiphilic molecules with surface-active (or more generally interfacial-active) properties (Helenius and Simons, 1975). They migrate to surfaces or interfaces in solution and act by decreasing the surface (or interfacial) tension, thereby assuming the most energetically favourable location in a particular system (Tanford, 1980). Detergents are broadly classified as non-ionic, zwitterionic and ionic in character (Tanford and Reynolds, 1976; Helenius *et al*, 1979). Representative

detergent structures are depicted in Figure 3.3 from each of these classes. Nonionic detergents in common use consist mainly of polyoxyethylenes (the Triton series) and the bile salts (for example, deoxycholate). The molecular structure of polyethylene glycol (PEG) (refer to Figure 3.3) is shown to share some commonality with the structure of the polyoxyethylene detergents.

3.1.5. Properties of a detergent.

A detergent can be characterised by the ability of its monomers to self-aggregate and form micelles. This change, (from monomer to micelle), occurs abruptly over a narrow concentration range, known as the critical micellar concentration (CMC). The CMC also refers to the maximum chemical potential of a monomer (Neugebauer, 1994). Micellization is illustrated in Figure 3.4. The structure of a monomer influences the structure and size of the micelle (Neugebauer, 1990). Micelle structure can also be influenced by other parameters such as temperature, pH, ionic strength, and residual impurities from detergent manufacture. Micelle structure and size are of consequence in the removal of detergent by final downstream purification techniques, which depend upon parameters such as size or charge discrimination. Another parameter used to characterise polyoxyethylene detergents is the hydrophile-lipophile balance (HLB) number (Griffin, 1949). This number expresses the hydrophilic character of a detergent. It can be either calculated or determined empirically. Thus, the larger the HLB number (usually between 12 to 20), the greater the hydrophilic nature of the detergent. The aggregation number refers to the number of monomers required to form a micelle. Table 3.1 gives the properties of some commonly used detergents including those selected for use in this study.

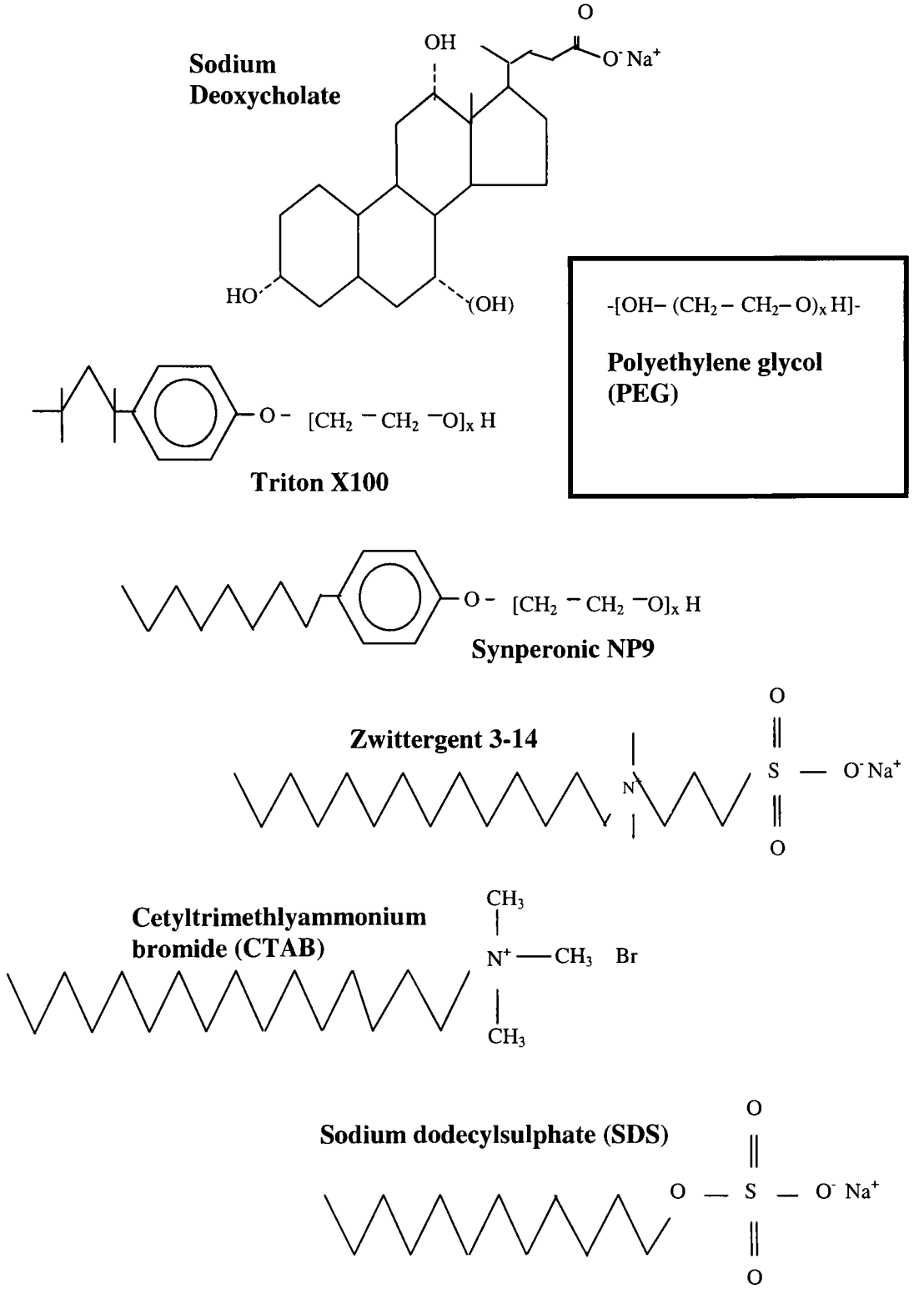

FIGURE 3.3. Structures of commonly-used detergents including those used in the solubilisation study.

The detergent structures illustrated are representative of the main detergent classes (see main text this Section). The structure of PEG is included in the insert for comparison with polyoxyethylene detergent structures.

Trade Name.	Monomer molecular weight.	CMC (mM).	Aggregation number (N).	HLB.	Micellar Mwt (kDa).
Triton X100	628	0.240	140	13.5	90 (in water)
Triton N101	625	0.085	No data	13.4	No data
Synperonic NP9	625	Similar to Triton N101	No data	12.8	Poss. larger than Triton X100
Sodium deoxycholate	415	* 4 **2.4	* 2-3 **19.9	N/A	1.7-4.2
Zwittergent 3-14	364	0.1-0.4	83	N/A	30
Sodium dodecyl sulphate (SDS)	288	8.2	60	N/A	18 (in water)
Cetylammonium bromide (CTAB)	336	3.5	169	N/A	62 (in 0.013M KBr)

TABLE 3.1. Properties of the detergents used in the solubilisation study.
The data was taken from Helenius and Simons, 1975; Hjelmland and Chrambach, 1984 and Neugbauer, 1990. Data for SDS and CTAB are shown for comparison. Data from Synperonic NP9 was disclosed by ICI.
** > pH 8 ** > pH 8 in 0.15M NaCl.*

3.1.6. Mechanism of antigen release from whole virus using a detergent.

The stages of lipid membrane solubilisation are well documented, (Hjelmland, 1990) and involve stepwise binding of detergent monomers to the membrane, structural lysis and formation of mixed micelles. Such micelles contain a combination of detergent-lipid, detergent-lipid-protein, or detergent-protein. Detergents selected for application in this

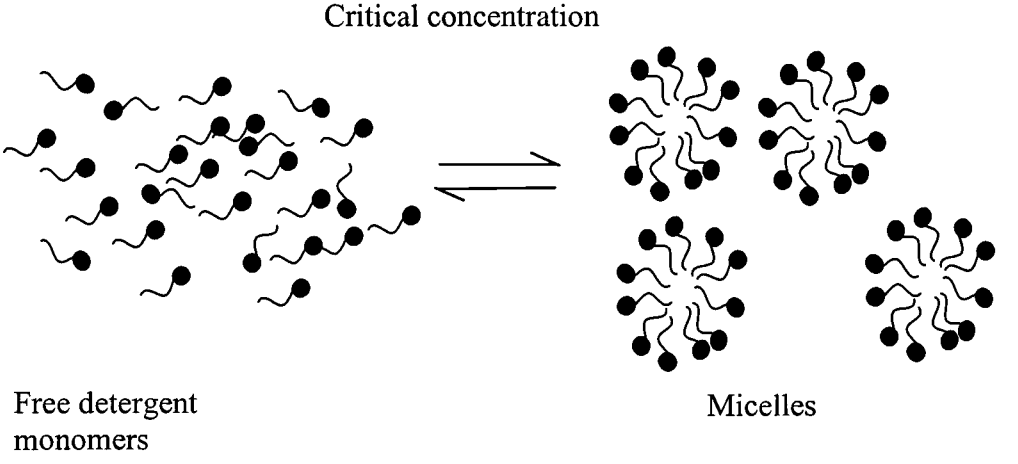

FIGURE 3.4. Micellization of detergent molecules.
Note the arrangement of the micelles. The hydrophilic head groups are in contact with the aqueous environment whilst the hydrophobic, hydrocarbon "tails" form an inner core. The micelles (illustrated in two-dimension) are actually spherical, typical of structural micelles formed by detergents such as Triton X100 used herein.

study included Triton X100, Synperonic NP9 and sodium deoxycholate Triton X100 was chosen because it is commonly used as a solubiliser of biological membranes (Helenius and Simons, 1975; Meyer *et al*, 1992; Hjelmland, 1990). Synperonic NP9 was used because it shares structural commonality with Triton N101 that is currently used in the Medeva Fluvirin™ Process. Sodium deoxycholate was used because it is representative of the bile salt class of non-ionic detergents (see Figure 3.3).

3.1.7. Selection of aqueous two-phase systems used in the optimisation study.

The aqueous two-phase system, ATPS (S25) consisting of PEG 300 22.2 % w/w/ phosphate 17.9 % w/w pH 7.5, concentrated the virus at the interface, whilst major contaminating proteins from allantoic fluid partitioned to the top phase (see Chapter Two). It was concluded that a system of relatively long tie-line length (TLL) and low PEG molecular weight was required for high recovery of virus within an interface and bulk removal of contaminants to the top phase. After the physical removal of the top phase, a successful second stage extraction would involve release of surface antigen (using a selected detergent) from the virus into the top phase. A system of short TLL and high molecular weight of PEG would be expected to promote the partition of viral surface antigens into one of the bulk phases (see Figure 3.5). The intermediate systems used were based on systems of short TLL previously used (refer to Table 3.2 and Appendix II).

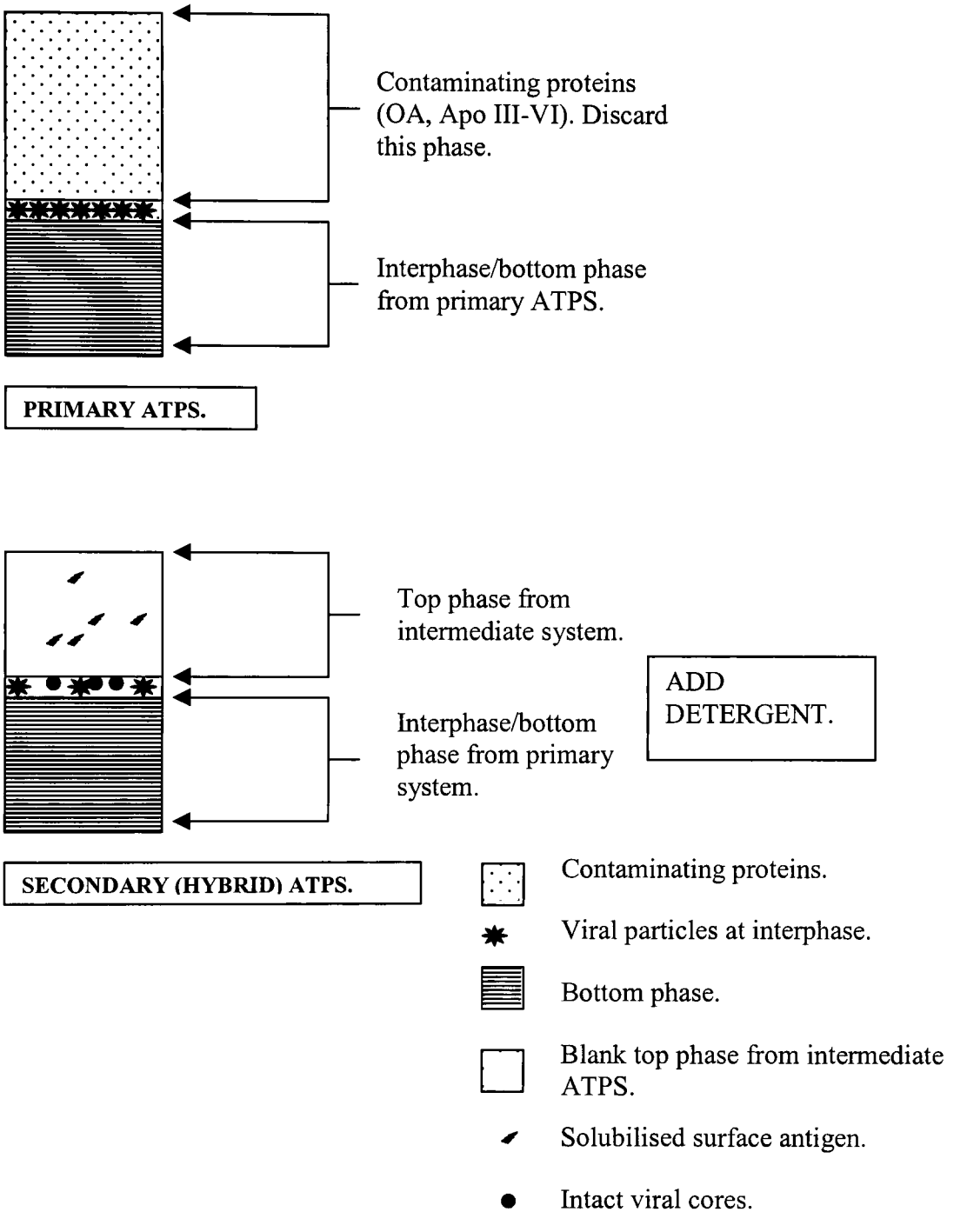

FIGURE 3.5. Schematic proposing the solubilisation of surface antigens (HA and NA) from influenza virus particles.
This figure gives a pictorial representation of the scheme outlined in Figure 3.1. The primary ATPS (S25) comprises PEG 300 22.2 % w/w/ phosphate 17.9 % w/w, pH 7.5. Identities of the intermediate and the resulting secondary (hybrid) ATPSs used are presented in Tables 3.2 and 3.3 respectively. The addition of detergent was expected to release HA and NA into a smaller top phase (thus concentrating the antigens).

3.1.7.1 System nomenclature.

As discussed previously (Section 2.1.9) ATPSs in the presence of biomass or detergent are not the same as their parent blank system. For convenience the same system number was used regardless of whether the system was loaded with biomass or detergent. For example, S39 used in this study (see Table 3.3) is also referred to as S39 in the presence of biomass or detergent.

3.1.8. Tangential flow ultrafiltration.

Once the antigens had been selectively released from whole partially purified virus, the final steps would necessarily involve removal of the phase formants, the detergent and contaminating proteins. (*British Pharmacopoeia* guidelines require the major contaminant ovalbumin, should be at a level of less than 1 μg ovalbumin per 15 μg HA dose in the final product). Although there are other ways in which this could be achieved (for example size exclusion chromatography or dialysis), ultrafiltration was selected because the material from the ADTPS could be both dialfiltered and concentrated, (Veide *et al*, 1984). Tangential flow filtration is a frequently used industrial protein separation process (van Reis *et al*, 1991; Millipore Technical Bulletin, 1992). Theoretically it could be used for handling the feedstock produced by the ADTPS study because of its ability to separate molecules on the basis of size. In contrast to size exclusion chromatography, the resulting solution would not be subject to dilution.

3.2. MATERIALS AND METHODS.

All materials were sourced from Sigma (Dorset, UK) unless otherwise stated.

3.2.1. Preparation of ATPS with detergent.

The primary ATPS S25 (described in Figure 3.1; see also Appendix II) used in this study was composed of PEG 300 (22.2 % w/w) and monobasic:dibasic phosphate in the ratio 18:7 (17.9 % w/w) pH 7.5 (± 0.5 pH units). System S25 was constructed by adding the required amounts of phase-forming chemicals along with 2 g Inactivated Bulk Fluid (IBF) material and Milli-Q water into a clean, pre-weighed 15 ml centrifuge tube (Sarstedt) to give a system of total mass of 10 g. This amount of added IBF (A/Sydney batch 753134) represented a loading of 20 % w/w of the total ATPS. Strains A/Panama (Batch 756303) and B/Yamanashi (Batch 756302) were used in subsequent experiments. The intermediate ATPSs (in Figure 3.1; see also Table 3.2) were constructed as for the loaded system but without the IBF material. The ATPSs were mixed for one hour at 22 °C (± 3 °C) using a blood rotator (Stuart SB1) and then centrifuged at 2000 *xg* for 5 minutes (centrifuge: C422 Jouan). The top phase of S25 was collected for analysis. The combined masses of the collected interphase/bottom phase (from S25) and the top phase of the intermediate ATPSs were determined. The appropriate mass of a 10 % w/w detergent stock solution (in Milli-Q water) was added to give a final detergent concentration of 1 % w/w. The various detergents were all used without further purification. The resulting hybrid aqueous-detergent two-phase system, (ADTPS), see Figure 3.5 was mixed for selective periods between one or four hours and then centrifuged as previously described. The top phase and interphase/bottom phases were

separated and analysed by ELISA and SDS PAGE. Blank hybrids ADTPs were also constructed for characterisation and analytical purposes.

PEG molecular weight.	Intermediate ATPS. PEG (%)/ Phosphate (%).	Root ATPS. PEG (%)/ Phosphate (%).	TLL (% w/w).	Volume ratio (or Vrd).
PEG 300	10.0/30.0 (S34)	20.0/20.0 (S2)	43.4	0.38
PEG 300	10.0/25.0 (S35)	16.1/20.0 (S3)	28.3	0.36
PEG 1000	10.7/13.9 (S36)	12.0/13.0 (S9)	8.3	0.55
PEG 6000	10.0/ 9.1 (S37)	N/A	19.0	0.50
PEG 8000	8.3/10.0 (S38)	11.3/9.2 (S24)	13.8	0.52

TABLE 3.2. Intermediate ATPSs used in optimisation study.
Table 3.2 displays the intermediate ATPSs used in the optimisation study (refer to Figure 3.1 and the main text, Section 3.1.7). The systems S34 to S38 inclusive (see Appendix II) were chosen from systems of same TLL (and hence overall system composition) as the root ATPSs except the Vrd's were smaller. For convenience, the systems were identified by a number (S34 to S33 shown in brackets) next to the system composition to be used herein. See Appendix II for details of these systems. The Vrd's were estimated as described in Section 2.1.8.

PEG molecular weight of top phase used.	Secondary ATPS. PEG (%)/ Phosphate (%)	TLL (% w/w).	Volume ratio (Vrd).
PEG 300	16.8/22.9 (S39)	43.5	0.83
PEG 300	13.9/24.3 (S40)	35.3	0.93
PEG 1000	7.3/27.6 (S41)	29.4	0.56
PEG 6000	7.8/25.3 (S42)	34.7	0.52
PEG 8000	7.2/27.1 (S43)	33.9	0.44

TABLE 3.3. Secondary (hybrid) ATPSs used in optimisation study.
Table 3.3 displays the secondary ATPSs used in the optimisation study (refer to Figure 3.1 and the main text, Section 3.1.7). The system compositions and TLLs were estimated from corresponding blank systems (without IBF material or detergent), using the relationship between TLL and volume ratio (Huddleston et al, 1991b). For convenience, the Systems were designated with a number, (S39 to S43 shown in brackets) next to the system composition to be used herein. See Appendix II for details of these systems. . The Vrd's were estimated as described in Section 2.1.8.

3.2.2. Preparation of the sucrose ultracentrifuge gradient.

A 60 % w/w stock solution of sucrose was prepared in Milli-Q water. Sucrose densities and gradient preparation were described in Figure 3.6. Five millilitres of each gradient were layered into polycarbonate centrifuge tubes, maximum volume 38 mls, (Beckman). Each gradient component concentration contained detergent at a final concentration x % w/v selected from one of the following values: 0 % w/v, 0.01 % w/v, 0.05 % w/v, 0.1 % w/v, 0.5 % w/v, 1.0 % w/v or 5 % w/v. These concentrations were chosen to cover three magnitudes of concentration that might be used in solubilisation studies and so enable the determination of the optimal concentration(s) for membrane solubilisation. The detergents used were Triton X100, sodium deoxycholate and Synperonic NP9 (ICI, Middlesborough, UK). Once the gradients had been prepared and the purified zonal concentrate, (PZC, A/Beijing strain, batch 679) had been added, the centrifuge tubes were loaded onto a swinging bucket rotor (SW28, Beckman). The average radius (r_{av}) from rotor axis to the outer edge was 122.1mm (Beckman operation manual). The centrifuge (Beckman L-80) was programmed to run for 4 hours at 25,000 rpm (90, 000 *xg*) at 16 °C. After the run time had elapsed, fractions were carefully harvested by dipping the tip of a pipette into the top of the tube and withdrawing 3 ml aliquots. This procedure was repeated until all the fractions had been collected.

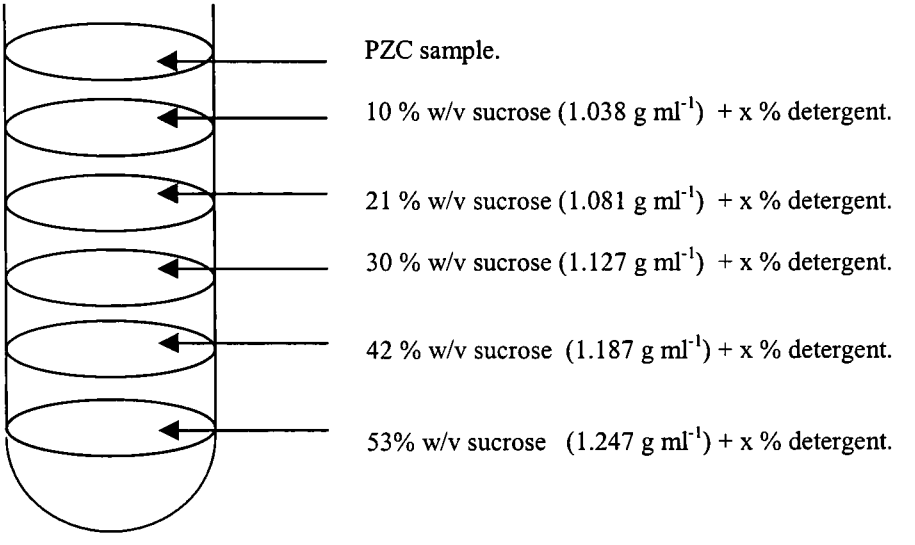

FIGURE 3.6. Schematic illustrating gradient preparation.
The gradient was loaded in order of densest to lightest sucrose solution. The sucrose densities (determined at 20 °C) were taken from Bates, (1942). The gradient were prepared either in the presence or absence of detergent at a final concentration of x % w/v (x can have a range of values from 0 to 5 % w/v (see main text Section 3.2.2).

3.2.2.1. Preparation of ultracentrifuge sucrose gradient (for assessment of antigen release post partition in an ADTPS).

Once the gradient had been prepared 3 to 5 ml of either top phase material or interphase/bottom phase material, which had been partitioned in the ADTPS hybrid system, was loaded onto the gradient (see Figure 3.6). The tubes were centrifuged as described in Section 3.2.2 except the period of centrifugation and temperature were altered to 16 hours at 4 °C to allow more time for migration of components in the gradient (see Section 3.3.1).

3.2.2.2. Determination of sucrose concentration using refractive indices.

The refractive index was determined for each fraction using a refractometer (Abbe), calibrated against distilled water at 20 °C. The sucrose concentration was estimated from a standard curve of sucrose or sucrose plus detergent.

3.2.3. Dialysis of samples to remove detergent and sucrose.

A cellulosic dialysis membrane (12 kDa MWCO) was used to dialyse samples generated in Section 3.2.2.1.

3.2.3.1. Preparation of the dialysis membrane.

This protocol was supplied by Sigma (Dorset, UK) and involved boiling the membrane for 30 minutes in a solution of 10 mM sodium bicarbonate plus 1 mM EDTA. This was followed by a five-minute wash in boiling Milli-Q™ water and two further washes in the same. After a cooling, the membrane was ready for use.

3.2.3.2. Sample Dialysis.

Fractions of volume 500 µl were added to microfuge tubes (with neat holes in their lid). The dialysis membrane was placed over the top of tube and the lid was closed firmly (Stage 1, Figure 3.7). The tubes were then briskly inverted to ensure their contents were in contact with the membrane (Stage 2, Figure 3.7), which was then immersed in the dialysis tank (containing 0.01M PBS pH 7.4). The contents of the tank were continually stirred for 18 hours ± 3 hours at 4 °C (Stage 3, Figure 3.7). After the dialysis, the tubes' exteriors were wiped dry and the samples were centrifuged for 30 seconds at 11,600 *xg*. The volume of each tube was noted. The dialysis efficiency was 70 % on the basis of total protein recovery BCA assay.

STAGE 1.
Preparing and loading the dialysis tube with sample.

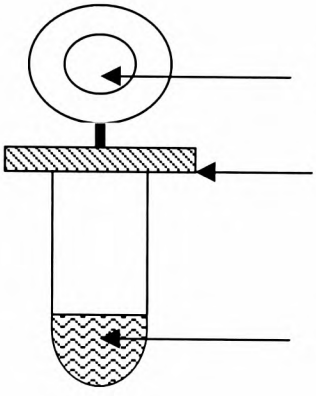

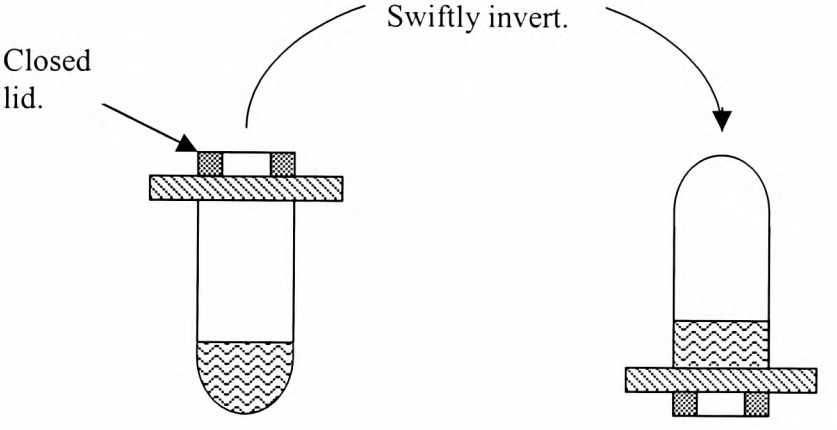

STAGE 2.
Placing dialysis membrane over the tube with sample and inversion.

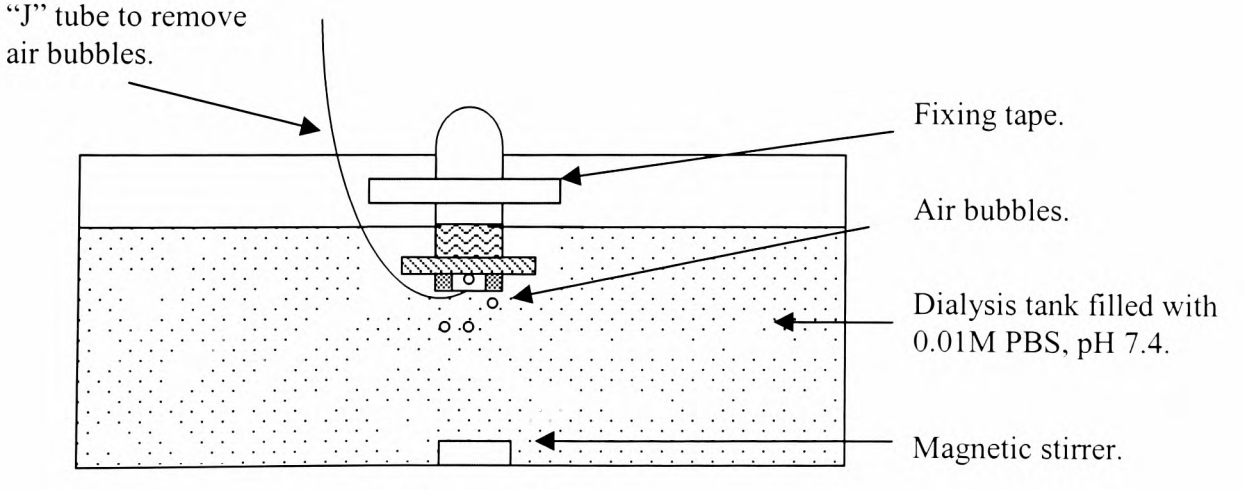

STAGE 3. Dialysis.

FIGURE 3.7. Illustration of the dialysis assembly used.
Details of dialysis are given in Section 3.2.3.

3.2.4. SDS PAGE/densitometry.

Homogenous mini gels containing 12 % acrylamide monomer and samples were prepared as described in Section 2.2.3 with the modification of using the method described by Bensadoun and Weinstein, (1976), which involved addition of 0.16 % w/v deoxycholate added to 50 % w/v cold TCA in a ratio of 1: 2. Volumes of 15 to 20 µl were loaded into each lane and the samples were electrophoresed at 125 V for approximately one hour. Low molecular markers (from AmershamPharmacia Biotech., Uppsala, Sweden) consisted of phosphorylase a (97 kDa), bovine serum albumin (67 kDa), ovalbumin (43 kDa), carbonic anhydrase (31 kDa), trypsin inhibitor, (21 kDa) and lysosyme (14 kDa). The gels were stained (Coomassie Brilliant Blue or silver stain), destained, dried and scanned (Ultroscan XL densitometer, LKB Pharmacia) as detailed in Section 2.2.4.

3.2.4.1. Estimation of total protein from fractions harvested in the Solubilisation Study using SDS PAGE gels.

Fractions from the Solubilisation Study (Section 3.1.2 and Figure 3.6) were analysed by SDS PAGE and one-dimensional densitometry. The amount of protein in each fraction was estimated by correlating the absorbance multiplied by area ratio (obtained by densitometry) from IBF relative to sample with the ratio of masses of protein in IBF relative to the sample. The amount of IBF loaded onto the gel and the proportion of haemagglutinin subunit 1, nucleoprotein and neuraminidase (HA_1/NP/NA) and haemagglutinin subunit 2 and matrix protein (HA_2/M) therein were known thus it was possible to deduce the amounts of these proteins in the samples.

3.2.4.2. Calculation of Purification factors.

Purification factors were used to assess the purity of material produced at each stage of the downstream process and to compare the efficiency of purification between ultracentrifugation and ATPS (refer to Section 3.3.8). This was undertaken using SDS PAGE/one-dimensional densitometry.

For example to calculate the purification factor between Inactivated Bulk Fluid (IBF), Stage 1 and Purified Zonal Concentrate (PZC), Stage 2:

Stage 1= Mass of surface antigen (HA_1 and HA_2) in IBF/ total proteins in IBF.

Stage 2 = Mass of surface antigen (HA_1 and HA_2) in PZC/ total proteins in PZC.

Purification Factor = Stage 2/ Stage 1 *Equation 3*

However the bands of viral proteins on the SDS PAGE gel not only included HA_1 and HA_2 surface antigens, but also matrix (M), nucleoprotein (NP) and neuraminidase (NA) proteins. The monoblend pool (MBP) material is the final stage product in the Medeva Fluvirin™ Process and consists essentially of surface antigen (no core material). To ensure accurate comparisons, the proportion of surface antigen in the viral bands on the gel in IBF and PZC was estimated to be 30 %. Thus the mass of viral protein on the gel was multiplied by 0.3 to estimate the amount of HA_1 and HA_2 in the intact virus.

3.2.5. HA antigen ELISA.

The HA standard was prepared by CBER, USA and consisted of purified whole virus. The total protein content was determined and the proportion of HA established by SDS PAGE and densitometry. A single radial immunodiffusion (SRD) test was undertaken to assign a potency value. This standard was referred to as the primary standard. A secondary standard was sourced at NIBSC and cross-calibrated with the CBER standard and assigned a potency value (50 to 100 μg HA antigen per ml depending on the batch). Where indicated, Tris- Buffered Saline (TBS) was used as a diluent instead of TBS/ 0.1% zwittergent 3-14.

3.2.5.1. Preparation of HA antigen standard.

The HA standards and antibodies used in these studies were kindly provided by Medeva Pharma, Liverpool, UK. The reference antigens used were: A/Beijing/262/95/X-127 and A/Sydney/5/97 Resvir -13 (CBER Ref. # 37). These were reconstituted in 1ml Milli-Q water. The anti-HA polyclonal antibodies used were: A/Beijing/262/95 CBER S-9606F2 and A/Sydney/97.

3.2.5.2. HA ELISA protocol.

A 96-well microtitre plate (Immunosorb™, Nunc) was coated with 0.1μg ml^{-1} concanavalin A (Con A) lectin. The plate was incubated overnight at 4 °C. The plate was washed twice in wash buffer (TBS/ 0.1 % v/v Tween 20) and then coated with 2 % w/v BSA/TBS to block non-specific binding. The plate was incubated at 25 °C (± 3 °C) for 90 minutes. The plate was washed again and the samples and HA standard were diluted in 0.1 % w/v zwittergent 3-14®, 3-(Tetradecyldimethylammonio) propane-1-sulfonate/ TBS and applied to the microtitre plate. After incubating the plate for 90 minutes, the

plate was washed and the anti-HA antibody was added (1/500 in 1 % w/v BSA/ TBS) and incubated for 60 minutes. The plate was washed and the donkey anti-sheep IgG peroxidase-labelled conjugate was added (1/1000 in 1% w/v BSA/ TBS) and the plate incubated for 90 minutes. After the wash step, the substrate para-nitrophenyl phosphate (pNPP) was added. Colour development at 405 nm was allowed to proceed until the top HA standard gave an optical density reading of 1. After subtracting the blank value from the reading, the HA concentration could be determined from the HA standard curve. The minimum level of detection of this assay was 0.1μg HA antigen per ml.

3.2.5.3. Estimation of mass balances for HA antigen.

The recovery of HA antigen from the ELISA was estimated as shown in Equation 3.1.

$$\text{Recovery (\%)} = \frac{C_{(\text{HA in Sample})} \times V_{(\text{Sample})}}{C_{(\text{HA in IBF})} \times V_{(\text{IBF})}} \times 100 \qquad \textit{Equation 3.1}$$

Where c = concentration of HA antigen (deduced from absorbance at 405 nm measurements) and v = volume of phase.

3.2.6. Tangential flow ultrafiltration.

A Millipore Labscale™ tangential flow system (see Figure 3.8) was used in conjunction with Pellicon Minicassettes containing a polyethersulfone membrane of nominal molecular weight cutoff of 100 kDa, (Pellicon XL™). The system was operated at an optimised transmembrane pressure (TMP) of 20 pounds per square inch (deduced from a flux versus TMP curve, see Figure 3.9).

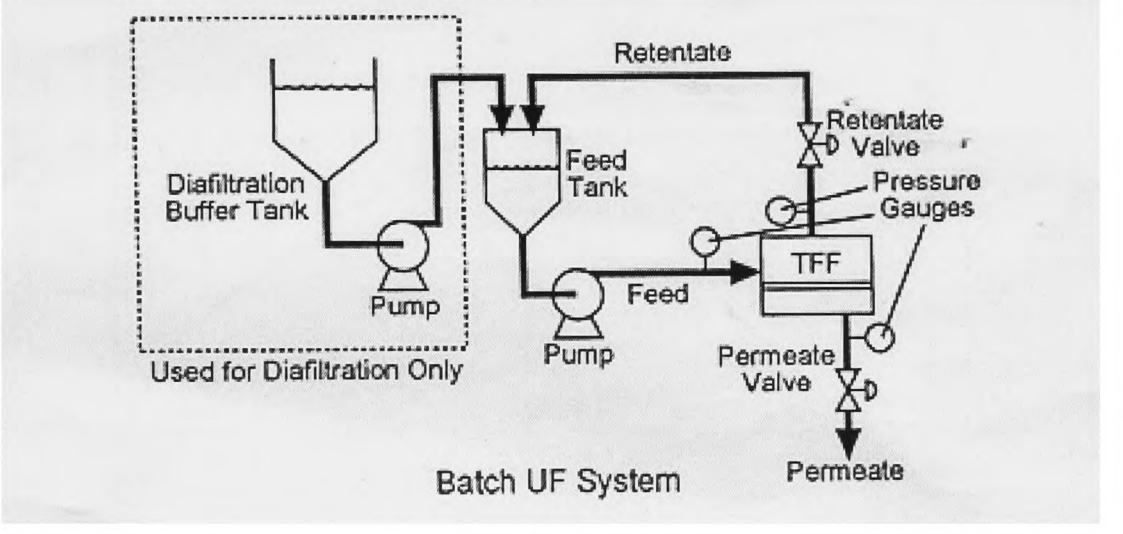

FIGURE 3.8. Experimental set-up used for diafiltration of ADTPS-partitioned IBF material.
This assembly, typical of the set-up described in Section 3.2.6, is reproduced from Zydney and Kuriyiel, (2000).

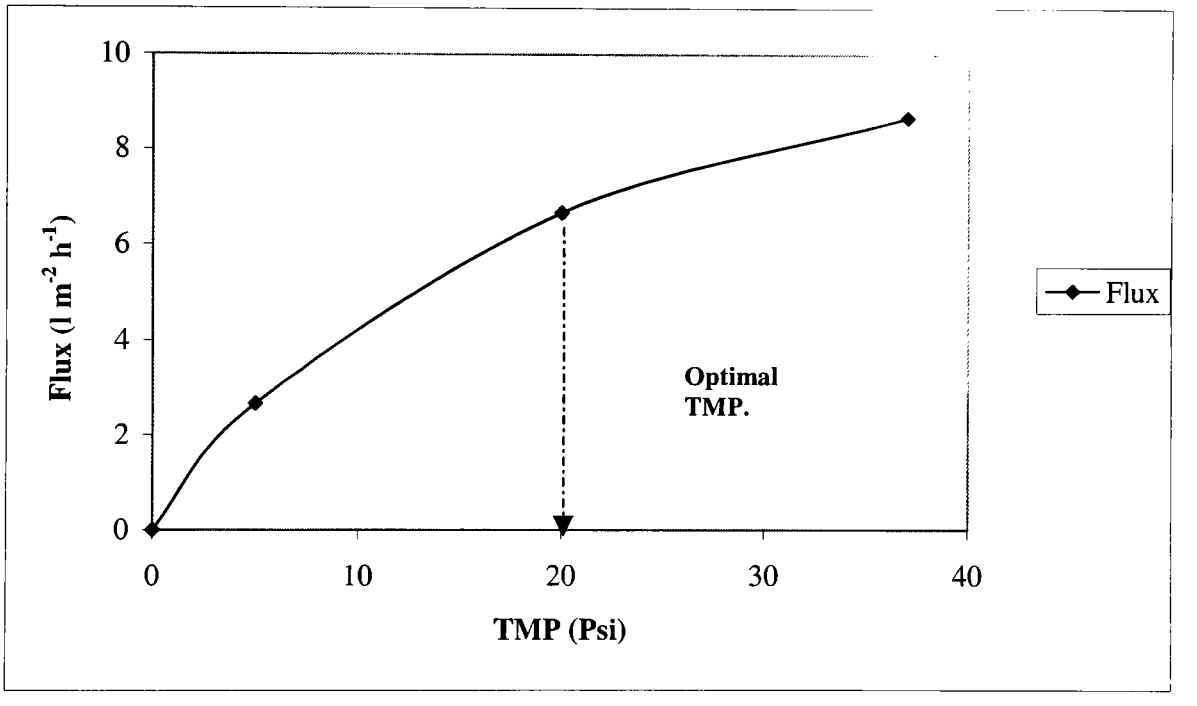

FIGURE 3.9. Estimation of optimum transmembrane pressure (TMP) from flux curve.
The maximum achievable TMP with minimal polarisation effect occurred at a TMP of 20 Psi (approximately 1.4 bar).

3.2.6.1. Membrane pre-conditioning.

The membrane was prepared by washing in Milli-Q water (2 litres), to remove membrane preservatives, followed by 0.1M NaOH (recirculation mode for 18 hours) to remove bacteria. A further 2 litres of Milli-Q water was flushed through membrane to remove the NaOH. Finally 0.1M NaCl primed the membrane to minimise charge-dependent binding (Millipore Technical Brief, Literature Number TB032, 1992).

3.2.6.2. Diafiltration in continuous mode.

Top phase material (80 ml) from the optimised hybrid ADTPS and containing partitioned influenza strain A/Panama, was diluted 1:4 in 0.01M PBS pH 7.4. This material was concentrated four-fold prior to diafiltration in continuous mode using times 2.5 diafiltration volumes. Permeate fractions (50 ml) were collected for mass balance analysis as described in Section 3.3.7.

3.2.7. A_{280} determination to estimate concentration.

The top phase samples were diluted 30 to 60 times in 0.01M PBS, pH 7.4, 100 µl placed in a small volume (100 µl) cuvette and read against an appropriate blank (accounting for the contribution of PBS and the phase-forming chemicals) at 280 nm (Ultrospec II, LKB). Bottom phase samples were analysed in the same manner, but without dilution.

3.2.7.1 A_{280} determination to estimate detergent mass balance in ADTPS.

The mass balances of detergent from absorbance at 280 nm was estimated as shown in Equation 3.2.

$$\text{Recovery (\%)} = \frac{C_{(A280 \text{ in partitioned sample})} \times V_{(\text{Sample})}}{C_{(A280 \text{ detergent})} \times V_{(\text{detergent used})}} \times 100 \qquad \textit{Equation 3.2}$$

Where c = concentration of detergent in sample (deduced from absorbance at 280 nm measurements) and v = volume of phase.

3.3. RESULTS AND DISCUSSION.

3.3.1. Solubilisation Study using PZC.

Purified Zonal Concentrate (PZC) was used in method development to ascertain the optimal detergent conditions to use in the ATPS. Ideally, the optimal detergent would be the lowest concentration of detergent that produced a profile similar to B (shown in Figure 3.2). The PZC was chosen since it contains purified viral proteins and other contaminant proteins would not complicate the profiles generated. Fractions from sucrose density ultracentrifugation (as described in Section 3.1.2) were analysed using SDS PAGE, one-dimensional densitometry and ELISA (specific for HA antigen). The amount of haemagglutinin subunit 1, nucleoprotein and neuraminidase (HA_1/NP/NA) and haemagglutinin subunit 2 and matrix protein (HA_2/M) in each fraction was estimated using SDS PAGE and one-dimensional densitometry as described in Section 3.2.4.1. Figures 3.10 to 3.12 depict typical data obtained when no detergent or relatively high and low concentrations of a detergent (for example 1 % w/w and 0.01 % w/w respectively) was added to the gradient. Triton X100 was selected here as an example. The total protein and HA antigen profiles track each other fairly well. In the absence of detergent, both the total protein and antigen signals were located at intermediate sucrose concentration (approximately 30 % to 35 % w/v sucrose). This was much lower than expected (in the Medeva Fluvirin™ Process, where intact viral particles were located in sucrose concentrations of 50 to 55 % w/v, personal communication with Medeva Pharma Development Scientists). Although the profile shown in Figure 3.10 (a) mimicked the expected profile for intact virus particles (Profile "C" in Figure 3.2), their precise location in the gradient was unexpected. The run time of four hours may have been insufficient to permit components to migrate to their true position in the gradient.

Although, under the conditions used, this profile still provided information as to where the intact particles were likely to be located. Subsequent use of ultracentrifugation employed longer processing times (see Section 3.2.2.1). The total protein profile depicted in Figure 3.10 (a) was broader than the corresponding profile obtained by monitoring the HA antigen (using absorbance at 405 nm). This was because the protein was estimated using SDS PAGE and densitometry (see Section 3.2.4.1) and thus includes NP and M protein as well as the HA proteins. The ELISA on the other hand, detects only the surface HA protein. The gradient location of virus in the presence of low Triton X100 concentration (0.01 % w/w) was similar to that in the absence of virus (compare Figures 3.10 and 3.11). However the total protein mass balance did not close. Since the ELISA mass balance data was not affected, it was suggested that this was due to the TCA method used (see Section 2.2.3.1). This method worked well in the absence of detergent but produced non-quantitative precipitation in the presence of low Triton X100 concentration. To confirm if this was the source of error, a standard protein of known concentration could be subjected to the precipitation in the presence and absence of Triton X100. In the presence of relatively high concentration of Triton X100 1 % w/w, a profile similar to Profile "B" (compare Figures 3.2 and 3.12a) resulted. This type of profile indicated that the surface antigens had been solubilised (in a sucrose concentration of 10 % to 20 % w/v), leaving intact core particles (in a sucrose concentration of approximately 45 % w/v). This is similar to the concentration in the Medeva Fluvirin™ Process. Possibly fraction pooling could have diluted the virus and thus account for the slightly lower concentration.

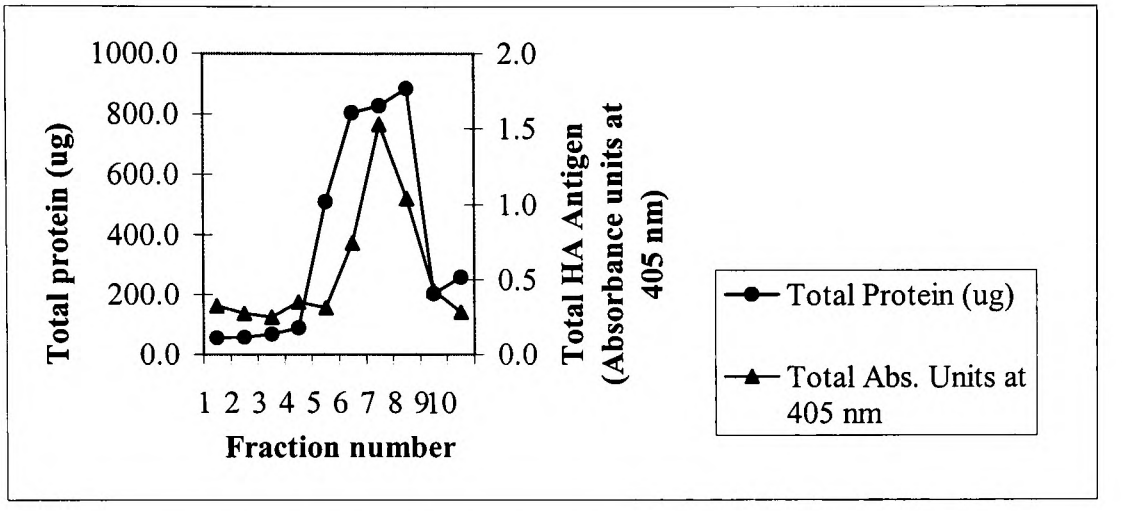

FIGURE 3.10 (a). Total protein (estimated using SDS PAGE and densitometry) and HA antigen profiles from sucrose density gradient ultracentrifugation in the absence of Triton X100.

Fractions of 3mls were collected and analysed (see main text) for total protein and HA antigen content. The resulting profile indicates that the protein is located in Fractions 5 to 10 (corresponding to sucrose concentrations of approximately 24 % to 47 % w/v).

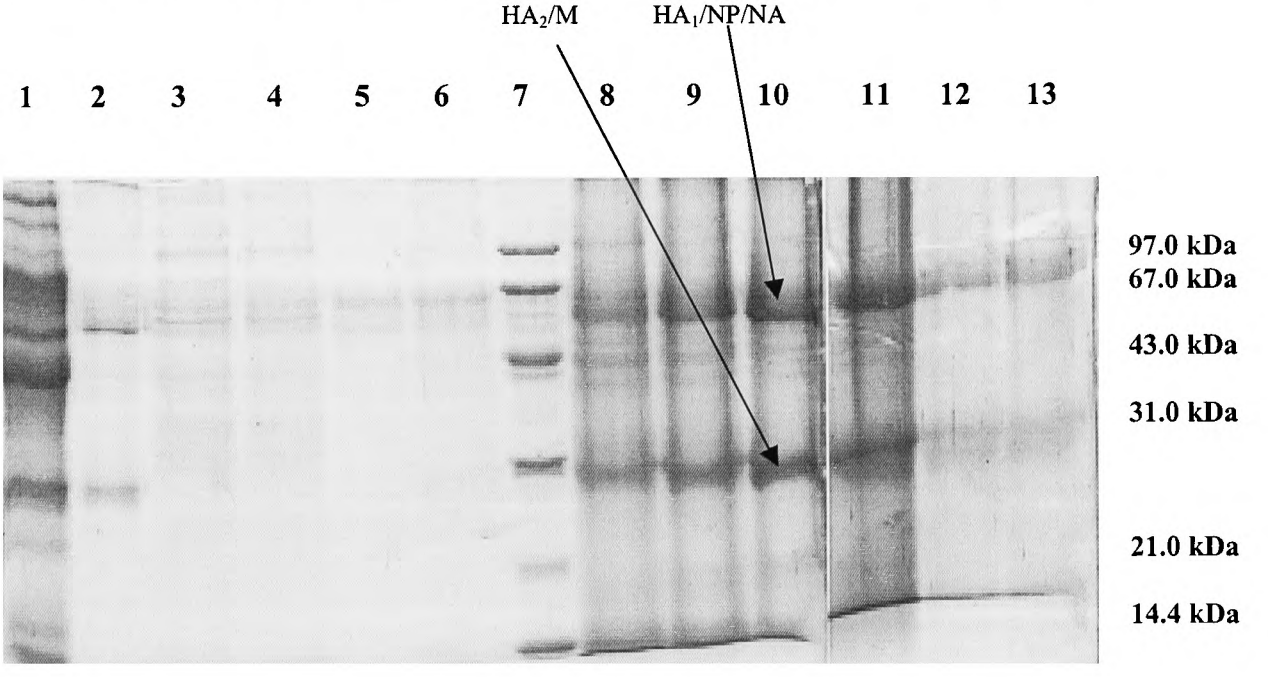

FIGURE 3.10 (b). The corresponding gel from Figure 3.10 (a).

Lane 1: *IBF,* ***Lane 2:*** *PZC,* ***Lanes 3 to 6 inclusive:*** *Fractions 1 to 4.* ***Lane 7:*** *Low molecular weight marker.* ***Lanes 8 to13 inclusive:*** *Fractions 5 to 10.*

Fractions of 3 mls (from ultracentrifugation, Section 3.2.2) were collected and analysed using SDS PAGE and one-dimensional densitometry. The resulting profile in the absence of Triton X100 indicates that the viral proteins (HA_1/NP/NA and HA_2/M) were located in Fractions 5 to 10 inclusive confirming the data presented in Figure 3.10 (a).

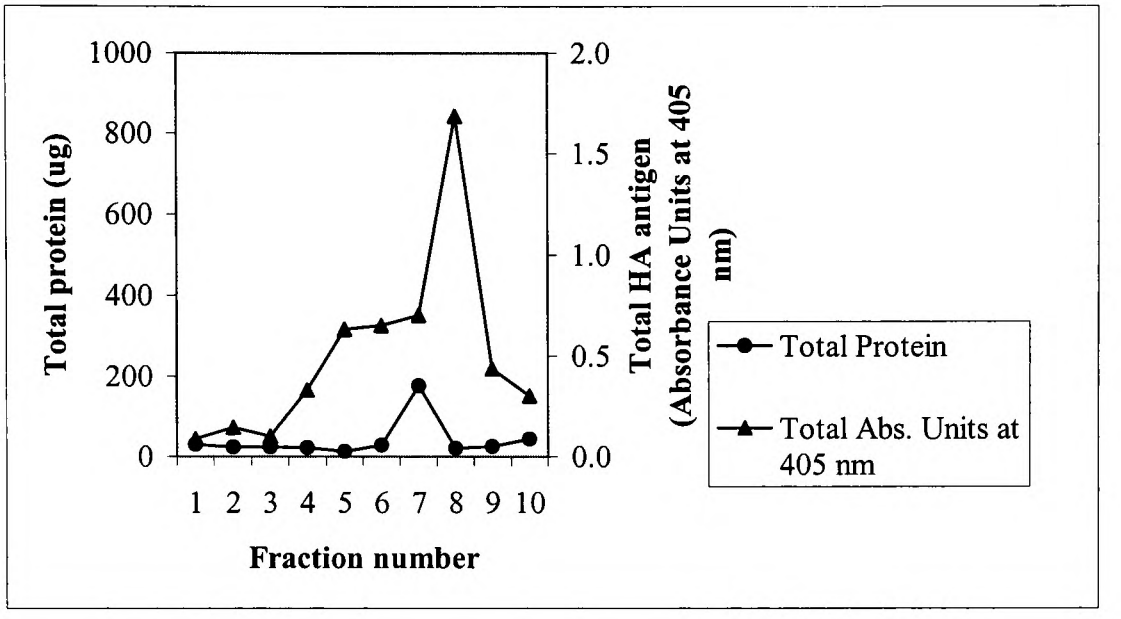

FIGURE 3.11 (a). Total protein (estimated using SDS PAGE and densitometry) and HA antigen profiles from sucrose density gradient ultracentrifugation in the presence of 0.01 % w/w Triton X100.

Fractions of 3mls were collected and analysed (see main text) for total protein and HA antigen content. The resulting profile is similar to that presented in Figure 3.10 (a) with respect to the location of the protein peak indicating that the protein is located in Fractions 5 to 10 (corresponding to sucrose concentrations of approximately 24% to 47 % w/v).

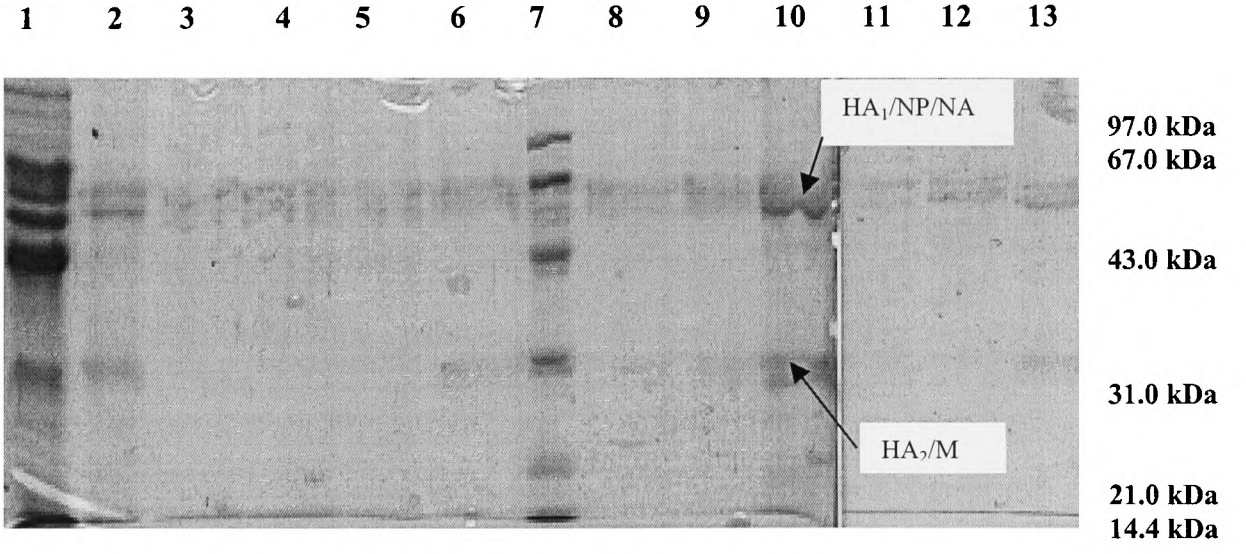

FIGURE 3.11(b). The corresponding gel from Figure 3.11 (a).

Lane 1: *IBF,* ***Lane 2:*** *PZC,* ***Lanes 3 to 6 inclusive:*** *Fractions 1 to 4.* ***Lane 7:*** *Low molecular weight marker.* ***Lanes 8 to 13 inclusive****: Fractions 5 to 10.*

Fractions of 3 mls (from ultracentrifugation, Section 3.2.2) were collected and analysed using SDS PAGE and one-dimensional densitometry. The resulting profile in the presence of 0.01 % w/w Triton X100 indicates that the viral proteins (HA_1/NP/NA and HA_2/M) were located predominantly at Fraction 7. This profile does not track the HA antigen profile presented in Figure 3.11(a) due to poor staining (and hence protein quantitation on the gel) see main text.

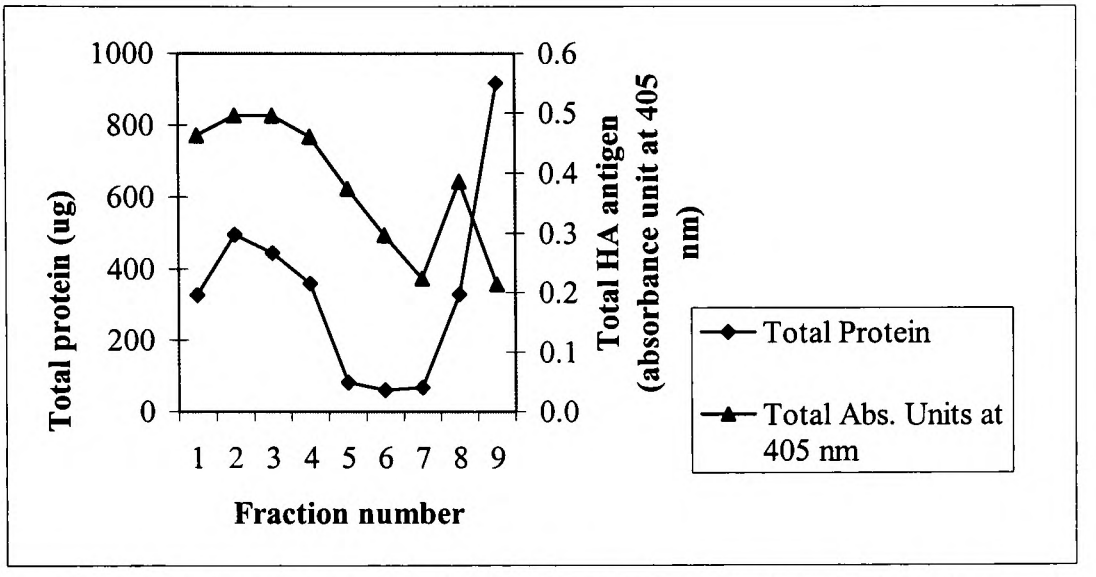

FIGURE 3.12 (a). Total protein (estimated using SDS PAGE and densitometry) and HA antigen profiles from sucrose density gradient ultracentrifugation in the presence of 1 % w/w Triton X100.

Fractions of 3mls were collected and analysed (see main text) for total protein and HA antigen content. The resulting profile is similar to that depicted by Profile "B", (Figure 3.2) with respect to the location of the protein peaks indicating that the protein is located at Fractions 1 to 4 (corresponding to sucrose concentrations of approximately 4 % to 15 % w/v) and also Fractions 8 and 9 (corresponding to sucrose concentrations of approximately 41 % to 49 % w/v).

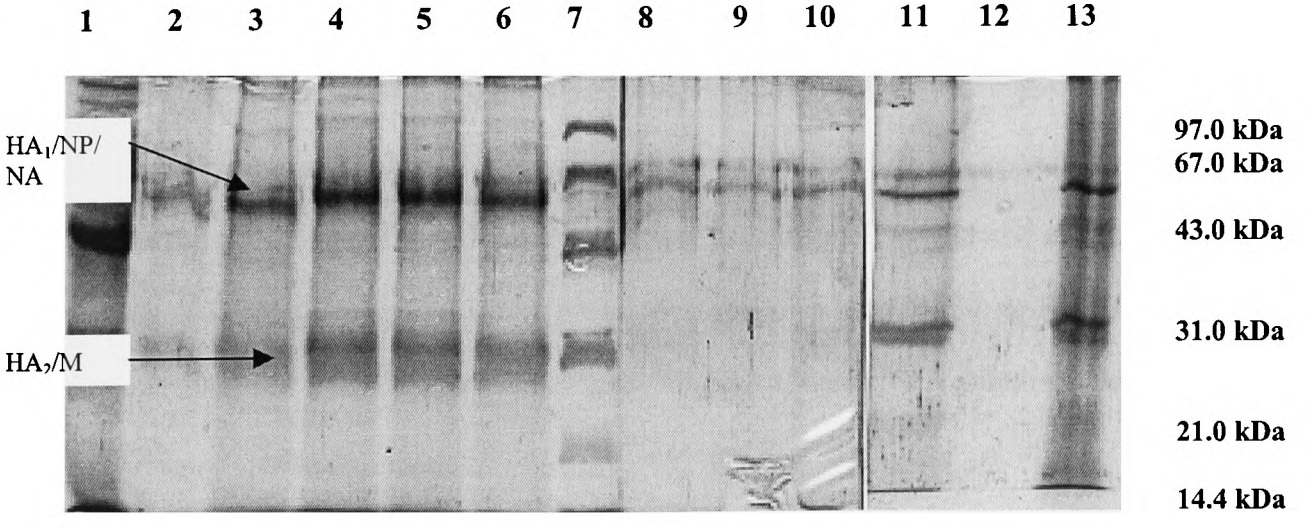

FIGURE 3.12 (b). The corresponding gel from Figure 3.12 (a).

Lane 1: *IBF,* ***Lane 2:*** *PZC,* ***Lanes 3 to 6 inclusive:*** *Fractions 1 to 4.* ***Lane 7:*** *Low molecular weight marker.* ***Lanes 8 to 11 inclusive****: Fractions 5 to 8.* ***Lane 12:*** *Unused.* ***Lane 13:*** *Fraction 9.*

Fractions of 3 mls (from ultracentrifugation, Section 3.2.2) were collected and analysed using SDS PAGE and one-dimensional densitometry. The resulting profile in the presence of 1% w/w Triton X100 indicates that the viral proteins (HA_1/NP/NA and HA_2/M) were located in Fractions 1 to 4 and Fractions 8 to 9. This data generally tracks the HA antigen data presented in Figure 3.12 (a).

3.3.1.2. The Effect of three non-ionic detergents upon solubilisation of surface from purified influenza virus particles.

Figures (3.13 to 3.16 respectively) depict a series of profiles that illustrate the effect of selection detergent and operating concentration upon purified whole virus loaded onto a sucrose density gradient. When no detergent was present, a characteristic broad peak of protein (Fractions 5 to 8 inclusive) was produced. The presence and position of this peak has been discussed in the previous section. The use of low concentrations (0.01 % to 0.1 % w/w) of deoxycholate yielded analyses that indicated that the viral particles remained intact. However, at concentrations of 0.5 % w/w and above, the deoxycholate profile produced a protein peak at approximately 20 % w/v sucrose (corresponding to a density of 1.08 g ml^{-1}), suggesting that solubilisation had occurred. These observations could be explained by the relatively high critical micellar concentration (CMC) of deoxycholate 2.4 to 4 mM compared to the other two detergents (see Table 3.1). Solubilisation is thought most likely to occur when a detergent is at or near its CMC (Hjelmland and Chrambach, 1984). Thus below this concentration range, the detergent monomers can only bind to the hydrophobic domain of the surface antigen. At higher concentrations (above the CMC), the surface antigens and other proteins are incorporated into micelles leading to solubilisation. This is true for all the detergents used herein, except that with deoxycholate the CMC is that much higher; therefore higher concentrations would be required to achieve solubilisation. In addition, deoxycholate at these higher concentrations produced lower levels of solubilised antigen as compared to the other two detergents at similar concentrations and tended to give over-exaggerated mass balances in both SDS PAGE analyses and the ELISA. This could be due to interactions with the antigen exposing additional sites for the Coomassie dye or for the anti-HA antibody to

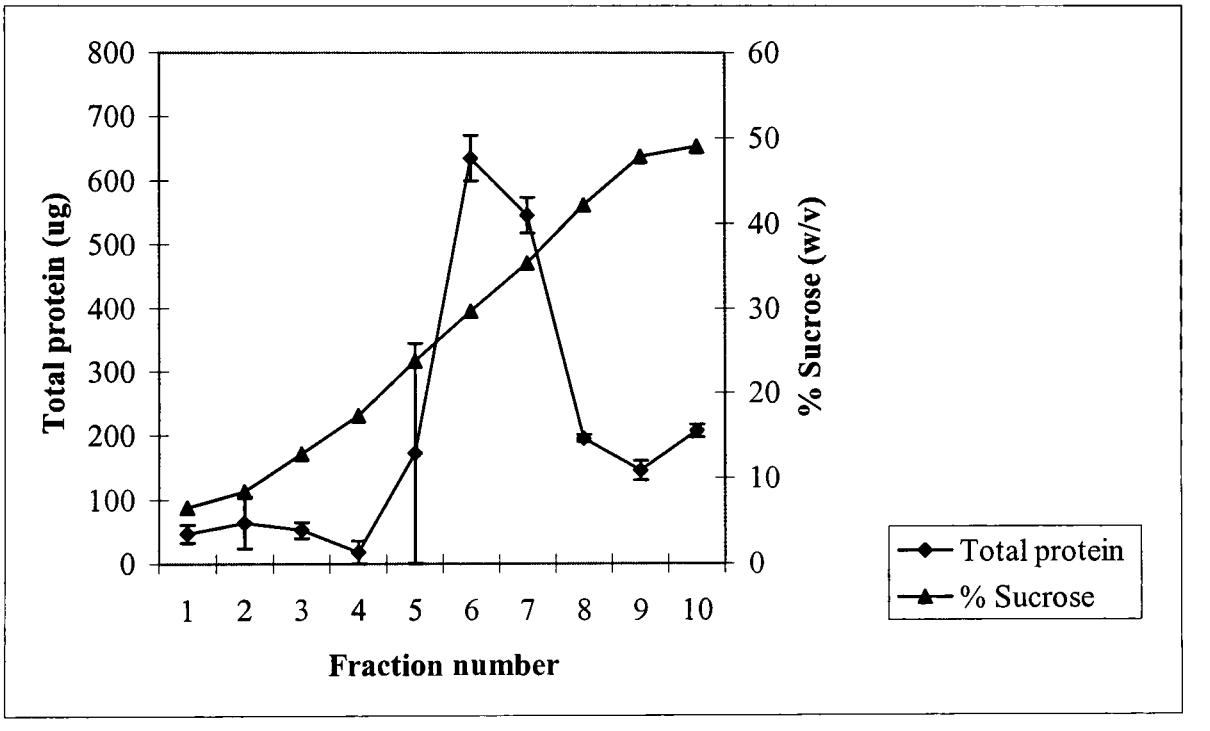

FIGURE 3.13. Total protein profile (deduced using SDS PAGE and one-dimensional densitometry) of PZC fractionation using sucrose density ultracentrifugation in the absence of detergent.

Three millilitres of PZC was layered onto a sucrose gradient (as described in Section 3.2.2) in the absence of detergent. The total protein profile is plotted as a mean of two consecutive ultracentrifuge runs. Total protein was estimated as described in Section 3.2.4.1. The broad protein peak (see Figure 3.10a) corresponded to intact viral particles located in sucrose concentration of 25 % to 40 % w/v.

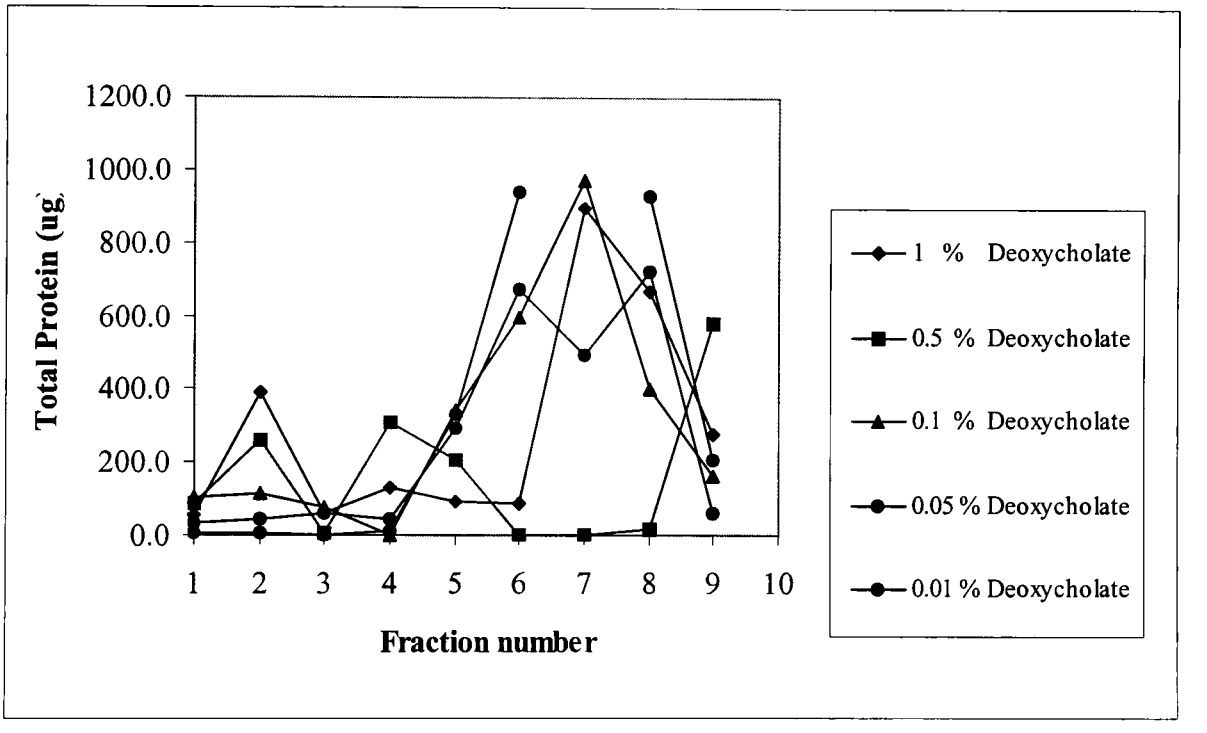

FIGURE 3.14. Total protein profiles (estimated using SDS PAGE and one-dimensional densitometry) in the presence of 0.01 % to 1 % w/v sodium deoxycholate.
A range of deoxycholate concentrations were employed to ascertain the optimal concentration for selective solubilisation of surface antigens (as described in Section 3.1.2. and Figure 3.2). Five millilitres of PZC of was layered onto a sucrose density gradient (as described in Section 3.2.2). Deoxycholate was added to the each gradient density layer (see Figure 3.6). Solubilsation of surface antigens occurred with deoxycholate concentrations in excess of 0.5 % w/v as indicated by the presence of protein peaks (Fractions 1 to 4) located in relatively low sucrose concentrations (approximately 7 % to 17 % w/v respectively). Intact viral particles are located in Fractions 5 to 9 (corresponding to approximate sucrose concentrations of 20 % to 50 % w/v). The recovery of total protein was over-inflated in the presence of this detergent (see main text for details).

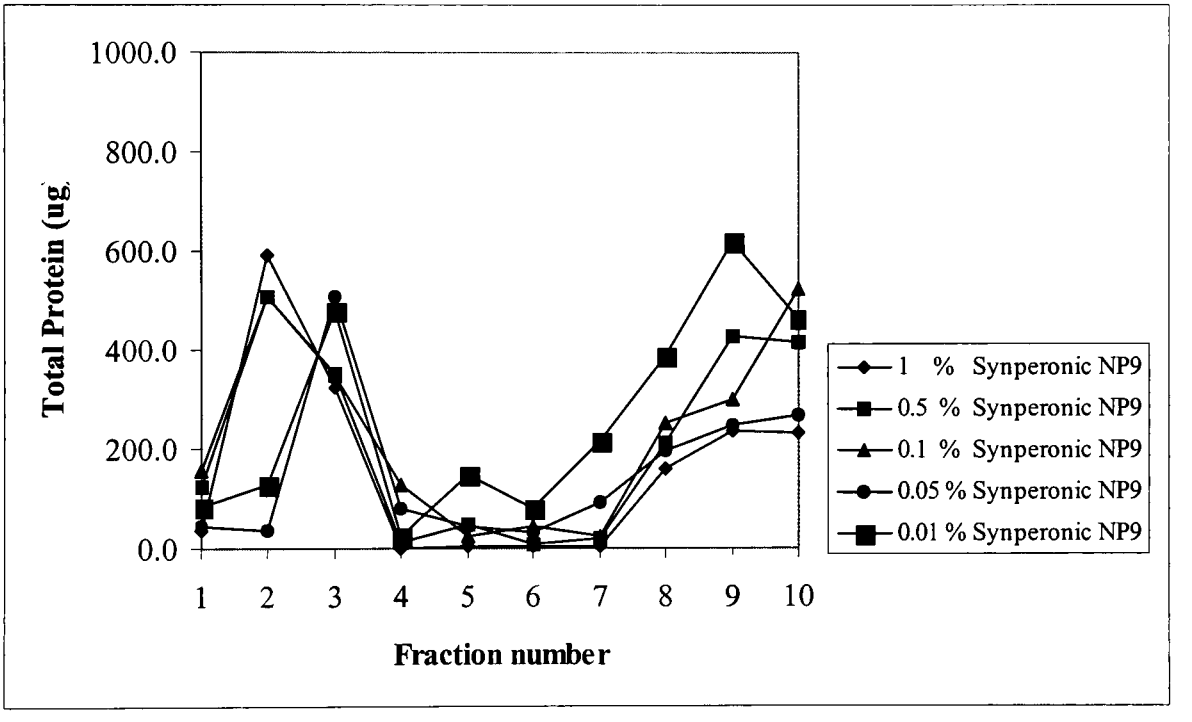

FIGURE 3.15. Total protein profiles (estimated using SDS PAGE and one-dimensional densitometry) in the presence of 0.01% to 1 % w/v Synperonic NP9.
A range of Synperonic NP9 concentrations were employed to ascertain the optimal concentration for selective solubilisation of surface antigens (as described in Section 3.1.2. and Figure 3.2). Five millilitres of PZC of was layered onto a sucrose density gradient (as described in Section 3.2.2). Synperonic NP9 was added to the each gradient density layer (see Figure 3.6). Solubilsation of surface antigens occurred with Synperonic NP9 concentrations in excess of 0.1 % w/v as indicated by the presence of protein peaks (Fractions 1 to 4) located in relatively low sucrose concentrations (approximately 4 % to 16 % w/v respectively). Intact viral particles are located in Fractions 7 to 10 (corresponding to approximate sucrose concentrations of 34 % to 51 % w/v).

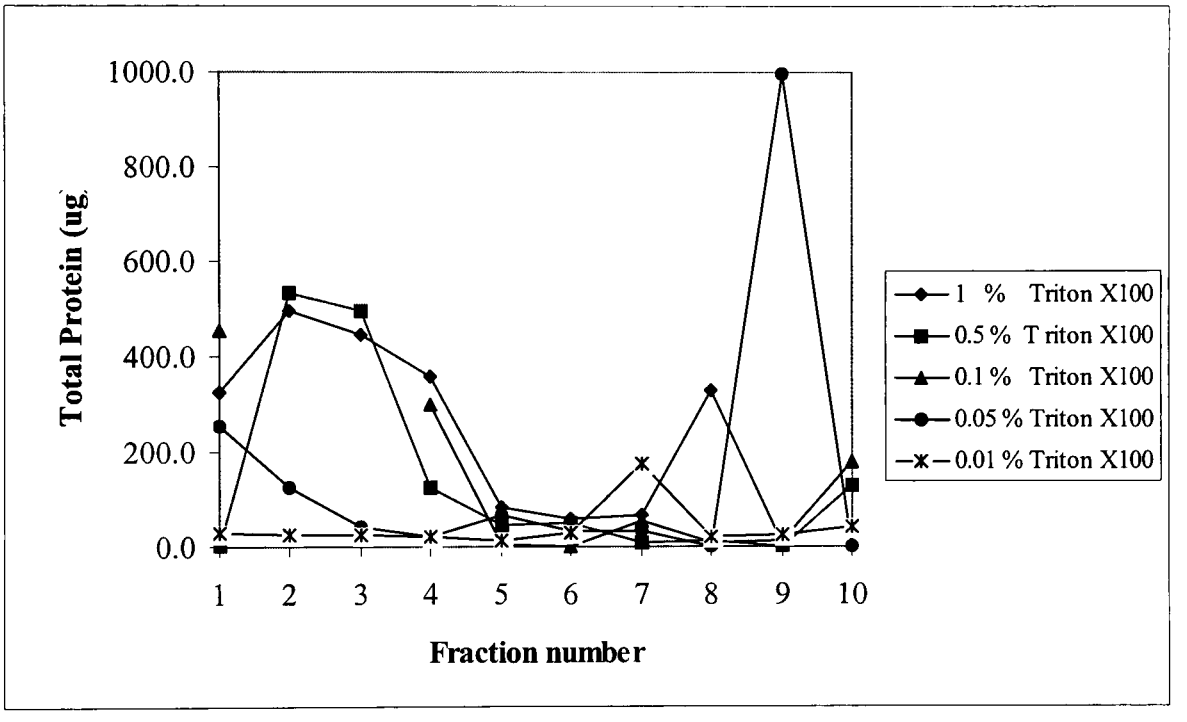

FIGURE 3.16. Total protein profiles (estimated using SDS PAGE and one-dimensional densitometry) in the presence of 0.01% to 1 % w/v Triton X100.
A range of Triton X100 concentrations were employed to ascertain the optimal concentration for selective solubilisation of surface antigens (as described in Section 3.1.2. and Figure 3.2). Five millilitres of PZC of was layered onto a sucrose density gradient (as described in Section 3.2.2). Triton X100 was added to the each gradient density layer (see Figure 3.6). Solubilsation of surface antigens occurred with Triton X100 concentrations in excess of 0.1 % w/v as indicated by the presence of protein peaks (Fractions 1 to 5) located in relatively low sucrose concentrations (approximately 4 % to 20 % w/v respectively). Intact viral particles are located in Fractions 7 to 10 (corresponding to approximate sucrose concentrations of 33 % to 49 % w/v). See also Figures 3.11 and 3.12.

bind. Thus this detergent was excluded from further use. Synperonic NP9 (Figure 3.15) produced almost "perfect" profiles with respect to its resemblance to that indicated by Profile "B" (Figure 3.2) except at the lowest concentration used. However, more solubilised antigen was produced when either 1 % w/w or 0.5 % w/w Synperonic NP9 was used. Triton X100 profiles showed a similar trend at these higher concentrations (Figure 3.16). At lower concentrations, Triton X100 yielded profiles suggesting that intact particles were the predominant species. The 100 % closure of mass balances could be variable. This was attributed to variable precipitation yields with TCA during sample pre-treatment (see Section 2.2.3.1). The 5 % w/w detergent concentration, (for all three detergents) was not considered for further use because the desired solubilisation effect had been obtained with much lower concentrations of detergent. The data for this was variable due to assay interference and therefore impossible to interpret accurately. On this basis, it was decided to use both Triton X100 and Synperonic NP9 in the construction of ADTPSs for solubilising the haemagglutinin antigens. It was difficult to assess the true benefit of using these detergents at 0.5 % w/w and 1 % w/w concentrations, so both of these were used in the next stage.

3.3.2. Effect of PEG molecular weight upon partition of detergents in secondary (hybrid) aqueous-detergent two-phase systems.

Prior to use of Synperonic NP9 and Triton X100 in an ATPS, it was essential to know where the detergent would partition in the experimental systems. The well-known property of these detergents absorbing ultraviolet light at 280 nm was utilised in this experiment. The top phase of each hybrid system was composed of PEG of varying molecular weight (as described in Section 3.2.1 and Figure 3.5). This was to assess the

contribution of PEG chain length to detergent partition. It was decided at this stage to re-display the system identifications since they were frequently used. These are presented in Table 3.4. The data presented in Figures 3.17 and 3.18 respectively indicated that both detergents preferentially partition to the top phase, regardless of the molecular weight of

System identification number.	Overall composition. PEG (%w/w)/ Phosphate (% w/w).	TLL (% w/w).
S39	PEG 300 16.8/22.9	43.5
S40	PEG 300 13.9/24.3	35.3
S41	PEG 1000 7.3/27.6	29.4
S42	PEG 6000 7.8/25.3	34.7
S43	PEG 8000 7.2/27.1	33.9

TABLE 3.4. List of secondary (hybrid) ADTPSs used in partition studies. *Refer also to Table 3.3 and Appendix II.*

PEG employed. This is unsurprising since the detergent structures are similar to PEG (refer to Figure 3.3). In particular, Triton X100 can be considered as PEG with a p-*t*-octylphenol head group). The A_{280} of a 1 % w/w solution of Triton X100 was determined to be 24.6 absorbance units (data not shown). This compared favourably to the published value of 22.0, (Furth *et al*, 1984). Mass balances were calculated as described in Section 3.2.8.1 and for Systems S39, S40 and S42 in the presence of Triton X100 (Figure 3.17), the mass balances were 72 %, 135 % and 49 % respectively; for Systems S39, S40, S41 and S43 in the presence of Synperonic NP9 (Figure 3.18), the mass balances were 81 %, 108 %, 10 % and 131 % respectively. The variability in the mass balance was more pronounced in PEG 1000 and PEG 6000- based ADTPSs (S41 and S42 respectively) and was attributed to precipitation of the detergent in these Systems. The PEG 300-based ADTPS of shorter TLL (S40, refer to Table 3.4) recorded a higher recovery of detergent compared to the PEG 300-based ADTPS of longer TLL (S39, refer to Table 3.4). This

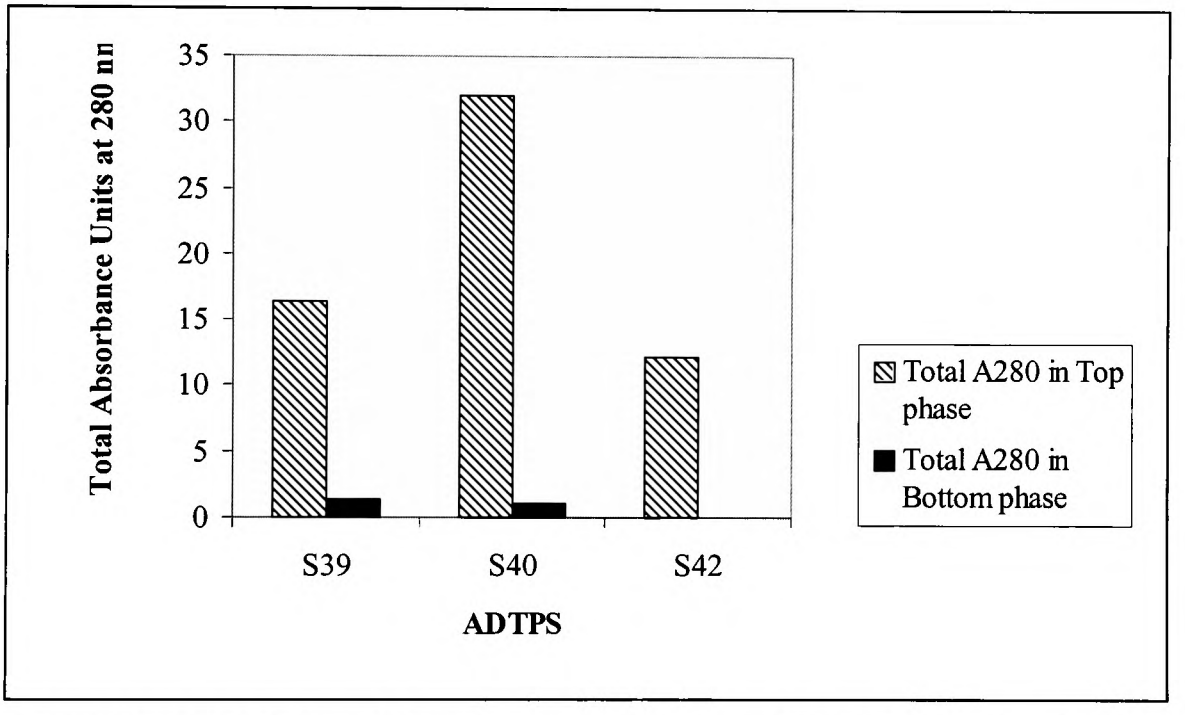

FIGURE 3.17. Utilisation of absorbance at 280 nm to monitor the distribution of Triton X100 (at a final concentration of 1 % w/w) in selected ATPSs.

The distribution of 1 % w/w Triton X100 was monitored (by absorbance at 280 nm) in a selection of ATPSs (see Table 3.4). The appropriate blanks were subtracted from the readings (see Section 3.2.7). The mass balances were estimated as described in Section 3.2.7.1. The data demonstrates that Triton X100 partitions preferentially to the top phase in these systems in a similar manner to that displayed by Synperonic NP9 (Figure 3.18).

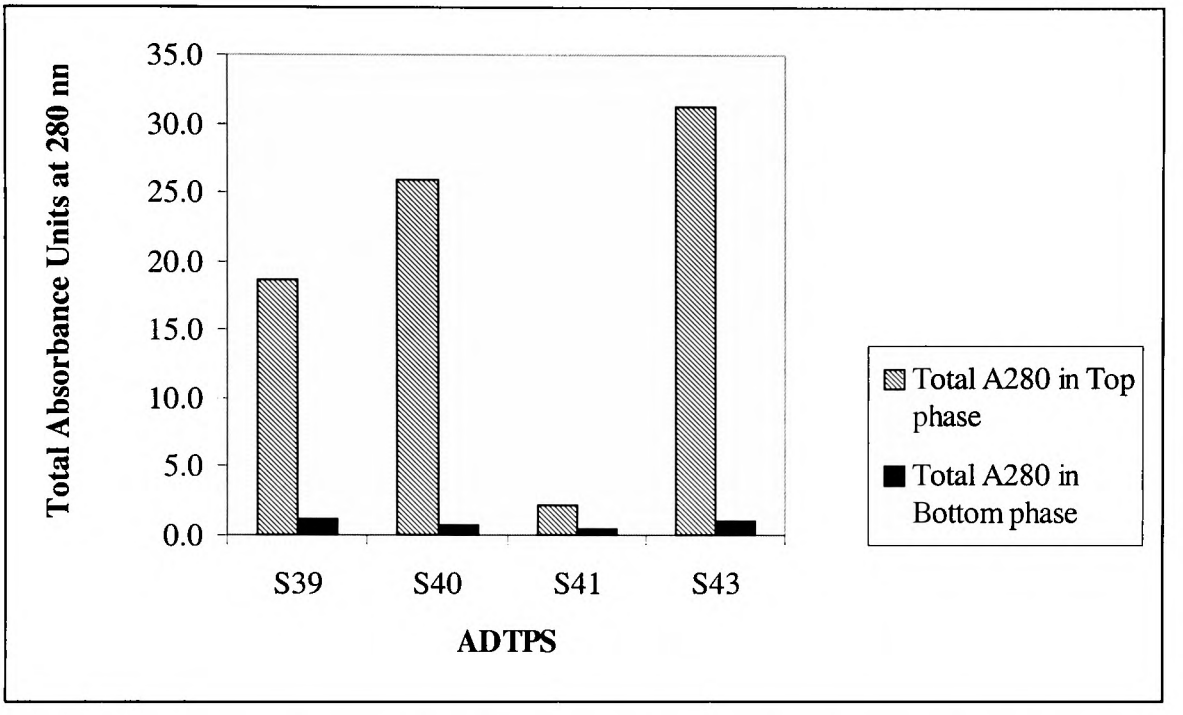

FIGURE 3.18. Utilisation of absorbance at 280 nm to monitor the distribution of Synperonic NP9 (at a final concentration of 1 % w/w) in selected ATPSs.
The distribution of 1 % w/w Synperonic NP9 was monitored (by absorbance at 280 nm) in a selection of ATPSs (see Table 3.4). The appropriate blanks were subtracted from the readings (see Section 3.2.7). The mass balances were estimated as described in Section 3.2.7.1. The data demonstrates that Synperonic NP9 partitions preferentially to the top phase in these systems in a similar manner to that displayed by Triton X100 (Figure 3.17).

could be explained by differences in the top phase concentration of PEG and resulting excluded volume and salting out mechanisms (Kim, PhD Thesis, 1986). System S39 contains a higher concentration of PEG and therefore a larger number of PEG molecules and hence an increased volume exclusion effect. In addition, an increased salting out effect causes precipitation (refer to Section 1.5.5) and hence less recovery (of detergent). An explanation for this observation is that water forms an ordered hydration layer around PEG (Huddleston *et al*, 1991b) and presumably around Triton X100 micelles too (due to its structural commonality with PEG, refer to Figure 3.3). As the PEG concentration increases, the PEG is hydrated in preference to the bulkier Triton X100 molecules since it is an energetically favourable arrangement. Thus the Triton head groups become dehydrated and the solution becomes turbid. This is similar to cloud point phenomenena described by Helenius and Simons, (1971). In extreme cases (PEG 1000 and 6000), precipitation occurs due to increased salting out effects (hence the non-closure of mass balances in these systems). The mass balance in the PEG 8000-based ADTPS, (S43) closed indicating that the detergent remained unaffected by the presence of PEG 8000 (although some cloudiness was observed in this System). An explanation for this could be that the long chain length of PEG 8000 and the bulky Triton X100 micelles are equally hydrated by the water molecules (that is they have no preference to hydrate), therefore the Triton X100 head groups are not subjected to dehydration to the same extent as PEG 300 and thus the turbidity is lower and the absorbance higher. Possibly the salting out effects are lower compared to the PEG 1000 and 6000-based ADTPSs therefore aggregation was not observed.

The aim of this experiment was to monitor the partition of detergent alone in ADTPSs. The detergent would be employed in the proposed purification scheme (see

Figure 3.1) using the optimised ADTPS to selectively release surface antigen from intact influenza virus particles. It was expected that the surface antigens would partition with the detergent to the top phase. Thus confirmation of the detergent partition undertaken in this study lends support to this proposal.

3.3.3. Effect of PEG molecular weight upon partition of Inactivated Bulk Fluid in secondary hybrid ADTPSs.

In the previous section, it was established that the detergent partitioned almost exclusively to the top phase in all systems tested. The experiment documented in Section 3.3.1 used purified zonal concentrate (PZC) and sucrose density ultracentrifugation as a means to determine optimal detergent and concentration for surface antigen release from the virus particles. This section employs the detergent(s) and concentration(s) considered optimal in selected ADTPSs containing Inactivated Bulk Fluid (IBF). The systems were constructed as in Section 3.2.1 and the HA ELISA was used as the analytical technique to monitor partition in the ADTPS because of its specificity and its capacity for high sample throughput. The neuraminidase (NA) was not monitored due to the lack of a suitable assay method to analyse samples partitioned in ATPSs. However, monitoring the HA antigen was more important because it is the main surface antigen and component in the Fluvirin™ vaccine. The following figures present ELISA mass balance data of IBF partitioned in a two-stage extraction (refer to Figure 3.1). Triton X100 and Synperonic NP9 were used at two different concentrations. Mass balances were estimated as described in Section 3.2.5.1. It should be noted that the starting IBF value for HA antigen content was approximately three-four fold lower than in the experiments of the previous chapter. It was concluded that this was because the material was taken

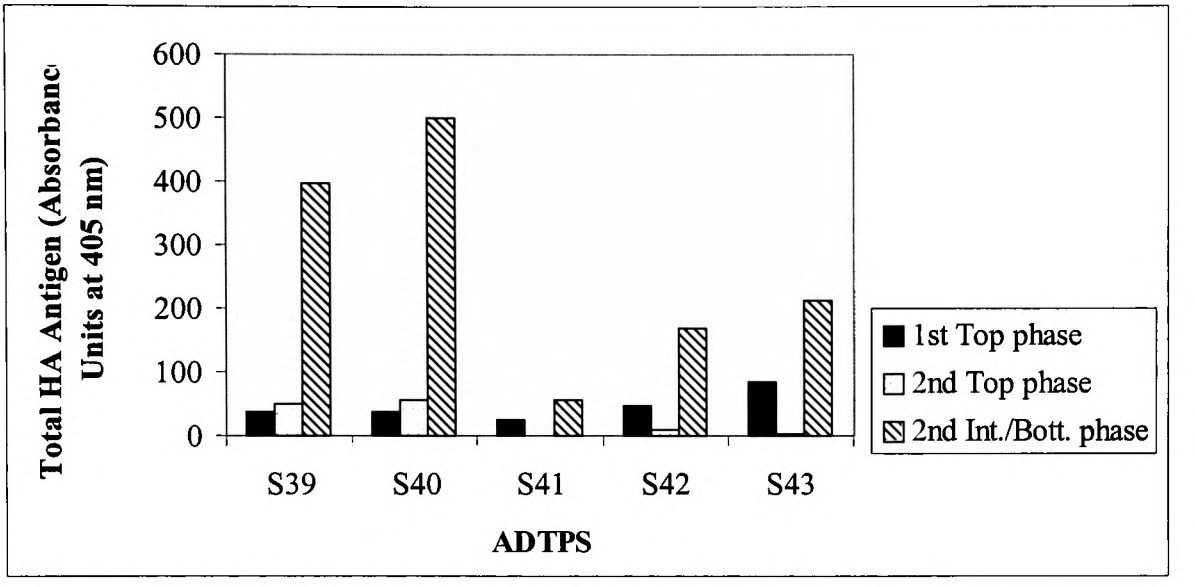

FIGURE 3.19. The effect of Triton X100 (1 % w/w) upon the distribution of HA antigen in selected ADTPSs.
The total HA antigen in each phase (see Section 3.2.5.1) is shown for ADTPSs comprising PEG of different molecular weights 300 to 8000 (see Table 3.4). Triton X100 was added to the hybrid system at a final concentration of 1 % w/w (see also Figure 3.20).

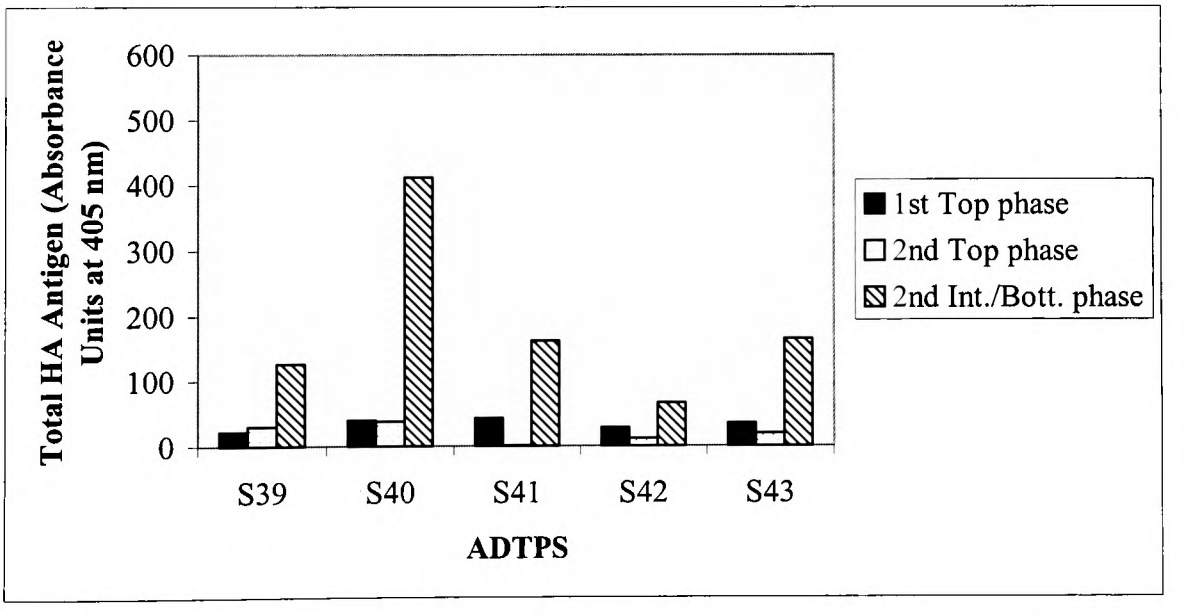

FIGURE 3.20. The effect of Triton X100 (0.5 % w/w) upon the distribution of HA antigen in selected ADTPSs.
The total HA antigen in each phase (see Section 3.2.5.1) is shown for ADTPSs comprising PEG of different molecular weights 300 to 8000 (see Table 3.4). Triton X100 was added to the hybrid system at a final concentration of 0.5 % w/w (see also Figure 3.19).

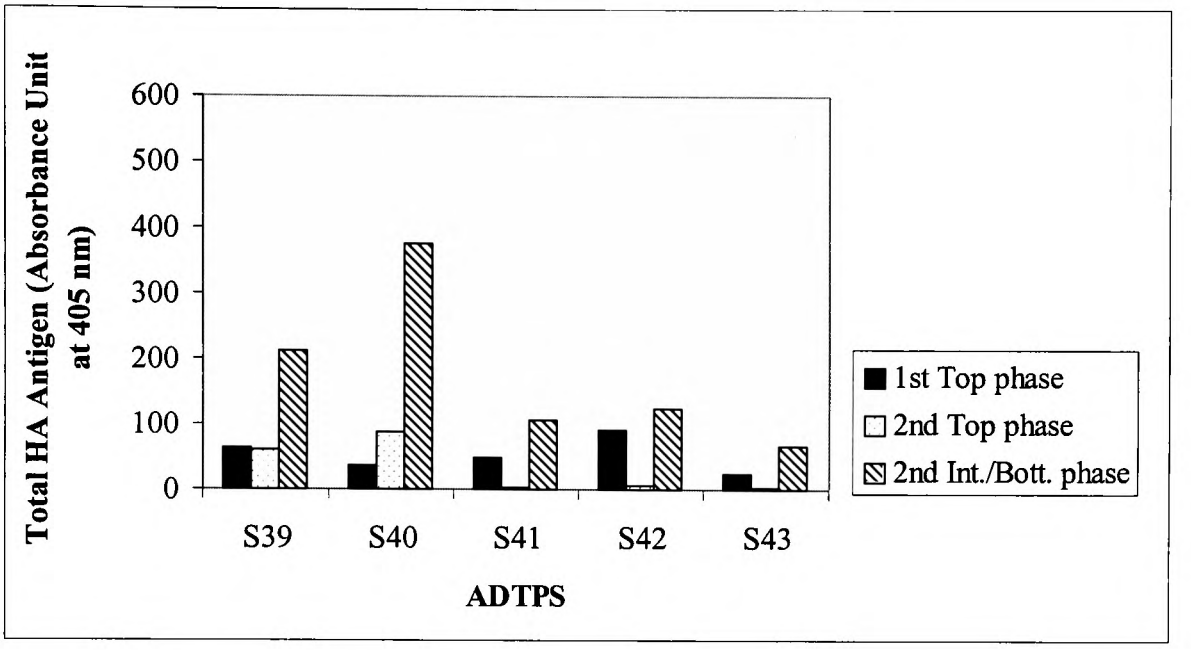

FIGURE 3.21. The effect of Synperonic NP9 (1 % w/w) upon the distribution of HA antigen in selected ADTPSs.

The total HA antigen in each phase (see Section 3.2.5.1) is shown for ADTPSs comprising PEG of different molecular weights 300 to 8000 (see Table 3.4). Synperonic NP9 was added to the hybrid system at a final concentration of 1 % w/w (see also Figure 3.22).

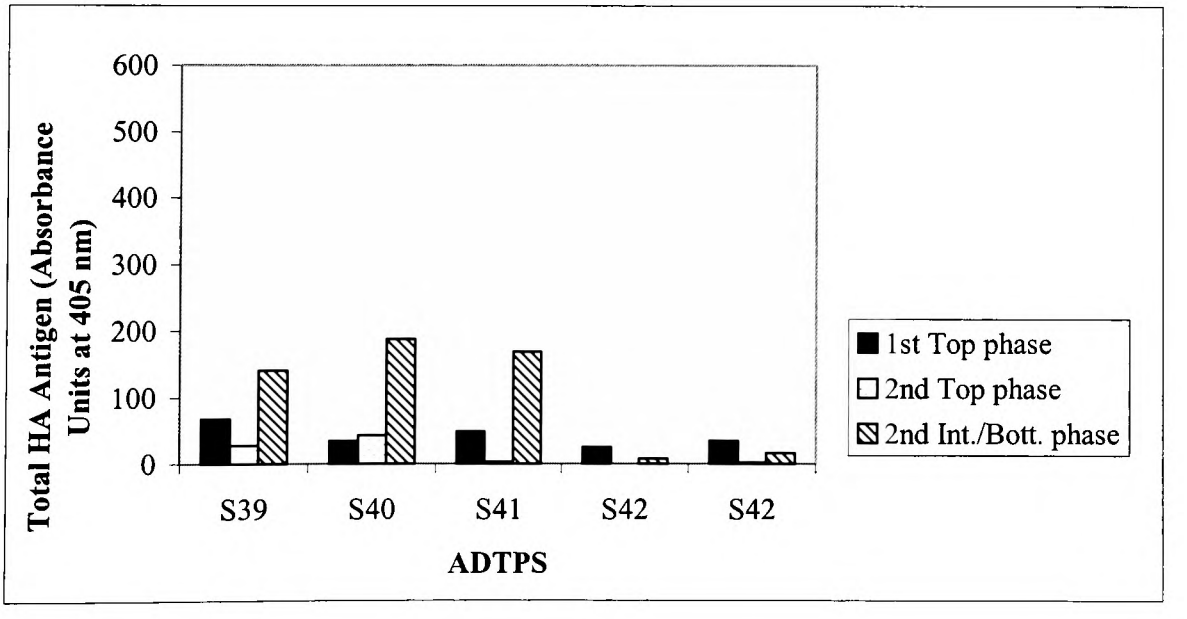

FIGURE 3.22. The effect of Synperonic NP9 (0.5 % w/w) upon the distribution of HA antigen in selected ADTPSs.

The total HA antigen in each phase (see Section 3.2.5.1) is shown for ADTPSs comprising PEG of different molecular weights 300 to 8000 (see Table 3.4). Synperonic NP9 was added to the hybrid system at a final concentration of 0.5 % w/w (see also Figure 3.21).

from a stock stored at –20 °C prone to proteolytic degradation (as opposed to –70 °C which had been completely used up in the previous experiments).

3.3 3.1. First extraction, top phase partitioned samples.

Results for HA recovery from the top phases in the first extraction, (see Figure 3.1) averaged out at around 40.0 A_{405} units. Densitometric analysis (data not shown) of an SDS PAGE gel of these samples confirmed that the HA antigen partitions to this phase was constant (refer to Figure 3.23). Detergent had not been added at this stage, suggesting that PEG has a relatively small impact upon surface antigen release or that the virus naturally "sheds" a small proportion of its surface antigens which partition to the top phase in PEG 300-based ATPSs.

3.3 3.2. Second extraction, top phase partitioned samples.

In the top phase of the second extraction samples, (see Figure 3.1) the greatest amount of HA antigen was quantitated in the PEG 300-based secondary hybrid ADTPSs. This occurred regardless of the detergent or detergent concentration used. The recovery in this same phase drops abruptly in the hybrid systems comprising PEG 1000 to 8000. This could be explained in terms of increased excluded volume effects as the PEG molecular weight was increased, coupled with the fact that the detergent preferentially partitions to the top phase. Detergent aggregation occurs as a result of preferential hydration of PEG as (discussed in Section 3.3.2). Thus less detergent is available to solubilise the surface antigens in ADTPSs of intermediate to high PEG molecular weight. In general, the proteins in such systems have an increasing natural preference for the bottom phase (see Section 2.2.3.4). Thus the low availability of detergent coupled

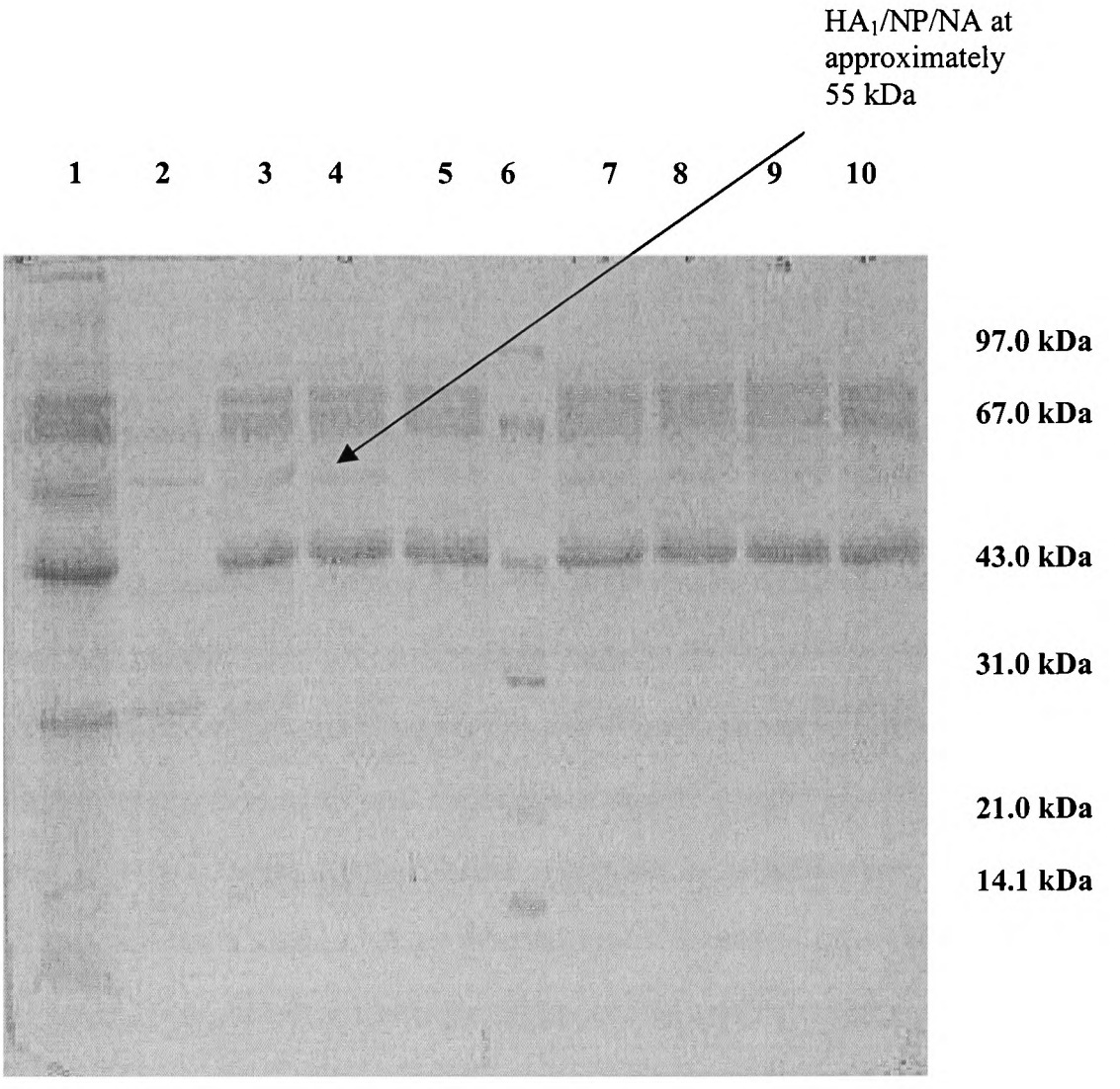

FIGURE 3.23. SDS PAGE gel depicting first extraction top phase samples.
Lane 1: *IBF;* ***Lane 2:*** *PZC;* ***Lanes 3 to 5 inclusive and 7 to 10 inclusive****: First extraction top phase samples from primary ATPS S25 (PEG 300 22.2 % w/w/ phosphate 17.9 % w/w, pH 7.5).* ***Lane 6:*** *Low molecular weight markers.*

The samples in Lanes 3 to 5 and 7 to 10 inclusive were partitioned in a series of S25 ATPSs loaded with 2 g IBF material (as described in Section 2.2.2). The interphase/bottom phases of these systems were destined to form a series of secondary hybrid ADTPS as illustrated in Figure 3.5. Replication of the top phase sample demonstrates the consistency in preparation of S25 and that the partition of HA antigen to this phase was similar.

with opposing partition preferences (of proteins and detergent) means that less solubilsation can occur (and hence less HA antigen detected in the top phase). In PEG 300-based ADTPSs, the proteins and detergent partition to the same phase, thus more solubilisation can occur.

3.3 3.3. Second extraction, interphase/bottom phase partitioned samples.

In the ADTPSs investigated using ELISA, most of the HA antigen was located in the interphase/bottom phase. This was attributed to detergent-solubilised antigen remaining at the interphase, unable to partition to the top phase due to entrapment with debris, combined with possible micelle breakdown upon contact with the phosphate phase (Save *et al*, 1995). This could be verified by transmission electron microscopy (TEM). Such a response was exaggerated in the presence of low molecular weight PEG. This could be explained as follows. Haemagglutinin exists as a trimer in its native. Low molecular weight PEG exposes a surface, which permits increased binding of antibody in the ELISA. Alternatively, detergent affects the antigen in such a way that high capacity, low affinity binding sites are uncovered (Hjelmland and Chrambach, 1984). Since Triton X100 and Synperonic NP9 share structural commonality with PEG (Figure 3.3) then they probably potentiate these effects. Support for the first explanation derives from previous analyses using the Haemagglutination Test (Appendix I) whereby decreased recoveries in this assay were attributed to conformation changes in the presence of low molecular weight PEG. It is widely accepted that PEG stabilises protein and protein intermediates (Mitraki and King, 1989). Stabilisation of antibody binding sites could result in increased antibody binding (as detected by ELISA). The alternative explanation could be verified by Scatchard analysis. These effects are observed in the presence of

presence of low molecular weight PEG because it has a smaller chain length thus permitting it to get closer to the surface antigen and exert the described effects.

3.3.3.4. Multiple phase formation in ADTPSs.

Another interesting observation was that ADTPSs containing detergent at a final concentration of 1 % w/w actually formed four-phase systems. That is: a clear bottom phase, a translucent interphase sometimes obscured by a turbid top phase and a thin pale yellow coloured phase on top due to lipoproteins (as described by Burley and Sleigh, 1975). The intensity of this colour increased as the PEG molecular weight increased. It was difficult to isolate this latter phase (on the scale of system used) thus it was harvested and analysed together with the top phase proper. In systems of high PEG molecular weight a white precipitate (due to salting out and increased excluded volume effects) was observed.

3.3.3.5. The optimal secondary ADTPS for release of HA from influenza virus.

Aqueous-detergent two-phase systems (ADTPSs) comprising PEG 300 (S39 and S40) were the most useful systems for recovering HA antigen in the top phase (as discussed in Section 3.3.3.2). System S40 was preferred because of its lower TLL (and lower tendency to precipitate the detergent as proposed in Section 3.3.2). Synperonic NP9 was marginally better than Triton X100 at releasing antigen to the top phase because it is more hydrophobic and can interact better with the lipid bilayer to release HA antigen. This is offset in ADTPSs of higher PEG molecular weights as preferential hydration of PEG leads to precipitation of Synperonic NP9 and poor recovery of antigen. However, Triton X100 was preferred because it is easier to remove further downstream (in

ultrafiltration or dialysis for example) because of its higher CMC (Furth *et al*, 1984). If further processing (including detergent removal) were to be carried out using ultracentrifugation (as in the Medeva Process), then either detergent would suffice. In addition, detergent at a final concentration of 1 % w/w was used since it released more HA antigen to the top phase (compare Figure 3.19 with Figure 3.20 and also Figure 3.21 with Figure 3.22). The increased viscosity of high molecular weight PEG ADTPSs (adding to the technical difficulty of harvesting the interphase) provided another reason for not using such systems.

3.3.3.6. Comparison of ADTPSs in the absence of detergent.

In light of data presented in Sections 3.3.31 to 3.3.3.3 inclusive, it was important to establish that the HA antigen recovered in the second extraction top phase was a true effect due to solubilisation. Figure 3.24 compares the partitioning of IBF material in a system that contains detergent (at a final concentration of 1 % w/w) with a system that does not. The ADTPS S40 (see Table 3.4) was used because it recovered more HA antigen in the top phase (refer to the previous section).

Figure 3.24 indicates that there was little difference between the amounts of HA antigen recovered in the top phase of the second extraction in the presence and absence of detergent. This could support the arguments discussed in Section 3.3.3.1. Approximately 60 to 70 % of the response was located in the interphase/bottom phase in the presence of detergent) for reasons previously discussed in Section 3.3.3.3. Other possibilities for the lack of difference in top phase recoveries could be that the detergent contact time had not been optimised, the detergent action was insufficient in solubilising

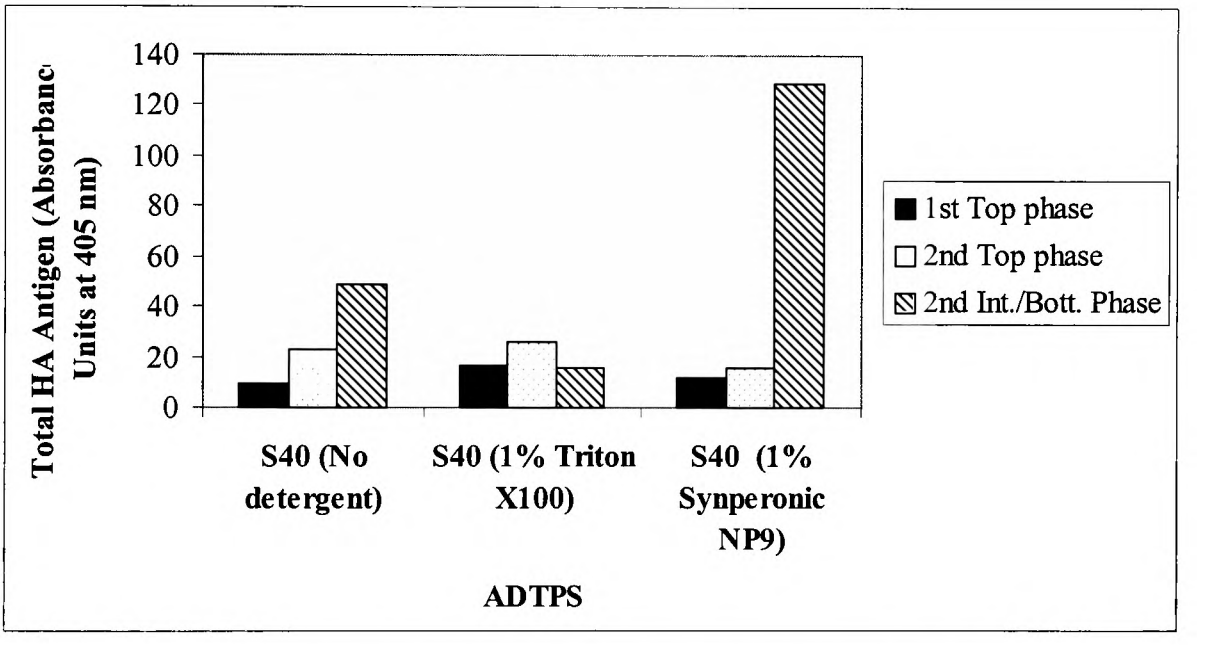

FIGURE 3.24. Recovery of HA antigen from IBF partitioned in ADTPS S40 in the absence and presence of 1 % w/w Triton X100 and 1 % w/w Synperonic NP9.
This Figure depicts the amount of HA antigen (determined by ELISA, see Section 3.2.5.1) in each phase of the two-stage extraction (illustrated in Figure 3.5). Comparison of the recovered amounts of HA antigen in the second extraction top phase (2^{nd} Top phase) reveals that there was no difference (in recovery) in the presence or absence of detergent. ADTPS S40 comprises PEG 300 13.9 % w/w/ phosphate 24.3 % w/w, see Table 3.4.

HA antigen or that solubilised antigen fragments had been produced and were aggregating at the interphase. The data in Figure 3.24 include significantly lower values for HA than data presented in Figures (3.19 to 3.22 inclusive). These systems had been constructed with IBF material that had previously been stored at –20 °C then thawed out and stored at 4 °C for a few days before use.

3.3.4. The effect of Triton X100 contact time upon solubilisation of HA antigen from influenza virus.

To evaluate the effect of detergent contact time upon solubilisation of HA antigen from influenza virus particles contained within IBF material, a series of ADTPSs S40 (refer to Table 3.4) were constructed. The IBF material was partitioned in the presence of 1 % w/w Triton X100 (see Section 3.2.1) for a period of time ranging from 0 to 24 hours. The top and bottom phases were analysed using the HA antigen ELISA. The total HA antigen recovery profile was biphasic suggesting that two species of molecules (containing HA antigen) were recognised by the anti-HA antibody and that detection of these species depended upon the length of time that the virus had been in contact with the detergent. A plot of total HA antigen versus detergent incubation time (Figure 3.25) demonstrated that there was a sustained response between 3 to 12 hours in the presence of Triton X100. This response peaked after an incubation period of three to four hours. The second peak response occurred at around 12 to 18 hours in the presence of Triton X100. The first peak was attributed to stabilisation of antibody binding sites in the presence of PEG leading to an increase in antibody binding (refer to Section 3.3.3.3). The fact that there was a concurrent increase in HA antigen to the top phase (in the second extraction suggests that there was HA antigen being released (see Figure 3.26).

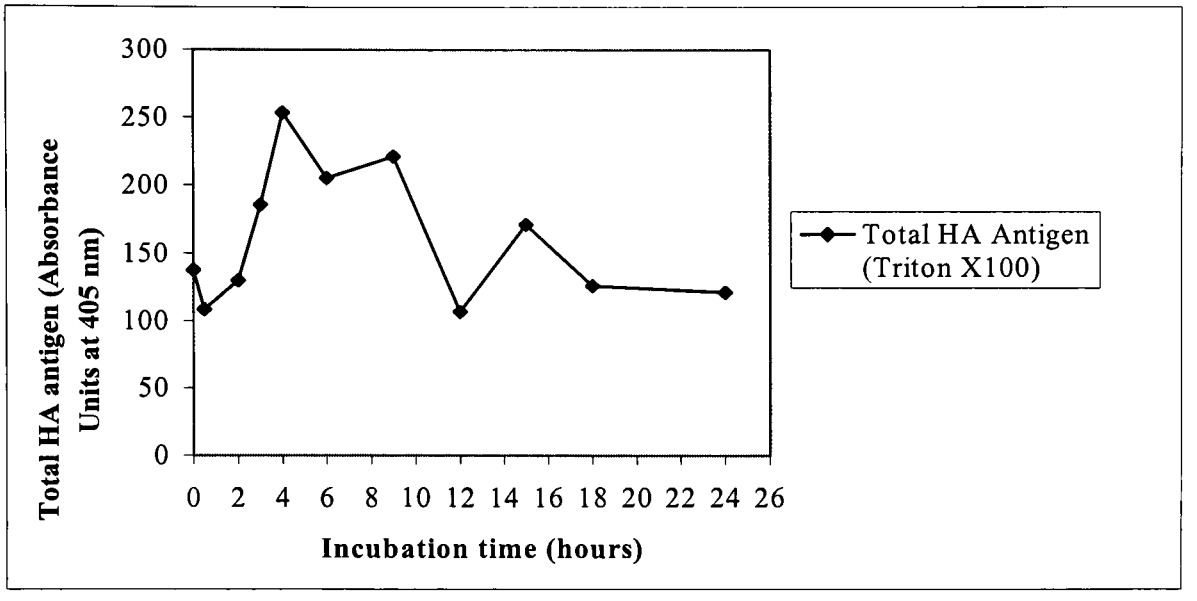

FIGURE 3.25. Impact of Triton X100 incubation time upon recovery of total HA antigen from IBF partitioned in ADTPS S40.
This profile of IBF material partitioned in ADTPS S40 (PEG 300 13.9 % w/w/ phosphate 24.3 % w/w, pH 7.5) incubated with Triton X100 (1 % w/w), illustrates the biphasic nature of the response (total recovery is defined as the sum of the amounts of HA antigen in the first extraction top phase, second extraction top phase second extraction and interphase/bottom phase).

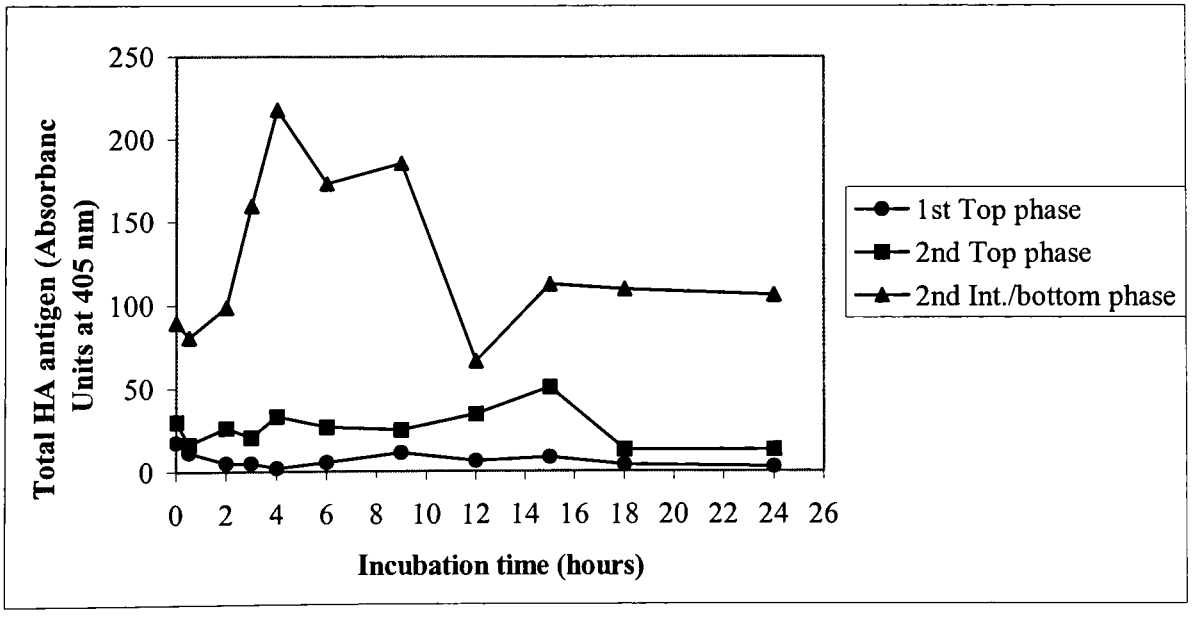

FIGURE 3.26. Impact of Triton X100 incubation time upon recovery of total HA antigen from each phase.
These profiles indicating IBF material partitioned in ADTPS S40 (PEG 300 13.9 % w/w/ phosphate 24.3 % w/w, pH 7.5) in the presence of Triton (1 % w/w), illustrate the HA antigen recovery in each phase (first extraction top phase, second extraction top phase and second extraction interphase/bottom phase). The sum of these profiles gives the total recovery in the system (refer to Figure 3.25). The response in the second extraction top phase was thought to be due to solubilised HA$_1$ antigen.

Gel analysis supports this. Lane 1 (Figure 3.27) demonstrated that there was a band at 55 kDa in the top phase (thought to be haemagglutinin subunit 1, HA_1 antigen). There was a similar band in the corresponding interphase/bottom phase sample (Lane 3) thought to be due to HA_1 and nucleoprotein (NP) because nucleic acid partition preferentially to the bottom phase in PEG-salt ATPSs (Cole, 1991). Bands at approximately 25 and 27 kDa representing the matrix (M) protein and haemagglutinin subunit 2 (HA_2) proteins respectively) were also observed. This suggested that there was a proportion of mostly HA_1, low concentrations of HA_2 and even M protein (since the latter were not detected clearly on a Coomassie-stained gel) being released in this first peak. As the sites became saturated with antibody, the binding decreased (hence a decreased ELISA response). The second peak could be due to the uncovering and stabilising of antigenic sites within the HA_2 domain since there was a band at 25 to 27 kDa also present in the interphase/bottom phase sample (Figure 3.27 Lane 3). The overall recovery of HA antigen appeared to be governed by recovery in the interphase/bottom phase since both HA antigen-detergent incubation time profiles were identical (compare Figures 3.25 and the interphase/bottom phase profile presented in Figure 3.26). Recovery in the top phase of the second extraction was approximately four times that of the top phase first extraction (Figure 3.26). The maximum recovery in the top and interphase/bottom phase of the second extraction was approximately two-fold higher than the corresponding phases of the systems containing no detergent. This suggests that a maximum action upon the virus had been reached under the conditions (of detergent concentration and ADTPS) used. Thus in conclusion an incubation time of four hours was selected as optimal and used in subsequent experimentation.

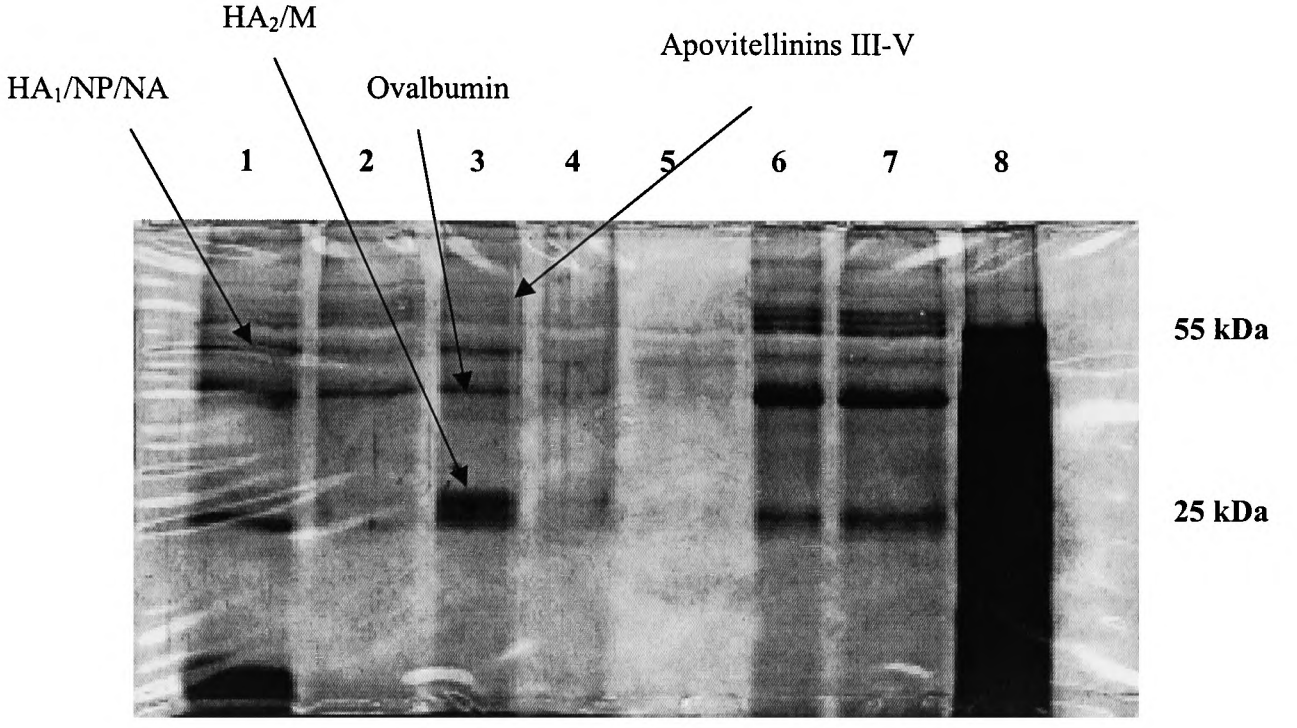

FIGURE 3.27. Silver stain gel depicting IBF material fractionated in PEG/phosphate ADTPs consisting of PEG 300 and 8000 respectively.

Lanes 1 and 2: *Second extraction top phase ADTPS (S40).*
Lanes 3 and 4: *Second extraction interphase/bottom phase ADTPS (S40).*
Lane 5: *Second extraction top phase ADTPS (S43).*
Lanes 6 and 7: *Second extraction interphase/bottom phase ADTPS (S43).*
Lane 8: *Low molecular weight marker (overloaded).*
Fifteen microlitres was of sample was loaded in each lane. Samples were prepared as described in Section 3.2.4. The differences in staining in Lanes 3and 4 are as a result differences in the amount of protein precipitated.

3.3.5. Proposed strategy to evaluate HA antigen solubilisation.

In the previous section, it was assumed that HA antigen detected in the top phase was as a result of selectively solubilised antigen. This assumption needed to be confirmed since it was possible that the response could have been due to disrupted viral fragments. A possible method to clarify this was to load the top phase material from an optimised ADTPS S40 onto a sucrose density gradient and centrifuge it (Section 3.2.2). If the solubilised antigen had partitioned to the top phase, one would expect to locate it in low-density sucrose. This would be repeated with the interphase/bottom phase material from the same ADTPS. If core material or intact virus were present, one would expect to locate it in the high-density sucrose. The harvested fractions were dialysed overnight (as described in Section 3.2.3) and analysed using the HA antigen ELISA, SDS PAGE and the BCA total protein assay. A control system was constructed (omitting the detergent) and treated in the same manner.

3.3.5.1. Evaluation of HA antigen solubilisation in second extraction top phase samples in the absence of detergent.

A sample from the second extraction top phase (refer to Figure 3.1) from partition of IBF material in ATPS S40 (see Table 3.4) without detergent was subjected to sucrose density ultracentrifugation (as described in Section 3.2.2.1). In the absence of detergent there is protein located in Fractions 1 to 7 inclusive (Figure 3.28 a). The SDS PAGE gel presented in Figure 3.28 (b), which indicates that the protein consisted of mainly ovalbumin and apovitellenins III to V as well as a low concentration of HA_1 antigen, (refer to Figure 2.14 and Table 2.4), supports this. The HA ELISA also confirms the presence of antigen in Fraction 15 (and the observations documented in Section 3.3.3.1).

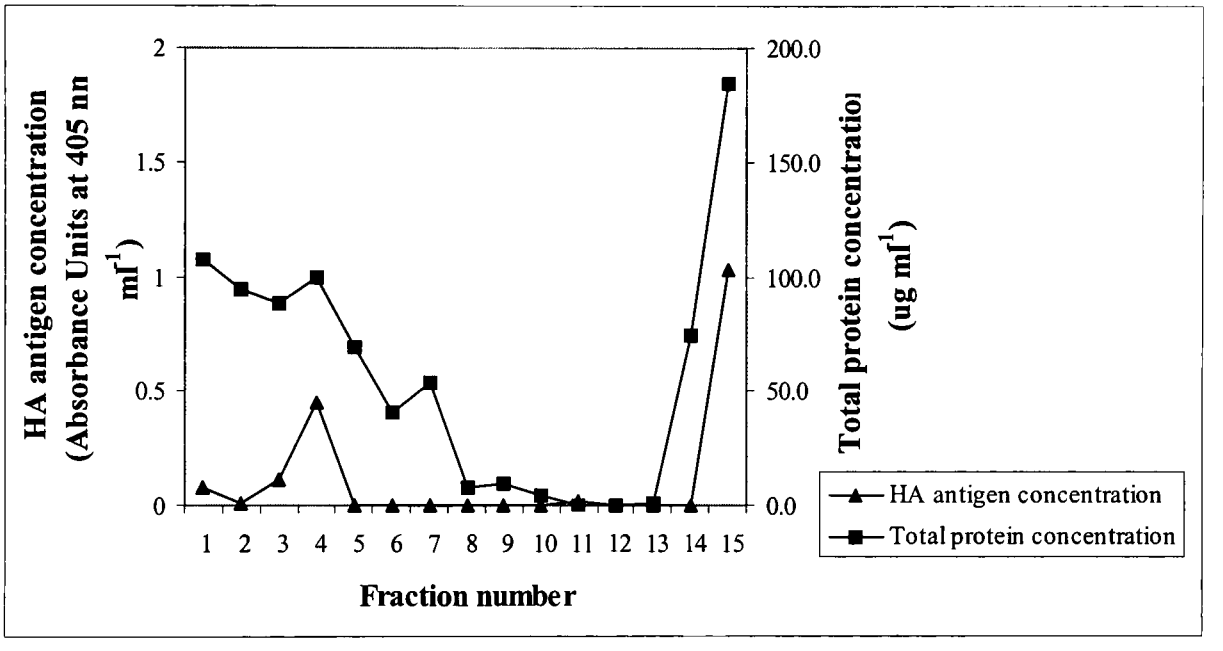

FIGURE 3.28 (a). Profiles illustrating distribution of HA antigen and total protein (as detected by ELISA and BCA assay respectively) from second extraction top phase fractions harvested from a sucrose density gradient in the absence of detergent.
A 5ml sample from the second extraction top phase of IBF material partitioned (without detergent) in ATPS S40 was layered onto a sucrose density gradient (see Section 3.2.2) and processed as described in Sections 3.2.3 and 3.2.4. SDS PAGE gels corresponding to these fractions are presented in Figures 3.28 (b) and 3.28 (c) respectively.

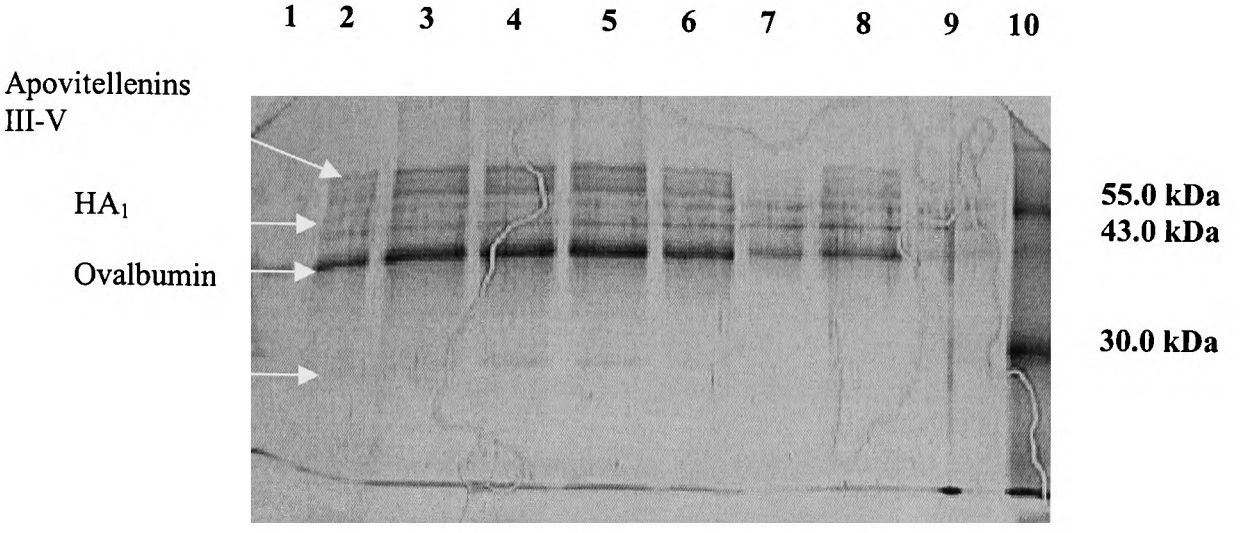

FIGURE 3.28 (b). Silver stain gel showing top phase Fractions 1 to 8 (in the absence of detergent) from Solubilisation Assessment Study.
The gel presented in this figure shows the fractions from the second extraction top phase (without detergent) analysed by SDS PAGE and silver stain. The corresponding protein and HA antigen concentration profiles are presented in Figure 3.28 (a).
***Lane 1:** Pre dialysis second extraction top phase sample. **Lanes 2 to 9:** Dialysed Fractions 1 to 8 inclusive. **Lane 10:** PZC. Fifteen microlitres of sample was loaded into each lane.*

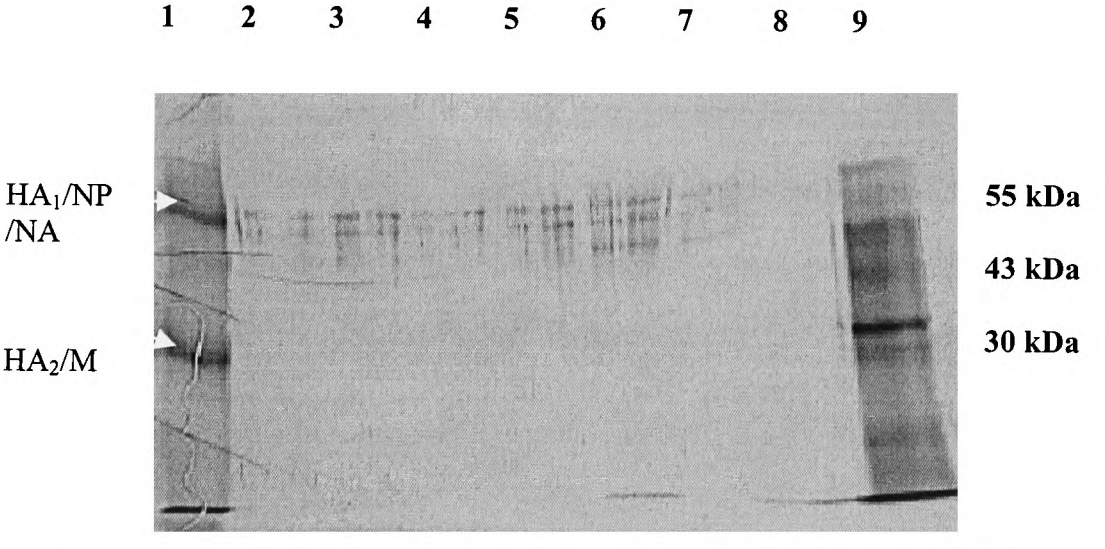

FIGURE 3.28 (c). Silver stain gel showing interphase/bottom phase Fractions 9 to 15 (in the absence of detergent) from Solubilisation Assessment Study.
The gel presented in this figure shows the fractions from the second extraction top phase (without detergent) analysed by SDS PAGE and silver stain. The corresponding protein and HA antigen concentration profiles are presented in Figure 3.28 (a).
***Lane 1:** PZC. **Lanes 2 to 7:** Dialysed Fractions 9 to 14 inclusive. **Lane 8:** Unused. **Lane 9:** Fraction 15. Fifteen microlitres of sample was loaded into each lane.*

The location of the antigen in the sucrose gradient suggests that the HA antigen derived from intact virus.

3.3.5.2. Evaluation of HA antigen solubilisation in second extraction interphase/bottom phase samples in the absence of detergent.

A sample from the second extraction interphase/bottom phase (refer to Figure 3.1) from partition of IBF material in ATPS S40 (see Table 3.4) without detergent was subjected to sucrose density ultracentrifugation (as described in Section 3.2.2.1). In the absence of detergent Figure 3.29 (a) depicted profiles (of protein and HA antigen concentration), which could be superimposed. Fractions 1 to 3 inclusive indicated large total protein and HA antigen responses, backed up by the corresponding silver stained gel, Figure 3.29 (b), confirming that virtually all of the total protein detected was due to the HA antigen. A comparison of profiles (Figures 3.28 a and 3.29 a) demonstrates that the interphase contains approximately 8 times more HA antigen compared to the corresponding top phase. The low protein concentration and silver staining appeared sensitive enough to resolve the two bands at approximately 25 to 27 kDa (due to matrix and HA_2 proteins respectively). The lack of protein in Fractions 4 to 15 (refer to Figures 3.29 a to 3.29 c) was mirrored by the absence of HA antigen in these Fractions (Fig 3.29 a). Thus in the absence of detergent, contaminant proteins (ovalbumin, apovitellenins III-V and phosvitin E_1) partitioned to the top phase in ATPS S40, whilst the viral proteins predominantly partitioned to the interphase/bottom phase in this same ATPS. The location of the interphase/bottom phase material (refer to Figures 3.29 a and 3.29 b) in the lower concentration sucrose (0 to 20 % w/v) was somewhat surprising and could be

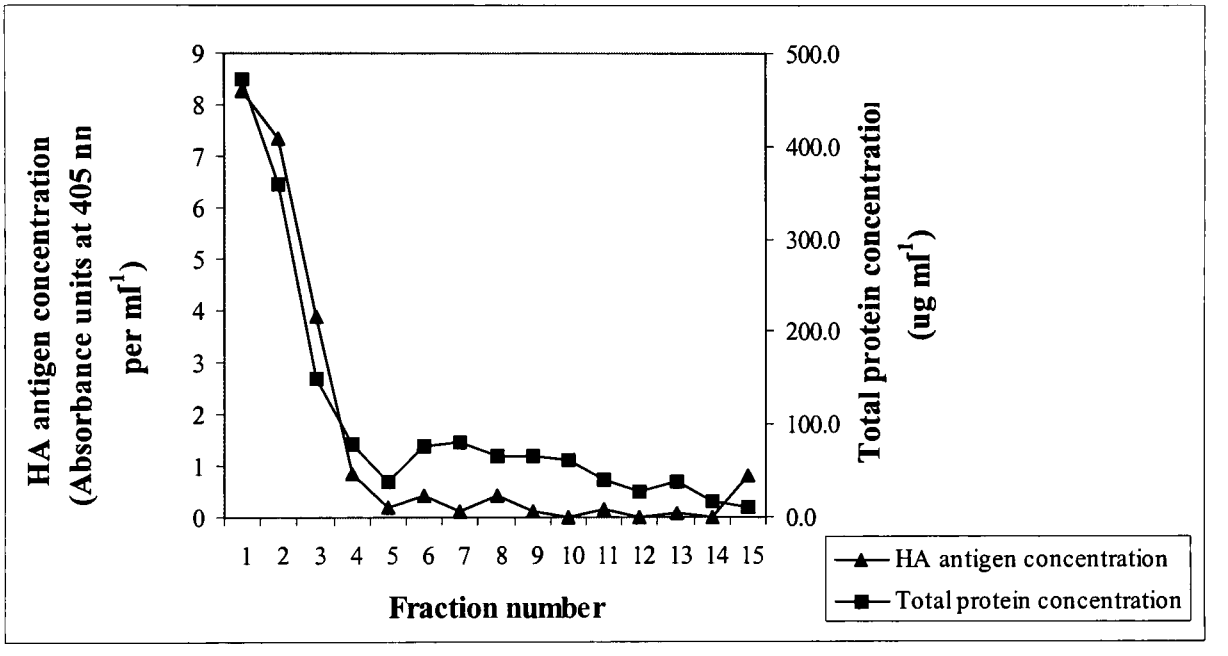

FIGURE 3.29 (a). Profiles illustrating distribution of HA antigen and total protein (as detected by ELISA and BCA assay respectively) from second extraction interphase/bottom phase fractions harvested from a sucrose density gradient in the absence of detergent.

A 3 ml sample from the second extraction interphase/bottom phase of IBF material partitioned (without detergent) in ATPS S40 was layered onto a sucrose density gradient (see Section 3.2.2) and processed as described in Sections 3.2.3 and 3.2.4. SDS PAGE gels corresponding to these fractions are presented in Figures 3.29 (b) and 3.29 (c) respectively. The HA antigen concentration can be compared with the corresponding top phase sample presented in Figure 3.28 (a).

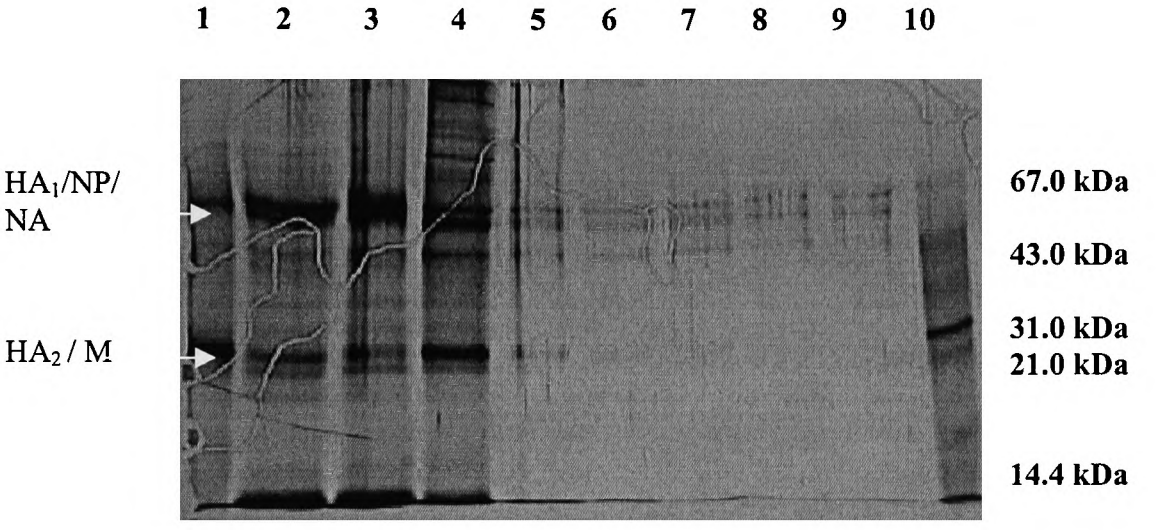

FIGURE 3.29 (b). Silver stain gel showing interphase/bottom phase Fractions 1 to 8 (in the absence of detergent) from Solubilisation Assessment Study.
The gel presented in this figure shows the fractions from the second extraction interphase/bottom phase (without detergent) analysed by SDS PAGE and silver stain. The corresponding protein and HA antigen concentration profiles are presented in Figure 3.29 (a).
***Lane 1:** PZC. **Lanes 2 to 9:** Dialysed Fractions 1 to 8 inclusive. **Lane 10:** Low molecular weight marker. Fifteen microlitres of sample was loaded into each lane.*

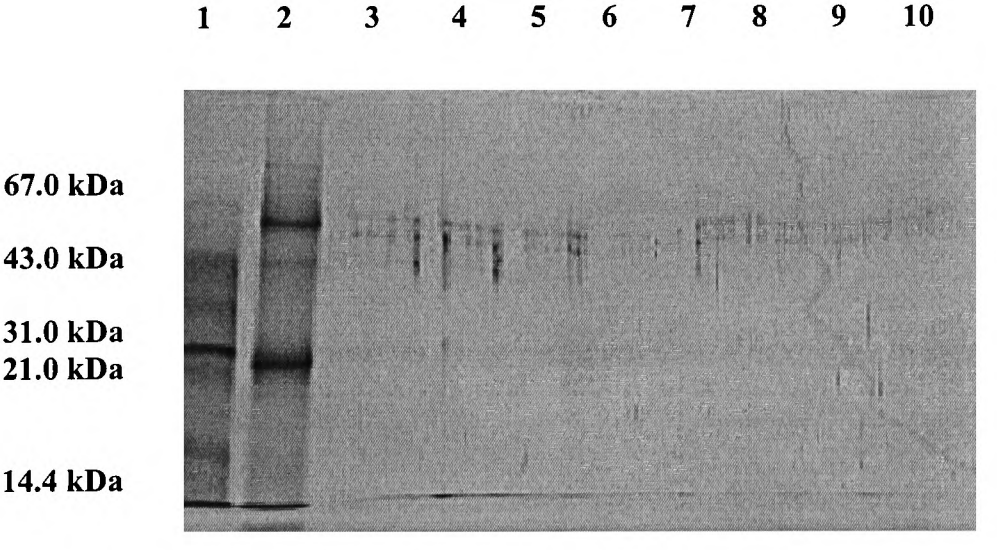

FIGURE 3.29 (c). Silver stain gel showing interphase/bottom phase Fractions 9 to 15 (in the absence of detergent) from Solubilisation Assessment Study.
The gel presented in this figure shows the fractions from the second extraction interphase/bottom phase (without detergent) analysed by SDS PAGE and silver stain. The corresponding protein and HA antigen concentration profiles are presented in Figure 3.29 (a).
***Lane 1:** Low molecular weight marker. **Lane 2:** PZC.*
***Lanes 3 to 9:** Dialysed Fractions 9 to 15 inclusive. **Lane 10:** Unused.*

attributed to traces of phosphate remaining post-dialysis, promoting aggregation of particles, which formed a (visible) carpet-like layer of lower density.

3.3.5.3. Evaluation of HA antigen solubilisation in second extraction top phase samples in the presence of detergent.

After a four-hour incubation period (refer to Section 3.3.4) with 1 % w/w Triton X100 and sample processing, the top phase total protein and HA antigen concentration profiles were depicted in Figure 3.30 (a). The profile presented in Figure 3.30 (a) indicated that protein and HA antigen were present in Fractions 1 to 4 inclusive, (corresponding to a sucrose concentration of approximately 0 to 20 % w/v). Another peak of protein and HA antigen was located at Fractions 9 and 10, (corresponding to a sucrose concentration of approximately 30 to 38 % w/v). These findings were confirmed with SDS PAGE/silver stain analysis (Figure 3.30 b and 3.30 c). The SDS PAGE gel presented in Figure 3.30 (b) demonstrated an increase in HA_1 antigen partitioning to the top phase in the presence of Triton X100 (as compared to Figure 3.28 b, no detergent). A species of HA antigen-containing fragments was also present in Fraction 9 and 10 (Figure 3.30 c). The location of this species in the gradient suggested that it was associated with denser material such as NP protein (although this was not confirmed by the gel). A two-fold increase in protein partition (and HA antigen) to the top phase was also detected (compare Figures 3.28 a and 3.30 a). This demonstrates that the increase in HA antigen release from the virus particles was due to the action of Triton X100 at 1 % w/w.

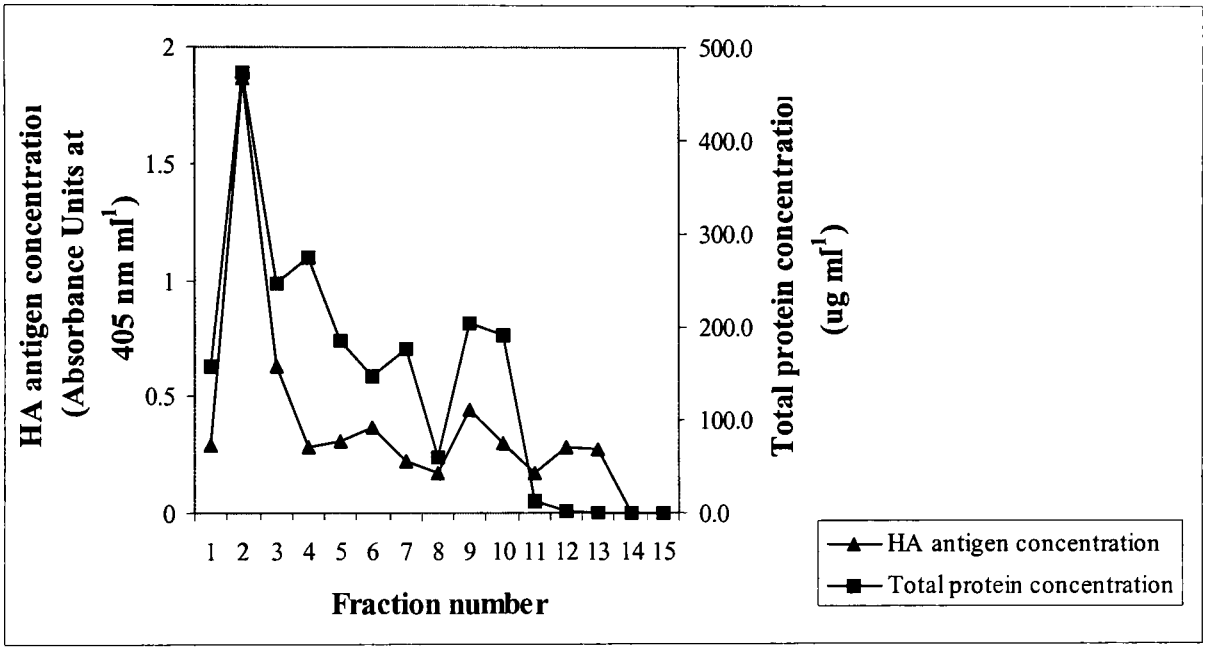

FIGURE 3.30 (a). Profiles illustrating distribution of HA antigen and total protein (as detected by ELISA and BCA assay respectively) from second extraction top phase fractions harvested from a sucrose density gradient in the presence of Triton X100.
A 5 ml sample from the second extraction top phase of IBF material partitioned (with 1 % w/w Triton X100) in ATPS S40 was layered onto a sucrose density gradient (see Section 3.2.2) and processed as described in Sections 3.2.3 and 3.2.4. SDS PAGE gels corresponding to these fractions are presented in Figures 3.30 (b) and 3.30 (c) respectively. The HA antigen concentration can be compared with the corresponding top phase sample without Triton X100 presented in Figure 3.28 (a).

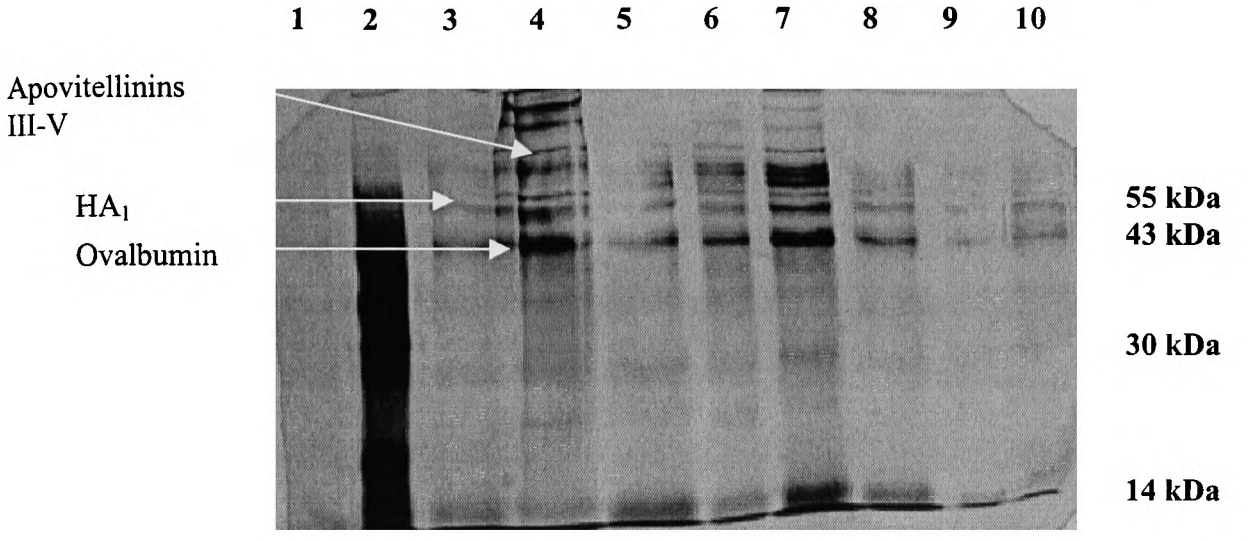

FIGURE 3.30 (b). Silver stain gel showing top phase Fractions 1 to 8 (in the presence of Triton X100) from Solubilisation Assessment Study.
The gel presented in this figure shows the fractions from the second extraction top phase (in the presence of 1 % w/w Triton X100) analysed by SDS PAGE and silver stain. The corresponding protein and HA antigen concentration profiles are presented in Figure 3.30 (a).
***Lane 1:** Pre dialysis second extraction top phase sample. **Lanes 2 to 9:** Dialysed Fractions 1 to 8 inclusive. **Lane 10:** PZC. Fifteen microlitres of sample was loaded into each lane.*

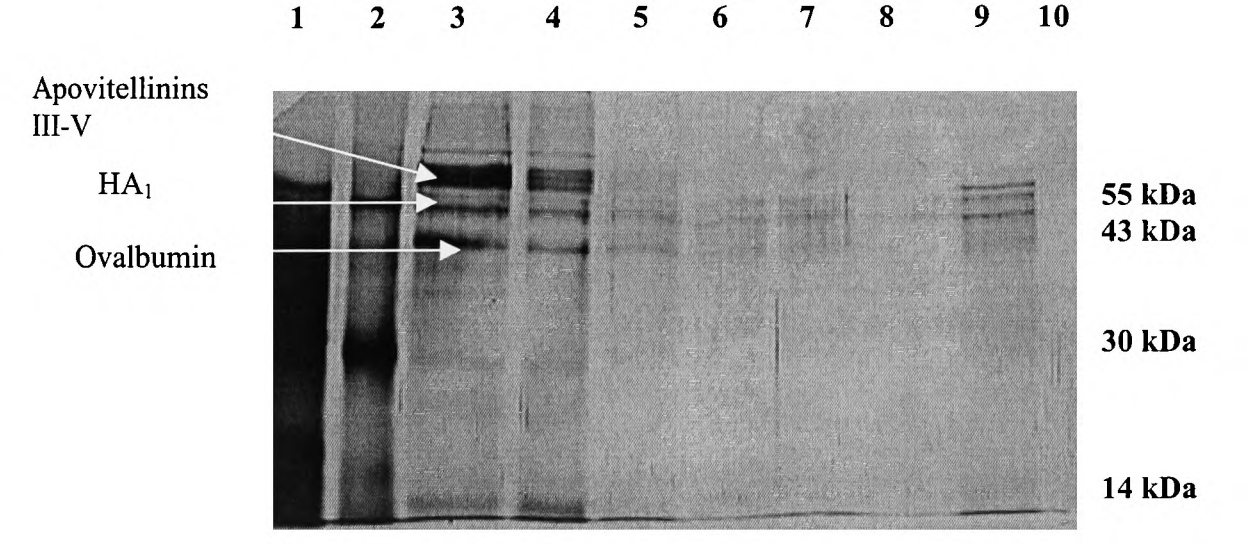

FIGURE 3.30 (c). Silver stain gel showing top phase Fractions 9 to 15 (in the presence of Triton X100) from Solubilisation Assessment Study.
The gel presented in this figure shows the fractions from the second extraction top phase (in the presence of 1 % w/w Triton X100) analysed by SDS PAGE and silver stain. The corresponding protein and HA antigen concentration profiles are presented in Figure 3.30 (a).
***Lane 1:** Low molecular weight marker. **Lane 2:** PZC.*
***Lanes 3 to 9:** Dialysed Fractions 9 to 15 inclusive. **Lane 10:** Unused.*

3.3.5.4. Evaluation of HA antigen solubilisation in second extraction interphase/bottom phase samples in the presence of detergent.

The interphase/bottom phase was removed for analysis (see Section 3.3.4) after IBF material was partitioned in ADTPS S40 in the presence of 1 % w/w Triton X100 for a period of fours hours. Total protein and HA antigen concentration profiles were depicted in Figures 3.31 (a). The profile presented in Figure 3.31 (a) indicated the presence of protein and relative absence of HA antigen in Fractions 1 to 4 inclusive. The protein concentration in Fractions 5 to 15 inclusive was relatively low. The HA antigen concentration profile generally mimics this (except for the peaks at Fractions 7 and 15. The former was thought to be an artifact and the latter, intact viral particles). The corresponding SDS PAGE gels of this profile (Figures 3.31 b and 3.31 c), back up the total protein profile in Figure 3.31 (a) except at Fraction 15 which suggests that it contains a low concentration of intact virus particles. The HA antigen data indicates that there is a low concentration of HA antigen in Fractions 1 to 14. The gels (Figures 3.31 b and 3.31 c) show protein bands at 55 and 30 kDa (corresponding to sucrose concentrations of approximately 0 to 30 % w/v). This means that the virus particles were disrupted to different extents and that the bands are predominantly due to NP and M respectively (because the ELISA detects HA antigen and more specifically, HA_1 antigen, see Figure 2.1). To summarise, most of the protein (including viral proteins) partitions to the top phase upon incubation with Triton X100. This suggests that the exaggerated HA ELISA responses observed with the interphase/bottom samples are due to the detergent and mask the fact that solubilisation has occurred. In order to confirm this, transmission electron microscopy (TEM) and negative staining was used to visualise the virus particles.

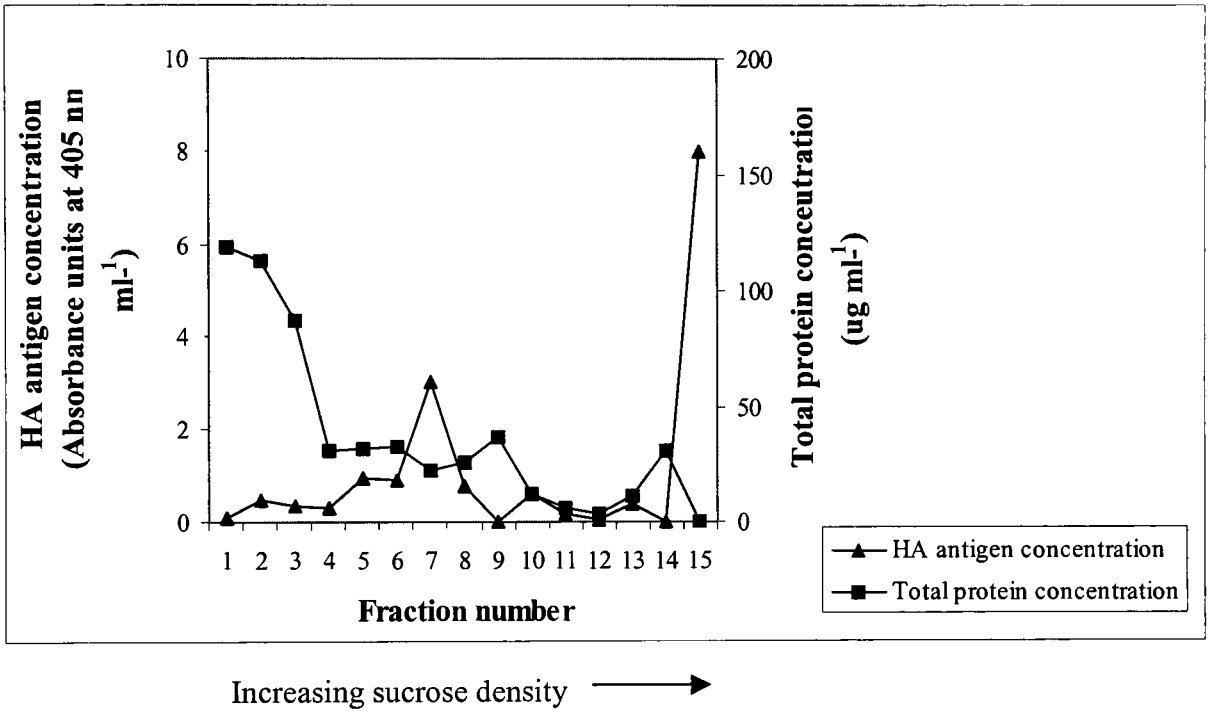

FIGURE 3.31 (a). Profiles illustrating distribution of HA antigen and total protein (as detected by ELISA and BCA assay respectively) from second extraction interphase/bottom phase fractions harvested from a sucrose density gradient in the presence of Triton X100.

A 5 ml sample from the second extraction top phase of IBF material partitioned (with 1 % w/w Triton X100) in ATPS S40 was layered onto a sucrose density gradient (see Section 3.2.2) and processed as described in Sections 3.2.3 and 3.2.4. SDS PAGE gels corresponding to these fractions are presented in Figures 3.31 (b) and 3.31 (c) respectively. The HA antigen concentration can be compared with the corresponding top phase sample without Triton X100 presented in Figure 3.29 (a).

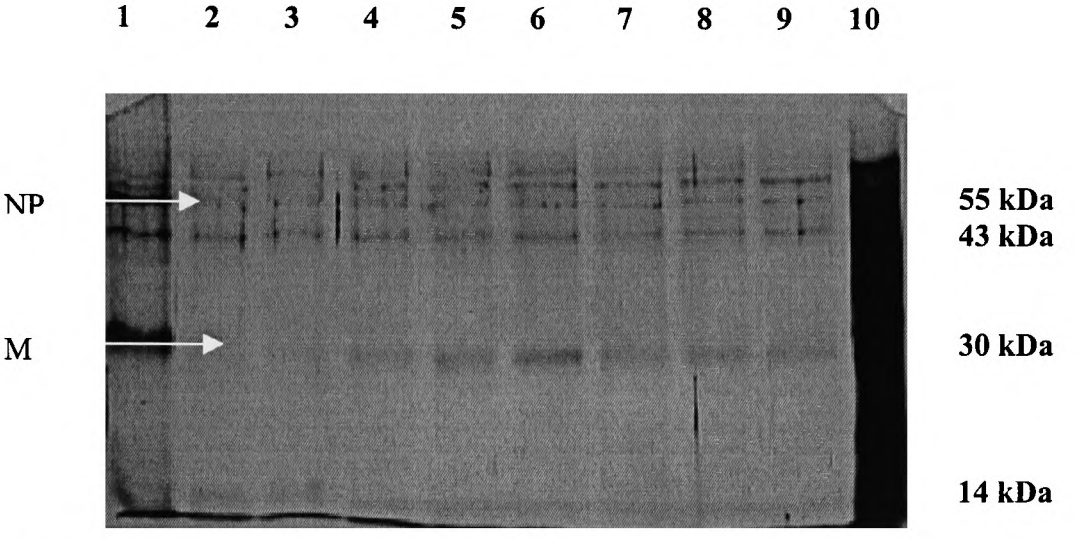

FIGURE 3.31 (b). Silver stain gel showing interphase/bottom phase Fractions 1 to 8 (in the presence of Triton X100) from Solubilisation Assessment Study.
The gel presented in this figure shows the fractions from the second extraction interphase/bottom phase (in the presence of 1 % w/w Triton X100) analysed by SDS PAGE and silver stain. The corresponding protein and HA antigen concentration profiles are presented in Figure 3.31 (a).
***Lane 1:** Pre dialysis interphase/bottom phase sample. **Lanes 2 to 9:** Dialysed Fractions 1 to 8 inclusive. **Lane 10:** Low molecular weight marker. Fifteen microlitres of sample was loaded into each lane.*

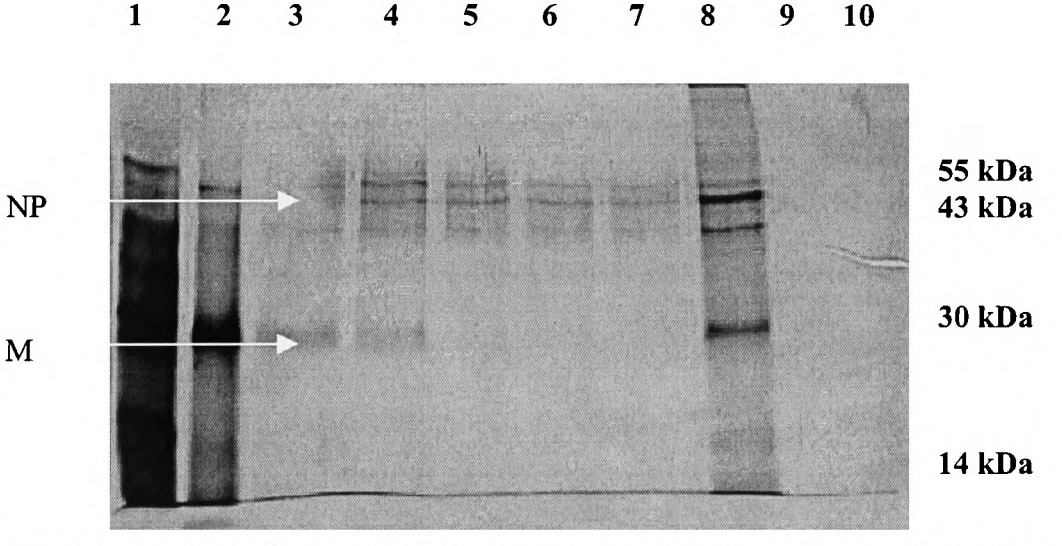

FIGURE 3.31 (c). Silver stain gel showing interphase/bottom phase Fractions 9 to 15 (in the presence of Triton X100) from Solubilisation Assessment Study.
The gel presented in this figure shows the fractions from the second extraction top phase (in the presence of 1 % w/w Triton X100) analysed by SDS PAGE and silver stain. The corresponding protein and HA antigen concentration profiles are presented in Figure 3.31 (a).
***Lane 1:** Low molecular weight marker. **Lane 2:** PZC.*
***Lanes 3 to 9:** Dialysed Fractions 9 to 15 inclusive. **Lane 10:** Unused.*
Fifteen microlitres of sample was loaded into each lane.

3.3.6. Analysis of second extraction top and interphase/bottom phases using transmission electron microscopy.

Samples described in the previous Section 3.3.5. were sent to Medeva Pharma and analysed by B. Getty. Negative staining and transmission electron microscopy (TEM) using 2 % w/v phosphotungstic acid (PTA), pH 6.8 and a Phillips TEM 300 were used at a magnification of 150,000 times. Despite dialysing the samples prior to analysis, it was only possible to capture images of the virus in the absence of detergent. Thus it was not possible to confirm the presence of different disrupted species (as presented in Figures 3.31 b and 3.31 c) and discussed in the previous section. Low concentrations of partially stripped virions were present in second extraction top phase pooled Fractions 1 to 4 (see profile in Figure 3.28 a), in the absence of detergent (Figures 3.32 a). This confirmed previous observations regarding antigen release in the absence of detergent (see Section 3.3.3.1). Pooled second extraction top phase Fractions 14 and 15 pooled (see profile in Figure 3.28 a), in the absence of detergent, also produced the same result Figure 3.33. This suggests that there were two species present in the top phase with different densities possibly due to more HA antigen being released in the former species compared to the latter. Second extraction interphase/bottom pooled Fractions 1 and 2 pooled in the absence of detergent, showed a fairly high concentration of essentially whole virus as shown in Figure 3.34 a. In addition, some of the virions were stripped and there was a high concentration of membranous debris present (Figure 3.34 b). Pooled Fractions 3 and 4 from this phase showed a low concentration of partially stripped virions amongst debris (electron micrograph not shown) This confirms the data presented in the profile shown in Figure 3.29 (a). Methods to improve the detection of components in the presence of detergent would be to submit the sample to ultracentrifugation (300,000 *xg*)

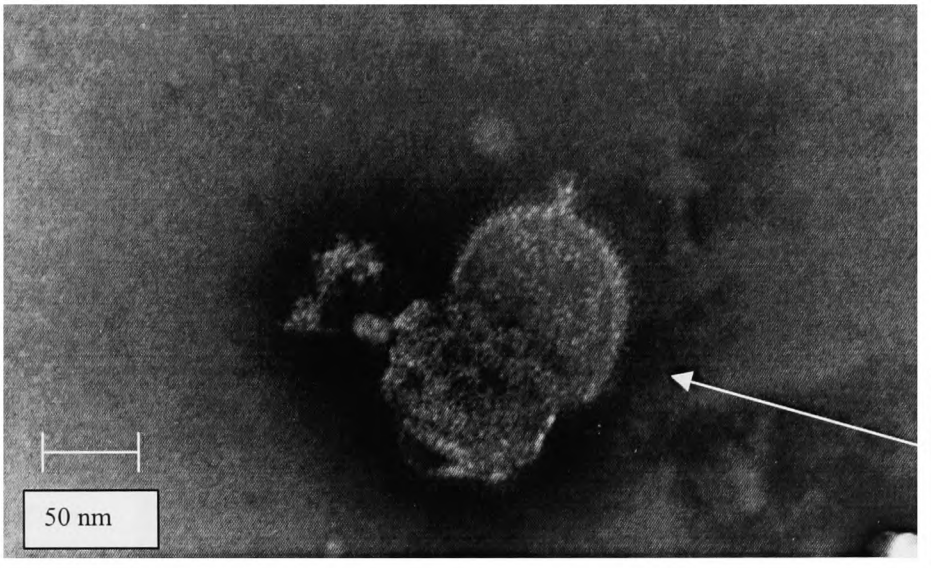

FIGURE 3.32. Electron micrograph showing a typical influenza A/Panama virion from pooled top phase. Fractions 1 to 4 in the absence of detergent.

The sample was negatively stained with 2 % w/v PTA pH 6.8 and deposited on a carbon coated copper grid. The electron micrograph was taken at a magnification of 150,000. (Refer to also Figure 3.28 a).

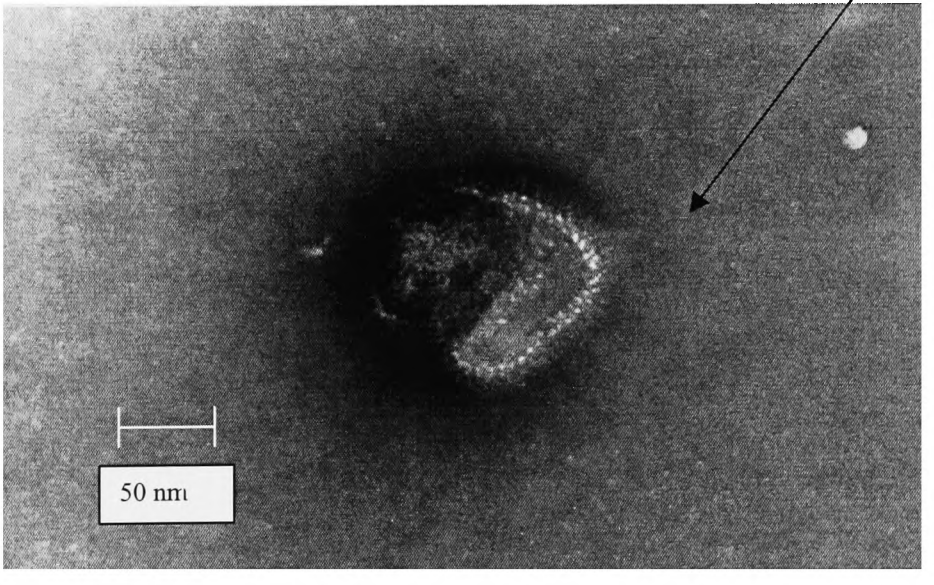

FIGURE 3.33. Electron micrograph showing a typical influenza A/Panama virion from pooled top phase. Fractions 14 to 15 in the absence of detergent.

The sample was negatively stained with 2 % w/v PTA pH 6.8 and deposited on a carbon coated copper grid. The electron micrograph was taken at a magnification of 150,000. (Refer to also Figure 3.28 a).

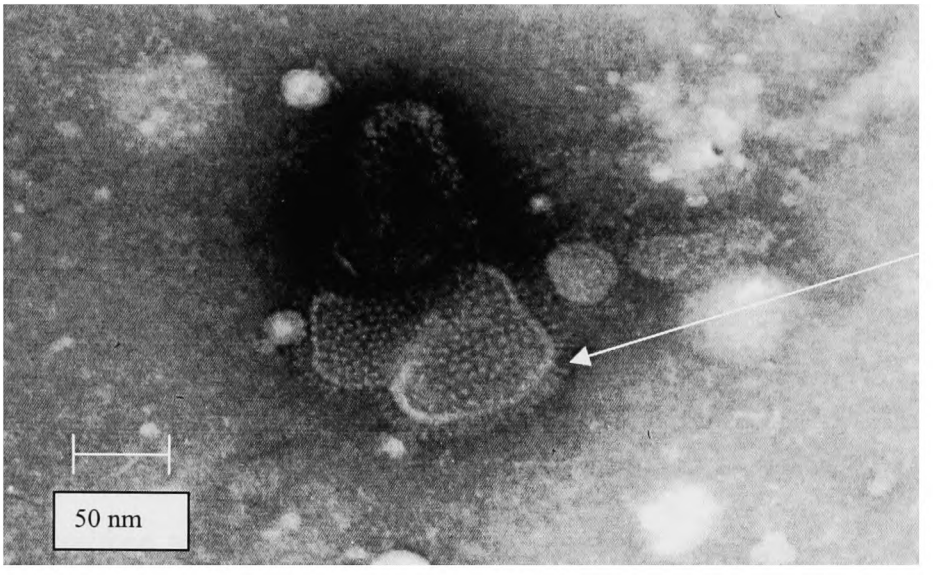

Influenza virus particle. Note HA spikes and intact nature of particle.

FIGURE 3.33 (a) Electron micrograph showing a typical influenza A/Panama virion from interphase/bottom phase Fractions 1 and 2 in the absence of detergent.
The sample was negatively stained with 2 % w/v PTA pH 6.8 and deposited on a carbon coated copper grid. The electron micrograph was taken at a magnification of 150,000. (Refer to also Figure 3.29 a).

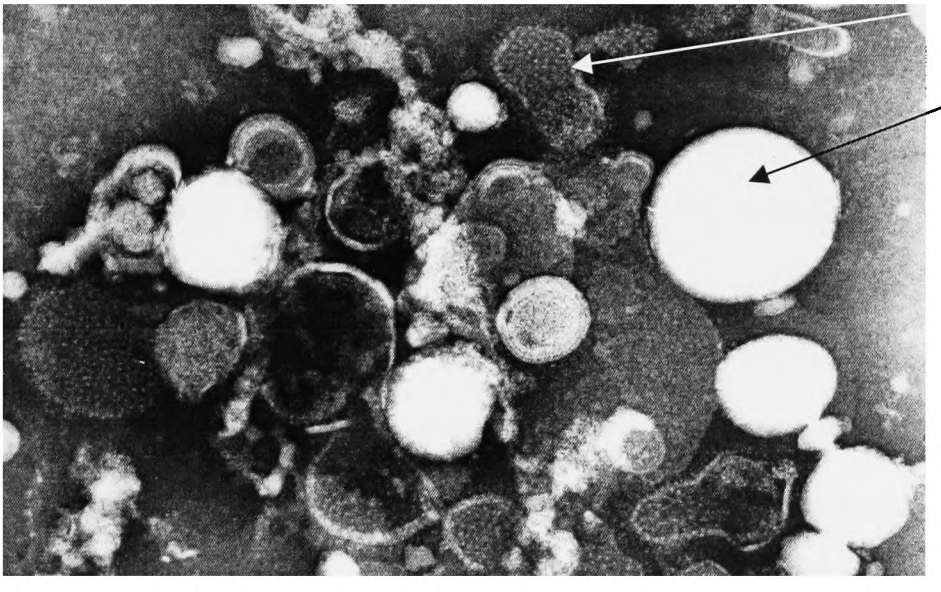

FIGURE 3.33 (b) Electron micrograph showing a typical influenza A/Panama virion from interphase/bottom phase Fractions 1 and 2 in the absence of detergent.
The sample was negatively stained with 2 % w/v PTA pH 6.8 and deposited on a carbon coated copper grid. The electron micrograph was taken at a magnification of 150,000. (Refer to also Figure 3.29 a).

and then resuspend the pellet in water. This would effectively remove salt, PEG and concentrate the sample. Also the ADTPS could be scaled up to create more particles for analysis.

3.3.7. Tangential flow ultrafiltration (TF UF).

The solubilised HA antigen recovered in the second extraction top phase of ADTPS S40 required further processing. Tangential flow ultrafiltration (TF UF) using a 100 kDa polyethersulfone membrane was employed to remove detergent in order to promote aggregation of solubilised antigen leading to the formation of aggregates approximately 300 kDa in size (Brady, PhD Thesis, 1974). These aggregates could then be separated from contaminants proteins (refer to Table 2.4). The removal of Triton X100 was to be facilitated by diluting below its critical micellar concentration (CMC) of 0.24 mM (or 0.02 %, see Table 3.1), so that monomers predominated in solution, which can easily pass through the membrane pores. The scheme outlined in Figure 3.35 illustrates the protein recoveries in an experiment designed to isolate solubilised HA antigen from other impurities. With regards to this study, the post UF (ultrafiltration) retentate material would be the end product of the purification scheme using ATPS. This would permit a comparison with end stage material generated by the Medeva Fluvirin™ Process (refer to Figure 3.1). Almost all the protein was recovered post first and second extraction stages. Although the recovery of protein could be accounted for post UF, 90 % of the protein was recovered in the permeate (see Figure 3.35). This suggests that the detergent had not been removed and that formation of the 300 kDa aggregates did not occur. Thus the HA antigens remained as (80 kDa) monomers which passed through the pores along with the apovitellenins and ovalbumin.

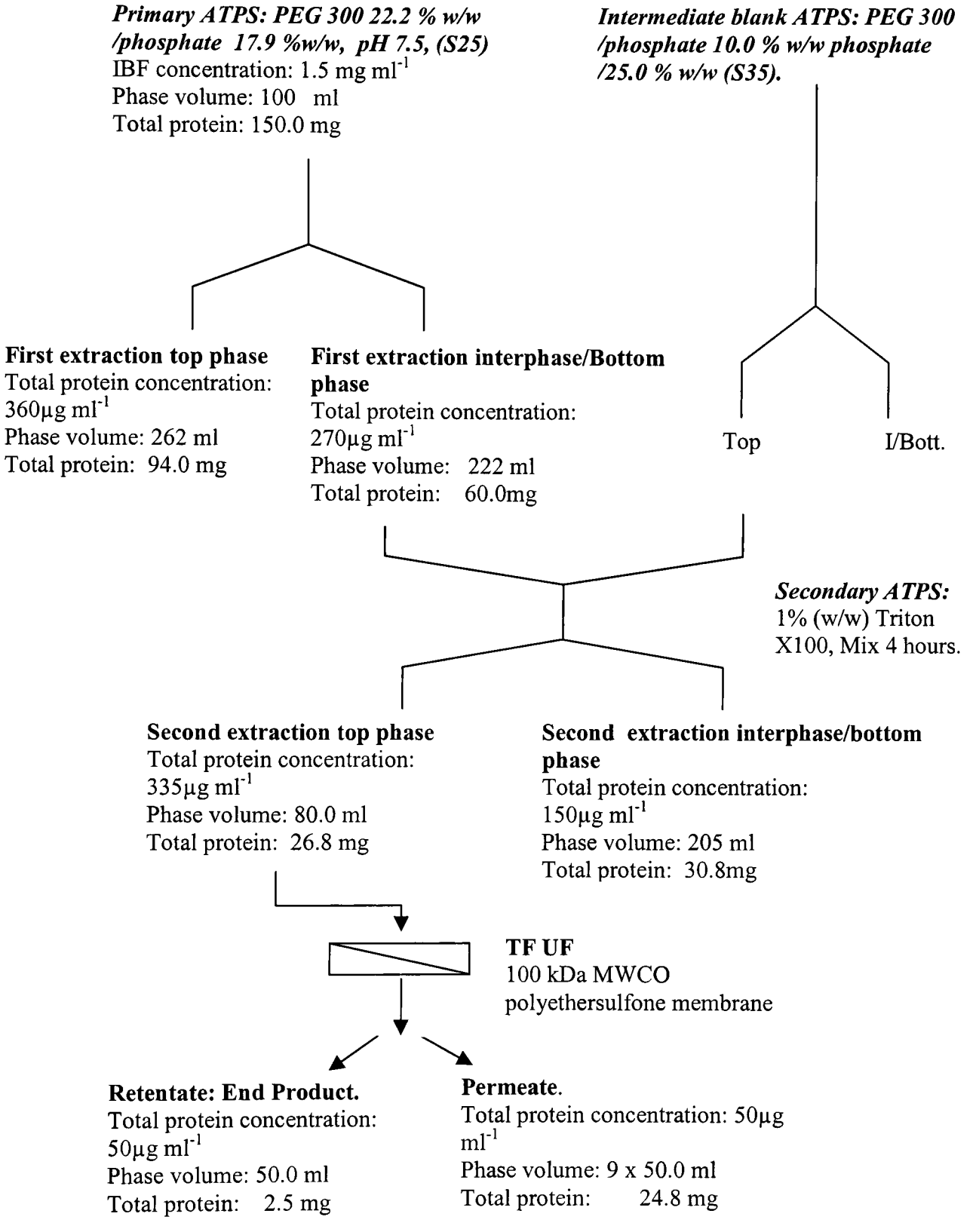

FIGURE 3.35. Scheme showing process stages using ATPS and TF UF along with recoveries of total protein. Quantities were estimated using SDS PAGE and densitometry.

The presence of detergent micelles is likely because the sample was not sufficiently. In the proposed scheme (Figure 3.35), assuming that all the detergent was available for solubilisation, the sample would need to be diluted at least fifty times (to disperse the micelles into monomers) giving a protein concentration of 0.007 g ml^{-1} and negligible HA antigen content. This unit operation can be improved by further elimination of impurities and a means of removing detergent, which does not require such dilution.

3.3.8. Comparison of ATPS performance against ultracentrifugation in the processing of IBF from the Medeva Fluvirin™ Process.

Aqueous two-phase systems (ATPS) capable of partitioning whole virus contained within inactivated bulk fluid (IBF) to fractionate influenza virus particles from process-related contaminants were initially investigated in Chapter Two and further studied in this chapter. The stages in the Medeva Fluvirin™ manufacturing process (outlined in Chapter Two and re-displayed in Figure 3.36), utilises sucrose density gradient ultracentrifugation. The initial ultracentrifugation procedure (Stage 5, Figures 3.36 and 3.37) eliminates debris and contaminant proteins, producing a whole virus- purified zonal concentrate (PZC). Addition of detergent, (Stage 6, Figures 3.36 and Figure 3.37) promotes the selective release of surface antigens, (haemagglutinin, HA and neuraminidase, NA) from the viral lipid envelope. The solubilised antigens and core material are then separated on the basis of size and density differences. Added detergent is removed by salting out (achieved by the inclusion of 2M phosphate) and finally, low molecular weight contaminants including the added salt are removed by diafiltration. This section compares the performance of ATPS with that of sucrose density gradient ultracentrifugation.

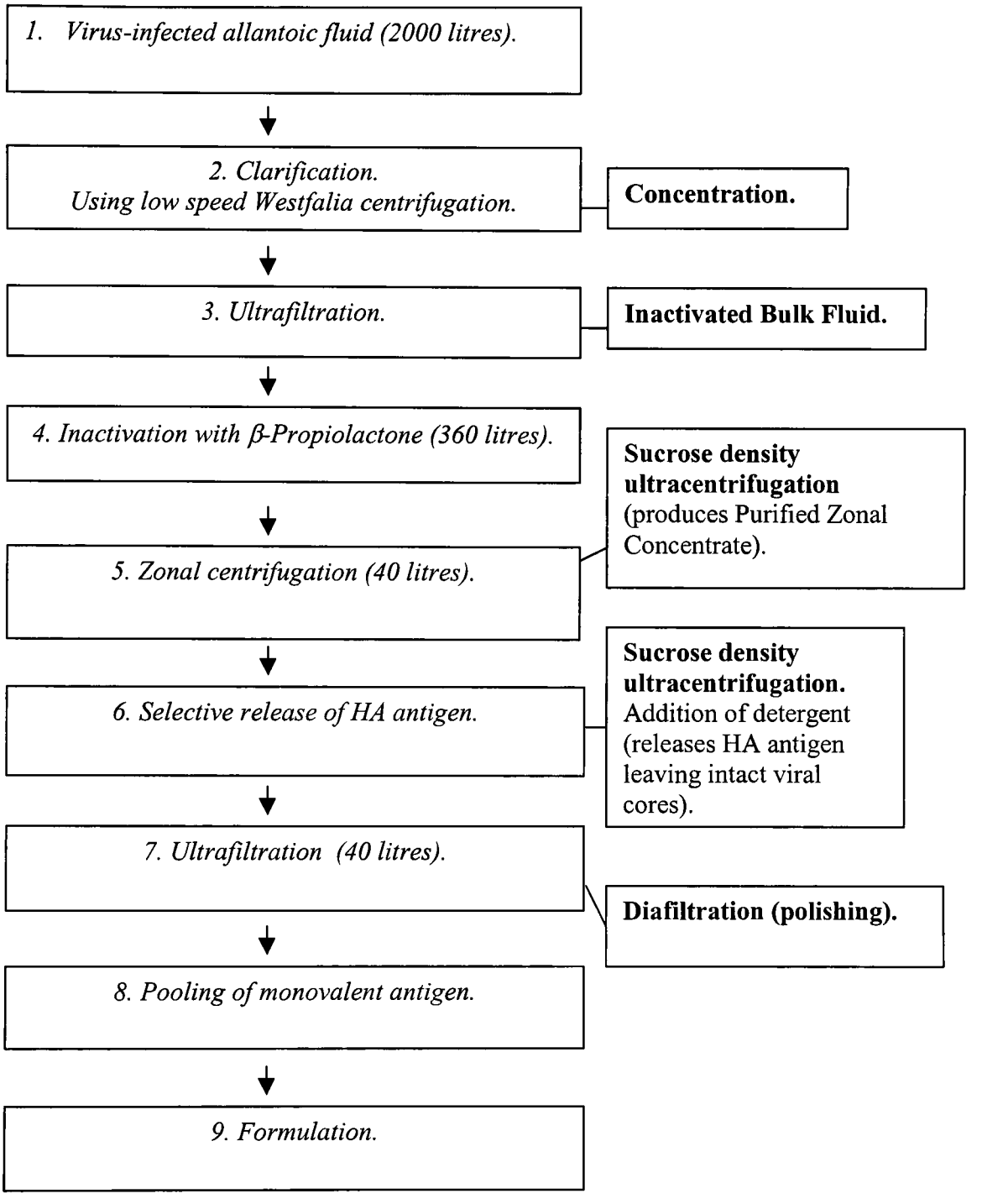

FIGURE 3.36. An outline of the downstream processing stages in the current Medeva Fluvirin™ Process.

Process Stage and brief description of process material.		*Process Stage and brief description of process material.*	
Stage 4: Inactivated Bulk Fluid (IBF). Whole virus and contaminating proteins in allantoic fluid.	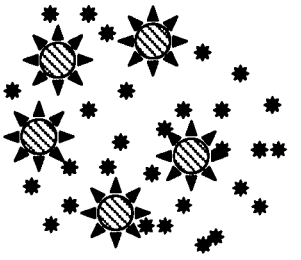	**First Key Stage: Inactivated bulk fluid (IBF).** Whole virus and contaminating proteins in allantoic fluid.	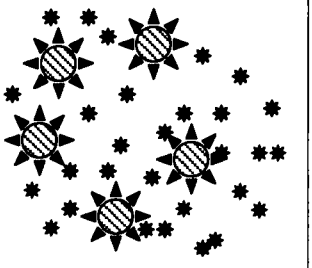
Stage 5: Purified zonal concentrate (PZC). Purified whole virus (very little contaminating protein- apovitellenins III- VI in PBS.	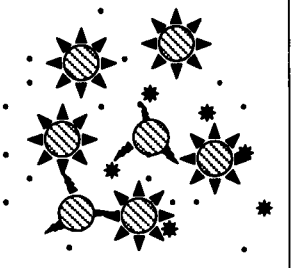	**Second Key Stage: Interphase/bottom phase1st extraction.** Debris, semi-purified, mainly whole virus; some stripped virions, contaminating proteins (OA, apovitellenins III-VI and residual phosvitins in (mainly) phosphate.	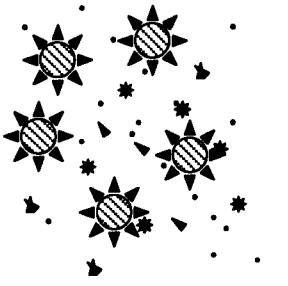
Post stage 7, pre stage 8: Mono-blend pool (MBP). Purified surface antigen (no core material).		**Third Key Stage: Retentate.** Low concentration of solubilised surface antigen, traces of detergent and carotenoids.	

KEY:

Whole virus 

Partially stripped virus 

Contaminating protein 

Surface antigen

Aggregated surface antigen 

Phosphate ions

FIGURE 3.37. Brief description of process feedstock and comparison of material at key stages of each purification strategy: ultracentrifugation (the Medeva Fluvirin™ process) and ADTPS/ATPS (the candidate process).

3.3.8.1. Using ATPS as a comparative technique.

As discussed previously, certain bottlenecks exist in the current process, which severely impact upon the volumetric throughput, the time to batch completion and ultimately, the process costs. These "process-limits" exist primarily at Stages 5 and 6 (Figure 3.36). The aim of this investigation was to use ATPS technology as a potential direct replacement for such process stages (refer to the schematic presented in Figure 3.38). Since the ultracentrifugation process could not be directly mimicked in this study (due to non-availability of the rotors used in the Medeva Fluvirin™ procedure), it was decided to use end-process material (post-Stage 7, pre-Stage 8, Figure 3.36), the mono-blend pool (MBP) to compare the material generated at the end of partition in the aqueous-detergent two-phase systems (ADTPS). The ATPS process performance was evaluated as follows: (i) a comparison of the material generated by ATPS with the MBP (from Medeva Fluvirin™ process) with respect to purity and yield (as deduced by SDS PAGE, a method recommended in the European Pharmacoepia) and (ii) the time taken to produce a batch from IBF to MBP (or its equivalent as generated by ATPS). It was expected that the ATPS process would yield a different profile of contaminants to that produced by the Medeva Fluvirin™ Process (refer to Figure 3.37). This was because the contaminants were removed sequentially, in the latter (contaminating proteins, core material and finally detergent). In contrast, material generated by partition in an ADTPS would still possess varying concentrations of these contaminants.

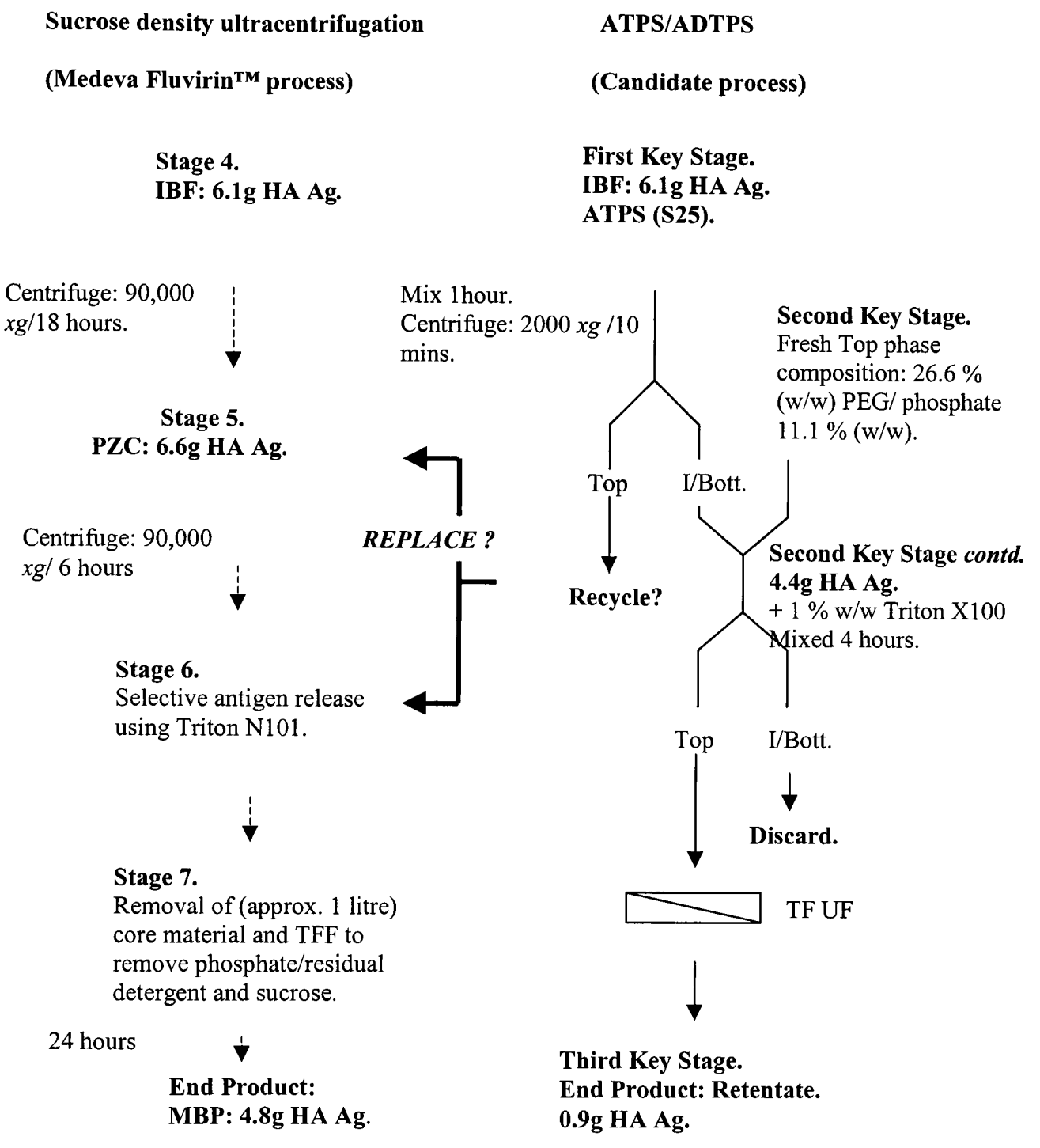

FIGURE 3.38. Purification of haemagglutinin (HA) antigen from influenza virus particles contained within IBF material. Comparison of down-stream purification steps used to (Medeva prepare a 90 litre batch of purified HA antigen using sucrose density ultracentrifugation Fluvirin™process) and ATPS (proposed process).

The bold arrows indicate process stages that could be potentially replaced by ATPS. The ATPS process has been scaled up for direct comparison with the Medeva Fluvirin™ process. In the up-scaled process, the use of an intermediate blank ATPS was replaced with phase-forming chemicals of identical composition to the intermediate ATPSs' top phase.

3.3.8.2. Characterisation of material from the Medeva Fluvirin™ Process.

Purity as defined by the Food and Drug administration (FDA) is the relative freedom of a product from extraneous matter including pyrogens. Since the bulk of impurities were protein in nature, the process was monitored for purity using SDS PAGE reduced gels. Purity with respect to mycoplasmas and potential adventitious viruses was not assessed here. The IBF and PZC from ultracentrifugation sourced from the Medeva Fluvirin™ process were representative of materials from the key process Stages 4 and 5 respectively (Figures 3.36 and 3.37). The IBF, (Lane 1, Figure 3.39) the starting material for this study, consists of many proteins (as described in Section 2.3.2.1) the major contaminants being the apovitellenins III-VI, ovalbumin and phosvitins. The viral proteins: HA (haemagglutinin), M (matrix protein), NA (neuraminidase) and NP (nucleoprotein) are also shown on the gel. The PZC (Lane 2, Figure 3.39) represents material from the next key process stage (Stage 5, Figures 3.36 and 3.37). Three bands are shown, from top to bottom, at approximately 80 kDa, 55 kDa and 25 kDa. The 80 kDa band represented residual apovitellenins III to VI. The 55 kDa band corresponded to HA_1/NP/NA and the 25 kDa band, was due to HA_2/M. There was a significant reduction in protein contaminants, notably ovalbumin, the phosvitins and the apovitellenins III to VI. The MBP material (Lane 9, Figure 3.39) is representative of material from the final process stage (with respect to this study), post-Stage 7, pre-Stage 8, Figures 3.36 and 3.37. This material showed three bands with identical molecular weights to those seen in PZC (Lane 2, Figure 3.39). From top to bottom, Lane 9, Figure 3.39, the first band (at approximately 80 kDa) represented residual apovitellenins III to VI. Since the core material had been removed by ultracentrifugation, the second band (at approximately 55

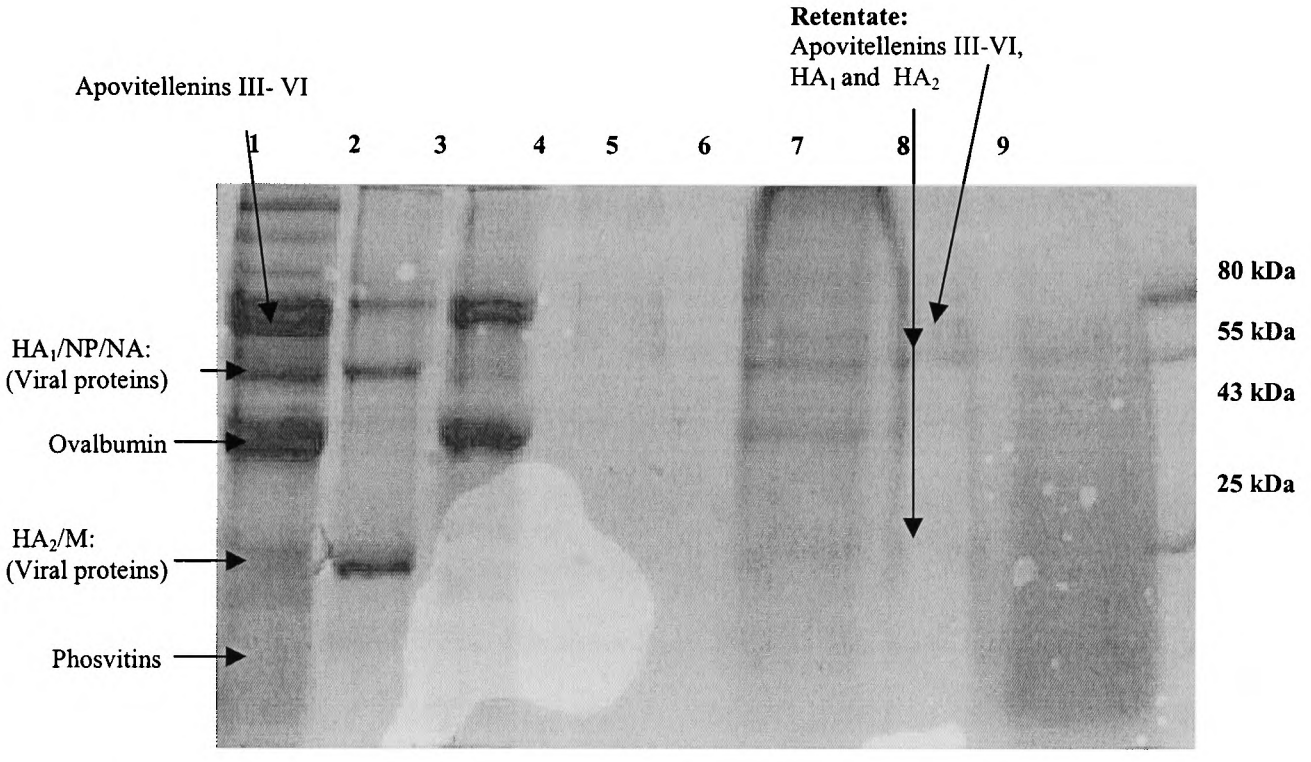

FIGURE 3.39. The purification of IBF purified using sucrose density gradient ultracentrifugation (Medeva Fluvirin™ process) was compared with purification of IBF using ATPS/ADTPS (candidate process) and monitored using SDS PAGE and one-dimensional densitometry.

Samples from key stages of both purification processes (Figure 3.37) were run on a 12 % homogeneous gel under reducing conditions. The IBF and PZC (Lanes 1 and 2) originated from Stages 4 and 5 of the Medeva Fluvirin™ process respectively (Figures 3.36 and 3.37). The mono-blend pool (MBP) material (Lane 9) represented post Stage 7, pre Stage 8 material from this process (Figures 3.36 and 3.37).

For comparison, the IBF and the interphase/bottom phase from the first extraction samples (Lanes 1 and 6 respectively) represented the first and second key stages of the ATPS process (Figure 3.37). The sample in Lane 6 formed the basis of the ADTPS (Figure 3.38). Lanes 4 and 8 represent purification of semi-purified IBF in the ADTPS. The top phase second extraction sample (Lane 4) was subjected to TFF. The retentate sample is shown in Lane 7. Thus the final stage comparison should be between the MBP (Lane 9) from the Medeva Fluvirin™ process and the retentate (Lane 7) from the ATPS/ADTPS process.

***Lane 1:** IBF 14.1 µg protein. **Lane 2:** PZC 4.2 µg protein.*
***Lane 3:** Top phase, first extraction (pre UF) 9.6 µg protein.*
***Lane 4:** Top phase, second extraction (pre UF)<1 µg protein.*
***Lane 5:** Unused. **Lane 6:** Interphase/bottom phase, first extraction (pre UF) 2.0 µg protein. **Lane 7:** Post UF Retentate 1.0 µg protein **Lane 8:** Interphase/bottom phase, second extraction (pre UF) µg protein. **Lane 9:** MBP 1.7 µg protein.*

kDa) corresponded to HA_1/NA and the third band (at approximately 25 kDa) was due to HA_2.

3.3.8.3. Characterisation of material generated by partitioning IBF in an ATPS.

The optimal primary ATPS for processing IBF material (as deduced in Chapter Three) was system S25, PEG 300, 22.2 % w/w/ phosphate 17.9 % w/w, pH 7.5, TLL 43.3 % w/w. The secondary ADTPS (including Triton X100) was system S40 corresponding to a blank ATPS of PEG 300 13.0 % w/w/ phosphate 24.3 % w/w. The composition of the top phase from ATPS S40 was PEG 300 26.6 % w/w/ phosphate 11.1 % w/w (refer to Figure 3.38). Fractions from the partition were electrophoresed (as described in Section 3.2.5). In addition to displaying material generated from the Medeva Fluvirin™ process, Figure 3.39, Lanes 3 to 8 (except Lane 5 which was unused) showed material from the ATP-partitioned fractions for comparison. The first extraction, top phase sample (from the primary ATPS) clearly shows that approximately 60 % of total proteins (including ovalbumin and the apovitellenins) have been eliminated (Figure 3.39, Lane 3). The resulting interphase/bottom phase of the first extraction, representing the start of the Second Key Process Stage (Figure 3.37), was similar to Stage 5 in the Medeva Fluvirin™ process, inasmuch as it contained a preparation of intact virus particles. (Lane 6, Figure 3.39) shows bands of residual apovitellenins III-VI (at approximately 80 kDa) and ovalbumin (at 43 kDa) as well as HA_1/NP/NA at approximately 55 kDa. The staining of the bands was poor and there was evidence of lane spreading. This was due to the high salt content remaining despite TCA precipitation. Samples from partition in the secondary ADTPS (including Triton X100) are shown in lanes 4 and 8 (the top phase and interphase/bottom phase respectively). The

presence of high concentrations of detergent in the top phase samples and high salt concentration in the interphase/bottom sample interfered with the TCA precipitation of protein leading to poor visualisation of the bands in these lanes. The retentate sample (Lane 7, Figure 3.39) shows three faint bands corresponding to residual apovitellenins III to VI (approximately 80 kDa) and HA_1 (approximately 55 kDa) and HA_2 (approximately 25 kDa). The recovery of this fraction was poor due to non-optimisation of the diafiltration step in which the presence of detergent and lack of HA antigen aggregation, meant that the technique could not separate the HA from the other proteins thus they passed through into the permeate (Section 3.3.7).

3.3.8.4. Assessing the performance purification processes using SDS PAGE and densitometry.

The behaviour of major proteins at all stages of both processes (Medeva Fluvirin™ and ATPS) has already been described (Sections 3.8.2 and 3.8.3). The key protein contaminants at similar key stages in both processes are illustrated in Figure 3.37. The data in Table 3.5 compares the yield and purity of material produced at each Key Stage in each process as well as overall. The end product from the Medeva Fluvirin™ Process is MBP, which consists essentially of HA surface antigen devoid of viral core material. Thus for calculation of yield and purity (and process comparison), the amount of surface antigen in the IBF and PZC materials was estimated from the total viral proteins on the gel and the proportion of surface antigen that the viral proteins represented (30 %) see Section 3.2.4.2. The estimation could only be applied for intact viral particles. It was assumed that the HA antigen in the retentate was due only to solubilised HA antigen.

The quantitative recovery of surface antigen between Stages 4 and 5 of the Medeva Fluvirin™ Process

SUCROSE DENSITY GRADIENT ULTRACENTRIFUGATION			AQUEOUS TWO-PHASE PARTITION		
Process stage	**Yield (%)**	**Purification Factor**	**Process stage**	**Yield (%)**	**Purification factor**
IBF (Stage 4)	N/A	N/A	**IBF (1st Key Stage)**	N/A	N/A
PZC (Stage 5)	109.0	4.0	**1st extraction Ib (2nd Key Stage)**	72.1	4.2
MBP (pre-Stage 7, post Stage 8)	73.0	1.8	**Retentate (3rd Key Stage)**	35.7	3.3
OVERALL PROCESS	80.0	7.3	**OVERALL PROCESS**	14.7	8.9

TABLE 3.5. Comparison of purity obtained at each key process stage (Table 4.1), from sucrose density ultracentrifugation and ATPS as determined by SDS PAGE and one-dimensional densitometry.
The total amount of protein was estimated by one-dimensional densitometry (Section 2.2.6). By subtracting the amount of contaminating protein from this, the amount of viral proteins were deduced. It was estimated that the surface antigens (HA and NA) comprised 30 % of the viral protein. Thus the amount of these antigens could be estimated in all the samples (except the MBP).

indicates how effective the ultracentrifugation step is since the intact viral particles are both purified and concentrated in the sucrose gradient. In comparison, the recovery of surface antigen between the First and Second Key Process Stages, (IBF to interphase/bottom phase, 1st extraction) using ATPS was 72.1 %. An uneven distribution of virus resulted when IBF was partitioned in ATPS S25 with most of the intact viral particles located in the interphase/bottom phase. Transmission electron microscopy (TEM) analysis (Section 3.3.6) confirmed this. In addition this technique showed that, a proportion of surface antigen partitioned to the top phase of this ATPS. This accounts for

the lower recovery of surface antigen obtained in the interphase/bottom phase. The purification factors obtained between Stages 4 and 5 of the Medeva Fluvirin™ Process (IBF to PZC) and between the First and Second Key Stages of the ATPS process (IBF to interphase/bottom phase, 1st extraction) were similar, (indicating that there was a similar degree of efficiency in the removal of bulk protein contaminants ovalbumin and apovitellenins). Between Stage 5 and post Stage 7 of the Medeva Fluvirin™ Process, (PZC to MBP), 73 % of the surface antigen was recovered. The losses were possibly due to non-solubilised surface antigen remaining attached to the core material (and thus banding out in higher density sucrose). The yield at the equivalent stage (between the Second and Third Key Process Stages, 1st extraction, interphase/bottom phase to retentate) using ATPS was substantially lower (35.7 %). This was due to non-optimisation of the ultrafiltration step (discussed in Section 3.3.7). The purification factor of the PZC to MBP stage (for the Medeva Fluvirin™ Process) was lower, indicating that a greater proportion of protein was surface antigen. The purification factor of the equivalent stage of the ATPS process (Third Key Process Stage) was 3.3. This showed that further removal of contaminating proteins was still occurring at this stage. The data demonstrated that the overall protein purity was marginally better using ATPS (overall purification factor of 8.9) but the overall yield was reduced, thus the Medeva Fluvirin™ process produced end material that was of similar purity to the ATPS material but is produced in much higher yield (80 %). This study demonstrated that material containing semi-purified intact virus particles (1st Key Process Stage) could be produced in one hour (combined with a lower energy input). The time to produce the equivalent Stage 5 material (from the Medeva Fluvirin™ Process) was 18 hours (using energy-intensive ultracentrifugation). Thus a scaled-up process could be beneficial

(particularly if centrifugal separators were used to decrease the time to equilibrium). In the light of the data obtained, the procedure proposed (in Figure 3.38) appears to be too ambitious in attempting to remove all the contaminants at once rather than sequentially. Thus ATPS has demonstrated advantages in the primary processing of viral particles in IBF, but further work is required to in order to fully realise these benefits. The scheme outlined in Figure 3.38 compares the process stages followed using sucrose density ultracentrifugation (as Medeva) and ATPS. Implementation of ATPS to replace Stage 5 (and eventually Stage 6) may be advantageous. The advantages would be realised primarily through the high volumetric throughput of material and the significant decrease in time required to obtain this material, thereby significantly minimising the process bottlenecks described at the outset of this work.

3.3.9 CONCLUDING DISCUSSIONS.

The aim of this study was to further the investigations undertaken in Chapter Two, using the primary ATPS S25 (PEG 300 22.2 % w/w/ phosphate 17.9 % w/w, pH 7.5) as a starting point to propose a purification scheme that yielded an end product similar to that obtained in the Medeva Fluvirin™ Process. A simple two-stage extraction process was undertaken to achieve selective release of HA antigen from intact virus and removal of impurities (see Figure 3.38). Nonionic detergents were evaluated to assess their ability to mimic selective release of surface antigens (which occurs in the Medeva Fluvirin™ Process). The effect of PEG chain length (molecular weight) was also assessed in the ATPSs used. The detergent examined were sodium deoyxhcholate, Triton X100 and Synperonic NP9. The former detergent was discounted from further use because of it interfered significantly in SDS PAGE gel analysis. Triton X100 and Synperonic NP9

partitioned preferentially to the top phase in the PEG-salt ATPSs due to these detergents sharing structural commonalities with PEG (see Figure 3.3). The amount of available detergent was affected by the molecular weight of PEG in the system. In general, the higher the PEG molecular weight, the poorer recovery of detergent. This was explained by preferential hydration of PEG leading to dehydration of the detergent head groups and aggregation. Excluded volume and salting out effects also contribute to aggregation (hence an ADTPS of shorter TLL would be better for use). A detergent concentration of 1 % w/w was determined to be optimal for recovery of solubilised HA antigen and Triton X100 was preferred to Synperonic NP9 for use in the ATPS. Recovery of IBF material in the ADTPSs was greatest in PEG 300-based systems. In addition a greater proportion of HA antigen was detected in the second extraction top phase samples as compared to secondary systems comprising other PEG molecular weights (see Section 3.3.3.2). This was explained in terms of protein and detergent partitioning to the same phase, less detergent dehydration in the presence of short chain PEG 300 and less excluded volume effects (therefore greater availability of detergent for solubilisation purposes). The HA recovery was over-estimated in the presence of PEG 300. It is thought that PEG 300 (by virtue of its small size) stabilises the antibody binding domains leading to an increase in binding. The presence of detergent probably potentiated this effect. This over-estimation was not observed with the other PEG molecular weights employed in the presence of detergent. The optimal ADTPS for solubilsation was S40 (PEG 300 13.9% w/w/ phosphate 24.3 % w/w, containing 1 % w/w Triton X100). The Solubilisation Assessment Study (Section 3.3.5) confirmed that HA antigen was released to the top phase in the presence of 1 % w/w Triton X100 (refer to Figure 3.30 a). It was proposed that solubilisation was non-selective leading to the release of different species

of HA antigen-containing fragment (refer to profile in Figure 3.30 a). This could be confirmed by TEM with samples prepared as discussed in Section 3.3.6. It is also necessary to confirm the identity of the high-density species (Fraction 15 in Figure 3.31 c), since a significant response was generated in the HA ELISA (refer to corresponding profile, Figure 3.31 a). This could be a species of core particles with some HA still attached which is responsible for the over-exaggerated response in the interphase/bottom phase. A more hazardous method for detecting solubilsed antigen (as distinct from core material) could involve radiolabelling the viral core and membrane with ^{32}P (Bachmayer, 1975).

3.9.1. Analytical methodology.

A number of analytical challenges had to be surmounted in this study. The method of sample preparation using TCA precipitation for SDS PAGE analysis was at times problematic giving non-quantitative recovery. Other methods had been tried previously, (Wessel and Flügge, 1984 and Sauvé *et al*, 1995) with varying degrees of success. An attempt to back up data presented in the Solubilisation Study (Section 3.3.1) which exploited TCA precipitation followed by monitoring absorbance at A_{280} did not work well because (despite repeated washing of the precipitate), the detergent could not be sufficiently removed to obtain reproducible results. Thus it was concluded that under the circumstances, the best method had been used. In the presence of PEG 300, the HA antigen ELISA gave exaggerated responses in the interphase/bottom phase (attributed to stabilisation by PEG and an increase in antibody binding in the ELISA). The samples from which the data in Figure 3.28 to 3.30 is presented have been dialysed thus the interference from PEG and detergent was removed. The fact that the magnitude of the

responses varied due to the instability of IBF upon storage raised concerns about the nature of the biomass loaded into the systems.

3.9.2. Effect of storage temperature upon IBF material.

It was possible that the components in the –70 °C batch differed slightly from those in the –20 °C batch (there may be more proteases and degradation products which could subtly affect the partition characteristics). Under such circumstances it would not be pertinent to compare data generated from these batches. The instability problem was not encountered at Medeva Pharma because the material is processed immediately onto the next stage (the production of the more stable PZC).

3.9.3. Partition and removal of other components in IBF material.

The main focus of this chapter was to address elimination during virus protein purification since they were by far the major source of contamination. However it was also recognised that a successful purification strategy should involve the removal of other contaminants such as lipids, carbohydrates, nucleic acids and metabolic by-products such as uric acid. Although this aspect was not studied in detail (with the exception of uric acid), some inferences can be made on the basis of observation, knowledge regarding the composition of the starting material and the handling process used. In the ideal situation (that is selective solubilisation of surface antigens), viral lipids and nucleic acid (RNA) should not increase the complexity of the purification problem. This is because the virus particle should remain intact. It is known that nucleic acids prefer to partition to the bottom phase in PEG-salt ATPs (Hustedt *et al*, 1985; Albertsson, 1986). A possible method to detect the RNA could involve developing the

SDS PAGE/densitometry method used in this study, but using agarose gel electrophoresis and RNA standards. It was thought that lipids (mainly in the form of low-density lipoproteins) partition to the uppermost phase in a four-phase system (as discussed in Section 3.3.3.4). Thus removal of this yellow coloured phase could facilitate lipid removal. Carbohydrates should not pose a problem since they are associated with the viral protein. Uric acid, an excretory product has a purine-based structure. The levels of this metabolite in IBF were estimated to be 0.1 % (by monitoring the absorbance at 293 nm, Wharton and Wharton, 1960). This would be diluted ten-fold in the ATPS that would be negligible. Further analyses indicated a bottom phase preference for this product (like nucleic acids).

3.9.4. The effectiveness of ultracentrifugation in selective release of HA antigen.

It was possible that during the mixing of the particulate suspension with solid phase forming chemicals and detergent, the particles encountered a wide range of dynamic changes in PEG and phosphate concentration (described by Walker, PhD Thesis, 1998). This proposal has been lent some credence in that researchers have reported differences in partition characteristics depending on whether wet or dry phase formants are used. This is attributed to the locally high PEG concentration (Hammar *et al*, 1989b). The particles cross the interface (so-called "trans-interfacial transport"), which could have imposed stresses on the particles leading to disruption of virus and generation of HA antigen-containing fragments (because even PEG on its own had some ability to remove antigen even before detergent addition). In the ultracentrifugation method, the virus passes downward through a stabilised localised band of detergent at approximately 30 % w/v sucrose (personal communication, P. Sinclair, 2000), with a high concentration of

micelles per square area gives a higher opportunity to strip more antigen creating a releasing antigens to the less dense sucrose and core material travels onwards towards denser sucrose concentration. Thus the antigen release is more consistent. If this was true, then the method used to select the detergent conditions (using purified whole virus and sucrose density ultracentrifugation) could not be satisfactorily applied to selecting the optimal detergent conditions in an ADTPS. If time had permitted, the pure intact virus (PZC) would have been partitioned in hybrid ADTPS containing different concentrations (or more importantly, different detergent: protein ratios).

3.9.4.1. Methods to improve ATPS.

Strategies require developing which permit more solubilised antigen to be recovered in the top phase. For example, the volume ratio could be varied (to determine the optimum top phase volume for antigen recovery). In this study, a small top phase volume was selected in order to concentrate antigen in the top phase and additionally to facilitate the ease of handling. This however could have placed restraints upon the recovery of antigen in the top phase since other proteins and detergent (so-called competing contaminants) also had a preference for the top phase. Indirectly manipulating the volume ratio could aid re-partition of the interphase.

3.9.5. Characterisation of loaded ADTPSs.

The naming of secondary hybrid systems ADTPSs was undertaken by using the phase composition of the corresponding blank hybrid. This is not strictly correct because by the time the IBF and detergent had been added, the system would have changed (refer to

Section 3.17.1). Characterisation could be performed by observing the distribution of radiolabelled amino acids, (Lebreton, PhD Thesis, 1998) in the ADTPs.

3.9.6. The potential of ATPS as a fractionation technique for processing of nanoparticles.

Aqueous two-phase partition (ATPS) as a commercially viable purification technique is pretty much in its infancy in the UK. Although the data showed that overall, the current process (using sucrose density ultracentrifugation) performed better than ATPS (for reasons already discussed), this candidate technology displays much potential. It demonstrated its worth as a purification technique: by rational selection of appropriate systems, bulk protein contaminants were significantly removed from the viral particles. Aqueous two-phase partition established its potential not only as a protein purification tool, but also as a nanoparticulate purification method (affirming the work of other researchers: Braas, 2000; Walker and Lyddiatt, 1999). This technique illustrated that it has a major role to play in the purification of commercialised therapeutic products with respect to processing large volumes of medium, in the fastest time possible, as economically as possible.

CHAPTER FOUR.

4. FINAL CONCLUSIONS AND FUTURE WORK.

4.1 Restatement of objectives.

In order to conclude whether the objectives of the study were met, it is necessary and helpful to remind one what these aims are. The main aim was to investigate the potential of a liquid-liquid fractionation technique, utilising aqueous two-phase systems (ATPS) towards the primary purification and recovery of inactivated influenza virus particles sourced from allantoic fluid within fertile hens' embryos. These nanoparticles were destined to formulate a commercial subunit vaccine, Fluvirin™ (produced by Medeva Pharma, Liverpool, UK). The requirement for such a study was highlighted by various limitations identified in the current process. Performance of this novel fractionation technique was then compared to the current method of manufacture, sucrose density ultracentrifugation. The final ultracentrifugation stage utilised Triton N101 in the gradient to solubilise the immunoprotective surface antigens haemagglutinin (HA) and neuraminidase (NA). Separation was brought about by buoyant density differences between the detergent micelles, surface antigens and the intact core material. These antigens were further purified and formulated into Fluvirin™ subunit vaccine. Comparison between ATPS and ultracentrifugation was undertaken with respect to purity, yield and time taken to produce a batch. The possibility of integrating ATPS in the established purification and recovery protocol was also investigated leading to the proposal of where in the current process ATPS could be used for maximal effect. Demonstration of the utility of ATPS in the successful handling of influenza virus

particles could provide further grounds for embracing it as a serious purification technique for handling nanoparticles.

4.2. Investigations undertaken.

Investigations were initially undertaken using purified, intact virus particles (as supplied by Medeva Pharma). One of the major influences upon partition in ATPS is the molecular weight of PEG employed (as previously discussed). Thus the effect of PEG (in the average molecular weight range 300 to 8000 kDa) upon partition was evaluated. The analytical procedures developed were SDS PAGE and quantitative one-dimensional densitometry to determine fractional mass ratios (FMRs) to monitor partition of contaminating proteins and viral proteins and a HA ELISA (originating from Medeva Pharma) in order to monitor partition of HA from the virus. Thus it was possible to assess the impact of the PEG molecular weight, TLL (with volume ratio being fixed at unity). The viral particles partitioned to the interphase in all systems used. Although it would have been simpler (from the viewpoint of FMR determination) to ignore this phase (on the basis of the small volume occupied), the majority of the virus (>80 % of the antibody signal as judged by HA ELISA) was located in this phase. An ATPS comprising PEG 300 (S2, refer to Appendix II) was useful at directing major contaminating proteins (namely apovitellinins III-VI and ovalbumin) away from the virus at the interphase. In addition, manipulation of volume ratio to concentrate the virus into a smaller volume was also undertaken providing the candidate ATPS S25 (refer to Appendix II). This system demonstrated the value of ATPS for the primary purification

of influenza viral particles. The next stage was to attempt to design a strategy whereby final stage material (monoblend pool, MBP) equivalent to that produced by the Medeva Fluvirin™ Process (using sucrose density ultracentrifugation) could be produced using ATPS. Equivalence in this context entailed a comparison using SDS PAGE of the proteins present. The process design incorporated addition of a fresh top phase (to replace the original one now contaminated with undesirable proteins) and addition of 1 % w/w Triton X100 (to solubilise the surface antigens) generating an aqueous detergent two-phase system (ADTPS), system- S40 (see Appendix II). A comparison of processes was undertaken and discussed with ultracentrifugation designated as the benchmark process.

4.3 Main conclusions.

The results demonstrated that in the PEG-phosphate ATPS examined, pH 7.5 (with varying PEG molecular weight and TLL with volume ratio of unity), the virus preferentially partitioned to the interface. This finding was not unexpected since it is well known that particles prefer partition to the interface since this lowers the free energy of the system (Albertsson, 1986). As the polymer concentration increases (with increased TLL and interfacial tension), the number of particles partitioning to the interface increases. Particles with diameters in excess of 10 nm adsorb non-specifically (regardless of their surface properties) to the interface leading to partition between this phase and a bulk phase (Bamberger, *et al*, 1985). According to Walter *et al*, (1991), partition is dominated by surface properties per unit area in larger particles (with surface areas in excess of 0.2 μm^2). In the case of particles smaller than this, partition is governed by size

(surface area). Assuming that the influenza particles are spheres with a radius of 0.05 μm and using the equation: surface area = $4\pi r^2$, then the calculated surface area is 0.03 μm^2, which suggests that it is the size that governs partition of these particles. However, the surface area is much greater than that calculated for a sphere because influenza possesses surface HA and NA projections. Therefore one concludes that surface properties dominate partition (similar to α-glucosidase inclusion bodies used by Walker, PhD Thesis, 1998). In the case of influenza the surface properties must be extremely large to elicit almost total adsorption of virus to the interface (as judged by HA antigen ELISA) because this occurred in systems of low TLL (for example S9, TLL, 8.3 % w/w). Debris also partitions to this phase suggesting that it is of similar density, particle size with similar surface properties.

Comparison of process performance between ATPS and sucrose density ultracentrifugation was undertaken using SDS PAGE and densitometry to monitor purity and to quantitate the recovery. The purification was divided into equivalent stages (refer to Table 3.5): IBF to PZC- Stages 4 to 5 (corresponding to the First to Second Key extraction stages using ATPS); and PZC to monoblend pool (MBP)- Stages 5 to Post Stage 7 corresponding to the Second to Third Key Stages using ATPS. The results demonstrated that the first purification stage produced a higher quantitative recovery when using ultracentrifugation (109 %) as compared with 72 % using ATPS.

However product purity at this first stage using either process was similar (purification factor 4.0, ultracentrifugation, purification factor 4.2, ATPS). The lower recovery using ATPS was attributed to a small proportion of solubilised HA antigen partitioning to the top phase. The time to produce this material using ATPS was significantly lower (1

hour) compared to the time taken to produce equivalent material using ultracentrifugation (18 hours). ATPS did not perform well in the second stage of purification with respect to quantitative recovery of the HA antigen. This was due to the attempts at trying to remove remaining impurities simultaneously rather than sequentially and by non-optimisation of the ultrafiltration step. Thus it was proposed that ATPS could find a use in the early stage of the purification process. It was not confirmed in this study whether the particles remained intact during the first purification stage although evidence from TEM analysis (Section 3.3.6) suggested this to be the case. Data (not presented) showed that HA and NA in PZC partitioned to the same phase, which suggests that the particles did remain intact. This study also emphasised the importance of having sensitive, specific assays to allow characterisation of the feedstock components. Thus the use and potential of ATPS for selectively fractionating influenza virus was demonstrated.

4.4. Future work to improve existing process using ATPS to fractionate allantoic fluid containing influenza particles.

The processing of influenza virus particles using ATPS (as documented in Chapters Two and Three) demonstrated great potential. However, in order to implement such a technique for commercial use a number of investigations need to be undertaken. The first stage of the purification proved relatively successful (as discussed in Section 4.3), but the second stage was subject to various problems. Due to time constraints, these problems were unable to be adequately addressed, thus it was decided to integrate the current ATPS process into downstream stages of the Medeva Fluvirin™ Process. The

fullest benefits of ATPS could be realised if ultracentrifugation was not used at all. Walker, (1998) demonstrated that repartitioning of the interphase into an identical ATPS lead to further removal of impurities as this gave the interphase components another opportunity to release contaminating proteins. Such an occurrence would have been beneficial for the purification scheme using influenza. Two strategies could be employed to process further the particles at the interphase. The first strategy involves direct harvesting of the interphase and incubating it directly with detergent (to enhance to the solubilising step) followed by re-partition into an ATPS. Thus the antigens could be solubilised and partition into a bulk phase whilst the core material and debris remained at the interphase. Confirmation of solubilisation could be performed by TEM. The reasons this had not been previously confirmed, pointed to the preparation of samples for analysis (see Section 3.3.6). If solubilsation did not occur, then the detergent and detergent conditions would require re-evaluation. Instead of using ultracentrifugation to assess the potential of a detergent (as described in Section 3.2.2), ATPS would be used. The second strategy would involve increasing the loading and (perhaps) manipulation of system pH to obtain a sediment, thus mimicking the inclusion body partition experiments undertaken by (Walker and Lyddiatt, 1998). The former strategy would probably be the most useful since the surface antigens could be isolated and it is these components that are ultimately required. The latter strategy *may* be useful for maximising the number of intact particles in the system (that is utilising the full capability of the system capacity). However, the type of manipulations involved such as changing the pH would affect the conformation of the surface antigens or aggregation properties (Henderson *et al*, 1973)

and hence the immunoprotective antibodies generated from any potential vaccine formed thereof.

Other important investigations include assessing the impact of allantoic fluid (contains uric acid) and β-propiolactone upon the binodal curve. The latter hydrolyses (into hydracrylic acid) and it would be useful to know if these affect partition of the feedstock. This could be done by determining the phase diagram in the presence and absence of (0.05 % v/v) β-propiolactone and then to determine the phase diagram at different time points β-propiolactone addition. Superimposition of the phase diagrams would indicate β-propiolactone has no effect upon the phase diagram. If ATPS was to be employed routinely for handling influenza virus, a generic purification strategy must be demonstrated for different strains (for example A/Beijng and B/Panama). In addition, it is important to characterise the ATPSs used. This could be done using distribution of radiolabelled amino acids, a method used to deduce TLL in loaded ATPSs and hence redefine co-ordinates on the binodal curve (Lebreton, PhD Thesis, 1998).

It was believed that the influenza virus partitioning (at the biomass load used) was directed by its surface properties and independent to that of the proteins. Partitioning of the virus alone would confirm this (at the time of undertaking experiments with pure virus, the interpretation of the interphase belonging to a bulk phase was used, therefore it was not treated as a discrete phase). The proteins may have exerted some influence on each other. Partitioning blank bulk fluid (without influenza virus) and using the SDS PAGE/quantitative one-dimensional densitometry to ascertain the fractional mass ratios (FMRs) of the main proteins could verify this. Studies on the impact of load are required because this would impact on partition of the proteins, manifesting in increased salting

out effects and the prevention of protein access due to the interphase acting as a physical barrier.

A means of estimating the total number of particles and the ability to monitor their distribution in an ATPS is required. This would assist in comparison of partition behaviour with different feedstock in different ATPSs. However it would be insufficient to comment solely on the number of particles, a better correlation involves the number of particles per unit area to facilitate comparisions with other particulate feedstocks.

4.5. How ATPS could impact further upstream in the processing of Fluvirin™.

Further upstream of the process described in this study, the influenza particle-containing allantoic fluid is harvested from the eggs. It is during this stage that presumably the impurities (from fragments of cell membrane and within the allantois) and protein contaminants (from the yolk and albumin sacs, Figure 2.2) are introduced. A gross clarification step using a continuous flow Westfalia centrifuge (and if necessary, microfiltration) is used to separate solids (debris from the embryo) from the soluble proteins. It is not envisaged that ATPS could be useful at very early stages due to the high solids content produced. However prior to inactivation the bulk fluid is dilute and is normally ultrafiltrered (using a Pellicon™ ultrafiltration system and 8.0 μm filter) to reduce processing volumes. A possible extension of ATPS is identified to replace this ultrafiltration step and provide the initial concentration of the feedstock as well as fractionation of the proteins. However the analytical problems associated with the pre-concentrated feedstock are likely to be exacerbated in the presence of a more dilute feedstock (see Section 2.3.2).

4.6 The potential of ATPS in processing other nanoparticles.

Advances in the field of genomics and recombinant DNA technology have impacted upon the field of biochemical engineering (Shanks and Stephanopoulos, 2000) to provide molecular therapies that can treat or prevent acquired and inherited diseases (Alton, 1995; Cooper, 1996). The portfolio of molecules, which in this context have a particle diameter of 2.0×10^1 to 2.0×10^2 nm are referred to as nanoparticles (as stated in Section 1.3.1.3) and include gene therapy vectors (viral and non viral) viruses, plasmid DNA, virus-like particles and protein aggregates: small inclusion bodies and prion proteins. Meeting the demand for the production of these particles is a tough challenge for the bioprocess engineer but one that has to be surmounted if they are to be produced at the required levels. In a situation analogous that is to that of influenza virus processing, ATPS may be *the* bioseparation technique to handle this diverse class of particles. The following discussion introduces these nanoparticles and proposes how ATPS could be used to circumvent limitations of the conventional techniques that are currently employed.

4.6.1. A brief description of other nanoparticles with potential use as therapeutics.

Viral gene therapy vectors are replication-deficient viruses containing relevant gene(s) (coding for defective or missing proteins) that infect target cells and deliver the gene(s) to the nucleus. Their description and application are reviewed (see Bonnet *et al*, 2000; Mountain, 2000; Romano *et al*, 2000 and Wu and Ataai, 2000 for a discussion of the advantages and disadvantages). Non-viral gene vectors include plasmid DNA and virus-like particles. Plasmids can be used as delivery vehicles (delivering relevant genetic

information to the nucleus leading to the generation immunoprotective proteins) or as "third generation" vaccines which themselves act as the immunostimulant, stimulating both humoral and cellular arms of the immune response (see Section 1.2). This discussion refers to small plasmids (containing 5-10 kb genetic information, with particle diameters of approximately 1.5 x 10^2 to 2.5 x 10^2 nm in their extended form). Virus-like particles (vlp's) are artificial structures constructed with the subunit(s)-immunoprotective protein(s) of the infectious organism, which can be used as vaccines or as delivery vehicles (DaSilva *et al*, 1999; Neumann *et al*, 2000). Genes encoding the subunit(s) and structural components capable of particle formation are spliced together and expressed under strongly inducing conditions to form particles (Andrews *et al*, 1995). These particles of diameter of 3.0 x 10^1 to 8.0 x 10^1 nm, have some advantages over viral vaccines because a range of immunoprotective proteins identified from various diseases can be expressed and the genes encoding these proteins can be selected to circumvent problems of infectivity or inappropriate immune reactions (Netter *et al*, 2001); Protein aggregates include inclusion bodies and prion proteins. In some cases over-expression of recombinant proteins may lead to the production of inclusion bodies (Misawa and Kumagai, 1999), which can be solubilised and correctly refolded to give active high value therapeutic proteins including antibody fragments (Tomlinson and Holliger, 2000). Most of the inclusion bodies formed are too large to be considered as nanoparticles 150 to 300 nm, (Walker, PhD Thesis, 1998), however one example of a small inclusion body, α-glucosidase (approximately 150 nm) has been used.

4.6.2. Prerequisites for the production of nanoparticulates to be used as therapeutics.

The viral vectors and plasmid DNA described in the previous section have been produced for Phase II or Phase III clinical trials (whereas the other nanoparticles are still undergoing laboratory investigations). Thus there are a number of requirements that must be met if the particle is to succeed in these stages as well as for intended commercial production. The foremost requirement is that the particles should be safe to use. Unlike traditional vaccine manufacture (from organisms such as influenza viruses), there is no safety precedent, thus the regulatory requirements are very strict (Braas *et al*, 1996). A high level of purity is desired to minimise potential toxicity, immunogenicity or in the case of gene therapy vectors, inappropriate activation/deactivation of regulatory genes (Wu and Ataai, 2000). In addition, the safety of the viral vectors has been thrown under the spotlight with the recent fatality in an adenovirus trial due to a strong host immune response (Stephenson, 2001). Other important issues regarding nanoparticles production is the specificity of the targeting mechanisms employed. This is one of the factors that currently make plasmid delivery disappointing (Ferreira *et al*, 2000). Once the delivery of genetic material has taken place, expression must occur at therapeutic levels (Romano *et al*, 2000). Thus to achieve these objectives, large quantities of these particles must be produced 10^{12} to 10^{20} particles (Braas *et al*, 1996).

4.6.3. Current DSP of nanoparticles and application of ATPS.

The unit operation utilised in the primary purification of these nanoparticles are much the same as those used in the manufacture of traditional viral vaccines and include filtration, centrifugation and adsorption chromatography (see Section 1.3.1.2). These unit

operations can work well but often have some limitation when applied on large scale (refer to Table 4.1 and Section 1.3.1.3).

It is proposed that ATPS when used as primary purification technique could circumvent many of the problems encountered. To start with, ATPS is mild (thus it should not impair the infectivity of viruses or harm shear sensitive molecules such as plasmid DNA); it can be highly selective (and could be used in discriminating between the different types of plasmid DNA, currently being looked at in Biochemical Recovery Group at the University of Birmingham, UK); the volumetric capacity is high (inclusion body work demonstrated a potential capacity of 10^9 to 10^{12} pfu ml^{-1}, Walker and Lyddiatt, 1999) and scale-up is relatively simple; this method is capable of processing large volumes in a relatively short time (as demonstrated in this study and thereby eliminating the limitations suffered by ultracentrifugation); each conventional unit operation has disadvantages when used to process a specific nanoparticle. ATPS can overcome these for a range of particles at a range of scales. This technique could prove invaluable if generic systems could be developed and applied and is discussed in the following section.

4.7. A generic mechanism for partition.

There are many inter-related factors that impact upon the partition of nanoparticles. The main ones are identified as: the surface properties of the nanoparticles; the biomass load; the presence of debris; the location of the nanoparticles; the feedstock type. Partitioning of a variety of nanoparticles within PEG-salt ATPSs was previously investigated (Braas and Lyddiatt, 2000). Analogies were drawn between adenoviruses

and washed (small) α-glucosidase inclusion bodies (Ib's) and also non-washed α-glucosidase Ib's and retroviruses, based on their surface properties and distribution in an ATPS. The washed Ib's presented a more hydrophilic surface, whereas the non-washed Ib's presented a more hydrophobic surface. On this basis one would expect the influenza virus particles to behave in a manner similar to the non-washed Ib's and retroviruses ATPS S24, PEG 8000 11.3 % w/w/ phosphate 9.2 % w/w, pH 7.5 was used to partition influenza virus. This was similar to the PEG 8000 10.0 % w/w/ phosphate 10.0 % w/w, pH 9.4 ATPS used in the studies undertaken by Braas and Lyddiatt (2000). Partition of the influenza virus in S24 showed that the majority of the influenza virus partitioned to the interface (see Figure C4). This confirmed the similarities with the non-washed inclusion bodies and retrovirus particles (see Table 4.1). A report also suggested an evolutionary link between orthomxyoviruses (such as influenza) and retroviruses (Harris *et al*, 1999).

UNIT OPERATION.	**Filtration.**	**Centrifugation.**	**Adsorption chromatography.**
Particle size range (nm).	**MF:** 5.0×10^2 2.0×10^4 **UF:**5.0×10^0 - 2.0×10^3	2.0×10^1 - 2.0×10^3	3.0×10^1 - 4.0×10^2
Nanoparticle description.			
VGTV.	-Scale limited. - Expensive.	-CsCl gradients can damage enveloped viruses. - Scale limited (requires large number of particles, 10^{11} particles ml^{-1} per ml). -Time-consuming (could affect viral infectivity).	-Low capacity. -Can impair infectivity
NVGTV.	-Large hydrodynamic radius blocks pores. Not sufficiently discriminating for different DNA's.	-Plasmid, shear sensitive (breakdown of plasmid, leads to worse purification problem). - Separation from other DNA's.	-Low capacity. -Can impair infectivity. -Expensive -Rigorous sanitation.
AGG. **Inclusion bodies.** **Prion protein fibrils.** **Vlp's.**		-Can get co-purification of contaminating proteins. -Requires long process times.	

TABLE 4.1. A comparison of the advantages and disadvantages of conventional unit operations when applied to the processing of nanoparticles to be used as therapeutics,
Key: *VGTV- viral gene therapy vector; NVGTV- non viral gene therapy vector; VLP- virus-like particle; AGG.- protein aggregate (refer to text for detailed descriptions). The ranges in brackets below the unit operation heading, refer to the particle diameters that the technique can handle.*

The observed differences in distribution of the nanoparticles in the ATPSs (such as the absence of a sediment) were accounted for by differences in biomass loading (Braas and Lyddiatt, 2000). The presence of biomass increases the TLL and interfacial tension. This in turn, increases adsorption of particles to the interphase up to a saturation limit. This limit would be exceeded relatively quickly in a sensitive system compared to those of a robust system. Increasing biomass load would increase the debris content and also affect the partition of the proteins and other components. The presence and quantity of debris and possible interactions with the nanoparticles impact upon the type of interphase formed (for example whether the interphase is dispersed or compact as observed in Chapter Three). The presence of debris is known to increase the precipitation concentration by decreasing the volume available to the salt phase (Zhou *et al*, 1998) and presumably the presence of particles, would by analogy, affect this also. Investigations are required to observe and to quantitate the impact of debris upon the binodal curve. The type of feedstock and the location of the nanoparticles would affect the type of debris produced (and hence the interphase formation, TLL, volume ratio and partition of components contained therein). Therefore for generic application of ATPSs for nanoparticles processing, methods are required to characterise the feedstocks

4.8. Future Indications in context of regulatory climate, acceptance as technique of choice for nanoparticle processing.

The investigations undertaken in this thesis addressed to some extent potential successes and problems encountered when using ATPS to fractionate nanoparticulates as applied to an industrially relevant particulate model- influenza virus. Thus this thesis has attempted to give an insight as to how ATPS may be employed in the fractionation of commercially relevant therapeutic nanoparticles.

Abbott, N. L., Blankschtein, D. and Hatton, T. A. (1990) On protein partitioning in two-phase aqueous polymer systems. *Bioseparation* **1** 191-225.

Ada, G. L., French, E. L. and Lind, P. E. (1961) Purification and properties of neuraminidase from *Vibrio cholerae*. *Journal of General Microbiology* **24** 409-421.

Albertsson, P., Å. (1958) Partition of proteins in liquid polymer-polymer two-phase systems. *Nature* **182** 709-711.

Albertsson, P., Å. (1986) Partition of cell particles and macromolecules. 3rd Edition, Wiley and Sons Publishers (Interscience), New York, NY.

Alton, E. W. (1995) Gene therapy for cystic fibrosis. *Journal of Inherited Metabolic Disease* **18 (4)** 510-507.

Ananthapadmanabhan, K., P. and Goddard, E., D., (1987) *Langmuir* **3** 25-31.

Andrews, B. A., Huang, R.-B. and Asenjo, J. A. (1995) Purification of virus like particles from yeast cells using aqueous two-phase systems. *Bioseparations* **5** 105-112.

Asplund, M., Bhikhabhai, R., Westerfors, M. and Haglund, R.(2000)
Purification of insulin from crude feedstock by employing a novel ligand for specific adsorption. Summary of a presentation at the EBA Conference 2000. *In: Downstream* **33**, 20-21, Amersham pharmacia Biotech., Uppsala, Sweden.

Awadé A.C. and Efstathiou, T. (1999) Comparison of three liquid chromatographic methods for egg-white protein analysis. *Journal of Chromatography B* **723** 69-74.

Azari, M., Boose, J.A., Burhop, K.E., Camacho, T., Catarello, J., Darling, A., Ebeling, A.A., Estep, T.N., Pearson, L., Guzder, S., Herren, J., Ogle, K., Paine, J., Rohn, K., Sarajari, R., Sun, C.S. and Zhang, L. (2000). Evaluation and validation of virus removal by ultrafiltration during the production of diaspirin crosslinked haemoglobin (DCLHb). *Biologicals* **28 (2)** 81-94.

Bachmayer, H. (1975) Selective solubilization of hemagglutinin and neuraminidase from influenza viruses. *Intervirology* **5** 260-272.

Bamberger, S., Brooks, D. E., Sharp, K. A., Van Alstine, J. M. and Webber, J. J. (1985) In: *Walter, H., Brooks, D.E. and Fisher, D. (eds.) Partitioning of Proteins in Aqueous Two-phase Systems. Theory, Methods, Uses and Applications to Biotechnology.* 85-130. Academic Press.

Bamberger, S., Seaman, G. V. F., Sharp, K. A. and Brooks, D. E. (1984) The effects of salts on the interfacial tension of aqueous dextran poly (ethylene glycol) phase systems. *Journal of Colloid and Interface Science* **99 (1)** 194-200.

Barrett, T. and Inglis, S.C. (1985) Growth, Purification and Titration of Influenza viruses. In: Mahey, B. W. J. (ed.) *Virology: A practical approach.* 119-150. IRL Press, Oxford.

Bartels, C. R., Kleinman, G., Korzon, N. J. and Irish D. B. (1958) A novel ion-exchange method for the isolation of streptomycin. *Chemical Engineering Progress* **54** 49-52.

Bates, F. J. (1942) Polarimetry, Saccharimetry and the Sugars, US Department of Commerce, National Bureau of Standards, Washington DC.

Batt, B. C., Yabannavar, V. M. and Singh, V. (1995) Expanded bed adsorption process for protein recovery from whole mammalian cell culture broth. *Bioseparation* **5** 41-52.

Bensadoun, A. and Weinstein, D. (1976) Assay of proteins in the presence of interfering materials. *Analytical Biochemistry* **70** 241-250.

Bierau, H., Zhanren, Z. and Lyddiatt, A. (1999) Direct process integration of cell disruption and fluidised bed adsorption for the recovery of intracellular proteins. *Journal of Chemical Technology and Biotechnology* **74** 208-212.

Boland, M. J., Hesselink, P.G. M., Papamichael, N. and Hustedt, H. (1991) Extractive purification of enzymes from animal tissue using aqueous two phase systems: pilot scale studies. *Journal of Biotechnology* **19** 19-34.

Boland, M. J., Hesselink, P.G. M. and Hustedt, H. (1989) Extractive purification of enzymes from animal tissue using aqueous two phase systems. *Journal of Biotechnology* **11** 337-352.

Bonnet, M. C., Tartaglia, J., Verdier, F., Kourilsky, P. Lindberg, A., Klein, M. Moingeon, P. (2000) Recombinant viruses as a tool for therapeutic vaccination against human cancers. *Immunology Letters* **74** 11-25.

Braas, G. M. F., Walker, S. G. and Lyddiatt, A. (2000) Recovery in aqueous two-phase systems of nanoparticulates applied as surrogate mimics for viral gene therapy vectors. *Journal of Chromatography B: Biomedical Applications* **743 (1-2)** 409-419.

Braas, G.M. F. (2000) Aqueous two-phase systems for the recovery of nanoparticulates bioproducts: relevance to the manufacture of gene therapeutics. *PhD Thesis, University of Birmingham, UK.*

Braas, G., Searle, P. F., Slater, N. K. H. and Lyddiatt, A. (1996) Strategies for the isolation and purification of retroviral vectors for gene therapy. *Bioseparation* **6** 211-228.

Bradford, M. M. (1976) A rapid and sensitive method for the quantitation of μg quantities of protein utilizing the principle of protein dye-binding. *Analytical Biochemistry* **72** 248-254.

Brady, M. I. and Furminger, I. G. S. (1976a) A surface antigen influenza vaccine. 1. Purification of haemagglutinin and neuraminidase proteins. *Journal of Hygiene Cambridge* **77** 161-172.

Brady, M. I. and Furminger, I. G. S. (1976b) A surface antigen influenza vaccine. 2. Pyrogenicity and antigenicity. *Journal of Hygiene Cambridge* **77** 173-180.

Brady M.I (1974) The immunogenic properties of purified components of influenza virus. *PhD Thesis, CNAA, London, UK.*

Breman, J. G. and Arita, I. (1980) The confirmation and maintenance of smallpox eradication. *New England Journal of Medicine* **303 (22)**1263-1273.

British Pharmacoepia, BP, HMSO (1997).

Burley, R. W. (1978) Studies on the apoproteins of the major lipoprotein of the yolk of hen's eggs III. Influence of salt concentration during isolation on the amount and composition of the apoproteins. *Australian Journal of Biological Science* **31** 587-592

Burley, R. W. (1975) Studies on the apoproteins of the major lipoprotein of the yolk of hen's eggs I. Isolation and properties of the low-molecular-weight apoproteins. *Australian Journal of Biological Science* **28** 121-132.

Burley, R. W. and Davies, W. A. (1976) Studies on the apoproteins of the major lipoprotein of the yolk of hen's eggs II. The dimer-tetramer transiton of apovitellin I. *Australian Journal of Biological Science* **29** 317-323.

Burley, R. W. and Sleigh, R.W. (1980) Studies on the apoproteins of the major lipoprotein of the yolk of hen's eggs. IV. Aggregation in urea of proteins of intermediate and high molecular weight and the isolation of four electrophoretically distinct proteins. *Australian Journal of Biological Science* **33** 255-268.

Burnet, F. M. (1941) Growth of influenza virus in the allantoic cavity of the chick embryo. *Australian Journal of Experimental Biology and Medical Science.* **19** 291.

Cabezas Jr., H., Kabiri-Badr, M. and Szlag, D. C. (1990) Statistical thermodynamics of phase separation and ion partitioning in aqueous two-phase systems. *Bioseparations* **1** 227-233.

Cabezas, J. A., Calvo, P., Eid, P., Martin, J. A., Perez, N., Reglero, A. and Hannoun, C. (1980) Neuraminidase from influenza virus A. (H3N2). Specificity towards several substrates and procedure of activity determination. *Biochimica et Biophysica Acta* **616** 228-238.

Cassidy, J. T., Jourdian, G. W., Roseman, S. (1965) The sialic acids VI. Purification and properties of sialidase from *Clostridium perfingens*. *The Journal of Biological Chemistry* **210 (9)** 3501-3506.

Choppin, P. W., Murphy, J. S. and Stoeckenius, W. (1961) The surface structure of influenza virus filaments. *Virology* **13** 548-550.

Cline, G. B. and Ryel, R. B. (1971) Zonal Centrifugation. *Methods in Enzymology* **22** 168-204.

Cole, K. D. (1993) Separation of lipoxygenase and the major soybean proteins using aqueous two-phase extraction and poly (ethylene glycol) precipitation *Journal of Agricultural and Food Chemistry*, **41 (2)** 334-340.

Cole, K. D. (1991) Purification of plasmid and high molecular mass DNA using PEG-salt two-phase extraction. *Bio/Techniques* **11** 18-24.

Colman, P. M, Varghese, J. N. and Laver, W. G. (1983). Structure of the catalytic and antigenic sites in influenza virus neuraminidase at 2.9 Å resolution. *Nature (London)* **303** 41.

Compans, R.W. and Choppin, P W. (1968) The nucleic acid of the parainfluenza virus SV5. *Virology* **35** 289-296.

Cooper, M. J. (1996) Noninfectious gene transfer and expression systems for cancer gene therapy. *Seminars in Oncology* **23 (1)** 172-187.

Corbel, M. J., Rondle, C. J. M. and Bird, R. G. (1970a) Degradation of influenza virus by non-ionic detergent. *Journal of Hygiene Cambridge* **68** 77-80.

Corbel, M. J. and Rondle, C. J. M. (1970b) Soluble antigens obtained from influenza virus by treatment with non-ionic detergent. *Journal of Hygiene Cambridge* **68** 81-96.

Cryz Jr., S J. (1991)Vaccines and Immunotherapy, McGraw-Hill.

Da Silva, D. M., Velders, M. P., Rudolf, M. P., Schiller, J. T. and Kast, W. M. (1999) Papillomavirus virus-like particles as anticancer vaccines. *Current Opinions in Molecular Therapy* **1** 82-88.

Donnelly, J. J., Ulmer, J.B., Shiver, J.W. and Liu, M. A. (1997) DNA vaccines. *Annual Review of Immunology* **15** 617-648.
Eitman, M. A. and Gainer, J. L. (1990) Peptide hydrophobicity and partitioning in poly(ethylene glycol)/magnesium sulfate aqueous two-phase systems. *Biotechnology Progress* **6** 479-484.

European Pharmacoepia, EP, HMSO (1997).

Evans, A. J. and Burley, R.W. (1987) Proteolysis of Apoprotein B during the transfer of very low density lipoprotein from hens' blood to egg yolk. *The Journal of Biological Chemistry* **62 (2)** 501-504.

Faff, O., Murray, B. A., Erfel, V. and Hehlmann, R. (1993) Large-scale production and purification of human retrovirus-like particles released to the mouse mammary tumour virus. *FEMS Microbiological Letters* **109** 289-296.

Ferreira, G. N. M, Monteiro, G. A., Prazeres, D. M. F. and Cabral, J. M. S. (2000) Downstream processing of plasmid DNA for gene therapy and DNA vaccine applications. *Trends in Biotechnology* **9** 380-388.

Flanagan, J. A., Huddleston, J. G. and Lyddiatt, A. (1991) Application of aqueous two-phase partition in PEG-phosphate systems. Design and implementations of a prototype process for recovery of bulk protein fractions from waste Brewer's yeast. *Bioseparation* **2** 43-61.

Forciniti, D. and Hall, C. K. (1992) Electrostatic effects on protein partitioning: simultaneous effect of pH and polymer molecular weight. *Chemical Engineering Science* **47 (1)** 165-175.

Furth, A. J., Bolton, H., Potter, J. and Priddle, J.D. (1984) Separating detergent from proteins. *Methods in Enzymology* **104** 318-328.

Graf, E.G., Jander, E., West, A., Pora, H. and Aranha-Creado, H. (1999) Virus removal by filtration. *Development of Biological Standards* **99** 89-94.

Guan, Y., Treffry, T., E. and Lilley, T., H. *E. Coli* penicillin acylase isolation by selective release, aqueous two-phase partitioning and ultrafiltration. *Biotechnology and Bioengineering* **40** 517-524.

Guan, Y., Wu, X. Y., Treffry, T., E. and Lilley, T., H. (1992) Studies on the isolation of penicillin acylase from *E. Coli* by aqueous two-phase partitioning. *Bioseparation* .
Gerin, J., L. and Anderson, N. G. (1969) Purification of influenza virus in the K-II zonal centrifuge. *Nature* **221** 1255-1256.

Hammar, L. and Gilljam, G. (1990) Extraction of HIV-1 in aqueous two-phase systems to obtain a high yield of gp120. *AIDS Research and Human Retroviruses* **6 (12)** 1379-1388.

Hammar, L., Eriksson, S., Malm, K., and Morein, B. (1989a) Concentration and purification of feline leukaemia virus (FeLV) and its outer envelope protein gp70 by aqueous two-phase systems. *Journal of Virological Methods* **24** 91-102.

Hammar, L., Merza, M., Malm, K., Eriksson, S. and Morein, B. (1989b) The use of aqueous two-phase systems to concentrate and purify bovine leukemia virus outer envelope protein gp51. *Biotechnology and Applied Biochemistry* **11** 296-306.

Hammond, P. M. and Scawen, M. D. (1989) High-resolution fractionation of proteins in downstream processing. *Journal of Chromatography* **11** 119-134.

Hariri, H., Ely, J. F. and Mansoori, G. A. (1989) Bioseparations: Design and engineering of partitioning systems. *Biotechnology* **7** 686-688.

Harris, A., Sha, B. and Luo, M. (1999) Structural similarities between influenza virus matrix protein M1 and human immunodeficiency virus matrix and capsid proteins: an evolutionary link between negative-stranded RNA viruses and retroviruses. *Journal of General Virology* **80** 863-869.

Hart, R. A. and Bailey, J. E. (1991) Purification and aqueous two-phase partitioning properties of recombinant *Vitreoscilla* hemoglobin. *Enzyme and Microbial Technology* **13** 788-795.

Helenius, A., McCaslin, D.R., Fries, E. and Tanford, C. (1979) Properties of Detergents. *Methods in Enzymology* **56** 734-749.

Helenius, A. and Simons, K. (1975) Solubilization of membranes by detergents. *Biochimica et Biophysica Acta* **415** 29-79.

Henderson, M. Wallis, C. and Melnick, J. L. (1973) Acid sensitivity of influenza virus haemagglutinin. *Applied Microbiology* **25** 685-687.

Hjelmeland, L. M. (1990) Solubilization of native membrane proteins. *Methods in Enzymology* **182** 253-265.

Hjelmeland, L. M. and Chrambach, A. (1984) Solubilization of functional membrane proteins. *Methods in Enzymology* **104** 305-318.

Hober, S., Gräslund, T., Hedhammar, M. and Uhlén, M. (2000) Charge engineering of a protein domain to allow efficient ion exchange recovery.. Summary of a presentation at the EBA Conference 2000. *In: Downstream* **33**, 22-23, Amersham Pharmacia Biotech., Uppsala, Sweden.

Hoffer, L., Schwinn, H., Biesert, L. and Josic, Dj. (1995) Improved virus safety and purity of a chromatographically produced Factor IX concentrate by nanofiltration. *Journal of Chromatography B: Biomedical Applications* **669** 187-196.

Hjorth, R. (1997) Expanded-bed adsorption in industrial bioprocessing: recent developments. *Trends in Biotechnology* **15** 230-235.

Hoyle, L., Horne, R. W. and Waterson, A.P. (1961) The structure and composition of the myxoviruses. II. Components released from the influenza virus particle by ether. *Virology* **13** 448-459.

Huddleston, J. G., Abelaira, J. C., Wang, R. and Lyddiatt, A. (1996) Protein partition between the different phases comprising poly (ethylene glycol)-salt aqueous two-phase systems, hydrophobic interaction chromatography and precipitation: a generic description in terms of salting-out effects. *Journal of Chromatography B: Biomedical Applications* **680** 31-41.

Huddleston, J. G., Ottomar, K. W., Ngonyani, D. M. and Lyddiatt, A. (1991a) Influence of system and molecular parameters upon fractionation of intracellular proteins from *Saccharomyces* by aqueous two-phase partition. *Enzyme and Microbial Technology* **13** 24-32.

Huddleston, J., Veide, A., Köhler, K., Flanagan, J., Enfors, S-O. and Lyddiatt, A. (1991 b) The molecular basis of partitioning in aqueous two-phase systems. *Trends in Biotechnology* **9** 381-388.

Huddleston, J. G. and Lyddiatt, A. (1991c) Aqueous two phase systems in biochemical recovery systematic analysis, design and implementation of practical processes for the recovery of proteins. *Applied Biochemistry and Biotechnology* **26** 249.

Huddleston, J. G. (1996) Polymer-salt aqueous two-phase systems in biochemical recovery Volume 1. PhD Thesis University of Birmingham, UK.

Hughes, P. and Lowe, C. R. (1988) Purification of proteins by aqueous two-phase partition in novel acrylic co-polymer systems. *Enzyme and Microbial Technology* **10** 115.

Hustedt, H., Kroner, K. H., Menge, U. and Kula, M-R. (1985) Protein recovery using two-phase systems. *Trends in Biotechnology* **3 (6)** 139-144.

Hustedt, H., Kroner, K. H., Stach, W.and Kula, M-R. (1978) Procedure for the simultaneous large-scale isolation of pullulanase and 1, 4-α-glucan phoshorylase from *klebsiella pneumoniae* involving liquid-liquid separations. *Biotechnology and Bioengineering* **20** 1989-2005.

Ingham. K.C. (1990) Precipitation of proteins with polyethylene glycol. *Methods in Enzymology* **182** 301-306 Academic Press Inc.

Ingham. K.C. (1984) Protein Precipitation with polyethylene glycol. *Methods in Enzymology* **104** 351-356. Academic Press Inc.

Johansson, G. (1985) Partitioning of protein. In: *Walter, H., Brooks, D.E. and Fisher, D. (eds.) Partitioning of Proteins in Aqueous Two-phase Systems. Theory, Methods, Uses and Applications to Biotechnology.* 161-226. Academic Press.

Joshi, J. B., Sawant, S. B., Raghava Rao, K.S.M.S., Patil, T. A., Rostami, K. M. and Sikdar, S, K. (1990) Continuous counter-current two-phase aqueous extraction. *Bioseparation* **1** 311-324.

Joubert, F. J. and Cook W. H. (1958) Separation and characterization of lipovitellin from hen egg yolk. *Canadian Journal of Biochemistry and Physiology* **36** 389-398.

Karger, A., Bettin, B., Granzow, H. and Mettenleiter, T. C. (1998) Simple and rapid purification of alphaherpesviruses by chromatography on a cation exchange membrane. *Journal of Virological Methods* **70** 219-224.

Kashyap, M. L., Hynd, B. A. and Robinson, K. (1980) A rapid and simple method for measurement of total protein in very low density lipoproteins by the Lowry assay. *Journal of lipid Research* **21** 491-495.

Kim, C., W. (1986) Interfacial condensation of biologicals in aqueous two-phase systems. *PhD thesis. Massachusetts Institute of Technology, MA, USA.*

Kroner, K. H. and Kula, M. –R. (1978) Extraction of enzymes in aqueous two-phase systems. *Process Biochemistry* **4** 7-9.

Kroner, K, H., Hustedt, H., and Kula, M. -R. (1984) Extractive enzyme recovery: economic considerations. *Process Biochemistry* **10** 1967-1988.

Kilbourne, E. D. (1987) Influenza. Plenum Medical.

Kilbourne, E. D. (1975) The influenza viruses and influenza. Academic Press, London.

Killington, R. A. and Powell, K. L. (1996) Growth, assay and purification of herpesviruses Chapter 10 207-236.

Kobasa, D., Rodgers, M. E., Wells, K. and Kawaoka, Y. (1997) Neuraminidase hemadsorption activity, conserved in avian influenza A viruses, does not influence viral replication in ducks. *Journal of Virology* **71 (9)** 6706-6713.

Kroner, K, H., Hustedt, H., and Kula, M. -R. (1984) Extractive enzyme recovery: economic considerations. *Process Biochemistry* **10** 1967-1988.

Kroner, K. H. and Kula, M. –R. (1982) Evaluation of crude dextran as phase-forming polymer for the extraction of enzymes in aqueous two-phase systems in large scale. *Biotechnology and Bioengineering* **24** 1015-1045.

Kroner, K, H., Hustedt, H., Granda, S. and Kula, M. -R. (1978) Technical aspects of separation using aqueous two-phase systems in enzyme isolation processes. *Biotechnology and Bioengineering* **20** 1967-1988.

Kulkarni, N., Vaidya, A. and Rao, M. (1999) Extractive cultivation of recombinant *Escherichia coli* using aqueous two phase systems for production and separation of extracellular xylanase. *Biochemical and Biophysical Research Communications* **255** 274-278.

Laemmli, U. K. (1970) Cleavage of structural proteins during the assembly of the head of bacteriophage T4. *Nature* **227** 680-685.

Lambré, C. R., Terzidis, H., Greffard, A. and Webster, R. G. (1991) An enzyme-linked lectin assay for sialidase. *Clinica Chimica Acta* **198** 183-194.

Lambré, C. R., Terzidis, H., Greffard, A. and Webster, R. G. (1990) Measurement of anti-influenza neuraminidase antibody using a peroxidase-linked lectin and mictrotitre plates coated with natural substrates. *Journal of Immunological Methods* **135** 49-57.

Laver, W. G. and Valentine, R. C. (1969) Morphology of the isolated hemagglutinin and neuraminidase subunits of influenza virus. *Virology* **38** 105-119.

Lebreton, B. and Lyddiatt, A. (2000) Application of two-phase partition to the production of homogeneous preparations of fluorescently labelled human serum albumin. *Journal of Chromatography B: Biomedical applications* **743** 263-269.

Lebreton, B. (1998) Practical exploitation of aqueous two-phase partitioning; molecular characterisation of working systems. *PhD Thesis, University of Birmingham, UK.*

Liljeqvist, S. and Stahl, S. (1999) Production of recombinant subunit vaccines: protein immunogens, live delivery systems and nucleic vaccines. *Journal of Biotechnology* **73 (1)** 1-33.

Liu, C.-L., Nikas, Y. J. and Blankschtein, D. (1995) Partitioning of proteins using two-phase aqueous surfactant systems. *American Institute of Chemical Engineering* **41 (4)** 991-995.

Lowry, O.H., Rosebrough, N. J., Farr, A. L. and Randall, R. J. (1951) Protein measurement with the folin phenol reagent. *Journal of Biological Chemistry* **193**, 265-275.

Madsen, T. (1933) *JAMA* **101** 187-188.

Makino, S., Reynolds, J. A. and Tanford, C. (1973) The binding of deoxycholate and triton X-100 to proteins. *The Journal of Biological Chemistry.* **248 (14)** 4926-4932.

Melander, W. and Horváth, C. (1977) Salt effects on hydrophobic interactions in precipitation and chromatography of proteins: An interpretation of the lyotropic series. *Archives of Biochemistry and Biophysics* **183** 200-215.

Meyer, O., Ollivon, M. and Paternostre, M-T. (1992) Solubilization steps of dark-adapted purple membrane by Triton X-100. A spectroscopic study. *Federation of European Biochemical Societies* **305 (3)** 249-253.

Millipore Technical Bulletin, 1992.

Miranda, M. V. and Cascone O. (1997) Partition of horseradish peroxidase in aqueous two-phase systems containing polyvinylpyrrolidone. *Bioseparation* **7** 25-30.

Misawa, S. and Kumagai, I. (1999) Refolding of therapeutic proteins produced in *Escherichia coli* as inclusion bodies. *Bioplymers* **51 (4)** 297-307.

Mitraki, A. and King, J. (1989) Protein folding intermediates and inclusion body formation. *Bio/Technology* **7** 690-697.

Morbidity and Mortality Weekly Report, 1997.

Mountain, A. (2000) Gene therapy: the first decade. *Trends in Biotechnology* **3** 119-128.

Murti, K. G. and Webster, R. G. (1986) Distribution of haemagglutinin and neuraminidase on influenza virions as revealed by immunoelectron microscopy. *Virology* **149** 36-43.

Murray, P. R., Kobayashi, G. S., Pfaller, M. A. and Rosenthal, K. S. (1994) Orthomyxoviruses Chapter 60 *In Medical Microbiology* International Student Edition Wolfe Imprint.

Netter, H. J., MacNaughton, T. B., Woo, W-P., Tindle, R. and Gowans, E. J. (2001) Antigenicity and immunogenicity of novel chimeric hepatitis B surface antigen particles with exposed hepatitis C virus epitopes. *Journal of Virology* **75 (5)** 2130-2141.

Neugebauer, J. (1994) A Guide to the Properties and Uses of Detergents in Biology and Biochemistry. Fifth Edition Calbiochem-Novabiochem International.

Neugebauer, J. M. (1990) Detergents: An overview. *Methods in Enzymology* **182** 239-253.

Neumann, G., Watanabe, T. and Kawaoka, Y. (2000) Plasmid-driven formation of influenza virus-like particles. *Journal of Virology* **74 (1)** 547-551.

O'Keeffe, R. S., Johnston, M. D. and Slater, N. K. H. (1999) The affinity adsorptive recovery of an infectious herpes simplex virus vaccine. *Biotechnology and Bioengineering* **62 (5)** 537-545.

O'Neil, P. F. and Balkovic, E. S. (1993) Virus harvesting and affinity-based liquid chromatography. A method ofr virus concentration and purification. *Biotechnology* **11** 173-178.

Paquet, V., Myint, M., Roque, C. and Soucaille, P. (1994) Partitioning of pristamycins in aqueous two-phase systems: A first step toward the development of antibiotic production by extractive fermentation. *Biotechnology and Bioengineering* **44** 445-451.

Peck, F., B. (1968) Purified Influenza virus vaccine. *Journal of the American Medical Association* 206 **(10)** 2277-2282.

Persson, J., Johansson, H-O., Galaev, I., Mattiasson, B. and Tjerneld, F. (2000) Aqueous polymer two-phase systems formed by new thermoseparating polymers. *Bioseparation* **9** 105-116.

Persson, J., Nyström, L., Ageland, H. and Tjerneld, F. (1999) Purification of recombinant proteins using thermoseparating aqueous two-phase system and polymer recycling. *Journal of Chemical Technology and Biotechnology* **74** 238-243.

Pharmacia Handbook, Expanded Bed Adsortion-Principles and Methods.Edition AA.

Pierce Technical Bulletin.

Planas, J., Kozlowski, A., Milton Harris, J., Tjerneld, F. and Hahn-Hägerdal, B. (1999) Novel polymer-polymer conjugates for recovery of lactic acid by aqueous two-phase extraction. *Biotechnology and Bioengineering* **66 (4)** 211-218.

Plotkin, S. A. (1993) Vaccination in the 21st century. *Journal of Infectious Diseases*. **168** 29-37.

Porter, M. C. (1972) Concentration polarization with membrane ultrafiltration. *Ind. Eng. Prod. Res. Develop.* **11 (3)** 234-248.

Richieri, S. P, Bartholomew, R., Aloia, R. C., Savary, J., Gore, R., Holt, J., Ferre, F., Musil, R., Tian, H. R., Trauger, R., Lowry, P., Jensen, F., Carlo, D. J., Maigetter, R., Z. and Prior, C. P. (1998) Characterization of highly purified, inactivated HIV-1 particles isolated by anion exchange chromatography. *Vaccine* **16 (2-3)** 119-129.

Reimer, C. B., Baker, R. S., vanFrank, R. M., Newlin, T. E., Cline, G. B. and Anderson, N. G. (1967) Purification of large quantities of influenza virus by density gradient centrifugation. *Journal of Virology* **1(6)** 1207-1216.

Rito-Palomares M. and Cueto, L. (2000) Effect of biological suspensions on the position of the binodal curve in aqueous two-phase systems. *Journal of Chromatography B: Biomedical Applications* **743** 5-12.

Rito-Palomares M. (1996a) Impact of cell disruption and polymer recycling upon aqueous two-phase processes for protein recovery *Journal of Chromatography B: Biomedical Applications* **680** 81-89.

Rito-Palomares M. (1995) Practical implementation of aqueous two-phase systems. *PhD Thesis University of Birmingham, UK.*

Romano, G., Michell, P., Pacilio, C. and Giordano, A. (2000) Latest developments in gene transfer technology: achievements, perspectives, and controversies over therapeutic applications. *Stem Cells* 18 (1) 19-39.

Romanoff A. L. and Romanoff, A. J. (1949) The Avian Egg. Wiley, NY.

Sabin, A. B. (1985) *Journal of Infectious Diseases.* **151** 420-430.

Rosenbergová, M., Slávik, I. and Hána, L. (1981) Zonal density gradient electrophoresis of influenza A virus. *Acta Virology* **25** 78-86.

Sadana, A. (1993) Interfacial protein adsorption and inactivation. *Bioseparation* **3** 297-320.

Salk, J. E. (1948) Reactions to concentrated influenza vaccines. *Journal of Immunology* **58** 369.

Sauvé, D. M, Duncan, T. H. and Roberge, M. (1995) Concentration of dilute protein for gel electrophoresis. *Analytical Biochemistry* **226** 383-386.

Save, S. V. and Pangarkar, V. G. (1995) Behaviour of surfactants in aqueous two phase systems. *Bioseparations* **5** 27-33.

Schmidt-Kastner, G. and Gölker, C. F. (1987) Downstream processing in biotechnology. Chapter 6 173-195. *In: Basic Biotechnology (Eds. J. Bu'lock and B. Kristiansen) Academic Press.Ltd.*

Sebastião, M. J., Martel, P. Baptista. A., Petersen, S. B., Cabral, J. M. S. and Aires-Barros, M. R. (1997) Predicting the partition coefficients of a recombinant cutinase in polyethylene glycol/phosphate aqueous two-phase systems. *Biotechnology and Bioengineering* **56 (3)** 248-257.

Shanks, J. V. and Stephanopoulos, G. (2000) Biochemical engineering. Bridging the gap between gene and product. *Current Opinion in Biotechnology* **11** 169-170.

Shearer, G. M. and Clerici, M. (1997) Vaccine strategies: selective elicitation of cellular or humoral immunity? *Trends in Biotechnology* **15** 106-109.

Sikdar, S., Cole, K. D., Stewart, R. M., Szlag, D. C., Todd, P. and Cabezas Jr., H. (1991) Aqueous two-phase extraction in bioseparations: An assessment. *Biotechnology* **9** 253-256.

Sivars, U. and Tjernfeld, F. (2000) Mechanisms of phase behaviour and protein partitioning in detergent/polymer aqueous two-phase systems for purification of integral membrane proteins. *Biochimica et Biophysica Acta* **1474** 133-146.

Skuse, D., R., Norris-Jones, R., Yalpani, M. and Brooks, D., E. Hydroxypropyl cellulose/poly(ethylene glycol)- co-poly(propylene glycol) aqueous two-phase systems: System characterization and partition of cells and proteins. (1992) *Enzyme Microbial Technology* **14** 785.

Smith, W. (1935) Cultivation of the virus of influenza. *British Journal of Experimental Pathology* **16** 508-512.

Stephenson, J. (2001) Studies illuminate cause of fatal reaction in gene-therapy trial. *Journal of the American Medical Association* **285 (20)** 2570.

Su, Z-G. and Feng, X-L. (1999) Process integration of cell disruption and aqueous two-phase extraction. *Journal of Chemical Technology and Biotechnology* **74** 284-288.

Tal, M., Silberstein, A. and Nusser, E. (1985) Why does Coomassie Brilliant Blue R interact differently with different proteins? A partial answer. *The Journal of Biological Chemistry* **260 (18)** 9976-9980.

Tanford, C. and Reynolds, J. A. (1976) Characterization of membrane proteins in detergent solutions.*Biochimica et Biophysica Acta* **457** 133-170.

Terstappen, G. C., Ramelmeier, R. A. and Kula, M-R. (1993) Protein partitioning in detergent-based aqueous two-phase systems. *Journal of Biotechnology* **28** 263-275.

Thömmes, J., Weiher, M., Karau, A. and Kula, M-R. (1995) Hydrodynamics in fluidized bed adsorption. *Biotechnology and Bioengineering* **48** 367-374.

Tomlinson, I. and Holliger, P. (2000). Methods of generating multivalent and bispecific antibody fragments.*Methods in Enzymology* **326** 461-479.

Towbin, H., Staehelin, T. and Gordon, L. (1979) Electrophoretic transfer of proteins from polyacrylamide gels to nitrocellulose sheets: procedure and some applications. *Proceedings of the National Academy of Science USA* **76** 4350-4354.

Ulmer, J. B., Sadoff, J. C. and Liu, M. A. (1996 c) DNA vaccines. *Current Opinions in Immunology* **8** (4) 531-536.

Ulmer, J.B., Donnelly, J. J., Parker, S. E., Rhodes, G, H., Felgner, P. L., Dwarki, V. J., Gromkowski, S. H., Deck, R. R., DeWitt, C. M., Friedman, A., Hawe, L. A., Leander, K. A., Martinez, D., Perry, H. C., Shiver, J.W., Montgomery, D. L. and Liu, M. A. (1993). Heterologous protection against influenza by injection of DNA encoding a viral protein. *Science* **259** 1745-1749.

Van Holde, K. E. (1986) Sedimentation, Chapter 5 *Physical Biochemistry, Edition 6.* 129-133.

van Reis, R., Leonard, L. C., Hsu, C. C. and Builder, S. E. (1991) Industrial scale harvest of proteins from mammalian cell culture by tangential flow filtration *Biotechnology and Bioengineering* **38** 413-422.

Varghese, J. N., Laver, W. G. and Colman, P.M. (1983) Structure of the influenza virus glycoprotien antigen neuraminidase at 2.9 Å resolution. *Nature* **303** 35-40.

Varley, D. L., Hitchcock, A. G., Weiss, A M., Horler, W, A., Cowell, R., Peddie, L., Sharpe, G. S., Thatcher, D. R. and Hanak, J. A. (1999) Production of plasmid DNA for human gene therapy using modified alkaline cell lysis and expanded bed anion exchange chromatography. *Bioseparation* **8 (1-5)** 209-217.

Veide, A., Lindbäck, T. and Enfors, S-O. (1984) Continuous extraction of β-D-galactosidase from *Escherichia coli* in an aqueous two-phase system: effects of biomass concentration on partitioning and mass transfer. *Enzyme and Microbial Technology* **6** 325-330.

Veide, A., Smeds, A-L. and Enfors, S-O. (1983) A process for large-scale isolation of β-Galactosidase from *E. coli* in an aqueous two-phase system. *Biotechnology and Bioengineering* **25** 1789-1800.

Walin, L., Tuma, R., G. J. Thomas, Jr. and Bamford, D. H. (1994) Purification of viruses and macromolecular assemblies for structural investigations using a novel ion exchange method. *Virology* **201** 1-7.

Walker, S. G. and Lyddiatt, A. (1999) Processing of nanoparticulate bioproducts: application and optimisation of aqueous two-phase systems. *Journal of Chemical Technology and Biotechnology* 74 250-255.

Walker, S. G. and Lyddiatt, A. (1998) Aqueous two-phase systems as an alternative process route for the fractionation of small inclusion bodies *Journal of Chromatography B*: *Biomedical Applications* 711 185-194.

Walker, S. G. (1998) Application of aqueous two-phase systems to the recovery of bioparticulates. *PhD Thesis , University of Birmingham, UK.*

Walker, S. G., Dale, C. J. and Lyddiatt, A. (1996) Aqueous two-phase partition of complex protein feedstocks derived from brain tissue homogenates. *Journal of Chromatography B* **680** 91-96.

Wallace, R.A. and Morgan, J. P. (1986a) Chromatographic resolution of chicken phosvitin. Multiple macromolecular species in a classic vitellogenin-derived phosphoprotein. *Biochemical Journal* **240** 871-878.

Wallace, R.A. and Morgan, J. P. (1986b) Isolation of Phosvitin: Retention of small molecular weight species and staining characteristics on electrophoretic gels. *Analytical Biochemistry* **157** 256-261.

Walsh, B. J., Barnett, D., Burley, R. W., Elliott, C., Hill, D. J. and Howden, M.E.H. (1988) New allergens from hen's egg white and egg yolk. *International Archives of Allergy and Applied Immunology* 87 81-86.

Walter, H., Johansson, G. and Brooks, D., E. (1991) Partitioning in aqueous two-phase systems: Recent results. *Analytical Biochemistry* 197 1-18.

Wang, Sho-Ya. and Williams, D. L. (1980) Identification, purification and characterization of two distinct avian vitellogenins. *Biochemistry* **19** 1557-1563.

Weber, K. and Osborn, M. (1969) The reliability of molecular weight determinations by dodecyl sulfate-polyacrylamide gel electrophoresis. *The Journal of Biological Chemistry* **244 (16)** 4406-4412.

Wells, C. M. and Lyddiatt, A. (1987) liquid fluidised bed adsorption of proteins. *In: Separations for Biotechnology.* 217-224. (Eds. M. J. Verrall and M. J. Hudson) Ellis-Horwood, Chichester UK.

Wessel, D. and Flügge, U. I. (1984) A method for the quantitative recovery of protein in dilute solution in the presence of detergents and lipids. *Analytical Biochemistry* **138** 141-143.

Wharton, M. L. and Wharton, D.R.A., (1960) The determination of uric acid I biological fluids: I. A modification of the method of Bergmann and Dikstein. *Analytical Biochemistry* **1** 213-217.

Wheelwright, S. M. (1989) The design of downstream processes for large-scale protein purification. *Journal of Biotechnology* **11(2,3)** 89-102.

Wu, N. and Ataai, M. M. (2000) Production of viral vectors for gene therapy applications. *Current Opinions in Biotechnology* **11** 205-208.

Zhang, Z., O'Sullivan, D. and Lyddiatt, A. (1999) Magnetically stabilised fluidised bed adsorption: practical benefit of uncoupling bed expansion from fluid velocities in the purification of a recombinant protein from *Escherichia coli. Journal of Chemical Technology and Biotechnology* **74** 270-274.

Zhou, Y. H. and Titchener-Hooker, N. J. (1999) Simulation and optimisation of integrated bioprocesses: a case study. *Journal of Chemical Technology and Biotechnology* **74** 289-292.

Zhou, Y. H., Bird, A. C., Alsaffar, L. and Titchener-Hooker, N. J. (1998) Modelling the effect of cell debris solids on protein precipitation. *IchemE research Event.* 1-6.

Zhou, F., Kakisaka, K., Ishidao, T., Iwai, Y. Arai, Y. and Furuya, T. (1997) measurement and correlation of partition coefficient of amino acids in dextran+ poly (ethylene glycol)+ water aqueous two-phase systems. *Journal of Chemical Engineering of Japan* **30 (2)** 349-353.

Zydney, A. L and Kuriyel, R. (2000) Protein concentration and buffer exchange using ultrafiltration. *Chapter 3 From Methods in Biotechnology* **9***: Downstream processing of proteins: Methods and Protocols, Humana Press Inc. New Jersey.*

APPENDIX I.

AI. Preliminary data regarding the partitioning and characterisation of Purified Zonal Concentrate (PZC) in selected ATPS. This feedstock was chosen as a representative nanoparticulate and originates from the Medeva Fluvirin™ Process. Such a feedstock was used since it could provide information helpful when partitioning the crude material.

A1. INTRODUCTION.

A.1.1 Partition of Purified Zonal Concentrate (PZC) and selection of ATPS.

Purified Zonal Concentrate (PZC) from Stage 5 in the Medeva Fluvirin™ Process (see Figure 2.4) was partitioned using a range of aqueous two-phase systems (ATPS) of varying PEG molecular weight, TLL and volume ratio (see Appendix II). Manipulating PEG molecular affects the system hydrophobicity, (Huddleston and Lyddiatt, 1991c), high PEG molecular weight, possesses longer chains and creates a more hydrophobic environment. Manipulating the TLL affects the interfacial tension of the system and manipulating the volume ratio can affect the distribution of target molecules. The reason for using PZC was to establish partitioning characteristics of the virus using a simpler feedstock (minus contaminating proteins) and to develop analytical methodologies to characterise the crude feedstock, Inactivated Bulk Fluid (IBF) from Stage 3 of the Medeva Fluvirin™ Process (see Figure 2.4). However from the viewpoints of subsequent comparison studies using IBF material and a published use of some ATPS, only a representative selection were discussed. Ideally, an ATPS showing potential would direct the partition of virus to one of the bulk phases.

A2. MATERIALS AND METHODS.

A.2.1.Construction of ATPS containing PZC.

The loaded ATPSs were constructed as in Section 2.2.2 with the addition of biomass. The biomass used included: Purified Zonal Concentrate (PZC), PZC spiked with egg white, egg white alone and IBF material. Medeva Pharma, Liverpool, UK, provided the IBF reserve material: A/Sydney batch 753134, and the PZC material: A/Beijing, batch 679. Eggs of uncertain age were used, originating from non-fertile hens medium eggs

(Crown Farm, Wychbold, UK, Lot: P59-4-692 best before 8/7/99). The eggs were used well within their best before date Separation of the egg white from the yolk was undertaken manually.

A.2.2. Haemagglutination Test (slight modification of WHO method, 1953).

The Haemagglutination (HA) Test was used in this study to quantify the amount of intact influenza virus. Haemagglutinin interacts with receptors (or more specifically, sialic acid residues on the receptors) of erythrocytes thereby promoting haemagglutination. This phenomenon formed the basis of the HA test. The virus was serially diluted in 0.01M PBS, pH 7.4 and challenged with an equivalent volume of a suitably low concentration (0.5 % v/v) solution of day-old chick erythrocytes in Alsevers, (TCS Microbiologicals, UK). The presence of virus was indicated by haemgglutination as observed by network formation and non-precipitation. Absence of the virus was indicated by pellet formation (Figure A1). Samples from phases of the blank and loaded ATPSs were serially diluted (50 µl per well), in a "U" -bottomed 96-well microtitre plate. The virus was challenged with an equivalent volume of the erythrocyte suspension and after gentle tapping, to mix the contents, the plate was incubated at 4 °C for one hour. A visual check was made to enable the deduction of the titre at which 50 % of the cells were agglutinated. After subtraction of the appropriate blanks, the haemagglutination units per ml HAU per ml (which is the titre at which 50 % of the virus is agglutinated by a 1 % v/v solution of erythrocytes) could be determined, (Barrett and Inglis, 1985). The total HAU was calculated by multiplying the HAU per ml by the phase volume. There was estimated to a 50 % error in this assay.

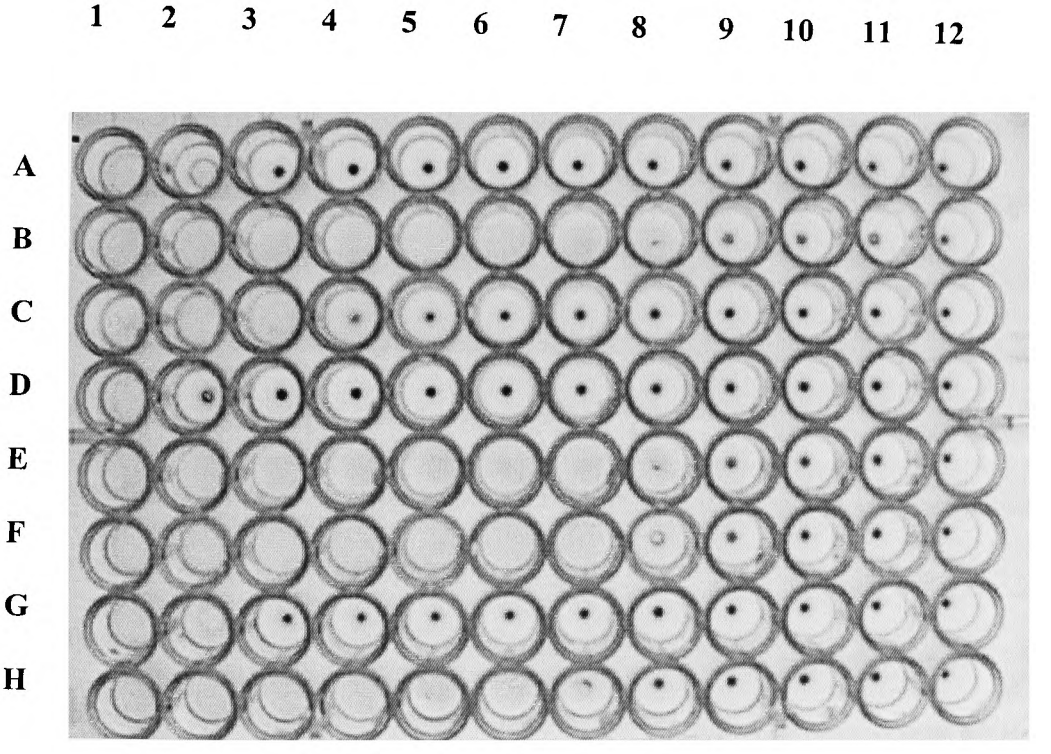

FIGURE A1. Microtitre plate illustrating typical results obtained using the HA test.
A negative result is indicated by pellet formation (for example, well 6C). A positive result is indicated by erythrocyte network formation (for example, well 3B). The virus was serially diluted across the plate (from 1 to 12) and challenged with a 0.5 % v/v suspension of erythrocytes.

A.2.3. *Neuraminidase enzyme-linked assay in microplates (NELLAM).*

This assay is outlined as follows (adapted from Lambré *et al*, 1991). Fetuin (a natural substrate of neuraminidase, NA), is attacked by NA in the influenza samples exposing) the carbohydrates N-acetyl neuramininc acid (NANA). The peroxidase-labelled peanut lectin (Po-PNA) recognises and binds to the NANA. Ortho-phenylamine diamine (OPD) is converted by the peroxidase to form a coloured complex that can be detected at 450 nm. The activity of NA is thus proportional to the amount of sialic acid removed, which is proportional to the amount of lectin bound and ultimately, to the quantified intensity of the coloured complex. A flat-bottomed 96-well microtitre plate was coated with fetuin (0.1 % w/v in 0.01M carbonate-bicarbonate buffer, pH 9.6). The plate was incubated overnight at 4 °C. Fetuin was removed and the binding sites were blocked with 1 % w/v BSA in 0.01M PBS pH 7.4 for one hour at 25 °C. The BSA blocking solution was removed and the PZC samples and calibration curve standards (neuraminidase Type II from *v. cholerae*) were then added to the plate. The plate was incubated for 5 hours at 37 °C then washed twice in 0.1 % v/v Tween 20/ 0.01M PBS pH 7.4 and the excess fluid removed by thorough blotting onto tissue. Peanut lectin peroxidase-labelled conjugate (3.3 $\mu g\ ml^{-1}$) was added to each well. The plate was incubated at 37 °C for a further two hours. After another wash/blot step, the substrate (10 mg O-PD in 25 ml citrate-phosphate buffer pH 5.0, plus 25 µl 30 % v/v hydrogen peroxide) was added. Colour development proceeded at room temperature for 15 to 20 minutes and the plate was read at 450 nm. After subtraction of the appropriate blanks, the neuraminidase content (in Units) could be determined from the calibration curve. The contents were corrected for dilution and then multiplied by the phase volume to obtain the total amount of NA Units in each phase. The minimum detection level of this assay was 1.0×10^{-3} NA units. The

definition of a Unit was as follows: 1 Unit releases 1 μmole NANA from NAN lactose min^{-1} at pH 5.0 at 37 °C. The decision was taken to present the results in Units because the NELLAM as described used fetuin (claimed to be better for viral NA's, Lambré *et al*, 1991) and the reaction was undertaken at 20 °C.

A.2.4. Bicinchinonic Acid (BCA) Assay.

The determination of total protein was undertaken using the Micro BCA assay kit (Catalogue number: 23235, Pierce, UK). This kit consisted of four reagents: MA (sodium carbonate, sodium bicarbonate and sodium tartrate in 0.2N sodium hydroxide), MB (4 % BCA in water), MC (4 % copper sulphate pentahydrate in water) and finally, BSA standard (2mg ml^{-1} total protein in 0.9 % saline and 0.05 % sodium azide). The principle of this assay involves the quantitative reduction of proteins in the presence of alkaline copper ions (Smith *et al*, 1985). The resulting purple-coloured complex can be spectrophotometrically detected between 540 to 590 nm (with the absorbance maximum occurring at 562 nm). For the purpose of this study, the assays were conducted in flat-bottomed 96-well microtitre plates (to increase throughput). Reagents MA, MB and MC were mixed in the ratio 25:24:1 to form a working reagent (stable for 24 hours at room temperature in a closed container). Equal volumes (150 μl) of sample (or blanks) and working reagent were incubated for 1 hour at 60 °C (with gentle shaking) and read using a plate reader at 540 nm. Total protein within the samples was calculated in BSA equivalents after subtraction of the appropriate blanks (consisting of the corresponding blank ATPS). The minimum detection limit of this assay using this protocol was 1.0 μg ml^{-1} total protein.

A.2.5. SDS PAGE and one-dimensional densitometry.

The methods deveoped using SDS PAGE and one-diensional densitometry formed the basis of Section 2.2.3.

A3. RESULTS AND DISCUSSIONS.

A.3.1. The effect of PEG molecular weight upon partition of PZC in selected ATPS.

The key proteins in the PZC material were identified using reduced SDS PAGE gels (Figure A5). The total protein concentration was also estimated using the BCA assay giving a value of approximately 0.5 mg ml^{-1} (Section A.2.4). It was not possible to use A_{280} measurements due to the presence of low levels (0.01 % w/v) of thiomerosal (which interfered with the analysis) that had been to PZC added as a preservative. The results recorded for the partition of purified zonal concentrate (PZC) were dependent upon both PEG molecular weight and tie-line length (TLL). The system comprising PEG 300 20..0 % w/w/ phosphate 20.0 % w/w, pH 7.5 and long TLL, 43.4 % w/w, (S2) partitioned the virus exclusively to the interphase (as shown in Figures A2 to A4). System S9 (comprising PEG 1000 12.0 % w/w/ phosphate 13.0 % w/w, pH 7.5, TLL, 8.3 % w/w) partitioned protein to all three phases, although assays detecting the viral components indicated that they partitioned preferentially to the bottom phase in this system (Figures A3 and A4). This suggested that either virus disruption had occurred (releasing other proteins not detected by the HA Test or neuraminidase enzyme-linked assay in microplates, (NELLAM) or there was an interfering agent in the top sample. This was also apparent in the partitioning of PZC in System S24 (PEG 8000 11.3 % w/w/ phosphate 9.2 % w/w, pH 7.5, TLL, 13.8 % w/w). The fact that the mass balances of total protein, HA and NA were variable, suggested that there was a source of

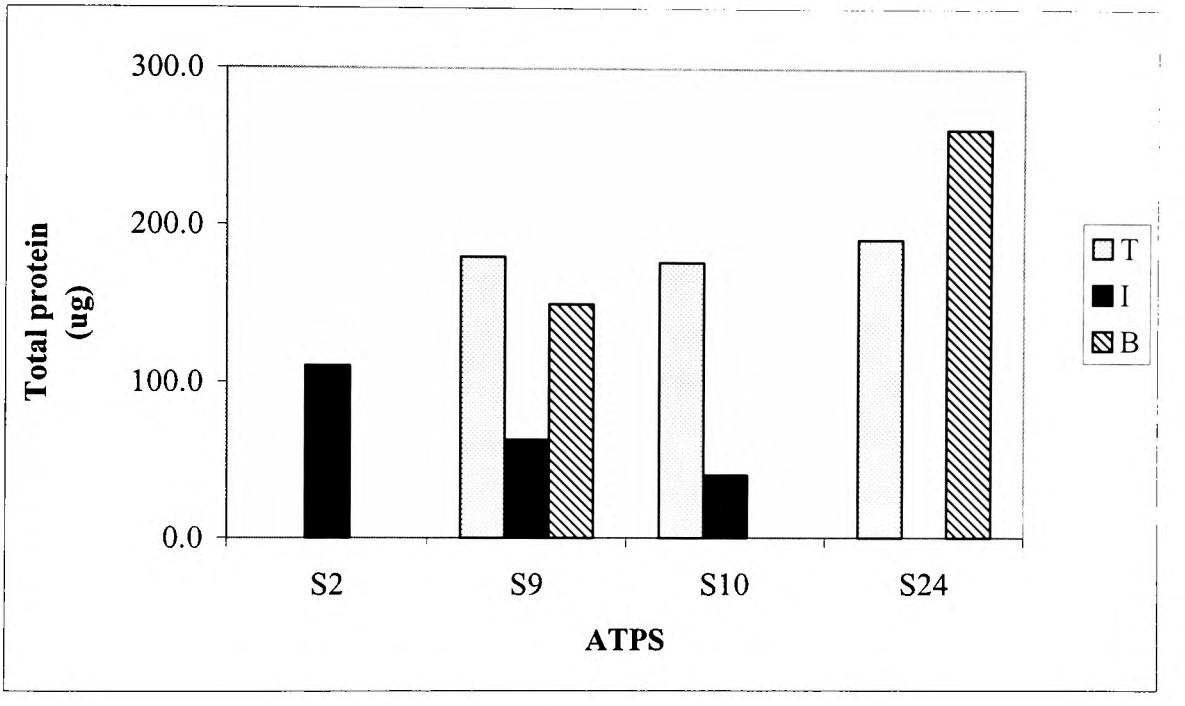

FIGURE A2. Partition of Purified Zonal Concentrate (PZC) in selected ATPSs monitored by BCA assay.

Four ATPSs were used to monitor the distribution of soluble protein in PZC. These systems were: S2 (PEG 300 20.0 % w/w/ phosphate 20.0 % w/w, pH 7.5), S9 (PEG 1000 12.0 % w/w/ phosphate 13.0 % w/w, pH 7.5), S10 (PEG 3350 20.0 % w/w/ phosphate 20.0 % w/w, pH 7.5) and S24 (PEG 8000 11.3 % w/w/ phosphate 9.2 % w/w, pH 7.5), refer to Appendix II for details. The mass balances were defined as the amount of protein in each phase divided by the load of protein to the system (585 µg in ATPSs S2, S9 and S24; 432 µg in ATPS S10). The mass balances were as follows: S2: 19.0 %, S9: 67.0 %, S10: 50.8 % and S24: 77.0 %. Refer also to Figures A3 and A4.

Key: T: Top phase; I: Interphase; B: Bottom phase.

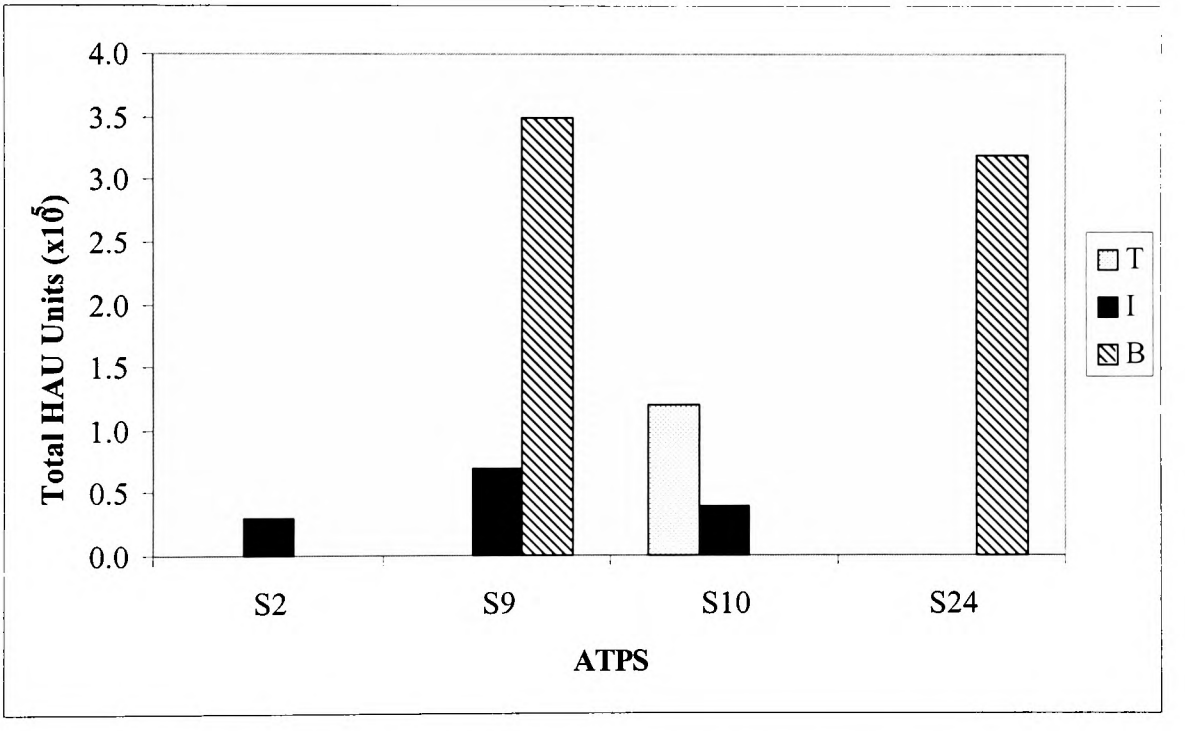

FIGURE A3. Partition of Purified Zonal Concentrate (PZC) in selected ATPSs monitored by HA Test.

Four ATPSs were used to monitor the distribution of HA antigen in PZC. These systems were: S2 (PEG 300 20.0 % w/w/ phosphate 20.0 % w/w, pH 7.5), S9 (PEG 1000 12.0 % w/w/ phosphate 13.0 % w/w, pH 7.5), S10 (PEG 3350 20.0 % w/w/ phosphate 20.0 % w/w, pH 7.5) and S24 (PEG 8000 11.3 % w/w/ phosphate 9.2 % w/w, pH 7.5), refer to Appendix II for details. The mass balances were defined as the amount of Haemagglutinin units (HAU) in each phase divided by the total added HAU to the system (5.5 x10^5 HAU). The mass balances were as follows: S2: 5.0 %, S9: 75.0 %, S10: 29.0 % and S24: 59.0 %. Refer also to Figures A2 and A4.

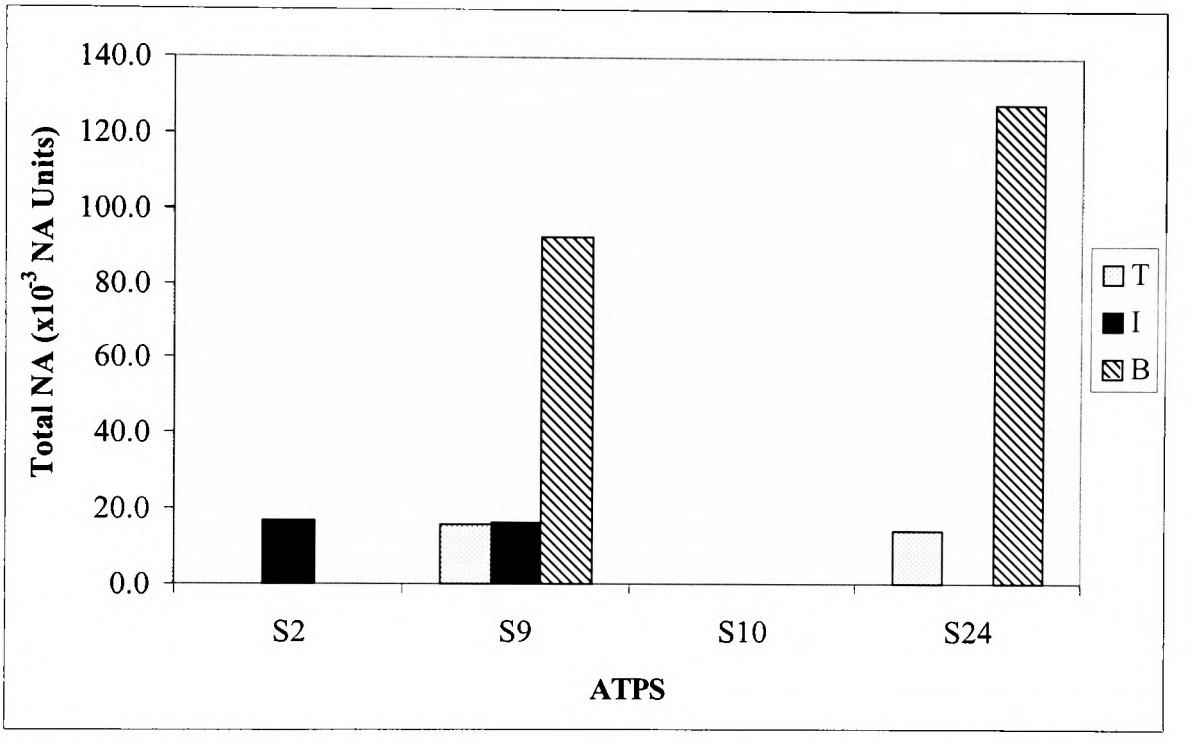

FIGURE A4. Partition of Purified Zonal Concentrate (PZC) in selected ATPSs monitored by neuraminidase enzyme-linked assay in microplates (NELLAM).
Four ATPSs were used to monitor the distribution of neuraminidase in PZC. These systems were: S2 (PEG 300 20.0 % w/w/ phosphate 20.0 % w/w, pH 7.5), S9 (PEG 1000 12.0 % w/w/ phosphate 13.0 % w/w, pH 7.5), S10 (PEG 3350 20.0 % w/w/ phosphate 20.0 % w/w, pH 7.5) and S24 (PEG 8000 11.3 % w/w/ phosphate 9.2 % w/w, pH 7.5), refer to Appendix II for details. The mass balances were defined as the amount of NA units in each phase divided by the total added NA to the system (46.3 x10^{-5} Units NA). The mass balances were as follows: S2: 36.0 %, S9: > 100 %, S10: Not determined and S24: > 100 %. Refer also to Figures A2 and A4.

interference. Thiomerosal was again suspected. This chemical is known to interfere in the BCA Assay (at the levels present in PZC), Pierce Technical Bulletin. Presumably thiomerosal partitions to the top phase producing false positives. The reason that this was apparently not observed in Systems S2 and S10 was because the proteins did not partition to the top phase in the former system and the effect of thiomerosal was included in the observed response in the latter system. In addition, the non-closure of mass balances in the systems was also attributed to aggregation of viral material at the interphase and inaccessibility of reagents in reaching virus in this phase. This suggested that the manner of harvesting the interphase needed to be re-evaluated. The fact that NA was detected in the top phase of whilst no haemagglutination was detected in Systems S9 and S24, could be explained by the difference in sensitivities of these assays (the former being more sensitive). System S10 (PEG 3350, 20.0 % w/w/ phosphate 20.0 % w/w, pH 7.5, TLL, 45.8 % w/w) produced a more one-sided partition. The formation of a dense interphase was responsible for the poor recovery and possibly prevented the partition of virus to the bottom phase. The HA result agreed with the protein distribution data in this system. From this study it was concluded that none of the systems could be rejected at this stage. System S2 demonstrated exclusive partition of virus to the interphase. The effect of 0.01 % thiomerosal upon the assays (BCA, HA and NA) could be monitored in order to identify it as a source of interference. If the source(s) could be verified and eliminated, then ATPSs S9 and S24 could prove useful in partitioning the virus to the bottom phase. If the recovery performance of S10 was verified then this may also have potential (in directing the virus to the top phase). In the first instance, the virus-specific assays demonstrated the partition preference of the virus. In addition, they provided

evidence that the virus remained intact (or that disrupted viral components containing HA and NA shared the same phase preference as the intact components).

A.3.2. The effect of PEG molecular weight and TLL upon partition of egg white proteins in selected ATPS.

Partition of egg white proteins was investigated using the Micro BCA assay and SDS PAGE/ one-dimensional densitometry. This would provide information on how the soluble proteins behaved in the ATPS and also the phase preference of individual proteins. The main contaminating protein in the crude Inactivated Bulk Fluid (IBF) feedstock (derived from the Medeva Fluvirin™ Process) was ovalbumin (personal communication P. Sinclair, 1999). Therefore with the data obtained from the partition of PZC, it was decided to spike the PZC with an ovalbumin source (a major impurity in the crude feedstock). The decision to use egg white was taken because it represented a readily available and more realistic (with respect to the proteinaceous process contaminants) source of ovalbumin. Analysis of the egg white showed it to be composed of a few proteins that could be easily identified by using SDS PAGE/densitometry and relative mobility (Rf) plots (Figure A5). The Rf values were deduced as follows:

$$\frac{\textit{The distance moved by the sample (mm)}}{\textit{The distance moved by the dyefront (mm)}} \qquad \textit{Equation A1.}$$

Ovalbumin, ovotransferrin (also known as conalbumin) and lysosyme were found to be present in the proportions listed in Table 2.2 (quantitation obtained from a calibration curve in ovalbumin equivalents). The other proteins present as shown in Table 2.2 (for example ovoglobin) were not observed due to their relatively low abundance and hence

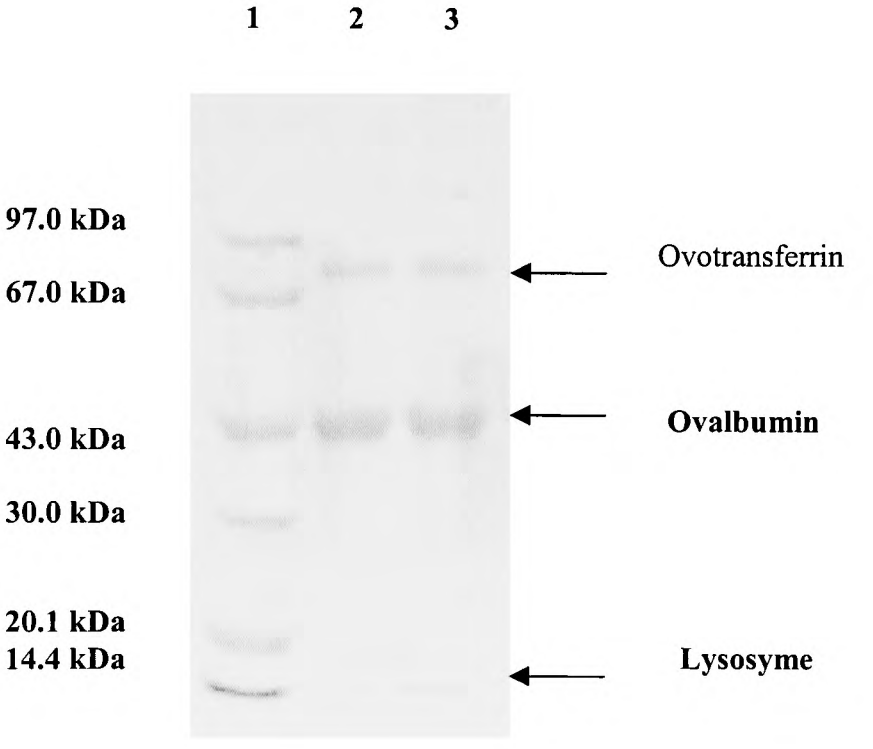

FIGURE A5. Proteins observed in egg white.
The egg white was obtained from a non-fertile hens egg. After separation from the egg yolk, the egg white fraction was prepared as and analysed using 9 % SDS PAGE gels (see Section 2.2.3). Approximately 5 μg total protein was applied to lanes 2 and 3.

Lane 1: *Low molecular weight markers (15 μl load).*
Lane 2: *100 μg ml^{-1} total egg white protein (10 μl load).*
Lane 3: *Duplicate of Lane 2 (10 μl load).*

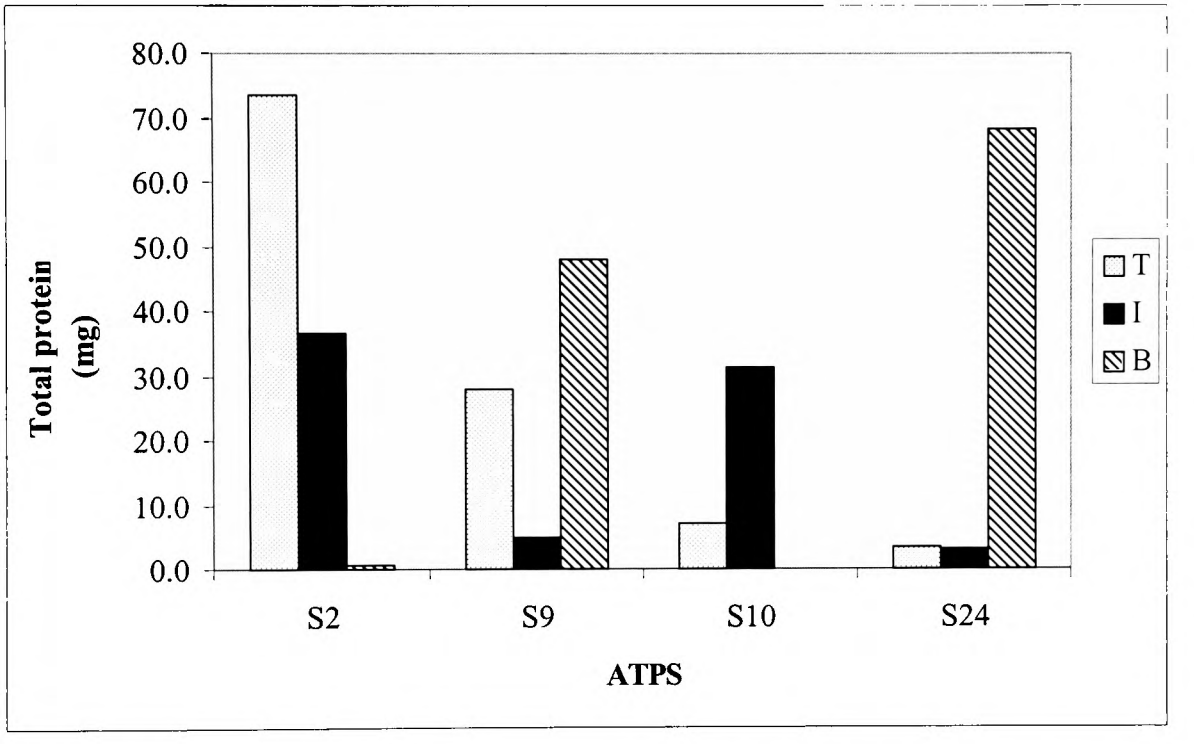

FIGURE A6.. Partition of egg white proteins in selected ATPSs monitored by BCA Assay.

Four ATPSs were used to monitor the distribution of egg white proteins loaded with 5 % w/w biomass. These systems were: S2 (PEG 300 20.0 % w/w/ phosphate 20.0 % w/w, pH 7.5), S9 (PEG 1000 12.0 % w/w/ phosphate 13.0 % w/w, pH 7.5), S10 (PEG 3350 20.0 % w/w/ phosphate 20.0 % w/w, pH 7.5) and S24 (PEG 8000 11.3 % w/w/ phosphate 9.2 % w/w, pH 7.5), refer to Appendix II for details. The mass balances were defined as the amount of protein in each phase divided by the total added protein to the system (78.8 mg). The mass balances were as follows: S2 and S9: 100.0 %, S10: 49.1 % and S24: 99.2 %. Refer also to Figures A7 and A8.

Key: T: Top phase; I: Interphase; B: Bottom phase.

less-intense staining and quantitation on the gel. The calculation of relative masses of each protein in each phase lead to the earliest definition of what eventually was termed a Fractional Mass Ratio (FMR), Section 2.3.2. This early work demonstrated the partition preference of individual proteins within a relatively simple protein mixture. Data from the partition of PZC suggested that the viral components partitioned exclusively to the interphase in S2. Data generated using SDS PAGE/ one-dimensional densitometry indicated that the majority of egg white proteins partitioned to the top phase (Figure A6). Thus such a system looked promising because it demonstrated selectivity for virus (refer to Figures A3 and A4). System S9 (Figures A3 and A4) showed that the viral components partitioned preferentially to the bottom phase and this trend was supported by SDS PAGE/ one-dimensional densitometry (data not shown). However, this ATPS would not be useful since a significant proportion of egg proteins in this ATPS also prefer the bottom phase. System S10 initially looked promising with respect to selectivity between the virus and contaminating proteins, but was hampered by poor recovery. Finally, S24 showed a bottom phase preference with respect to protein recovery. This was also mirrored in the recovery of the viral components (and supported by the SDS/ one-dimensional densitometry) thus it would seem that this ATPS would not be useful. Thus in summary, System S2 comprising PEG 300 appears selective in partitioning potential contaminating proteins away from the virus.

A.3.3. The effect of PEG molecular weight upon partition of PZC spiked with egg white selected ATPSs.

Thus far the discrete partitioning behaviour of PZC in selected ATPSs was investigated along with the partition of egg white proteins. This section investigates

whether the observed partition behaviour still held when both components were partitioned together. The distribution of egg white proteins in the presence of PZC was not significantly altered. A comparison of the total protein concentrations obtained using the BCA assay and SDS PAGE/ one-dimensional densitometry was presented in Table A1. The magnitude of protein concentration and trends were generally in agreement between the methods (except PEG 1000, because S9 is sensitive to changes in composition by virtue of it short TLL). This trend was also reflected in the SDS PAGE/ densitometry using egg white alone (data not shown). quantitation and monitoring of individual proteins. Differences in results were due to the differential staining of proteins with Coomassie Brilliant Blue partly due to the varied number of positive charges on the proteins, (Tal *et al*, 1985). It was therefore decided to produce separate calibration curves for each protein to account for this effect. The data from the HA Test (Figure A7) demonstrated that in all systems (including S10 although the value was very low) the HA antigen was predominantly located at the interphase except in S24 (where the preferred location was the bottom phase). The data could not be analysed quantitatively because the HA antigens were not binding adequately to the receptors on the erythrocytes. This was thought to be due to a conformation change or a possible antigen stripping mechanism exerted by the presence of PEG. The recovery was not affected by the presence of contaminating proteins in the egg white since the same total HAU was obtained with PZC alone. This suggested that the poor recovery was not due to masking of the receptor sites by the contaminating proteins. The magnitude of the values shown in Figure A8 was greater when compared to the data for PZC partitioned alone (Figure A4). This was attributed to the difference in scale of ATPS used and possibly due to the lower loading used (allowing greater accessibility of the enzyme to the substrate). The

ATPS (Analytical method).	**Top phase Total protein (mg).**	**Interphase Total protein (mg).**	**Bottom phase Total protein (mg).**	**Recovery (%).**
S2 (BCA)	11.9	0.6	0.4	103.0
S9 (BCA)	5.2	1.3	8.7	121.6
S9 (SDS PAGE)	9.1	0.0	3.5	101.6
S10 (BCA)	1.2	1.2	0.6	24.0
S10(SDS PAGE)	1.3	1.2	0.0	20.0
S24 (BCA)	0.2	N/A	14.4	116.8
S24(SDS PAGE)	0.0	N/A	41.3	330.0

TABLE A1. The partition of egg white proteins spiked with PZC within selected ATPSs comparing results produced by BCA assay and SDS PAGE /one-dimensional densitometry method.

Four ATPSs were used to monitor the distribution of egg white proteins spiked with PZC loaded with 5 % w/w biomass. These systems were: S2 (PEG 300 20.0 % w/w/ phosphate 20.0 % w/w, pH 7.5), S9 (PEG 1000 12.0 % w/w/ phosphate 13.0 % w/w, pH 7.5), S10 (PEG 3350 20.0 % w/w/ phosphate 20.0 % w/w, pH 7.5) and S24 (PEG 8000 11.3 % w/w/ phosphate 9.2 % w/w, pH 7.5), refer to Appendix II for details. The mass balances were defined as the amount of protein in each phase divided by the total added protein to the system (12.5 mg).

Key: ND: Not determined; N/A:Not applicable.

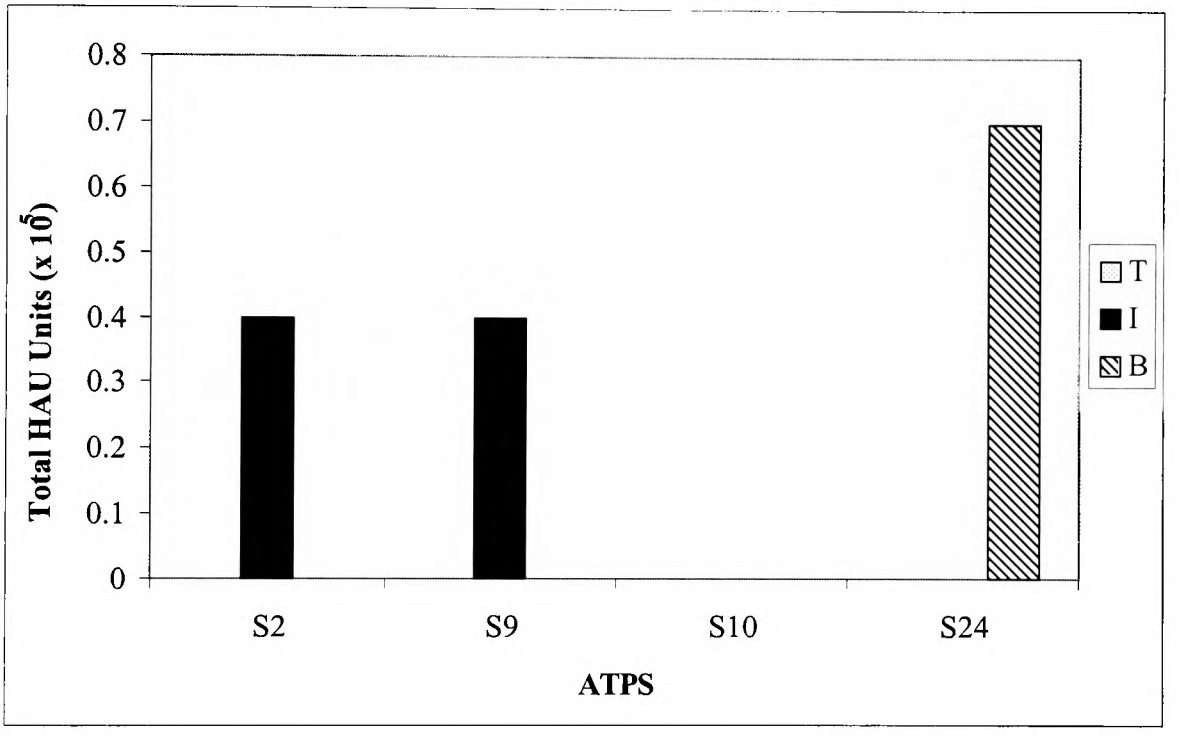

FIGURE A7. Partition of Purified Zonal Concentrate (PZC) in the presence of egg white proteins within selected ATPSs monitored by HA Test.

Four ATPSs were used to monitor the distribution of HA antigen of PZC in the presence of 12.5 mg egg white protein. These systems were: S2 (PEG 300 20.0 % w/w/ phosphate 20.0 % w/w, pH 7.5), S9 (PEG 1000 12.0 % w/w/ phosphate 13.0 % w/w, pH 7.5), S10 (PEG 3350 20.0 % w/w/ phosphate 20.0 % w/w, pH 7.5) and S24 (PEG 8000 11.3 % w/w/ phosphate 9.2 % w/w, pH 7.5), refer to Appendix II for details. The mass balances were defined as the amount of Haemagglutinin units (HAU) in each phase divided by the total added HAU to the system (1.5 x10^5 HAU). The mass balances were as follows: S2 and S9: 26.7 %, S10: 0.0 % and S24: 50.0 %. Refer also to Figures A6 and A8.
Key: T: Top phase; I: Interphase; B: Bottom phase.

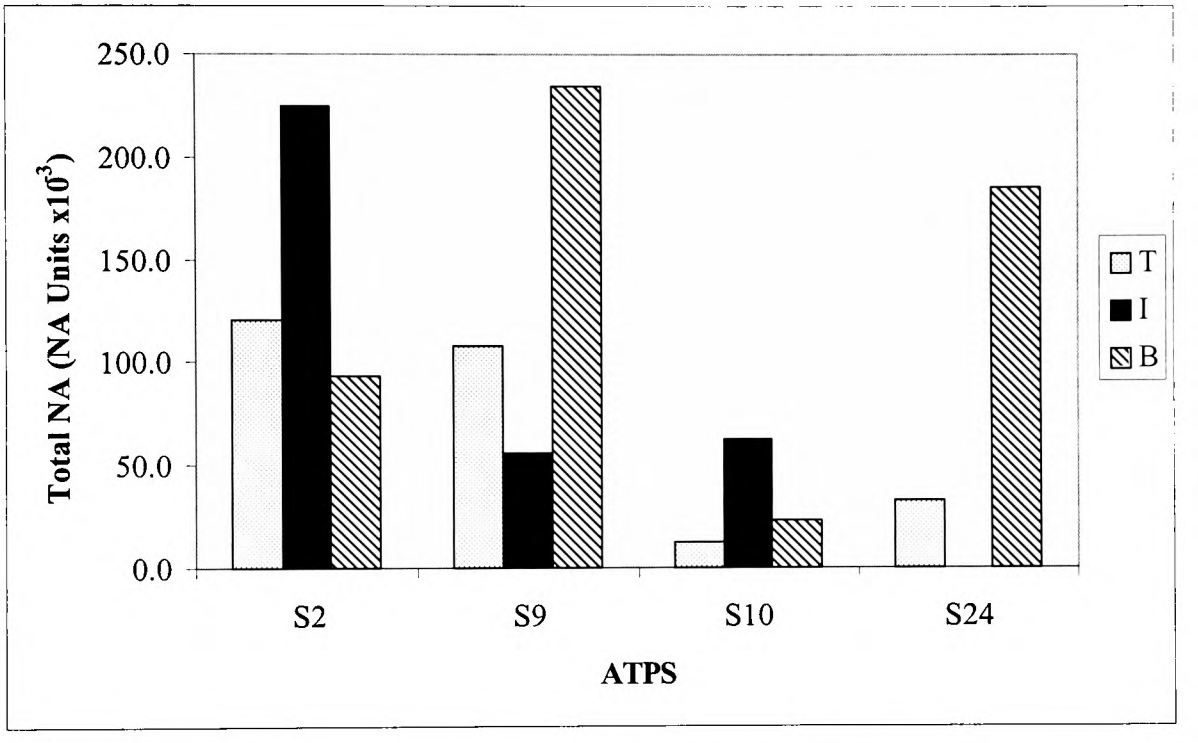

FIGURE A8. Partition of Purified Zonal Concentrate (PZC) in the presence of egg white proteins within selected ATPSs monitored by *neuraminidase enzyme-linked assay in microplates* ***(NELLAM).***

Four ATPSs were used to monitor the distribution of neuraminidase (NA) antigen of PZC in the presence of 12.5 mg egg white protein. These systems were: S2 (PEG 300 20.0 % w/w/ phosphate 20.0 % w/w, pH 7.5), S9 (PEG 1000 12.0 % w/w/ phosphate 13.0 % w/w, pH 7.5), S10 (PEG 3350 20.0 % w/w/ phosphate 20.0 % w/w, pH 7.5) and S24 (PEG 8000 11.3 % w/w/ phosphate 9.2 % w/w, pH 7.5), refer to Appendix II for details. The mass balances were defined as the amount of NA units (NA) in each phase divided by the total added NA to the system (28.0 x10^{-3} NA Units). The mass balances in all four systems were greater than 100 %. Refer also to Figures A6 and A7.

Key: T: Top phase; I: Interphase; B: Bottom phase.

presence of contaminating proteins did not affect the assay since PZC also gave the same result. In S2, the largest concentration of NA was present at the interphase. However this phase contributed the smallest volume. The top and bottom phase volumes were larger and contained lower concentrations of NA (hence the high recovery in these phases). The NELLAM was probably more sensitive than the HA test at detecting virus. There appeared to be no virus in these phases on the basis of haemagglutination. The same trend was observed in S9 and S24 and demonstrated that the majority of NA was detected in the bottom phase. Greater than 100 % closure of mass balances in the NELLAM was seen in majority of the systems used (in the absence or presence of egg white). This non-closure of mass balance occurs in the HA Test (less than 100 % closure) In both cases, this could be explained by changes in conformation. In the presence of phase forming chemicals leading to an increase in binding in the NELLAM and a decrease in binding in the HA Test. Methods to verify this would involve the analysis of the phases by binding studies. Alternatively, deliberate release the surface antigens using a detergent (Helenius and Simons, 1975), which would permit comparisons of the ability of haemagglutination and release of carbohydrates (by HA and NA respectively), with a non-disrupted preparation. The distribution of egg white proteins in the presence of PZC did not alter significantly. Also the magnitude of the concentration was as expected (an approximate five-fold decrease from the values shown in Figure A6). This study demonstrated that S2 (see Appendix II) would be useful for processing influenza since the virus favours the interphase whilst bulk proteins favour the top phase. The data obtained from S9 (see Appendix II) was not consistent. This was possibly because it was more sensitive (due to its low TLL) with respect to partition. System S10 was not useful from point of view of poor recovery and partial co-

purification of proteins with the virus and S24 was not useful since the viral proteins co-purified with the contaminating proteins.

A4. PRELIMINARY OBSERVATIONS.

The Haemagglutinin Test was useful as a qualitative indicator of the HA content, but not as a quantitative measure. Various factors affected the assay including the phase-forming chemicals (notably the PEG which lead to variable mass balances) and the age of the cells. It was best to use the cells for HA Tests within 5 days of receiving them) as they become prone to lysis, (leading to false positive results). Attempts to cryopreserve the cells using glycerol were unsuccessful. The assay was sensitive to the erythrocyte concentration used (although a well-suspended cell concentration of 0.5 or 1 % v/v was typically used. Another future (albeit lesser) concern was that if other viruses were present in the complex feedstock, they may also haemadsorb to the erythrocytes thus distorting the results. This was not thought to represent a huge problem since the adaptation techniques should passage out adventitious viruses. Other reasons for not using this test were that it only worked using chick, guinea pig or human erythrocytes. The reasons for this were unclear but were possibly linked to surface antigens present on these cells, which the virus recognises.

The volume of the interphase was estimated as though it were a disc of thin cylinder. This was probably a true representation of the volume but it did not provide an accurate picture for the estimation of components therein since (for example) aggregation of virus may not permit accessibility to assay reagents and so enable accurate quantitation. It was decided to suspend the interphase components in a known volume of buffer prior to their analysis. The Micro BCA assay was not suitable to analyse the PZC possibly due to

some interfering moiety (possibly thiomerosal) not seen in the egg white analysis. The Micro BCA assay had been selected in acknowledgement that the low concentration of PZC, (approximately 500 $\mu g\ ml^{-1}$), would be diluted even more in the ATPS, (approximately five-fold) and a further 50 to 100-fold to remove phase formants, might lead to problems of detection. The Bradford assay was not as sensitive as the Micro BCA assay and would still face the same problems regarding handling the interphase phase formants. Thus in conclusion, the HA and NA tracked each other fairly well suggesting that the viral particles remained intact or that there was release of antigens but they preferred the same phase. This could again be tested using electron microscopy and immunogold staining. System S2 (comprising PEG 300) so far looked the most promising ATPS. The behaviour of the individual components mimicked that of the spiked material. Differences were attributed to the differences in system loading. The importance of having supporting analytical techniques was highlighted as well as the problems of handling multiple phases. Suggested mechanisms for the observed partition behaviour are illustrated in Figure 2.10.

APPENDIX II.

B1 Aqueous Two phase systems employed for method scouting and optimisation studies.

A complete list of all the ATPS used in the method scouting and optimisation studies documented in Chapters Two, Three and Appendix I of this thesis. These systems were chosen such that a range of variables could be investigated in the partitioning of influenza virus particles contained in allantoic fluid (which served as an experimental vehicle for processing particulate feedstocks, see Appendix I). These variables included PEG molecular weight, tie-line length (TLL) and volume ratio (Vrd). This permitted the development of methods that could be applied to the influenza virus feedstock (Chapter Two and Three). Systems, which directed contaminating proteins away from the virus, were deemed useful. The partition of virus was monitored using SDS PAGE/ one-dimensional densitometry (on 12 % gels) and an ELISA specific for haemagglutinin (HA) antigen (one of the key surface projections on the virus, see Figure 2.1). The partition of the contaminants was monitored using SDS PAGE/ one-dimensional densitometry.

TABLES B1 to B9. Aqueous two-phase systems (ATPSs) employed in method scouting and optimisation studies.

The systems were prepared as described in Sections 2.2.1 and 2.2.2 (for blank and loaded systems respectively) and the Vrds were estimated as described in Section 2.1.8. Systems highlighted in bold typeface were key systems in the process development documented in this thesis.

TABLE B1. PEG 300/ potassium phosphate ATPS, pH 7.5.
These systems were used in the method scouting studies documented in Chapter Two. System S2 was the source ATPS from which System S25 (the primary ATPS, refer to Figure 3.1) arose.

.

System ID number.	PEG 300 (% w/w).	Phosphate (% w/w)	TLL (% w/w).	Vrd= (Vt/Vb).
S1	20.0	22.0	43.4	1.33
S2	**20.0**	**20.0**	**45.4**	**1.33**
S3	16.1	20.0	28.3	1.00
S25	**22.2**	**17.9**	**43.4**	**1.50**
S26	25.5	15.0	43.4	1.92
S27	32.2	10.0	43.4	6.00
S28	32.5	8.4	43.4	7.80
S29	32.2	7.3	Monophasic	N/A

TABLE B2. PEG 600/ potassium phosphate ATPS, pH 7.5.

System ID number.	PEG 600 (% w/w).	Phosphate (% w/w)	TLL (% w/w).	Vrd= (Vt/Vb).
S4	22.2	20.3	40.1	1.06
S5	16.1	15.6	23.0	1.13
S6	16.6	13.3	N/A	Monophasic

TABLE B3. PEG 1000/ potassium phosphate ATPS, pH 7.5.

System ID number.	PEG 1000 (% w/w).	Phosphate (% w/w)	TLL (% w/w).	Vrd= (Vt/Vb).
S7	17.0	16.8	36.6	0.93
S8	14.0	13.0	25.0	0.89
S9	12.0	13.0	8.3	0.89

TABLE B4. PEG 3350/ potassium phosphate ATPS, pH 7.5.

System ID number.	PEG 3350 (% w/w).	Phosphate (% w/w)	TLL (% w/w).	Vrd= (Vt/Vb).
S10	20.0	20.0	45.8	0.89
S11	14.4	12.4	26.1	0.89
S12	12.9	11.4	17.5	0.95

TABLE B5. PEG 6000/ potassium phosphate ATPS, pH 7.5.

System ID number.	PEG 6000 (% w/w).	Phosphate (% w/w)	TLL (% w/w).	Vrd= (Vt/Vb).

S13	20.0	15.0	37.7	1.03
S14	15.0	10.5	23.9	1.10
S15	13.9	10.8	18.8	1.00

TABLE B6. PEG 6000/ Dextran 464T (unbuffered) ATPS.

System ID number.	PEG 6000 (% w/w).	Dextran 464T (% w/w)	TLL (% w/w).	Vrd= (Vt/Vb).
S16	11.0	20.9	45.0	1.06
S17	7.5	15.4	31.4	1.08
S18	5.0	9.5	16.9	0.99

TABLE B7. PEG 6000/ Dextran 464T (buffered) ATPS, pH 7.5.

System ID number.	PEG 6000 (% w/w).	Dextran 500T (% w/w)	TLL (% w/w).	Vrd= (Vt/Vb).
S19	11.0	20.9	45.2	1.00
S20	7.5	15.4	30.5	1.08
S21	5.0	9.5	13.5	0.99

TABLE B8. PEG 8000/ potassium phosphate ATPS, pH 7.5.

System S23 was key in the volume ratio manipulation study undertaken (see Section 2.3.2.6) Systems S30 to S33 were generated on the back of S23.

System ID number.	PEG 8000 (% w/w).	Phosphate (% w/w)	TLL (% w/w).	Vrd= (Vt/Vb).
S22	22.8	16.8	42.9	1.07
S23	**15.0**	**11.1**	**22.4**	**1.06**
S24	11.3	9.2	13.8	1.18
S30	12.5	12.2	22.4	0.69
S31	10.0	13.5	22.4	0.50
S32	7.2	15.3	22.4	0.29
S33	5.3	16.3	22.4	0.20

TABLE B9. PEG / potassium phosphate ATPS, pH 7.5.
These systems were used as intermediate systems and secondary hybrid systems (refer to Figure 3.1). The effect of PEG molecular weight was evaluated to see which was optimal for processing Inactivated Bulk Fluid (IBF) material in Aqueous-detergent two-phase systems (ADTPSs). System S40 in the presence of Triton X100 was the optimal system (see Section 3.3.3.5).

System ID number.	**PEG 300 (% w/w).**	**Phosphate (% w/w)**	**TLL (% w/w).**	**Vrd= (Vt/Vb).**
S34	10.0	30.0	43.4	0.38
S35	10.0	25.0	28.3	0.36
S39	16.8	22.9	43.5	0.83
S40	**13.9**	**24.3**	**35.3**	**0.93**
System ID number.	**PEG 1000 (% w/w).**	**Phosphate (% w/w)**	**TLL (% w/w).**	**Vrd= (Vt/Vb).**
S36	10.7	13.9	8.3	0.55
S41	7.3	27.6	29.4	0.56
System ID number.	**PEG 6000 (% w/w).**	**Phosphate (% w/w)**	**TLL (% w/w).**	**Vrd= (Vt/Vb).**
S37	10.0	9.1	19.0	0.50
S42	7.8	25.3	34.7	0.52
S43	7.2	27.1	33.9	0.44
System ID number.	**PEG 8000 (% w/w).**	**Phosphate (% w/w)**	**TLL (% w/w).**	**Vrd= (Vt/Vb).**
S38	8.3	10.0	13.8	0.50